



PONTIFICIA UNIVERSIDAD CATOLICA DE CHILE
SCHOOL OF ENGINEERING

IMPLEMENTATION OF A COUNTER CURRENT PACKED COLUMN FOR FRACTIONATION OF KEY SIX-CARBON APPLE AROMAS USING SUPERCRITICAL CO₂

ARTURO BEJARANO CHAVARRO

Thesis submitted to the Office of Graduate Studies in partial fulfillment of
the requirements for the Degree of Doctor in Engineering Sciences.

Advisor:

Dr. JOSÉ M. DEL VALLE LLADSER

Santiago de Chile, (April, 2016)

© 2016, Arturo Bejarano Chavarro



PONTIFICIA UNIVERSIDAD CATOLICA DE CHILE
SCHOOL OF ENGINEERING

IMPLEMENTATION OF A COUNTER CURRENT PACKED COLUMN FOR FRACTIONATION OF KEY SIX-CARBON APPLE AROMAS USING SUPERCRITICAL CO₂

ARTURO BEJARANO CHAVARRO

Members of the Committee:

Dr. JOSÉ M. DEL VALLE LLADSER

Dr. JUAN C. DE LA FUENTE BADILLA

Dr. EDUARDO AGOSÍN TRUMPER

Dr. JOSÉ RICARDO PÉREZ CORREA

Dr. PEDRO M. CALADO SIMÕES

Dr. CRISTIAN VIAL EDWARDS

Thesis submitted to the Office of Graduate Studies in partial fulfillment of
the requirements for the Degree of Doctor in Engineering Sciences.

Santiago de Chile, (April, 2016)

*Dedicated to my loving wife, for her
immense heart, and to our promising
future. To my parents and sisters, that
despite everything that keeps us
apart, are always in my loving heart.*

ACKNOWLEDGEMENTS

My eternal gratitude is first for my loving wife, for her strength, patience, and understanding during hard times, but above all, for her enormous heart and infinite love, and for my parents, Eugenia and Diego, and my sisters Sonia and Laura which are always there for me.

I want to thank specially to my advisor Dr. José M. del Valle for his transparency and frankness, for the opportunity to work with him, his confidence in my capabilities, and support in every step of this work. His supervision made my work better. I would also like to thank Prof. Dr. Juan C. de la Fuente (*Universidad Técnica Federico Santa María*, Chile) for his friendship and support, Prof. Dr. Pedro C. Simões (*Universidade Nova de Lisboa*, Portugal) for the opportunity to work in his laboratory and coauthor one of my best publications, and Prof. Dr.-Ing. Arne Pietsch and Dr.-Ing. Philip T. Jaeger for their suggestions, constructive dialogues, and their kindness and work at Eurotechnica while my visit to Hamburg.

Special thanks to Pablo I López, for his dedicated effort and perseverance performing phase equilibria measurements, I believe both of us benefit from this work. Thanks to Maria Elena Ortiz, Gisela Bruhn, and Ana I. González for their assistance.

To Pedro F. Lisboa and Carmen A. Moreno Montoya for their help and the good times while my internship in Portugal (LAQV-REQUIMTE). Also thanks to my Lab partners from the *Laboratorio de Extracción de Materiales Biológicos* (LEMaB): Freddy Urrego, Gonzalo Nuñez, Fabián Reyes, Eduardo Richter, Julia Arango, Sofía Andrighetti, Caroline Sielfeld, and Soledad Murias.

Finally, thanks to the “*Dirección de Postgrados de la Escuela de Ingeniería DIPEI*” from the Pontificia Universidad Católica de Chile and “*Fondo de Fomento al Desarrollo Científico y Tecnológico FONDEF*”, specifically the R&D project N° D09I1207 of the Chilean agency CONICYT. Without these resources this work could not be completed, and therefore greatly acknowledged.

CONTENTS

AKNOWLEDGEMENTS	iii
CONTENTS	iv
LIST OF TABLES	vi
LIST OF FIGURES	viii
RESUMEN	xi
ABSTRACT	xiii
LIST OF PAPERS	1
1. INTRODUCTION	2
1.1 Hypothesis	4
1.2 Objectives	4
2. FRACTIONATION TECHNOLOGIES FOR LIQUID MIXTURES USING DENSE CARBON DIOXIDE	6
2.1 Introduction	6
2.2 Continuous CC-SFF fundamentals, research groups, and applications	19
2.2.1 Fundamentals	19
2.2.2 Modes of operation of packed columns and applications	31
2.3 Membrane contactors	37
2.4 Mixer-settler process and components	40
2.5 Spray processes	45
2.6 Phase equilibrium and relevant physicochemical properties.....	48
2.6.1 Phase equilibrium.....	48
2.6.2 Density and viscosity	56
2.6.3 Interfacial tension and contact angle.....	58
3. HIGH-PRESSURE (VAPOR + LIQUID) EQUILIBRIA FOR TERNARY SYSTEMS COMPOSED BY (<i>E</i>)-2-HEXENAL OR HEXANAL + CARBON DIOXIDE + WATER: PARTITION COEFFICIENT MEASUREMENT	66
3.1 Introduction	66
3.2 Experimental.....	70
3.2.1 Materials.....	70
3.2.2 Experimental apparatus and procedure	70
3.2.1 Analyses and quantification	73
3.3. Results and discussion	75
3.3.1 Validation of the experimental apparatus and methodology: (CO ₂ + ethanol) and (CO ₂ + ethanol + water) systems	75
3.3.2 Partition coefficients and separation factors of apple aroma constituents	80

4. COUNTERCURRENT FRACTIONATION OF AQUEOUS APPLE AROMA CONSTITUENTS USING SUPERCRITICAL CARBON DIOXIDE.....	88
4.1 Introduction	88
4.2 Materials and Methods	90
4.2.1 Materials.....	90
4.2.2 Experimental apparatus and procedure	90
4.2.3 Analyses and quantification	94
4.2.4 Data analysis and statistics.....	95
4.3 Results and discussion.....	95
4.3.1 Extraction yield of aromas and mass fractions of extract and raffinate streams.....	96
4.3.2 Total extraction yield of organics and organics loading	100
4.3.3 Selectivity of CO ₂ for aromas from 1-hexanol and water.....	104
5. CONCLUSIONS AND PERSPECTIVES	108
NOMENCLATURE	112
Acronyms	112
Variables and parameters	113
Greek symbols.....	114
REFERENCES	115
APPENDIXES.....	139
Appendix 1 Vapor pressures data for ethyl-2-methylbutyrate, hexanal, and <i>E</i> -2-hexenal at a pressure range of (25 to 190) kPa.....	140
Appendix 2 High-pressure VLE measurements vapor phase chromatograms.....	147
Appendix 3 Analytical reports of countercurrent supercritical fluid fractionation experiments: feed, raffinate, and extract samples.	148
Appendix 4 Interfacial Tension of aqueous apple aroma solutions surrounded by CO ₂ at elevated pressures.	164

LIST OF TABLES

Table 2.1	Edible oil components and derivatives fractionation applications, associated technology, equipment, or type of experimental set up, temperature and pressure conditions, and main objective of the work of selected references.....	9
Table 2.2	Essential oil fractionation and other deterpenation applications, associated technology, equipment, or type of experimental set up, temperature and pressure conditions, and main objective of the work of selected references.....	15
Table 2.3	Fractionation of alcoholic beverages and other aqueous mixtures applications, associated technology, equipment, or type of experimental set up, temperature and pressure conditions, and main objective of the work of selected references.	17
Table 2.4	Research lines of leading research groups and countercurrent packed columns dimensions and characteristics. Height (H), Inside diameter (ID), Operating pressures (P), Type of packing, Equipment used to compress CO ₂ , and Field of application for selected references.	20
Table 2.5	Phase equilibria. Studied system, temperature and pressure ranges, and type of equilibrium data of selected references.....	51
Table 2.6	Interfacial tension (IFT) datasets from selected references, system under study, experimental temperatures and pressures, and IFT measurement method.	60
Table 3.1	Chemical structure, aroma, occurrence, and odor threshold of some apple key odorants.	67
Table 3.2	Chemical material specifications.	70
Table 3.3	Quantification methodology of each component according to system studied, phase sampled and sampling method.	73
Table 3.4	Experimental (vapor + liquid) equilibria for the system (CO ₂ (1) + ethanol (2)). Liquid (x_i) and vapor phase (y_i) mole fractions and combined standard uncertainties (u_{comb}) at pressures (p) and at $T= 313$ K.....	77
Table 3.5	Experimental (vapor + liquid) equilibria for the system (CO ₂ (1) + ethanol (2) + water (3)). Liquid (x_i) and vapor phase (y_i) mass fractions and combined standard uncertainties (u_{comb}) at pressures (p) and at $T= 333$ K.	79
Table 3.6	Experimental (vapor + liquid) equilibria for the system (CO ₂ (1) + (<i>E</i>)-2-Hexenal (2) + water (3)). Vapor (y_i) and liquid phase (x_i) mole fractions, partition coefficients of (<i>E</i>)-2-Hexenal (k_2), and combined standard uncertainties (u_{comb}) at pressures (p) and temperatures (313, 323 and 333) K.	81

Table 3.7	Experimental (vapor + liquid) equilibria for the system (CO ₂ (1) + Hexanal (2) + water (3)). Vapor (y_i) and liquid phase (x_i) mole fractions, partition coefficients of Hexanal (k_2), and combined standard uncertainties (u_{comb}) at pressures (p) and temperatures (313, 323 and 333) K.	82
Table 4.1	Box-Behnken design and observed responses. Operational conditions of temperature (T), pressure (P), solvent-to-feed ratio (S/F), CO ₂ density (ρ_{CO_2}), mass flow rates of feed (q_F), extract (q_E) and raffinate (q_R); mass fractions of component i in extract (y_i) and raffinate (x_i) streams; selectivity of aromas (A) from 1-hexanol ($\alpha_{A,3}$) and water ($\alpha_{A,4}$); extraction yield of aromas (Y_A) and total organics (Y_{tot}), and Organics Loading (OL).....	97
Table 4.2	Analysis of variance (ANOVA) of total yield of organics (Y_{tot}) and Organics Loading (OL) models. First Order (FO), Two Factor Interaction (TFI), Pure Quadratic (PQ).	101
Table 4.3	Regression coefficient analyses for total yield model (Y_{tot}) and Organics Loading (OL) models. Coded variables X_1 temperature, X_2 pressure, and X_3 , solvent-to-feed ratio; regressed coefficients (β_0 , β_{ii} , β_{ij}); and model determination coefficient (R^2).	102
Table A4.1	Composition of aqueous solutions used in IFT measurements.....	164

LIST OF FIGURES

Figure 2.1	Modes of operation of packed columns. (A), Stripping mode; (B), Reflux mode; (C), Semi-batch mode.....	32
Figure 2.2	Immobilized phase interface in a membrane contactor.....	38
Figure 2.3	Schematic flow diagram of a mixer-settler arrangement of (k+1) stages.	42
Figure 2.4	Simplified schematic flow diagrams of high-pressure spray processes. (A), RESS; (B), PGSS; (C), Spray drying of loaded liquids; (D), CC-spray extraction; (E), Two-phase spray extraction.	46
Figure 2.5	Interfacial tensions (IFT) at various pressures (<i>P</i>) for pure Water in contact with CO ₂ . (*), Bachu & Bennion (2009) at 314 K; (○), Chiquet et al. (2007) at 308 K; (◇), Chun & Wilkinson (1995) at 311 K; (□), Dittmar, Oei, et al. (2002) at 313 K; (▽), Georgiadis, Maitland, et al. (2010) at 313 K; (△), Hebach et al. (2002) at 318 K; (×), Kvamme et al. (2007) at 318 (+), Sutjiadi-Sia et al. (2008a) at 313 K.	65
Figure 3.1	Schematic flow diagram of the experimental apparatus. (1) Equilibrium view cell, (2) Vapor phase auto-sampler (ROLSI™), (3) Liquid phase sampling valves, (4) Cold-trap, (5) Wet-test meter, (6) ROLSITM heated transfer line, (7) Gas chromatograph, (8) View cell pressure indicator, (9) View cell temperature control system, (10) CO ₂ tank, (11) Carrier gas tank, (12) Cooler, (13) Syringe pump, (14) Feed line check valve, (15) Three-way valves, (16) Vacuum pump, (17) Liquid expulsion valve, (18) Magnetic stirrer, (19) ROLSITM control unit.	72
Figure 3.2	Isothermal (vapor + liquid) equilibria for the system (CO ₂ (1) + ethanol (2)) at 313.2 K: (●) this work; (□) Meneses (2012); (○) Gutiérrez et al. (2010); (△) Secuianu et al. (2008); (◇) Tsivintzelis et al. (2004); (▽) Joung et al. (2001); (×) Chang et al. (1997); (*) Jennings et al. (1991); (+) Suzuki et al. (1990a).	76
Figure 3.3	Solvent free mass fractions of the ternary (vapor + liquid) equilibria for the system (CO ₂ (1) + ethanol (2) + water (3)) at 333.2 K and 10.1 MPa: (●) this work; (☆) Budich & Brunner (2003); (□) Lim et al. (1994); (○) Furuta et al. (1990); (△) Suzuki et al. (1990a); (◇) Furuta et al. (1989).	78
Figure 3.4	Ternary (vapor + liquid) equilibria for the system (CO ₂ (1) + ethanol (2) + water (3)) at 333.2 K and 10.1 MPa: (●) this work; (☆) Budich &	

	Brunner (2003); (\square) Lim et al. (1994); (\circ) Furuta et al. (1990); (\triangle) Suzuki et al. (1990a); (\diamond) Furuta et al. (1989).	80
Figure 3.5	Isothermal partition coefficients of (<i>E</i>)-2-hexenal (k_2) at various pressures (p). This work: (\blacksquare) 313 K; (\bullet) 323 K; (\blacktriangle) 333 K. (----) Trend line.....	83
Figure 3.6	Isothermal separation factor (a_{23}) of (<i>E</i>)-2-hexenal (2) from water (3) at various pressures (p). This work: (\blacksquare) 313 K; (\bullet) 323 K; (\blacktriangle) 333 K. (--- -) Trend line.	84
Figure 3.7	Isothermal partition coefficients of hexanal (k_2) at various pressures (p). This work: (\blacksquare) 313 K; (\bullet) 323 K; (\blacktriangle) 333 K. (----) Trend line.	85
Figure. 4.1	Schematic flow diagram of experimental apparatus. (1), packed column; (2), sapphire window; (3) and (4), upper and bottom heating mantles; (5), heating bath; (6) preheater; (7), temperature controllers; (8), backpressure regulator; (9), liquid piston pump; (10), liquid storage tank; (11), liquid mass flow meter; (12), CO ₂ piston pump; (13), CO ₂ buffer tank; (14), CO ₂ recovery cycle; (15), cooling bath; (16), CO ₂ mass flow meter; (17) and (18), cyclonic separators; (19), cold-trap; (20), needle valve; (21), flow control valve; (22), wet test-meter; (23), molecular sieve; (24), raffinate expansion tank; (25), temperature controller; (26), CO ₂ storage tank; (27), magnetic stirrer.	93
Figure 4.2	Raffinate mass fractions over time for steady state time estimation. (--- \circ ---), 1-Hexanol; (— \square —), (<i>E</i>)-2-Hexenal; (---- Δ ----), Hexanal. Open symbols represent experimental values and lines signals trends.....	94
Figure 4.3	Aroma content in Feed, Raffinate, and Extract samples of best experimental run (first line of Table 4.1). (\blacksquare), (<i>E</i>)-2-Hexenal; (\hbar) Hexanal; (\blacksquare), 1-Hexanol; (\square), Water.....	98
Figure 4.4	Super-concentrated extract, two-phase separation.	98
Figure 4.5	Aromas ((<i>E</i>)-2-Hexenal, Hexanal) extraction yield (Y_A). (--- \circ ---), 60 °C; (— \square —), 50 °C; (---- Δ ----), 40 °C. Open symbols represent experimental values and lines signals trends.	99
Figure 4.6	Response surface plot for total organics extraction yield (Y_{tot} , %) $Y_{\text{tot}} = 89.97 - 0.97X_1 + 3.39X_2 - 0.70X_3 + 1.89X_1^2 + 1.39X_3^2 - 1.23X_2X_3$. (A), effect of temperature and pressure; (B), effect of pressure and solvent-to-feed ratio; (C), effect of temperature and solvent-to-feed ratio.....	103

Figure 4.7	Response surface plot for Organics loading (OL, $\text{mg}\cdot\text{kg}^{-1}$ Org/ CO_2) $\text{OL} = 157.06 - 6.30X_2 - 81.88X_3 - 2.60X_2^2 + 32.64X_3^2$. Effect of pressure and solvent-to-feed ratio.....	104
Figure 4.8	Selectivity of apple aroma constituents (<i>E</i>)-2-Hexenal, Hexanal from 1- Hexanol ($\alpha_{A,3}=k_A/k_3$). (---○---), 60 °C; (—□—), 50 °C; (----Δ----), 40 °C. Open symbols represent experimental values and lines signals trends.....	105
Figure 4.9	Selectivity of individual aromas from water ($\alpha_{i,4}=k_i/k_4$) calculated from column experiments and (vapor + liquid) equilibria (VLE) data (Bejarano et al., 2015).(A), (<i>E</i>)-2-hexenal; (B), Hexanal; (C), 1-hexanol; (---○---), 60 °C; (—□—), 50 °C; (----Δ----), 40 °C. Open symbols represent experimental values, closed symbols experimental values from VLE, and lines signal trends.....	107
Figure A1	Vapor pressure article <i>J. Chem. Thermodyn.</i> 74 (2014) 16-21	141
Figure A4.1	Interfacial tension of aqueous aroma solutions surrounded by CO_2 at elevated pressures	164
Figure A4.2	Poster presented in the Annual ProcessNet meeting "High pressure technology" held in Merseburg, Germany 2014.....	165

PONTIFICIA UNIVERSIDAD CATOLICA DE CHILE

ESCUELA DE INGENIERIA

IMPLEMENTACIÓN DE UNA COLUMNA EMPACADA A CONTRA CORRIENTE
PARA EL FRACCIONAMIENTO DE COMPUESTOS DE SEIS CARBONOS CLAVES
PARA EL AROMA DE MANZANA USANDO CO₂ SUPERCRÍTICO

Tesis enviada a la Dirección de Investigación y Postgrado en cumplimiento parcial de los
requisitos para el grado de Doctor en Ciencias de la Ingeniería.

ARTURO BEJARANO CHAVARRO

RESUMEN

La extracción supercrítica de mezclas líquidas con CO₂ supercrítico es un proceso de fin de línea, típicamente utilizado para fraccionar materiales extraídos por métodos convencionales. Las principales aplicaciones de fraccionamiento son las mezclas de lípidos, aceites esenciales, y bebidas alcohólicas. El Fraccionamiento con Fluidos Supercríticos a Contra Corriente (FFS-CC) en columnas empacadas es un área de investigación no explorada en Chile. Por lo tanto, esta tesis entrega una revisión exhaustiva del uso del FFS-CC y de otras tecnologías menos comunes como contactadores de membrana, arreglos mezclador-decantador, y procesos de aspersión.

El FFS-CC es una tecnología alternativa para concentrar y fraccionar aromas de fruta natural ricos en agua. Un extracto de aroma súper-concentrado obtenido por FFS-CC es un producto de mayor valor agregado que los obtenidos por métodos convencionales, y por ende, el uso del FFS-CC puede ser atractivo para los concentradores de jugo de fruta.

El objetivo de este trabajo fue implementar una columna para el FFS-CC de compuestos de seis-carbonos (C-6) característicos del aroma de manzana. Para este propósito, y con el objetivo de obtener condiciones de operación razonables para el FFS-

CC, se realizaron mediciones de equilibrio (líquido + vapor) (ELV). Un nuevo aparato, armado en este trabajo, fue utilizado para medir datos experimentales de ELV de los sistemas ternarios (CO_2 + (*E*)-2-hexenal + agua) y (CO_2 + hexanal + agua). Especialmente, para (*E*)-2-hexenal se observó un muy alto factor de separación del agua ($\sim 10^4$). El valor más alto de éste, para ambos compuestos, ocurrió a una temperatura de 313 K y entre 12 a 14 MPa.

Una columna empacada de FFS-CC fue puesta en operación mediante el estudio del efecto de la temperatura, presión y la razón solvente-alimentación (*S/F*) sobre la concentración, y el fraccionamiento de los compuestos C-6 característicos del aroma de manzana de compuestos menos relevantes como 1-hexanol y agua.

Con la obtención de un extracto en dos fases claramente separables fue posible mostrar que el FFS-CC es altamente capaz de producir un extracto de aromas súper-concentrado y libre de agua. Sin embargo, el fraccionamiento de los compuestos importantes para el aroma de 1-hexanol fue muy pobre. La concentración máxima de aromas C-6 en el extracto total fue aprox. 20 %w/w, y el rendimiento de extracción de aromas fue >86%. La *S/F* tuvo el efecto más significativo en la extracción de los compuestos C-6 del aroma de manzana. Adicionalmente, los modelos de superficie de respuesta indicaron que las mejores condiciones para concentrar los compuestos C-6 del aroma de manzana son 40 °C, 14 MPa, y *S/F*= 5.

Miembros de la Comisión de Tesis Doctoral

Dr. José M. del Valle Lladser

Dr. Juan C. de la Fuente Badilla

Dr. Eduardo Agosín Trumper

Dr. José Ricardo Pérez Correa

Dr. Pedro M. Calado Simões

Dr. Cristian Vial Edwards

Santiago, Abril 2016

PONTIFICIA UNIVERSIDAD CATOLICA DE CHILE

ESCUELA DE INGENIERIA

IMPLEMENTATION OF A COUNTER CURRENT PACKED COLUMN FOR
FRACTIONATION OF KEY SIX-CARBON APPLE AROMAS USING
SUPERCRITICAL CO₂

Thesis submitted to the Office of Graduate Studies in partial fulfillment of the
requirements for the Degree of Doctor in Engineering Sciences by

ARTURO BEJARANO CHAVARRO

ABSTRACT

Supercritical fluid extraction of liquid mixtures with supercritical CO₂ is an end-of-line process that is typically used to fractionate materials extracted by conventional methods. Main fractionation applications include lipid mixtures, essential oils, and alcoholic beverages. CounterCurrent Supercritical Fluid Fractionation (CC-SFF) in packed columns is an unexplored area of research in Chile. Therefore, this thesis offers a comprehensive review on the use of CC-SFF in packed columns and less common SFF technologies for liquid mixtures such as membrane contactors, mixer-settler arrangements, and spray processes.

CC-SFF can be used as an alternative technology to concentrate and fractionate natural fruit aroma essences with large amounts of water. A super-concentrated aroma extract obtained by CC-SFF would be a product of higher added value than the actual products obtained by conventional methods, and therefore, the use of CC-SFF could be attractive to producers of concentrated fruit juices.

The objective of this work was to implement a newly acquired CC-SFF packed column for the fractionation of characteristic six-carbon (C-6) apple aromas. For this

purpose, fundamental (vapor + liquid) equilibria (VLE) measurements were carried out in order to obtain reasonable CC-SFF conditions. A new apparatus assembled in this work was utilized to measure and report new experimental VLE data for the ternary systems (CO_2 + (*E*)-2-hexenal + water) and (CO_2 + hexanal + water). Very high separation factors from water were observed ($\sim 10^4$) especially for (*E*)-2-hexenal. The highest separation factor, for both compounds, was found at a temperature of 313 K and pressures from (12 to 14) MPa.

The newly acquired CC-SFF packed column was started up by studying the effect of temperature, pressure, and solvent-to-feed ratio (*S/F*) on the concentration and fractionation of a model aqueous apple aroma solution of characteristic six-carbon (C-6) apple aromas ((*E*)-2-hexenal and hexanal) from less important compounds such as 1-hexanol and water.

Two separate phases were obtained in the extract, demonstrating that CC-SFF of aqueous apple aromas is highly capable of producing a water-free super-concentrated aroma extract. However, little fractionation of aromas from less important compounds such 1-hexanol was achieved. The highest concentration of C-6 apple aromas in the total extract was approximately 20 %w/w, and the extraction yield of aromas was >86%. The *S/F* had the most significant effect on the extraction of C-6 apple aroma compounds. Additionally, according to response surface models 40 °C, 14 MPa, and *S/F*= 5 to would be the best conditions to concentrate C-6 apple aromas.

Members of the Doctoral Thesis Committee:

Dr. José M. del Valle Lladser

Dr. Juan C. de la Fuente Badilla

Dr. Eduardo Agosín Trumper

Dr. José Ricardo Pérez Correa

Dr. Pedro M. Calado Simões

Dr. Cristian Vial Edwards

Santiago, April 2016

LIST OF PAPERS

This thesis is based on the next scientific articles:

1. Bejarano A. Simões P.C. & del Valle J.M. Fractionation technologies for liquid mixtures using dense carbon dioxide. *J. Supercrit. Fluids* 107 (2016) 321-348.
2. Bejarano A., López P.I., del Valle J.M. & de la Fuente, J.C. High-pressure (vapor + liquid) equilibria for ternary systems composed by (E)-2-Hexenal or Hexanal + Carbon Dioxide + Water: partition coefficient measurement *J Chem. Thermodyn.* 89 (2015) 79-88
3. Bejarano A., & del Valle J.M. Countercurrent fractionation of aqueous apple aroma constituents using supercritical carbon dioxide. (Accepted in the *J. Supercrit. Fluids*)

1. INTRODUCTION

Supercritical fluids are substances under temperature and pressure conditions above their respective critical values and where distinct liquid and gas phases do not exist. Supercritical Fluid Extraction (SFE) is a process that uses gases at high pressures as solvents to extract valuable materials. SFE has been studied to take advantage of the hybrid transport and solvent properties between gases and liquids of supercritical fluids. The most commonly used solvent in SFE is carbon dioxide (CO₂), mainly because it has a near-ambient critical temperature (T_c , 31.1 °C), it is innocuous, and it is completely removable from the extract and treated substrate by simple decompression. These characteristics coupled with its selectivity towards high-value compounds in biological matrices, make CO₂ an ideal solvent to extract bioactive and/or temperature-sensitive solutes for use in foods, cosmetics, and pharmaceuticals.

In contrast to SFE from solid matrices, in which the compounds of interest are directly extracted from its natural source, the SFE from liquid mixtures is considered as an end-line process, known as Supercritical Fluid Fractionation (SFF). SFF is typically used to fractionate materials extracted by conventional methods (Tabera et al., 2004), and is frequently carried out in the Counter Current mode (CC-SFF).

In general, among SFF applications, it is possible to identify two broad categories (fractionation of non-aqueous and aqueous mixtures) and three major areas of intense scientific research (triglycerides, essential oils, and alcoholic beverages). In the first category, the fractionation of edible oil components and derivatives is perhaps the furthestmost explored area followed by the deterpenation of essential oils. In the second category, the removal of ethanol and separation of the aromas from alcoholic beverages is the most studied application.

Concentration and fractionation of aroma constituents from aqueous solutions has been mainly applied to alcoholic beverages (Gamse, Rogler, & Marr, 1999; Macedo et al., 2008; Medina & Martínez, 1997; Ruiz-Rodríguez et al., 2010; Señoráns et al., 2003; Señoráns, Ruiz-Rodríguez, Ibáñez, et al., 2001; Señoráns, Ruiz-Rodríguez, Ibáñez, et al.,

2001). The recovery of aromas from other liquid mixtures such as juices or fruit essences is even more limited.

Apple juice is unique in the sense that consumers accept it both clarified and unclarified, and after orange juice, is the most sold in the US (Shaw, 1986). Chile is among the eleven top world producers of apples with almost 2% of the world production (Bravo Mina, 2011). Nearly 55% of the domestic production of apples is used to make concentrated juice with 95% being exported (Gálvez, 1996). This process is usually carried out by evaporation, and a significant amount of volatile aromas are lost. Actually, few companies in Chile recover the aroma fraction lost in the evaporation stage of the concentrated juice manufacturing process. Traditionally, fruit aromas are recovered from the concentrated juice using techniques based on distillation/evaporation or partial condensation (Belitz, Grosch, & Schieberle, 2009; Birjessön et al., 1996). CC-SFF can be used as an alternative technology to concentrate and fractionate natural fruit aroma essences with large amounts of water as described by Mukhopadhyay (2000).

CC-SFF is an unexplored field of research in Chile and a super-concentrated aroma extract obtained by CC-SFF would be a product of higher added value than the fresh fruit, concentrated juice, and aqueous essences obtained by condensation. Therefore, the use of CC-SFF could be attractive to local producers of concentrated fruit juices.

Apple aroma is a complex combination of numerous volatile compounds that contribute to the overall sensory quality of the fruit and is specific to the species and cultivar (Sanz, Olías, & Perez, 1997). Dimick et al. (1983) reviewed the apple aroma profile and reported an extensive list of over 300 volatile compounds that include alcohols, aldehydes, carboxylic esters, ketones, and ethers among others (Salas-Salazar & Olivas-Orozco, 2011). Approximately 20 compounds including C-6 aldehydes and alcohols, usually present in very low concentrations, are considered essential constituents that contribute to strong characteristics typical of apple aroma (Dixon & Hewett, 2000).

Considering that generally the most abundant constituents are not responsible for the characteristic aroma, it is necessary to separate them from which they are. Therefore, minor key apple aroma compounds (aldehydes, esters and ketones) need to be selectively

separated from volatile compounds such as water and certain alcohols. In simple terms the selective separation of key aroma constituents depends on their preference towards water, other compounds, and the solvent (CO_2). This preference is defined by the physiochemical nature of substance, and the thermodynamic principles of phase equilibria. Therefore, it is essential to conduct studies and experimental measurements of phase equilibrium-type model systems (CO_2 + water + [key odorant compound] + [non-odorant volatile compound]).

Given the limited information on the CC-SFF of nonalcoholic beverages to recover aromas, and in order to implement a methodology in Chile for the systematic study of SFF of liquid mixtures with CO_2 as solvent, it is relevant to study the operation of a pilot scale CC-SFF packed column to isolate key natural fruit aroma constituents, using representative model systems of juices or fruit essences, with known aroma profiles, *e.g.*, apple. In addition, to meet this purpose is essential to conduct studies and experimental measurements of phase equilibria for systems of the type (CO_2 + water + [key aldehyde, ester or ketone] + [key alcohols]).

1.1 Hypothesis

Through CC-SFF with CO_2 as solvent, it is possible to selectively separate key natural fruit aroma constituents.

1.2 Objectives

The main objective of this thesis is to start-up a newly acquired CC-SFF packed column and to implement a methodology to systematically study the fractionation of liquid mixtures using supercritical CO_2 as solvent.

The specific objectives of this thesis are:

1. Perform a comprehensive review of the different SFF technologies for liquid mixtures.
2. Define a model aqueous aroma solution resembling apple aroma.

3. Perform experimental high-pressure (vapor + liquid) equilibria measurements of the model solution in contact with CO₂ in order to obtain reasonable CC-SFF operation conditions.
4. Study the effect of temperature, pressure, and solvent-to-feed ratio on the selective separation of key apple aroma constituents in a pilot scale CC-SFF packed column, using CO₂ as solvent.

2. FRACTIONATION TECHNOLOGIES FOR LIQUID MIXTURES USING DENSE CARBON DIOXIDE

2.1 Introduction

Supercritical fluids are substances under temperature and pressure conditions above their respective critical values and where distinct liquid and gas phases do not exist. Supercritical Fluid Extraction (SFE) is a process that uses gases at high pressures as solvents to extract valuable materials. SFE has been studied to take advantage of the hybrid transport and solvent properties between gases and liquids of supercritical fluids. The most commonly used solvent in SFE is carbon dioxide (CO₂), mainly because it has a near-ambient critical temperature (T_c , 31.1 °C), it is innocuous, and it is completely removable from the extract and treated substrate by simple decompression. These characteristics coupled with the selectivity of CO₂ towards high-value compounds in biological matrices, make it an ideal solvent to extract bioactive and/or temperature-sensitive solutes for use in foods, cosmetics, and pharmaceuticals.

In contrast to SFE from solid matrices, in which the compounds of interest are directly extracted from its natural source, the SFE from liquid mixtures is considered as an end-of-line process, known as Supercritical Fluid Fractionation (SFF). SFF is typically used to fractionate materials extracted by conventional methods (Tabera et al., 2004), and is frequently carried out in the countercurrent mode.

Early developments of the SFF technology and its advantageous characteristics were first described in the late 1970's (Siegfried Peter & Brunner, 1978; Wilke, 1978; K. Zosel, 1978; Kurt Zosel, 1974). However, the number of applications of SFF nowadays is limited because the process has to be designed for each application, and the required know-how is not universally shared by all members of the chemical engineering community (Brunner, 2010). Continuous CounterCurrent (CC) SFF in packed columns is more commonly applied than other methods of fractionation and considerable information regarding this process is available in scientific literature.

In general, among SFF applications, it is possible to identify two broad categories (fractionation of non-aqueous and aqueous mixtures) and three major areas of

intense scientific research (lipids, essential oils, and alcoholic beverages). In the first category, the fractionation of edible oil components and derivatives is perhaps the furthestmost explored area followed by the deterpenation of essential oils. In the second category, the removal of ethanol and separation of the aromas from alcoholic beverages is the most studied application.

In non-aqueous mixtures, there is plenty of information available regarding edible oil components and derivatives (Table 2.1), specifically on fractionation and concentration of sterols, tocopherols, fatty acids, and carotenoids from pepper oleoresin (Fernández-Ronco et al., 2011), olive oils (T. Fornari et al., 2008; Ibáñez, Hurtado-Benavides, Señoráns, & Reglero, 2002; Luis et al., 2007; Simões et al., 1998; Vázquez et al., 2009), and other vegetable oils such as those of palm (Chuang & Brunner, 2006; Gast, Jungfer, Saure, & Brunner, 2005), sunflower (Vázquez et al., 2006), and soybean (Brunner, Malchow, Stürken, & Gottschau, 1991; Chang, Chang, Lee, Lin, & Yang, 2000; Fang et al., 2007; T. Fornari, Torres, Señoráns, & Reglero, 2009; Langmaack, Jaeger, & Eggers, 1996; Shi, Jin, Yu, & Zhang, 2011; Torres, Fornari, Torrelo, Señoráns, & Reglero, 2009). Another important application is the fractionation of fish oil fatty acid alkyl esters (Catchpole, Grey, & Noermark, 2000; Catchpole, von Kamp, & Grey, 1997; Catchpole & von Kamp, 1997; Catchpole, Simões, et al., 2000; Fleck, Tiegs, & Brunner, 1998; W B Nilsson, Gauglitz, Hudson, Stout, & Spinelli, 1988; William B. Nilsson, Gauglitz, & Hudson, 1989; Perretti et al., 2007; Riha & Brunner, 2000; Simões & Catchpole, 2002; Vázquez, Fornari, Señoráns, Reglero, & Torres, 2008) where the main issues that remain to be addressed are the appropriate representation of the phase behaviour for more complex or real mixtures, and the process scale-up (Rubio-Rodríguez et al., 2010). Further information on separation of fish oil constituents using supercritical fluids can be consulted in Staby & Mollerup (1993) and Sahena et al. (2009b).

A second area of intense research for non-aqueous mixtures is the deterpenation (removal of monoterpenes) from essential oils (Table 2.2). Monoterpenes hydrocarbons are associated with off-flavours and decomposition of essential oils. The most important contribution to the flavour of the essential oil comes from oxygenated compounds from which the monoterpenes hydrocarbons are partially removed. Citrus fruits essential oils

(Budich, 1999; Díaz, Espinosa, & Brignole, 2005; Gironi & Maschietti, 2008; M Kondo, Goto, Kodama, & Hirose, 2000; Reverchon, Marciano, & Poletto, 1997), and plants essential oils like lavender (Varona, Martín, Cocero, & Gamse, 2008) and oregano (Köse, Akman, & Hortaçsu, 2000; Kubat, Akman, & Hortaçsu, 2001) are the most studied systems for fractionation in countercurrent and semi-batch packed columns.

The third area of active research, in the aqueous mixture category, is the dealcoholization of alcoholic beverages (Table 2.3) and, to a more limited extent, the recovery of their aromas (Gamse et al., 1999; Macedo et al., 2008; Medina & Martínez, 1997; Ruiz-Rodríguez et al., 2010; Señoráns et al., 2003; Señoráns, Ruiz-Rodríguez, Ibáñez, et al., 2001). The recovery of aromas from other liquid mixtures as juices is even more limited (Señoráns, Ruiz-Rodríguez, et al., 2001; Simó et al., 2002). Tables 2.1–2.3 list the type of technology used, the operational conditions under study, and the objective of the work in an extensive compilation of references. For more detailed and comprehensive information regarding continuous countercurrent packed columns, their applications, and process design please refer to the reviews of G. Brunner (2009, 1998b, 2005).

This work reviews less common technologies than CC-SFF in packed columns, and their applications for fractionation of liquid mixtures using dense CO₂ or SuperCritical CO₂ (SC-CO₂). The technologies examined in this review are membrane contactors, devices based on the mixer settler principle, and spray processes. Aspects of the use of static mixers and nozzles are also briefly included. However, because of the importance of CC-SFF, this contribution includes a description of fundamental engineering topics of packed columns, their different modes of operation, and available equipment and installations in leading research groups around the world. This work also covers subjects transversal to all technologies such as phase equilibrium and relevant physicochemical properties like diffusivity, density, and surface tension.

Table 2.1 Edible oil components and derivatives fractionation applications, associated technology, equipment, or type of experimental set up, temperature and pressure conditions, and main objective of the work of selected references.

Technology / Equipment / Experimental set up	Extraction Temperature / K	Extraction Pressure / MPa	Objective	Reference
Countercurrent packed column	343	13.0–25.0	Enrich tocopherols from oil deodorizer distillates. Favourable conditions for separation. Phase equilibrium measurement and separation behaviour.	(Brunner et al., 1991)
Column-mixer-settler: pump and cyclone between stripping and enrichment sections.	323–343	17.0–20.0	Fractionate a (α -tocopherol + α -tocopherol acetate) mixture. Improve the longitudinal mixing of the column and wetting of the packing.	(Schaffner & Trepp, 1995)
Countercurrent packed column	323–353	13.0–25.0	Refine vegetables oils. Describe and predict fluid dynamics and mass transfer. Obtain a high concentration of tocopherols and sterols in the extract.	(Langmaack et al., 1996)
Countercurrent packed column	323; 333	10.7–27.4	Fractionate crude and refined palm oil by CC-SFF with SC-CO ₂ . Effect of pressure, temperature, and co-solvent on free fatty acids and carotenes content of extract and raffinate.	(Ooi et al., 1996)
Countercurrent packed column	323–353	13.0–25.0	Fractionate glyceride mixtures. Investigate the effects of process parameters in the separation efficiencies and yields of mono, di and tri-acylglycerols.	(Sahle-Demessie, 1997b)
Countercurrent packed column	353; 359	26.0–31.0	Deacidify olive oil. Study the technical feasibility for deacidification of olive oil.	(Simões et al., 1998)
Countercurrent packed column	313–363	13.6–25.0	Deacidify crude rice bran oil. Study the effect of isothermal and temperature gradient operation of the column on the composition of rice bran oil.	(Dunford & King, 2001)

Table 2.1 cont'd Edible oil components and derivatives fractionation applications, associated technology, equipment, or type of experimental set up, temperature and pressure conditions, and main objective of the work of selected references.

Technology / Equipment / Experimental set up	Extraction Temperature / K	Extraction Pressure / MPa	Objective	Reference
Countercurrent packed column	318–353	13.8–27.5	Phytosterol ester fortification in rice bran oil. Isothermal CC-SFF of rice bran oil for enrichment of oryzanol and phytosterol fatty acid esters.	(Dunford, Teel, & King, 2003)
Semi-batch screening unit	343; 353; 363	20.0; 20,5; 30.0	Deacidify rice bran oil. Study of pressure and CO ₂ consumption on free fatty acids removal, and triglycerides retention.	(Chen et al., 2008)
Countercurrent packed column	313	11.5	Fractionate edible oil mixtures. Separate squalene and methyl oleate from deodorizer distillates. Hydrodynamics and mass transfer behaviour.	(Ruivo, Cebola, Simões, & Nunes da Ponte, 2001)
Countercurrent packed column	313	20	Separate sterols and tocopherols from olive oil. Evaluate the efficiency of different random packing materials on the selectivity of sterols and tocopherols.	(Ibáñez et al., 2002)
Countercurrent packed column	308–323	7.5–20.0	Fractionate a raw extract of olive leaves in hexane. Separate waxes, hydrocarbons, squalene, β -carotene, triglycerides, α -tocopherol, β -sitosterol, and alcohols. Process parameter influence on selectivity	(Tabera et al., 2004)
Countercurrent packed column	340; 370	20.0–30.0	Purify tocochromanols from edible oil. Enrich of vitamin E from crude palm oil and a soy oil deodorizer distillate. Phase equilibrium measurements theoretical description of the separation.	(Gast et al., 2005)
Five stage mixer-settler (pump-cyclone) device	333	14.0	Enrich minor constituents from crude palm oil. Enrich carotenoids and tocochromanols, in a pilot-scale mixer-settler apparatus.	(Chuang & Brunner, 2006)
Countercurrent packed column	338	15.0–23.0	Fractionate sunflower oil deodorizer distillates. Influence of the feed composition in the extraction process. Analysis of the tocopherol and phytosterol yields and enrichment factors obtained.	(Vázquez et al., 2006)

Table 2.1 cont'd Edible oil components and derivatives fractionation applications, associated technology, equipment, or type of experimental set up, temperature and pressure conditions, and main objective of the work of selected references.

Technology / Equipment / Experimental set up	Extraction Temperature / K	Extraction Pressure / MPa	Objective	Reference
Mixer-settler (static mixer-gravimetric phase separator).	313–343	11.0–24.0	Selective fractionation of squalene from methyl oleate. Hydrodynamics and mass transfer study of a Kenics-type static mixer. Pressure drop and overall mass transfer coefficient calculations.	(Ruivo, Paiva, & Simões, 2006)
Countercurrent packed column	343	15.0–23.0	Recover squalene from olive oil deodorizer distillates. Simulate the separation process and find optimal process conditions with the GC EoS.	(Luis et al., 2007)
Countercurrent packed column	318–328	20.0–28.0	Separate phytosterol esters from soybean oil deodorizer distillates. Study the CC-SFF of an enzymatically modified soybean oil deodorizer distillate for concentration of phytosterol esters.	(Torres, Fornari, et al., 2009)
Countercurrent packed column	298	8.3	Purify 1,2-diacylglycerols from vegetable oils. Compare molecular distillation and CC-SFF in terms of the removal of the fatty acid propyl ester by-products while reducing the migration of the 1,2-diacylglycerols to 1,3-diacylglycerols.	(Compton, Laszlo, Eller, & Taylor, 2008)
Countercurrent packed column	296–298	11.0	Purify a model crude reaction mixture from the enzymatic synthesis of SoyScreen TM . Use of liquid CO ₂ for the fractionation of a model mixture of ethylferrulate, fatty acid ethyl esters and, soybean oil triacylglycerides. Study the effect of column length and S/F ratio.	(Eller, Taylor, Compton, Laszlo, & Palmquist, 2008)
Countercurrent packed column	313	18.0; 234; 250	Recover squalene, tocopherols and phytosterols from oil deodorizer distillates. Use of GC EoS to simulate the separation process, phase equilibrium, and find optimal process conditions.	(T. Fornari et al., 2008)
Membrane module apparatus (small flat sheet membrane test cell)	313	18.0	Fractionate squalene from oleic acid. Compare membrane performance to separate squalene from a model mixture. Feasibility of coupling membrane separation with SC-CO ₂ extraction.	(Ruivo, Couto, & Simões, 2008)

Table 2.1 cont'd Edible oil components and derivatives fractionation applications, associated technology, equipment, or type of experimental set up, temperature and pressure conditions, and main objective of the work of selected references.

Technology / Equipment / Experimental set up	Extraction Temperature / K	Extraction Pressure / MPa	Objective	Reference
Countercurrent packed column	313	18.0; 234; 250	Deacidify olive oil. Use of GC EoS to simulate the separation process, representing the oil as a simple pseudo-binary oleic acid + triolein mixture.	(Vázquez et al., 2009)
Countercurrent packed column	298	8.3	Fractionate of partially deacylated sunflower oil. Remove by-product fatty acid propyl esters of partial deacylated sunflower oil using liquid CO ₂ . Study the effect of S/F ratio to optimize separation.	(Eller, Taylor, Laszlo, Compton, & Teel, 2009)
Semi-batch screening unit / Countercurrent packed column	298; 313; 353	14.7; 19.6; 24.5	Fractionate triglycerides from the unwanted polar fraction present in used frying oil using liquid and supercritical ethane and CO ₂ .	(Rincón et al., 2011)
Countercurrent packed column	298	8.62	Purify 2-monoacylglycerols. Use of liquid CO ₂ to remove fatty acid ethyl esters and diacylglycerols from 2-monoacylglycerols from the enzymatic alcoholysis of triolein with ethanol.	(Compton, Eller, Laszlo, & Evans, 2012)
Two phase flow spray column	373	75	Present new device of deoiling of soy lecithin based on jet extraction wit SC-CO ₂ . Viscosity and surface tension determination.	(Eggers, Wagner, & Wag, 1993)
Two phase flow spray column	373; 393; 413	48.0; 60.0; 70.0	Deoil lecithin and extraction of liposomes. Mathematical modelling and optimization of mixing and extraction zones. Measurement of viscosity and surface tension.	(Eggers, Wagner, & Schneider, 1999a; H. Wagner & Eggers, 1996)
Countercurrent packed column	298	9.3	Remove hexane from soybean oil. Investigate the use of liquid CO ₂ in place of SC-CO ₂ to remove hexane from soybean oil.	(Eller, Taylor, & Curren, 2004)
Countercurrent packed column	313	24.1	Fractionate anhydrous milk fat. Study the mass transfer rates for low, medium, and high -melting triglycerides of anhydrous milk fat.	(Bhaskar, Rizvi, & Harriott, 1993)

Table 2.1 cont'd Edible oil components and derivatives fractionation applications, associated technology, equipment, or type of experimental set up, temperature and pressure conditions, and main objective of the work of selected references.

Technology / Equipment / Experimental set up	Extraction Temperature / K	Extraction Pressure / MPa	Objective	Reference
Countercurrent packed column	313–348	3.4–24.1	Fractionate anhydrous milk fat. Determinate physicochemical properties of anhydrous milk fat. Observe the effects of operating conditions on fatty acids, triglycerides and cholesterol distribution in anhydrous milk fat and its fractions.	(Bhaskar, Rizvi, & Sherbon, 1993)
Countercurrent packed column	313–348	3.4–24.1	Fractionate anhydrous milk fat. Pilot-scale fractionation of anhydrous milk fat. Studies for scale-up of larger plants. Compare physicochemical properties obtained by different methods.	(Rizvi & Bhaskar, 1995)
Countercurrent packed column	313	24.1	Fractionate anhydrous milk fat. Develop a mathematical model for continuous extraction of multicomponent mixture anhydrous milk fat.	(Yu, Bhaskar, & Rizvi, 1995)
Countercurrent packed column	323–333	2.4–24.1	Fractionate anhydrous milk fat. Study the conjugated linoleic acid, and carotenes content of various fractions from milk fat, obtained in cascade separators.	(Romero, Rizvi, Kelly, & Bauman, 2000)
Countercurrent packed column	321; 333	8.9–18.6	Fractionate fatty acid ethyl esters from butter oil. Obtain highly concentrated fractions of short- and long- chain fatty acids for use as starting material for the production of highly valuable functional lipids for nutritional applications.	(Torres, Torrelo, Señoráns, & Reglero, 2009)
Countercurrent packed column	333–353	14.5–19.5	Fractionate fatty acid ethyl esters from fish oil. Study the influence of the size of the column on separation efficiency and yield.	(Fleck et al., 1998)
Countercurrent packed column	323–353	13.0–25.0	Fractionate acid ethyl esters from fish oil. Separate between low-molecular-weight components (C14 to C18) and (C20 and C22).	(Riha & Brunner, 2000)

Table 2.1 cont'd Edible oil components and derivatives fractionation applications, associated technology, equipment, or type of experimental set up, temperature and pressure conditions, and main objective of the work of selected references.

Technology / Equipment / Experimental set up	Extraction Temperature / K	Extraction Pressure / MPa	Objective	Reference
Static mixer and packed column.	333	25.0	Squalene recovery from shark liver oil and olive oil deodorizer distillate. Compare the performance of a static mixer and countercurrent packed column for the fractionation of shark liver oil.	(Catchpole, Grey, et al., 2000; Catchpole, Simões, et al., 2000)
Countercurrent packed column	333–353	6.0	Fractionate deep-sea shark liver oil. Study the effects of temperature, S/F, and squalene separation from oleic acid in model mixtures and two shark liver oils using R134a as solvent.	(Simões & Catchpole, 2002)
Countercurrent packed column	313; 323; 338	14.0–18.0	Fractionate non esterified alkoxyglycerols obtained from shark liver oil	(Vazquez et al., 2008)
Countercurrent packed column	363; 353–368	2.9	Determine the best processing conditions to fractionate used lubricant oil for the formulation of new lubricants by means of SFF with supercritical ethane.	(Rincón, Cañizares, & García, 2007)

Table 2.2 Essential oil fractionation and other deterpenation applications, associated technology, equipment, or type of experimental set up, temperature and pressure conditions, and main objective of the work of selected references.

Technology / Equipment / Experimental set up	Extraction Temperature / K	Extraction Pressure / MPa	Objective	Reference
Countercurrent packed column	313; 318	7.7–9.0	Separate a mixture of (δ -limonene and 1,8-cineole) SFF. Mass transfer study and feasibility of application to the purification of eucalyptus oil.	(Simões, Matos, Carmelo, Gomes de Azevedo, & Nunes da Ponte, 1995)
Semi-continuous packed column	313; 333; 313–333	8.8–11.8	Citrus oil deterpenation. Study the effect of an internal reflux induced by a temperature gradient on the separation behaviour of a model mixture of linalool, limonene and citral. Compare with isothermal operation.	(Sato, Goto, & Hirose, 1995)
Semi-continuous packed column	313; 313–343	8.8	Citrus oil deterpenation. Study the selectivity of terpenes vs. oxygenated terpenes (limonene vs. linalool) at isothermal and temperature gradient conditions.	(Sato, Goto, & Hirose, 1996)
Semi-continuous packed column	333	8.8; 9.8	Orange oil deterpenation. Observe the effects of pressure and (S/F) ratio on the separation selectivity for a model mixture (limonene + linalool) and raw orange oil.	(Goto, Sato, Kodama, & Hirose, 1997)
Semi-continuous packed column	313; 313–333	8.8	Citrus oil deterpenation. Study of limiting operation conditions. Study the effect of reflux on separation selectivity. Total reflux and with internal and external reflux.	(Sato, Kondo, Goto, Kodama, & Hirose, 1998)
Semi-continuous packed column	313–353	7.8–10.8	Bergamot oil deterpenation. Phase equilibrium measurement and fractionation by semi-batch operation. Internal reflux fractionation by temperature gradient. Study the effect of temperature profile, S/F ratio on composition of extracts.	(M Kondo et al., 2000)
Semi-continuous packed column	313; 333; 353; 313–373	8.8–34.3	Bergamot oil deterpenation. Study the effects of feed composition, feed inlet position, reflux ratio, and stage number on extraction ratio of limonene, separation, selectivity, and recovery of linalyl acetate. Isothermal and temperature gradient operation.	(Mitsuru Kondo, Goto, Kodama, & Hirose, 2002)

Table 2.2 cont'd Essential oil fractionation and other deterpenation applications, associated technology, equipment, or type of experimental set up, temperature and pressure conditions, and main objective of the work of selected references.

Technology / Equipment / Experimental set up	Extraction Temperature / K	Extraction Pressure / MPa	Objective	Reference
Countercurrent packed column	323–343	8.0–13.0	Orange peel oil deterpenation. Phase equilibrium measurements and limit of separation and flooding-point calculations.	(Budich, Heilig, Wesse, Leibkuchler, & Brunner, 1999)
Screening unit	313–326	8.1–9.5	Citrus essential oil deterpenation. Simulate extraction process with PR-EoS for a model mixture of limonene and citral. Compare experiments with simulation results, and assess the model prediction capability.	(Jaubert, Gonçalves, & Barth, 2000)
Semi-continuous packed column	313; 313–343	8.8	Lemon oil deterpenation. Compare with countercurrent continuous contacting.	(Mitsuru Kondo, Akgun, Goto, Kodama, & Hirose, 2002)
Countercurrent packed column	313; 323; 333	7.5; 9; 11	Fractionate Lavandin essential oil. Experiment and modelling of the separation of linalool and linalyl acetate. Study of the influence of process parameters and optimum conditions for the process.	(Varona et al., 2008)
Semi-continuous packed column	313–373	8.8–20.0	Yuzu oil deterpenation. Study the effect of temperature, and pressure on the extraction yield, extract composition, and recovery factor of aroma components of Yuzu cold pressed oil.	(Terada et al., 2010)
Semi-batch screening unit	313–323	6.0–12.0	Fractionation of essential oils with biocidal activity. Equilibrium distribution and selectivity of monoterpenes, oxygenated terpenes and sesquiterpenes of <i>Salvia officinalis</i> , <i>Mentha piperita</i> and <i>Tagetes minuta</i> oil.	(Gañán & Brignole, 2011)

Table 2.3 Fractionation of alcoholic beverages and other aqueous mixtures applications, associated technology, equipment, or type of experimental set up, temperature and pressure conditions, and main objective of the work of selected references.

Technology / Equipment / Experimental set up	Extraction Temperature / K	Extraction Pressure / MPa	Objective	Reference
Semi-continuous column	298	6.3	Fractionate volatile compounds from fruit essences. Extraction experiments to obtain highly concentrated fruit aroma using liquid CO ₂ .	(T. H. Schultz et al., 1967; W. G. Schultz & Randall, 1970; W. G. Schultz, Schultz, Carston, & Hudson, 1974)
Mixer-settler (static mixer-gravimetric phase separator).	333–353	28	Regenerate caffeine-loaded CO ₂ . Investigate the performance of the mixer–settler principle in application with a Kenics-type static mixer	(Pietsch & Eggers, 1999)
Countercurrent packed column	313	16.0	Extract antioxidants from orange juice. Study the effect of the solvent-to-feed ratio (S/F) on the content of antioxidant compounds.	(Señoráns, Ruiz-Rodríguez, et al., 2001)
Countercurrent packed column	313	16.0	Extract antioxidants from orange juice. Analysis of antioxidants from orange juice obtained by CC-SFF with micellar electro-kinetic chromatography (MEKC) technique.	(Simó et al., 2002)
Countercurrent packed column	303–353	7.0–30.0	Fractionate alcoholic beverages. Optimization of process variables (extraction temperature and pressure, and liquid feed flow) for isolation of brandy aroma.	(Señoráns, Ruiz-Rodríguez, Ibáñez, et al., 2001)
Countercurrent packed column	313	20.0	Fractionate alcoholic beverages. Optimize the separation conditions for fractionation of spirits.	(Señoráns, Ruiz-Rodríguez, Ibáñez, et al., 2001)
Countercurrent packed column	313	10.0; 20.0; 30.0	Fractionate alcoholic beverages. Selective extract aromatic components of brandy flavour. Study the effect of flow, temperature and extraction pressure on flavour quality.	(Señoráns et al., 2003)
Countercurrent packed column	313	10.9–18.0	Fractionate alcoholic beverages. Recover wine must aroma. Study the influence of process parameters (S/F and density) on the aromatic fraction of <i>Muscatel</i> wine, and <i>Muscatel</i> must wine.	(Macedo et al., 2008)
Countercurrent packed column	308	9.5; 13.0; 18.0	Fractionate alcoholic beverages. Use of GC-EoS model to simulate the dealcoholization of red and white wines.	(Ruiz-Rodríguez et al., 2010)

Table 2.3 cont'd Fractionation of alcoholic beverages and other aqueous mixtures applications, associated technology, equipment, or type of experimental set up, temperature and pressure conditions, and main objective of the work of selected references.

Technology / Equipment / Experimental set up	Extraction Temperature / K	Extraction Pressure / MPa	Objective	Reference
Single hollow fiber membrane contactor	298	6.9; 6.9; 3.45	Extraction of fermentation products (acetone and ethanol). Study of the feasibility of extracting aqueous ethanol and acetone with dense CO ₂ .	(Bothun et al., 2003)
Hollow fiber contactor	298	6.9; 3.45	Extract organic solvents and sulphur aroma compounds from aqueous solutions. Modelling extraction, in series mass transfer resistance theory.	(Bocquet, Torres, Sanchez, Rios, & Romero, 2005)
Three module hollow fiber membrane contactor	294–298	9.0–27.6	Extract isopropanol or acetone from water. Experimental results and mathematical modelling, validation with data of extraction of caffeine, ethanol, dimethyl formamide.	(Gabelman & Hwang, 2005)
Three module hollow fiber membrane contactor	294–298	9.0–27.6	Extract isopropanol or acetone from water. Experimental results and mathematical model development. Validate experimental results with dimensionless numbers.	(Gabelman, Hwang, & Krantz, 2005)
Two module hollow fiber membrane contactor	305	13.5	Extract of acetone from water. Study mass transfer as function of membrane geometry and operating parameters.	(Gabelman & Hwang, 2006)
Single and three module hollow fiber contactor	296–298	3.45; 9.6; 20.7;	Extract acetone or caffeine from water. Simulate membrane characteristics and operating parameters.	(Bocquet, Romero, Sanchez, & Rios, 2007)

2.2 Continuous CC-SFF fundamentals, research groups, and applications

This section includes a description of fundamental engineering topics regarding CC-SFF, specifically how mass transfer and other column operational issues as pressure drop and flooding points are approached in the literature. Even though CC-SFF has been extensively reviewed in the past, this work contributes with a detailed list (Table 2.4) of packed column facilities in leading research institutions and companies around the world. Additionally, this section includes a description of different modes of operation of packed columns. Table 2.4 contains dimensions, operating pressures, column packing, type of equipment used to compress CO₂, and research areas of the leading institutions.

2.2.1 Fundamentals

Basically, CC-SFF is a mass transfer operation that can be considered as a stripping process, and is usually developed in a packed column. In an ordinary stripping process, the liquid-gas contact in a packed column is continuous and non-staged, unlike in plate or other types of columns. The solute of interest is transferred from a descending liquid stream to an ascending dense gas stream. In the particular case of CC-SFF, due the liquid-like density of the dense gas, its velocity through the packing conduits can be about 100 times lower (around $\text{cm}\cdot\text{s}^{-1}$ instead of $\text{m}\cdot\text{s}^{-1}$) than in distillation (De Haan & De Graauw, 1991). In order to achieve the separation it is essential that operational conditions warrant the presence of a two-phase region inside the column. Therefore, phase equilibrium, interfacial tension, and differences in density between phases, are of great importance to ensure the partial immiscibility and separation of the contacting streams.

Table 2.4 Research lines of leading research groups and countercurrent packed columns dimensions and characteristics. Height (H), Inside diameter (ID), Operating pressures (P), Type of packing, Equipment used to compress CO₂, and Field of application for selected references.

Research group	Column dimensions and characteristics							References
	H / m	ID / mm	P / MPa	Column packing	Equipment used to compress CO ₂	Mode of operation	Field of Application	
TUHH	3.0	17.5	6.5–50.0	Sulzer Mellapak 500.X® (ε: 0.975 <i>a</i> : 500 m ⁻¹); Sulzer EX; Sulzer EX-Laboratory; Sulzer BX (ε: 0.97 <i>a</i> : 492 m ⁻¹); 6 mm random wire mesh (ε: 0.9 <i>a</i> : 820 m ⁻¹); 3 x 3 mm SS spirals - Teflon rings for liquid distribution; Shott Durapak (ε: 0.7 <i>a</i> : 280 m ⁻¹).	Pump / Compressor.	Continuous reflux mode / middle liquid feed / partial extract reflux.	Edible oil components and derivatives / deterpenation of essential oils / dealcoholization of alcoholic beverages.	(Brunner & Machado, 2012; Brunner et al., 1991; Budich & Brunner, 2003; Budich et al., 1999; Danielski et al., 2008; Danielski, Zetzl, Hense, & Brunner, 2005; Gast et al., 2005; Langmaack et al., 1996; Riha & Brunner, 2000).
	4.0 [†]	17.5 25.0 [†]						
	6.0	17.5						
	7.0	17.5						
	7.5	40.0						
	12.0	68.0						
CIAL-UAM-CSIC	1.5	30.0	15.0–30.0	3 mm Raschig rings (ε: 0.46), Fenske rings (ε: 0.76), Dixon rings (ε: 0.83), Glass beads (ε: 0.39), 2 mm and 5 mm (i.d) 316 SS balls.	Pump.	Continuous stripping mode / no reflux / upper, middle and bottom liquid feed.	Edible oil components and derivatives / deterpenation of essential oils / aroma of alcoholic beverages and dealcoholization.	(Hurtado-Benavides, Señoráns, Ibáñez, & Reglero, 2004; Ibáñez et al., 2002; Luis et al., 2007; Ruiz-Rodríguez et al., 2012; Señoráns et al., 2003; Señoráns, Ruiz-Rodríguez, Ibáñez, et al., 2001; Torres, Torrelo, et al., 2009; Vazquez et al., 2008; Vázquez et al., 2009).
	1.0 [†]	10.0						
	3.0 [†]	17.6						
	2.8 [†]	29.7						
	4.0 [†]	40.0						
LAQV-REQUIMTE	1.0	24.0	7.7–18.0	24 mm Sulzer EX (ε: 0.86 <i>a</i> : 1,710 m ⁻¹); 24 mm Sulzer CY (ε: 0.90 <i>a</i> : 890 m ⁻¹).	High-pressure membrane pump / Gas compressor.	Continuous stripping mode / partial extract reflux with upper liquid feed.	Edible oil components and derivatives / dealcoholization of alcoholic beverages.	(Fernandes, Ruivo, & Simões, 2007; Macedo et al., 2008; Ruivo, Cebola, Simões, & Nunes da Ponte, 2002; Simões et al., 1995).
	2.5 [†]	24.0						
	4.0 [†]	40.0						

Table 2.4 cont'd Research lines of leading research groups and countercurrent packed columns dimensions and characteristics. Height (H), Inside diameter (ID), Operating pressures (P), Type of packing, Equipment used to compress CO₂, and Field of application for selected references.

Research group	Column dimensions and characteristics							References
	H / m	ID / mm	P / MPa	Column packing	Equipment used to compress CO ₂	Mode of operation	Field of Application	
Northern USDA	0.6	17.5	8.3–35.0	4 mm Pro-Pak protruded metal (ϵ : 0.94).	Gas booster pump.	Continuous stripping mode / no reflux / upper, middle, and bottom liquid feed / temperature gradient (internal reflux).	Edible oil components and derivatives.	(Dunford et al., 2003; Eller et al., 2008; Eller, Taylor, & Palmquist, 2007; Sahle-Demessie, 1997a, 1997b).
	1.2	17.5						
	1.7	14.3 44.5						
	1.8	102 (O.D)						
	2.5	14.3						
Kumamoto Univ.	1.0	9.0	7.8–11.8	2 mm and 3 mm Dixon packing	High-pressure pump	Semi-batch mode / linear temperature gradient (internal reflux).	Deterpenation of essential oils / Edible oil components and derivatives.	(Fang et al., 2007; Goto et al., 1997; Sato et al., 1995; Terada et al., 2010).
	2.4	20.0						
Cornell Univ.	0.6	17.5	2.4–24.1	SS 304 Goodloe knitted mesh (ϵ : 0.95 α : 1,920 m ⁻¹).	High-pressure positive-displacement pump.	Continuous Stripping mode.	Edible oil components and derivatives.	(Bhaskar, Rizvi, & Harriott, 1993; Ooi et al., 1996).
	1.8	49.0						
Industrial Research Limited	1.2	24.3	6.0–30.0	SS wire wool; 6 mm and 8.5 mm glass Raschig rings; 4 mm glass Fenske helices.	High-pressure compressor / Triplex diaphragm pump.	Continuous stripping mode and reflux mode / upper and middle liquid feed.	Edible oil components and derivatives.	(Catchpole, Grey, et al., 2000; Catchpole et al., 1997; Catchpole & von Kamp, 1997; Catchpole, Simões, et al., 2000; Simões & Catchpole, 2002).
	1.9	20.3						
	2.5	56.0						

Table 2.4 cont'd Research lines of leading research groups and countercurrent packed columns dimensions and characteristics. Height (H), Inside diameter (ID), Operating pressures (*P*), Type of packing, Equipment used to compress CO₂, and Field of application for selected references.

Research group	Column dimensions and characteristics							References
	H / m	ID / mm	<i>P</i> / MPa	Column packing	Equipment used to compress CO ₂	Mode of operation	Field of Application	
University of Stellenbosch	4.3	29.0	8.7–30.0	Sulzer DX.	Positive displacement pump / compressor.	Continuous stripping and reflux mode / upper, middle, and bottom liquid feed.	Oligomer (C16 to C24), and (C10 to C16) alkanes and alcohols fractionation. Fractionation of wax derivatives using supercritical propane and ethane	(Bonthuys, Schwarz, Burger, & Knoetze, 2011; Nieuwoudt, Crause, & du Rand, 2002; C. E. Schwarz et al., 2011; Cara E Schwarz, Nieuwoudt, & Knoetze, 2010).
Univ. degli Studi di Roma “La Sapienza”	1.9	20.0	84.0–10.5	Sulzer EX.	Volumetric compressor.	Semi-batch mode.	Deterpenation of lemon peel oil.	(Gironi & Maschietti, 2005, 2008).
Univ. of Technology Graz	2.0	35.4	7.5–18.0	10x10x0.3 mm ³ Pall® Raschig rings; Sulzer DX.	High-pressure diaphragm pump.	Continuous stripping and Semi-batch mode / no reflux.	Deterpenation of essential oils / dealcoholization of alcoholic beverages, removal of organic solvents from aqueous mixtures.	(Gamse et al., 1999; Varona et al., 2008).

Table 2.4 cont'd Research lines of leading research groups and countercurrent packed columns dimensions and characteristics. Height (H), Inside diameter (ID), Operating pressures (*P*), Type of packing, Equipment used to compress CO₂, and Field of application for selected references.

Research group	Column dimensions and characteristics							References
	H / m	ID / mm	<i>P</i> / MPa	Column packing	Equipment used to compress CO ₂	Mode of operation	Field of Application	
Lund Univ.	1.1	25.0	15.0; 20.0	SS Sulzer; 6x6 mm Raschig rings	High-pressure diaphragm pump.	Continuous stripping mode / no reflux.	Removal of phenolic compounds from aqueous mixtures. Removal of dioxins from fish oil.	(Jakobsson, Sivik, Bergqvist, Strandberg, & Rappe, 1994; Persson, Barisic, Cohen, Thörneby, & Gorton, 2002).
	1.0	14.0	15					
NOAA's National Marine Fisheries Service	1.8	17.5	11.0–17.2	9 mm 304 SS ball bearings and 4 mm 316 SS Propak.	Diaphragm compressor	Semi-batch mode.	Edible oil components and derivatives	(W B Nilsson et al., 1988; William B. Nilsson et al., 1989).
Univ. of Texas at Austin	1.2	25.4	8.2–15.2	Sieve trays; 12.7 mm ceramic Raschig rings; 6.4 mm ceramic Raschig rings (a : 722 m ⁻¹); Intalox saddles N° 15.	Positive displacement pump.	Continuous stripping mode.	Mass-transfer performance of spray, tray, and packed columns to extract ethanol and isopropanol from water.	(Lahiere & Fair, 1987; Seibert & Moosberg, 1988).
	2.2	98.8						
Univ. di Salerno	1.9	17.5	70.0	5 mm Steel berl (ϵ : 0.9 a : 1600 m ⁻¹); 5 mm Raschig rings (ϵ : 0.66 a : 1050 m ⁻¹).	High-pressure diaphragm pump.	Continuous reflux mode / upper, middle, and bottom liquid feed.	Edible oil components and derivatives / Deterpenation of essential oils.	(Osséo, Caputo, Gracia, & Reverchon, 2004; Reverchon, 1997).
Bogazici Univ.	1.5	9.0	7.0; 8.5	1.5 mm Dixon wire mesh (ϵ : 0.8); 5 mm glass beads.	Diaphragm pump.	Semi-batch mode.	Deterpenation of essential oils.	(Köse et al., 2000; Kubat et al., 2001).

Table 2.4 cont'd Research lines of leading research groups and countercurrent packed columns dimensions and characteristics. Height (H), Inside diameter (ID), Operating pressures (*P*), Type of packing, Equipment used to compress CO₂, and Field of application for selected references.

Research group	Column dimensions and characteristics							References
	H / m	ID / mm	<i>P</i> / MPa	Column packing	Equipment used to compress CO ₂	Mode of operation	Field of Application	
Clemson Univ.	2.0	18.0	3.5–8.4	4 mm Pro-Pak protruded metal.	Two-piston reciprocating pump.	Continuous stripping and Semi-batch mode / reflux finger.	Fractionation of petroleum pitches.	(Edwards & Thies, 2006).
Delft Univ. of Technology	1.0	35.0	10.0–20.0	Sulzer BX Gauze Packing (ϵ : 0.90 <i>a</i> : 890 m ⁻¹); 5-mm metal Raschig ring.	Membrane pump.	Continuous stripping mode / no reflux.	Hydrocarbon processing / Flavours from milk fat.	(De Haan & de Graauw, 1990).
Univ. de Castilla-La Mancha	1.7	20.0	2.9–24.5	3 mm Pall® Raschig rings (ϵ : 0.46 <i>a</i> : 1185 m ⁻¹); 3 mm irregular steel packing (ϵ : 0.85 <i>a</i> : 195 m ⁻¹).	Membrane pump.	Continuous stripping mode / Semi-batch mode.	Edible oil components and derivatives using SC-CO ₂ and ethane	(Rincón et al., 2011, 2007).
Univ. of Birmingham	1.5	11.5	10.0–20.0	Glass beads	Piston pump	Continuous stripping mode isothermal and with temperature gradient (internal reflux).	Edible oil components and derivatives.	(Al-darmaki et al., 2012).
Beijing Univ. of Chemical Technology	3.3	25.0	20	3.2 mm θ ring (ϵ : 0.93 <i>a</i> : 2400 m ⁻¹); 2 mm triangle (ϵ : 0.84 <i>a</i> : 2700 m ⁻¹)	Diaphragm compressor.	Continuous stripping mode / Middle liquid feed with temperature gradient (internal reflux).	Edible oil components and derivatives.	(Shi et al., 2011).

Table 2.4 cont'd Research lines of leading research groups and countercurrent packed columns dimensions and characteristics. Height (H), Inside diameter (ID), Operating pressures (P), Type of packing, Equipment used to compress CO₂, and Field of application for selected references.

Research group	Column dimensions and characteristics							References
	H / m	ID / mm	P / MPa	Column packing	Equipment used to compress CO ₂	Mode of operation	Field of Application	
Ehime Univ.	1.0	12.7 (O.D)	15.0–30.0	3.0 mm Dixon.	High-pressure pump.	Continuous stripping mode	Edible oil components and derivatives.	(Kawashima, Watanabe, Iwakiri, & Honda, 2009).
Institut National Polytechnique de Lorraine	0.4	23.0	8.0–9.5	5 mm glass beads	High-pressure pump.	Semi-batch mode.	Deterpenation of essential oils.	(Jaubert et al., 2000).
Isfahan Univ. of Technology	0.5	9.0 10.0 22.0 (*)	10.0–14.0	Glass beads.	Reciprocating pump.	Bottom liquid feed with temperature gradient (internal reflux).	Glycerol acetates extraction from biofuels by-products.	(Rezayat & Ghaziaskar, 2011).
Korea Inst Sci & Technol	1.5	31.7	9.1–112.2	31.5x100 mm knit mesh (ϵ : 0.95 α : 1400 m ⁻¹).	High-pressure metering pump.	Continuous stripping mode / no reflux.	Mass-transfer in packed and spray columns for the ethanol water mixture.	(J. S. Lim, Lee, Kim, Lee, & Chun, 1995).
National Chung Hsing Univ.	0.8	22.0	20.0–30.0	Ø type SS.	Syringe pump.	Semi-batch mode.	De-acidification of rice bran oil.	(Chen et al., 2008).
Univ. of Udine	4.5	30.0	10	Sulzer EX.	High-pressure pump.	Continuous stripping mode.	Aroma compounds from alcoholic beverages.	(da Porto & Decorti, 2010).

Table 2.4 cont'd Research lines of leading research groups and countercurrent packed columns dimensions and characteristics. Height (H), Inside diameter (ID), Operating pressures (*P*), Type of packing, Equipment used to compress CO₂, and Field of application for selected references.

Research group	Column dimensions and characteristics							References
	H / m	ID / mm	<i>P</i> / MPa	Column packing	Equipment used to compress CO ₂	Mode of operation	Field of Application	
Univ. of Alberta	3.1	17.5	20.0; 25.0	4.1 mm SS Propak.	Syringe pump.	Bottom liquid feed with temperature gradient (internal reflux).	Edible oil components and derivatives.	(Güçlü-Üstündağ & Temelli, 2007).
Fachhochschule Lübeck	2.4 [†]	40.0	50	10 mm VFF Interpack®	Membrane pump.	Continuous stripping mode / no reflux.	Edible oil components and derivatives.	(Pietsch & Swidersky, 2012).
FAU-Erlangen-Nuremberg	7.5 [†]	67.0	16.0	Sulzer CY, BX.	Compressor.	Continuous reflux mode / middle liquid feed / partial extract reflux.	Edible oil components and derivatives / deterpenation of essential oils / dealcoholization of alcoholic beverages.	(S Peter, Zhang, Grüning, & Weidner, 2001; Siegfried Peter et al., 1987).
	8.0	33.0						
VTT Chem. Technol.	2.0	35.0	40.0	Oldshue-Rushton column: flat-blade paddle-type impeller.	Compressor.	Continuous stripping mode / no reflux.	Removal of pyridine and ethanol from water.	(Laitinen & Kaunisto, 1998, 1999, 2000).
LAEPSI, INSA	2.0	100.0	1.0–1.3	6.4 mm Beryl Saddles, Raschig rings, Sulzer Mellapak 250Y	n.a.	Continuous stripping mode / no reflux.	Mass transfer and hydrodynamics of CO ₂ absorption in NaOH solutions.	(Assaoui, Benadda, & Otterbein, 2007; Benadda, Kafoufi, Monkam, & Otterbein, 2000; Benadda, Otterbein, Kafoufi, & Prost, 1996).
	1.0	62.0						
Aix-Marseille Univ.	2.0	19.0	35.0	VFF Interpack®.	High-pressure pump.	Continuous stripping mode / no reflux.	Fractionation of microalgae oil.	(Pieck, Crampon, Chanton, & Badens, 2013).

Table 2.4 cont'd Research lines of leading research groups and countercurrent packed columns dimensions and characteristics. Height (H), Inside diameter (ID), Operating pressures (P), Type of packing, Equipment used to compress CO₂, and Field of application for selected references.

Research group	Column dimensions and characteristics							References
	H / m	ID / mm	P / MPa	Column packing	Equipment used to compress CO ₂	Mode of operation	Field of Application	
SSEA-Univ. of Reggio Calabria	3.0	30.0	8.0	Raschig rings	High-pressure membrane pump.	Continuous stripping mode / no reflux.	Deterpenation of essential oils	(Poiana, Mincione, Gionfriddo, & Castaldo, 2003).
EXTRALIA NS Plataform	4.0 [†]	45	30.0	(n.a)	High-pressure pump.	(n.a)	Edible oil and derivatives / deterpenation of essential oils.	(Perre, Delestre, Shrive, & M, 1994).
	8.0 [†]	126	35.0					
Solvay Specialty Polymers, R&D Center.	1.1	38	30.0	Sulzer CY	High-capacity metering diaphragm pump.	Continuous stripping mode / no reflux.	Perfluoropolyethers (PFPEs) fractionation.	(Valsecchi, Mutta, De Patto, & Tonelli, 2014).
Muller extract Co.	3.0	30.0	8.0–30.0	10 mm x10 mm SS Raschig rings.	High-pressure pump.	Continuous stripping mode / Upper, middle and, bottom liquid feed with temperature gradient (internal reflux).	(n.a.)	(Bondioli et al., 1992; Stockfleth & Brunner, 2001b).
FLAVEX Naturextrakte	3.0	46.0	30	SS spirals.	(n.a.)	(n.a.)	(n.a.)	(Manninen, Pakarinen, & Kallio, 1997).
F. Hoffmann-La Roche AG	13.6	35.0	14.5–19.5	Sulzer CY.	Membrane pump.	Continuous reflux mode / middle liquid feed / partial extract reflux.	Edible oil components and derivatives.	(Fleck et al., 1998).

(ε), void fraction; (a), specific surface m²·m⁻³; (n.a.), Not available on scientific literature; (SS), Stainless steel; (†), Actually active, personal communication; (*), The same column has three sections of different internal diameters.

In general, for the design of packed columns, the separation is treated as a staged process, and uses the packed bed Height Equivalent to a Theoretical Plate (HETP) to convert the required number of ideal stages to a packing height. The basic model for the mass transfer performance of a packed column in distillation or absorption/stripping processes is often expressed by the HETP. According to the double-film theory the relationship between HETP and the Height of the mass-Transfer Unit for the gas phase (HTU_G) and for the liquid phase (HTU_L) is given by the following equations (Wang, Yuan, & Yu, 2005):

$$HETP = \frac{Z}{N}, \text{ and} \quad (1a)$$

$$HETP = \frac{\ln(\lambda)}{\lambda - 1} \cdot (HTU_G + HTU_L), \quad (1b)$$

where Z is the height of packing, N is the number of theoretical stages, and λ is the stripping factor defined as the ratio between the slope of the equilibrium line and that of the operating line (mass balance equation). Combining Eq. (1b) with the definitions of HTU_G and HTU_L (Sinnott, 1999), the expression becomes:

$$HETP = \frac{\ln(\lambda)}{\lambda - 1} \cdot \left(\frac{G_m}{k_G \cdot a_e} + \lambda \cdot \frac{L_m}{k_L \cdot a_e} \right), \quad (2)$$

where G_m and L_m are the molar flow rates per unit cross sectional area of the gas and liquid phase, respectively; k_G and k_L are the corresponding gas and liquid phase mass-transfer coefficients; and a_e is the effective interfacial area for mass transfer provided by the packing. It is simple to perceive that Eq. (2) will be accurate if the correlations used to predict the basic parameters are accurate.

When assuming binary or pseudo-binary systems, low concentrations of the solute, straight equilibrium and operation lines (generally true in CC-SFF), and constant

molar overflow throughout the column, Eq. (1a) and Eq. (2) can be solved using conventional methods. The number of stages can be estimated using graphical methods such as those of McCabe-Thiele or Ponchon-Savarit as described by G. Brunner (2009b, 1994, 1998a), or using numerical integration of traditional expressions for the Number of Transfer Units (NTU) (Sinnott, 1999). For multicomponent separations a more complex approach, based on the Stefan-Maxwell equation to estimate multicomponent diffusivities, is necessary. Literature reporting diffusion coefficients in multicomponent mixtures at elevated pressures is scarce and this topic is beyond the scope of this work. However, studies of multicomponent diffusion using the Stefan-Maxwell approach under high pressure for the ternary system ($\text{CO}_2 + \text{methanol} + \text{water}$) can be found in the work of Unlusu & Sunol (2004a, 2004b). Recent improvements to the HETP model are also reported by Hanley & Chen (2012).

In general, the mathematical description of CC-SFF considers only axial dispersion and the mass fluxes in terms of overall mass-transfer coefficients for the solutes into the dense gas (SC- CO_2 , $K_{i,\text{SC}}$) and of the SC- CO_2 into the liquid phase ($K_{\text{CO}_2,\text{L}}$, non-negligible in non-aqueous systems). Due to back mixing effects, a correction factor dependent on the densities of both phases (ρ_{SC} , ρ_{L}) and the corresponding superficial velocities (u_{SC} , u_{L}) is usually introduced in the expression for the mass fluxes, Eq. (3a) and Eq. (3b), to take into account the buoyancy effects produced by the slight density difference between the SC- CO_2 and the liquid phase (Ruivo, Paiva, Mota, & Simões, 2004).

$$J_i = K_{i,\text{SC}} \cdot \rho_{\text{SC}} \sqrt{\frac{\rho_{\text{SC}}}{\rho_{\text{L}} - \rho_{\text{SC}}}} \cdot \frac{u_{\text{SC}}}{u_{\text{L}}} \cdot (y_i^* - y_i) \quad (3a)$$

$$J_{\text{CO}_2} = K_{\text{CO}_2,\text{L}} \cdot \rho_{\text{L}} \sqrt{\frac{\rho_{\text{SC}}}{\rho_{\text{L}} - \rho_{\text{SC}}}} \cdot \frac{u_{\text{SC}}}{u_{\text{L}}} \cdot (x_{\text{CO}_2}^* - x_{\text{CO}_2}) \quad (3b)$$

From Eq. (2), Eq. (3a), and Eq. (3b) it is seen that phase equilibrium mole fractions (y_i^* , $x_{\text{CO}_2}^*$) are essential in the description of the process. Comprehensive reviews on correlations for estimating basic parameters, *i.e.*, mass-transfer coefficients of both phases, and effective interfacial area for different types of packing can be found in literature (De Haan & De Graauw, 1991; Oliveira, Silvestre, & Silva, 2011; Wang et al., 2005). Several mass-transfer and hydrodynamics studies, along with CC-SFF process modelling and simulation, can be found in literature, mainly for non-aqueous systems and very few applications related with aqueous systems. Hydrodynamics of countercurrent packed columns consists of studying dry and wet pressure drops, liquid holdups, and flooding points. The work of Stockfleth & Brunner (1999, 2001a, 2001b) demonstrated that the hydrodynamic behaviour of countercurrent columns at high pressure could be described with models developed for normal pressure operation if specific peculiarities, such as the real mixture properties of miscible systems at the relevant conditions of high-pressure operation, are appropriately addressed. Becker & Heydrich (2004) contributed greatly to clarify the fluid dynamic dispersion of the mixture ($\text{CO}_2 + \text{ethanol} + \text{water}$). The authors studied the separation efficiency and hydrodynamics of two types of packing, wiremesh and Sulzer BX. They found lower separation efficiencies and very irregular flow patterns for the wiremesh packing. The authors also predicted axial dispersion coefficients using a conventional liquid/liquid model and found that experimental data obtained for the wiremesh packing did not follow the general trend. In general, as it can be seen from Table 2.1, the fractionation of edible oil components and derivatives has been relatively well studied. Much less is known about hydrodynamics of aqueous systems, other than ethanol + water, in contact with dense gases, and experimental investigation of these systems is more challenging.

Availability of information regarding phase equilibrium, interfacial tension, and other physicochemical properties, transversal and relevant to all fractionation technologies will be described in Section 2.6.

2.2.2 Modes of operation of packed columns and applications

As mentioned before, CC-SFF in packed columns is the type of technology more commonly used in SFF. It is possible to identify three different modes of operation in CC-SFF in packed columns: stripping mode, reflux mode, and batch or semi-batch modes. Because the applications of CC-SFF in packed columns have been reviewed in the past by G. Brunner (2009b, 1998a, 2005), in this section we will describe the applications and mode of operation used by the first six institutions listed in Table 2.4. The applications mentioned in this section are listed along with the applications of the other fractionation technologies described in this work, classified according to the three major areas of research; edible oil components and derivatives (Table 2.1), essential oils (Table 2.2), and alcoholic beverages (Table 2.3). As it can be understood, the equipment listed in Table 2.4 can be used also for other applications that may not fall in the defined areas of research, and/or use other solvents such as ethane and propane. These studies are very scarce in literature, and therefore were only included in Table 2.4 and not listed in Tables 2.1 to 2.3.

Research groups in Table 2.4 are organized according to number of publications associated with the equipment found in the literature. Considerable effort was devoted to make Table 2.4 as complete and actualized as possible, and to include all equipment available at the research groups. However, some installations may have been modified, discarded, or upgraded, and are no longer operational.

Stripping mode

The stripping mode of operation is achieved when the liquid mixture is fed from the top of the column and the dense gas is fed at the bottom of the column causing the countercurrent flow (Fig. 2.1A). The extract is recovered by the expansion of the loaded CO₂ in the separator. In this type of operation there is no partial reflux of the extract.

Slight variations of the stripping mode are found in the investigations of the *Instituto de Investigación en Ciencias de la Alimentación* (CIAL) from the *Universidad Autónoma de Madrid* (UAM) and the *Consejo Superior de Investigaciones Científicas* (CSIC) (CIAL-UAM-CSIC). The feed point of liquid phase can be in different positions of the column (upper, middle and low). The extract is obtained in two separators where

cascade decompression takes place. No reflux of the extract is used in this way of operation. CIAL-UAM-CSIC research group has developed investigations in two areas of research. Regarding edible oil components and derivatives, it has studied the removal of free fatty acids (Fernández-Ronco et al., 2011; Vázquez et al., 2009), recovery and concentration of minor lipids such as tocopherols, phytosterols, phytosterol esters, carotenoids, and squalene from olive oil and other lipids (T. Fornari, Torres, et al., 2009; T. Fornari et al., 2008; Ibáñez et al., 2000, 2002; Luis et al., 2007; Tabera et al., 2004; Torres, Torrelo, et al., 2009; Vázquez et al., 2006). It has also studied the fractionation of alcoholic beverages (Señoráns et al., 2003; Señoráns, Ruiz-Rodríguez, Ibáñez, et al., 2001; Señoráns, Ruiz-Rodríguez, Ibáñez, et al., 2001), and isolation of antioxidants from orange juice (Señoráns, Ruiz-Rodríguez, et al., 2001; Simó et al., 2002).

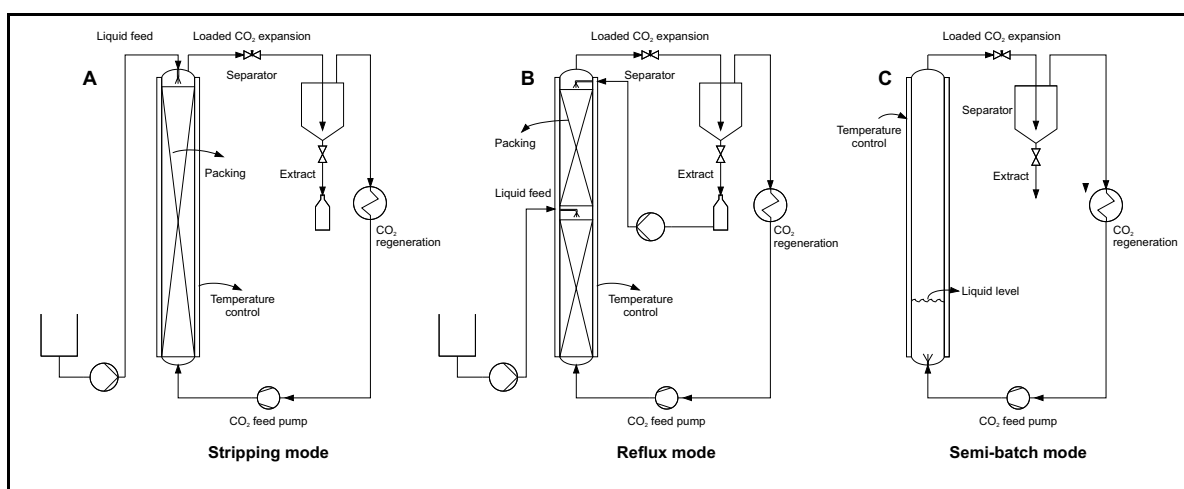


Figure 2.1 Modes of operation of packed columns. (A), Stripping mode; (B), Reflux mode; (C), Semi-batch mode.

The research group of Portugal at the *Laboratório Associado para a Química Verde – Tecnologias e Processos Limpos* (LAQV-REQUIMTE) has operated their columns in both the stripping, and reflux mode of operation. LAQV-REQUIMTE research is related mainly to edible oil components and derivatives: fractionation and deacidification of olive oil deodorized distillates (Catchpole, Simões, et al., 2000; Simões et al., 1998) and separation of squalene from methyl oleate (Ruivo et al., 2001). Additionally, they have reported one work on wine must aroma (Macedo et al., 2008) and have

contributed with mass-transfer studies in packed columns (Ruivo et al., 2002; Simões et al., 1995), dynamic simulation of coupled mass and energy balances (Fernandes, Lisboa, Barbosa Mota, & Simões, 2011; Fernandes, Ruivo, Mota, Simoes, & Simões, 2007; Fernandes, Ruivo, & Simões, 2007; Ruivo et al., 2004), and the use of Computer Fluid Dynamics (CFD) for pressure drop calculations (Fernandes et al., 2008; Fernandes, Lisboa, Simões, Mota, & Saatchian, 2009).

Another group that applies a slight variation of the stripping mode is the one at the Northern United States Department of Agriculture (USDA). The column is divided into different sections and the liquid is fed in the first section of the column, just above the bottom feed of CO₂, in order to achieve the countercurrent flow. Northern USDA research group also applies an ascending temperature gradient from the bottom to the top of the column. The increase in temperature decreases CO₂ density allowing the higher vapor-pressure compounds to concentrate at the top of the column. The main area of research of the Northern USDA is the edible oil components and derivatives; fractionation of mixtures composed of mono-, di-, and tri-acylglycerols (Compton et al., 2012, 2008; Eller et al., 2008; Sahle-Demessie, 1997b), removal of free fatty acids from vegetable oils (Dunford & King, 2001; Eller et al., 2009), enrichment of phytosterol esters of rice bran oil (Dunford et al., 2003), and removal of the organic solvent from an hexane-extract of soybean oil (Eller et al., 2004).

The research group of Cornell University applies the stripping mode with no variations, *i.e.*, no extract reflux and liquid feed on top of the column. The main applications of this group are related to non-aqueous solutions: refining palm oil (Ooi et al., 1996), and anhydrous milk fat fractionation (Bhaskar, Rizvi, & Harriott, 1993; Bhaskar, Rizvi, & Sherbon, 1993; Rizvi & Bhaskar, 1995; Romero et al., 2000; Yu et al., 1995).

Reflux mode

In the reflux mode of operation the liquid feed is introduced in the middle section of the column and the extract is partially returned to the top of the column to achieve the countercurrent flow. The partial reflux of the extract is done in order to obtain

an extract richer in light components (Fig. 2.1B). Other possibility is to partially reflux the raffinate to the feed supply in order to increase extraction yield but at the expense of lower product volumes at the bottom of the column.

Perhaps the world leader research group in supercritical fluid technology is that of the *Technische Universität Hamburg-Harburg* (TUHH). Researchers at TUHH operate their available columns in the reflux mode (as a distillation column) and they have developed research in the three main areas of application described in this work. This group has influenced the way in which supercritical fractionation is addressed. The approach of the TUHH research group can be divided in four important steps: (i) phase equilibrium measurements; (ii) pilot scale experiments in order to adjust velocities, solvent-to-feed ratio, and measure real compositions of extract and raffinate samples; (iii) determination of hydrodynamic characteristics such as dry and wet pressure drops, flooding points, and liquid holdups; and, (iv) graphical or computer-aided determination of NTU and HTU or HETP. Detailed information on the steps of the approach followed by the TUHH group and their applications are described in detail in the reviews of Gerd Brunner (2009b, 1998a, 2005) and the work of Gerd Brunner & Machado (2012).

A less common technique is the semi-batch mode of operation. Particularly the research group of Kumamoto University has applied this mode of operation for the deterpenation of citrus oils.

Semi-batch contacting equipment

Semi-batch contacting can be achieved in columns with continuous flow of CO₂ through a quiescent portion of liquid held in the bottom of the column. The extract is recovered by pressure reduction in a separator at controlled temperature and pressure as depicted in Fig. 2.1C. This mode of operation is a much less common technique than the stripping and reflux modes of operation. The infrastructure needed for this type of operation is simpler than for the stripping and reflux modes, and the same equipment used for SFE of solids may be used for SFF of liquid mixtures using laboratory-size equipment. Phase equilibrium, extraction kinetic curves, and derived information can be obtained with this kind of arrangement.

For the reasons exposed above, only for this mode of operation a detailed description of the applications found in literature is given below. A few comparisons with the stripping and reflux modes were carried out by the research group of Kumamoto University and are described below.

Rincón et al. (2011b) studied the separation of triglycerides from the unwanted polar fraction in used frying oil using liquid and supercritical ethane. In order to determine the best conditions for the separation, preliminary semi-batch experiments were performed in a 940-cm³ vessel packed with an irregular steel material. Rincón et al. (2011b) performed the same separation by CC-SFF using the best pressure and temperature conditions found in the semi-batch experiments (24.5 MPa and 298.2 K). By the use of CC-SFF, the authors recovered 85% of the triglycerides in the used frying oil, and the content of polar compounds decreased from 29.9 to 11.2%, close to the value of the fresh sunflower oil (7.3%). The CC-SFF with ethane showed better separation efficiencies than obtained by CC-SFF with CO₂ in a previous work Rincón et al. (2007b). In the work of Chen et al. (2008) on de-acidification of rice bran oil, the removal of free fatty acids reached 97.8% in a 75-cm packed column operated in the semi-batch mode.

Regarding essential oils, Jaubert et al. (2000b) modelled accurately the extraction profiles of citrus oil components with SC-CO₂. The authors applied a theoretical model to the separation of limonene and citral in a 40-cm vessel operated in the semi-batch mode packed with glass beads. Gañán & Brignole, (2011b) studied the fractionation of essential oils from plants (*Salvia officinalis*, *Tagetes minuta*, and *Mentha piperita*) with biocidal activity. The experimental set up used in this study was a conventional screening unit with a 50-cm³ vessel where a small quantity of oil (1.0 to 1.5 cm³) was embedded in 80-mesh glass beads. After two hours of approaching equilibrium, CO₂ was allowed to flow through the column and extracts were collected for analysis. Solubility of main components of different fractions of essential oil in CO₂ were determined and correlated using the Group Contribution Equation of State (GC-EoS). The study concluded that the active biocidal fraction of *Tagetes minuta* oil could be extracted in a semi-continuous or countercurrent column without external reflux.

The research group of Kumamoto University has studied the deterpenation of essential oils of lemon and other citrus fruits on larger columns. Researchers from this group observed that when performing continuous fractionation, the selectivity was not significantly influenced by the use of an external reflux (reflux mode). On the other hand, they found that the solvent-to-feed ratio, and feed-inlet position were important variables in the fractionation of citrus fruit essential oils (Goto et al., 1997; M Kondo et al., 2000; Mitsuru Kondo, Akgun, et al., 2002; Mitsuru Kondo, Goto, et al., 2002; Sato et al., 1995, 1996; Terada et al., 2010). In fact, better results were obtained operating the column in the stripping mode (Sato et al., 1998).

A countercurrent flow in the semi-batch mode can be obtained by applying a temperature gradient on the column. Sato et al. (1996) studied the effect of the operation of the column under isothermal and linear temperature gradient conditions on the selectivity in the extraction of terpenes (limonene) *versus* oxygenated terpenes (linalool). An internal reflux was induced by a temperature gradient, from 313 K at the bottom to 333 K at the top of the column. Under these conditions selectivity increased significantly because physical properties such as solubility, density, and viscosity changed remarkably. Mitsuru Kondo, Akgun, et al. (2002) compared the continuous countercurrent operation of the column with semi-batch experiments for the fractionation of lemon essential oil (with and without temperature gradient). The continuous operation of the column at higher solvent-to-feed ratios increased the selectivity between limonene and citral, and the highest value was obtained with the column working at 8.8 MPa under the temperature gradient from 313 K at the bottom to 333 K at the top.

An application that stands out from the three outlined areas is the recovery of aroma compounds from non-alcoholic beverages such as fruit juices or essences. Early researchers of the Western Regional Research Laboratory of the USDA (California) applied the semi-batch mode of operation. In the work developed by T. H. Schultz et al. (1967) and W. G. Schultz & Randall (1970b), aqueous apple juice essence was dispersed into liquid CO₂. After ~3.3 cycles of aqueous essence passing through the column, the concentration went from 150-fold to 10,000-fold although steady state was not achieved. The authors also compared different gases as solvents for the extraction; CO₂ showed good

recovery of the major essence constituents. Later, W. G. Schultz, Schultz, Carston, & Hudson (1974a) built a pilot plant for continuous liquid-liquid extraction of fruit aroma in order to reach steady-state conditions.

Very limited applications of this methodology were found in literature. All experiments using the semi-batch mode of operation were made using laboratory-size equipment (from 0.4–2.4 m of column height) and model mixtures were considered.

2.3 Membrane contactors

This section describes the use of membrane contactors to fractionate liquid mixtures using dense CO₂ along with its main applications (Table 2.3). Liquid fractionation with supercritical fluids in a separation device containing a porous membrane is characterized by a two-phase immobilized phase interface. As shown in Fig. 2.2, one fluid phase (phase 2, usually the dense gas) is on one side of the membrane occupying the pores, and an immiscible fluid phase (phase 1, usually aqueous) is on the other side of the membrane. The pressure of the fluid phase 1 (P_1) must be equal to or greater than the pressure of the second fluid phase (P_2) in order to immobilize the immiscible phase interface at the pore mouth. However, the pressure difference ($P_1 - P_2$) should not exceed a critical value (ΔP_{crit}); otherwise the fluid phase 1 will be forced through the pores and disperse into the fluid phase 2 as drops or bubbles. As no drops or bubbles are formed in either phase, the process becomes an equilibrium-based separation, and the separation device is generally called membrane contactor (Sirkar, 2008). Other membrane technologies and their applications can be consulted in the work of Sarrade, Guizard, & Rios (2003).

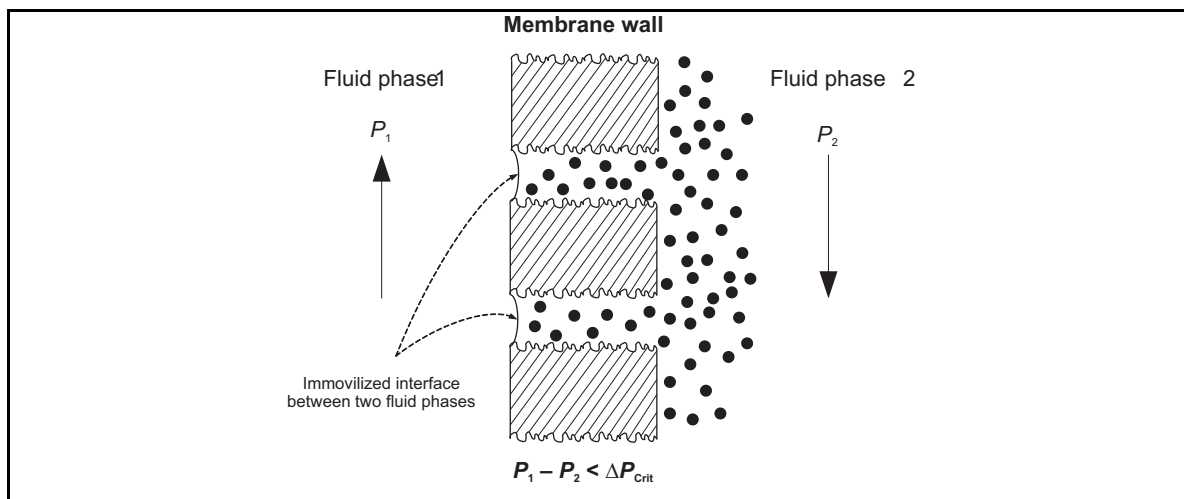


Figure 2.2 Immobilized phase interface in a membrane contactor

Most of literature regarding applications of membrane contactors deals with the separation of different organic solvents from aqueous solutions, probably because water solutions have favorable wetting behavior for membrane contactors and an immobile interphase is better achieved. Bothun et al. (2003) used a model solution of fermentation products, acetone and ethanol, to separate them from water in a Hollow Fiber Membrane Contactor (HFMC) with three different dense gases: CO₂, ethane, and propane.

Gabelman & Hwang (2005) made a comparison between the predictions of a mathematical model and the experimental results for the separation of various solutes (caffeine, ethanol, dimethylformamide, 1,2-dichloroethane, and ethyl acetate) from aqueous solutions into dense CO₂ and propane. A previous work (Gabelman et al., 2005) presented the mathematical model that described the HFMC process for the separation of isopropanol and acetone from water into dense CO₂. When applying the model to the new aqueous solutions, it predicted the steady-state fluid velocities and solute concentrations, and it estimated mass transfer coefficients. The mass transfer predictions made in both works agreed with experimental results.

Another interesting study made by Gabelman & Hwang (2006) compared sieve and spray towers, and packed columns with HFMC. The authors simulated HFMC using experimental information reported by others on the fractionation of isopropanol and ethanol from water. The comparison was made in terms of the HETP. The simulated HETP

was compared with the experimental data reported in the literature. The experimental data was obtained in sieve-tray columns, spray columns, and columns packed with Sulzer and Raschig rings of 0.5 to 4 m of active height. In some cases, the simulated HETP was significantly lower than compared with sieve tray, packed (Sulzer and Raschig rings), and spray columns. Consequently, Gabelman & Hwang (2006) claimed that HFMC technology is more efficient in most cases.

Perhaps the most common alcoholic beverage in the world is wine and its ethanol content and aroma profile is of great interest to producers. Thus, separation of organic solvents such as ethanol or isopropanol from aqueous solutions by HFMC can be used as an alternative to dealcoholize alcoholic beverages. Diban, Athès-Dutour, Bes, & Souchon (2008) tested the validity of HFMC to partially dealcoholize wine without compromising the aroma profile. They used model solutions with typical compositions of real wines and found that the technology was feasible to reduce ethanol to 2% (v/v) without perceptible loss of quality of the product. However, they observed that prolonged retention times of the mixture into the HFMC caused adsorption of highly hydrophobic flavours in the membrane with almost complete disappearance of aroma from the feed solution.

Simulation and mathematical modelling of the process is an intensive area of research. Simulation for the separation of organic solvents (ethanol and acetone), sulphur aroma components, and caffeine from aqueous matrices by single and multiple fiber modules is available in literature (Bocquet et al., 2007, 2005; Estay et al., 2007; Shirazian & Ashrafizadeh, 2010). In general, the mass transfer of the process was described by a resistance-in-series model, taking in consideration four steps for solute transport: (i) the solute flows through the aqueous boundary layer, from the bulk phase to the interface; (ii) the solute goes across the aqueous/solvent interface; (iii) the solute diffuses in the pore filled with the solvent phase; and, (iv) the solute flows through the solvent boundary layer. More recent advances are the application of CFD to model the separation of ethanol and acetone from water in a HFMC with dense CO₂ (Estay et al., 2007) and the simulation and optimization of an industrial scale HFMC to separate organic solvents such as ethanol, methanol, and acetone from water (Vyhmeister, Estay, Romero, & Cubillos, 2012).

Examples of SFF with membrane contactors and other membrane technologies that use dense CO₂ to fractionate liquid mixtures are relatively recent. More complex or real mixtures need to be studied to improve the knowledge of the process and scale it up to industrial size. Application of this technology is limited to one equilibrium stage and to aqueous systems mainly because fractionation for non-aqueous systems would probably lead to a mobile interphase in the pores causing the liquid phase to break into the CO₂ as drops or bubbles. Additionally, care must be taken to not exceed ΔP_{Crit} especially when the HFMC is operated in countercurrent mode. Typical values of ΔP_{Crit} are in the range of 0.1 to 0.5 MPa.

In membrane contactors, the main function of membranes is increasing interfacial area for mass transfer. However, membranes can be used for other purposes. For example, they can be coupled to CC-SFF for enhanced separation of the extract at the top of the column for CO₂ recycling. Ruivo et al. (2008) carried out a comparison of six different membranes for the separation of squalene from oleic acid with CO₂. Polydimethyl siloxane and polyamide membranes gave significant enrichment of squalene in the permeate side. The authors suggested that this technology could be used as an additional reflux step in a SFF packed column where the less-pure extract stream from the packed column would be diverted to the membrane cell. The permeate side, which has a higher squalene content, would be partially refluxed to the top of the SFF column, increasing the squalene content of the “enrichment section” of the column. Carlson, Bolzan, & Machado (2005) used similar approach to compare four different commercial membranes (one nano-filtration and three reverse osmosis) to separate limonene from a solution with CO₂. They found that the best was a thin film polyamide reverse osmosis membrane achieving a limonene retention factor as high as 0.94.

2.4 Mixer-settler process and components

This section describes devices that take advantage of mixer-settler and the spray extraction processes to fractionate liquid mixtures. The role of the mixing devices (*e.g.*, static mixers and nozzles) is discussed, and in each case a discussion of the main applications, findings, developments, and future directions is provided.

Several mixer-settler equipment and configurations exist. Nevertheless, they work based on the same principle, a separation process that consists of two steps: the first mixes the solvent and the solution with the solute(s) of interest, that together follow to a second step where a quiescent settling takes place allowing phases to separate by gravity. The use of mixer-settler arrangements in SFF is desirable when (i) the liquid phase flow is low and does not cover all the mass transfer equipment, causing a limited mass transfer rate; (ii) the viscosity of substances in the liquid phase is high, even with dissolved supercritical fluids; (iii) the flow differences between liquid and gaseous phases are large, compromising stable operation of the column; and, (iv) there are small density differences between phases causing limited flow in columns driven by gravity. Using a mixer-settler arrangement circumvents these problems. The main drawback of this technology is its limitation to mixtures that require a relative small number of stages for a reasonable separation (Brunner, 2009).

The mixer-settler arrangement must accomplish two purposes: provide the adequate mixing of the liquid and gaseous phase, so as to approach phase equilibrium, and allow separation of phases after mass transfer has occurred in the mixing device. Typically, multiple mixer-settler units are used for a multistage process; this is achieved by driving the separated liquid phase to the mixing device of the next stage, and the gaseous phase to the preceding stage as shown in Fig 2.3. Each stage requires at least one mixing device, and one separator. Usually, for fast and intense phase contact and segregation, side channel pumps with a diffusor or static mixers are used as mixing devices in order to approach equilibrium. At high pressures, quiescent phase separation is not practical and induced vortexes in cyclonic separators are typically used to speed up phase separation.

It is well known that static mixers, also known as motionless mixers, are engineered devices for continuous mixing of fluid materials, that show significant advantages over conventional mixers for both turbulent and laminar flow. A typical design of a static mixer consists of a series of inserts commonly called elements, which can be contained in pipes, columns, or reactors. The purpose of the elements is to redistribute the fluid direction tangentially and radially to the main flow. In both laminar and turbulent flow, static mixers can significantly improve heat and mass transfer due to enhanced

turbulence and fast and intense mixing even near walls (Thakur, Vial, Nigam, Nauman, & Djelveh, 2003).

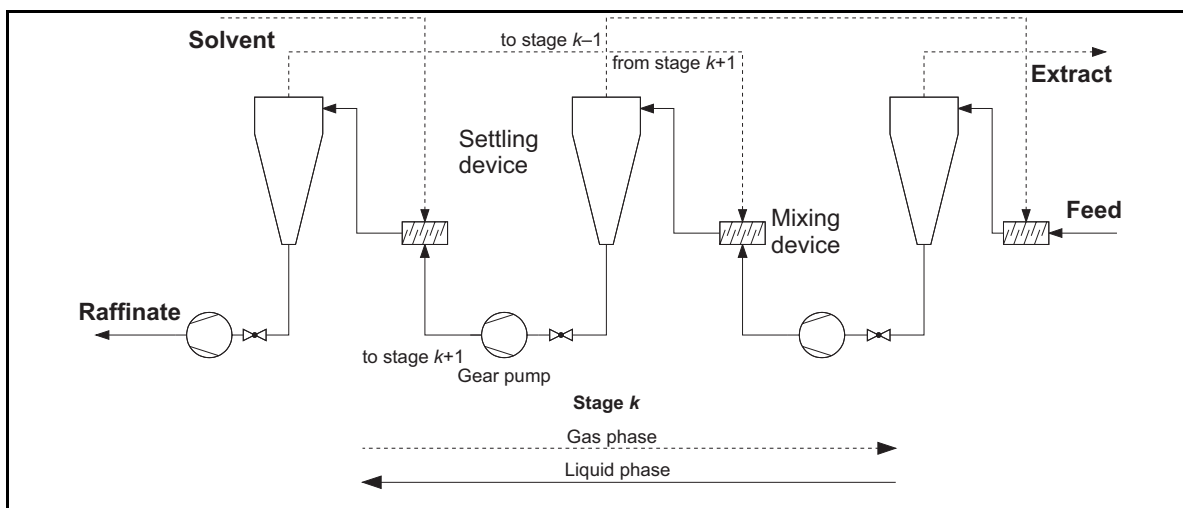


Figure 2.3 Schematic flow diagram of a mixer-settler arrangement of $(k+1)$ stages.

There are few studies regarding mixer-settler arrangements. Chuang & Brunner (2006) used a pilot scale five-stage mixer-settler device to study the fractionation of minor components (tocochromanols, sterols, β -carotene, and squalene) in crude palm oil. Each stage used a side-channel pump as mixing device and a cyclone for separation. The authors estimated four theoretical stages for the mixer-settler arrangement. After the third stage, tocochromanols were concentrated from 600 to 60,000 ppm, β -carotene from 550 to 105,000 ppm, squalene from 400 to 33,000 ppm, and sterols from 300 to 30,000 ppm. Thus, the enrichment of carotenoids (200-fold) was higher than that of tocochromanols (90-fold), and because β -carotene is the least volatile of the minor components in crude palm oil it has the largest concentration factor.

The results obtained by Chuang & Brunner (2006) are consistent with the findings of other authors (Catchpole, Simões, et al., 2000; Ruivo et al., 2006) for olive oil deodorizer distillate systems suggesting that the separation of carotenes from fatty acid methyl esters is suitable for the mixer-settler systems. For mixtures that need a larger number of theoretical stages like C18/C20-methyl esters, a reasonable separation of these fractions can be achieved in a countercurrent packed column and the mixer-settler principle

is not suitable. Most of the works reported are based in known phase behavior of the mixtures and use model systems in experiments.

Schaffner & Trepp (1995) modified a conventional countercurrent column, to address the lack of longitudinal mixing and of packing wetting, by installing a mixer-settler device, composed of a pump and a cyclone, between the stripping and enrichment sections of the column. The authors used a synthetic model solution in the range of 51 to 55% by weight of α -tocopherol and α -tocopherol acetate and evaluated the Murphee Efficiency, the separation efficiency of the cyclone, and the performance of the pump as mixing device. Schaffner & Trepp (1995) reported Murphee Efficiencies in the range of 81 to 96%. The separator was a homemade cyclone and achieved separation efficiencies from 92 to 99%. The authors also found that the separation efficiency could be improved significantly by entraining a fraction of the gas phase into the liquid phase. Regarding the performance of the mixing device (pump), the mixing performance was evaluated by studying the hydrodynamics and particle size distribution generated by the pump. Schaffner & Trepp (1995) correlated the specific surface area with the Reynolds number obtaining a maximum surface area of $3,000 \text{ m}^2 \cdot \text{m}^{-3}$.

As an alternative to using a pump as mixer, a Kenics-type static mixer was evaluated in the separation of the system (caffeine + water + CO_2) by Pietsch & Eggers (1999). The authors used a single stage mixer-settler arrangement and compared the performance of an empty tube and a tube with a static mixer in its interior. Separation efficiencies were found to be higher at low gas-to-liquid phase flow and at high temperatures (353 K), and the Kenics static mixer increased significantly the efficiencies of the empty tube. Moreover, there were no significant differences observed when replacing the static mixer with wire-mesh packing. The separation efficiencies achieved were around 65% for a phase ratio in the range of $10:20 \text{ kg} \cdot \text{kg}^{-1} \text{ CO}_2\text{-to-H}_2\text{O}$. Additionally, Pietsch & Eggers (1999) made pressure drop calculations across the static mixer concluding that the later can be neglected in supercritical fluid processes.

As the use of the mixer-settler principle avoids some of the disadvantages of conventional columns, Catchpole, Simões, et al. (2000) compared the use of a single stage

co-current mixer-settler arrangement with a countercurrent packed column for the fractionation of shark liver oil (SLO) and olive oil deodorizer distillate (OODD). The objective of the work was to evaluate squalene recovery from SLO and OODD. Experiments were made in a pilot and laboratory column and using a static mixer. Results indicated that CC-SFF pilot and laboratory columns were more efficient than the static mixer for the fractionation of SLO, but equally efficient for the fractionation of OODD. Catchpole, Simões, et al. (2000) suggested using multiple stages to obtain high-purity squalene due to the very low separation factor of squalene in OODD. Additionally, mass transfer coefficients and pressure drop in the static mixer were correlated to Reynolds and Schmidt dimensionless numbers. Another study leading to similar results was developed by Ruivo et al. (2006). The comparison between a CC-SFF column and a Kenics static mixer on the selective fractionation of squalene from methyl oleate was carried out with a model mixture representing OODD. Hydrodynamics and mass transfer of the static mixer was studied and the conclusion was that even though the static mixer showed higher extraction efficiency per transfer unit, the packed column presented higher yield of extraction. The later can be explained by the fact that the countercurrent packed column had a higher number of transfer units than the static mixer.

Due to the design characteristics of static mixers, it is common finding them in heat or mass transfer operations related to SFF or SFE. Regarding mass transfer, Catchpole, Simões, et al. (2000) as well as Pietsch & Eggers (1999) suggested that static mixers could be used for phase equilibrium measurements as done by Fonseca, Simões, & Nunes da Ponte (2003). Regarding enhanced heat transfer, Pedro C Simões, Afonso, Fernandes, & Mota (2008) studied their performance with satisfactory results compared with the traditional tube-in-tube heat exchanger. Additionally, Lisboa, Fernandes, Simões, Mota, & Saatdjian (2010) performed CFD simulations to analyze the use of a Kenics static mixer as heat exchanger in supercritical processes. The authors proved that static mixers had thermal efficiencies three times greater than conventional heat exchangers. Static mixers and nozzles are also of interest in spray extraction with supercritical fluids.

2.5 Spray processes

High-pressure spray processes are a group of five similar technologies that have in common the atomization of the mixture (liquid + CO₂) or suspension in an empty column or recipient. Fig. 2.4 shows a simplified schematic flow diagram of the five processes: (i) Rapid Expansion of Supercritical Solutions (RESS); (ii) Particles from Gas-Saturated Solutions (PGSS); (iii) Spray drying of gas loaded liquids; (iv) CC Spray Extraction (SE); and, (iv) Two-Phase (TP) SE. Supercritical fluids have been intensively applied in spray processes in many diverse configurations derived from those listed above, mainly to produce solid particles. Several applications of particle formation methods are available in the literature and are not extensively reviewed here. However, some examples of precipitation of flavonoids from green tea and *Ginkgo biloba* leaf extracts can be found in Meterc, Petermann, & Weidner (2008) and Miao et al. (2010). Additionally, recent works on precipitation of rosemary antioxidants can be reviewed in Visentín, Cismonti, & Maestri (2011) and Visentín, Rodríguez-Rojo, Navarrete, Maestri, & Cocero (2012). Comprehensive reviews on different methods to produce solid particles and liposomes can be found elsewhere (Charbit, Badens, & Boutin, 2004; Meure, Foster, & Dehghani, 2008). Additionally, high-pressure micronization and product formulation using supercritical fluids for food and pharmaceutical applications can be found in the excellent reviews of Weidner (2009) and Knez, Knez Hrnčič, & Škerget (2015).

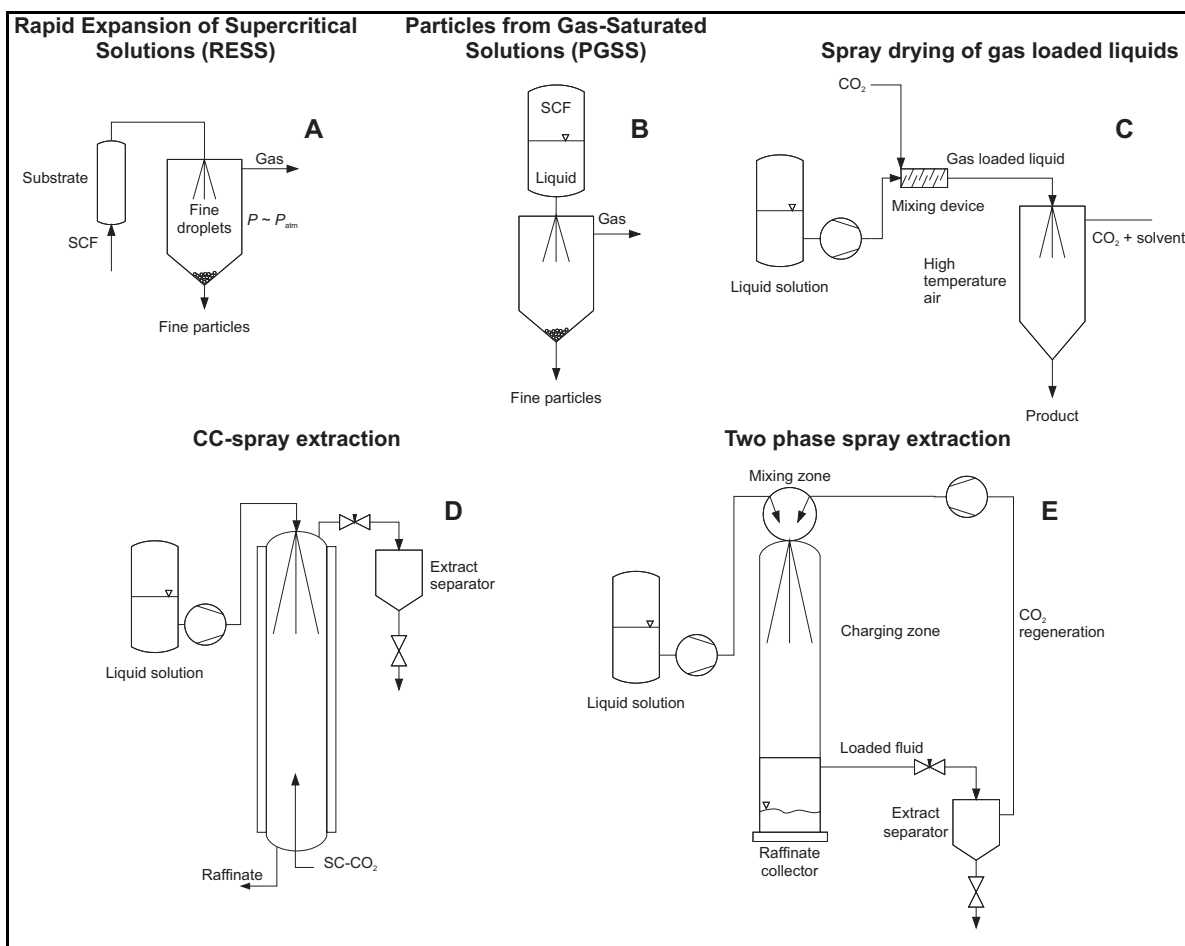


Figure 2.4 Simplified schematic flow diagrams of high-pressure spray processes. (A), RESS; (B), PGSS; (C), Spray drying of loaded liquids; (D), CC-spray extraction; (E), Two-phase spray extraction.

This work focuses in less common spray extraction processes like CC-SE (Fig. 2.4D) and TP-SE (Fig. 2.4E). As the other spray processes, CC-SE and TP-SE are suitable for mixtures with high separation factors because only one equilibrium stage can be achieved. Additionally, CC-SE and TP-SE are carried out in empty columns. Therefore, in contrast to CC-SFF in packed columns, there is no external element that provides high specific surface. Compared to the other spray processes, CC-SE and TP-SE offer the advantage that the prevailing process conditions have a positive effect on the spraying of the liquid phase. The solubility of the gas in the liquid, which increases significantly under pressure, leads to a considerable reduction in liquid viscosity allowing it to disperse into

droplets more easily. However, particularly the reduction of interfacial tension causes small drops to form, leading to a high specific surface for mass transfer.

Eggers & Wagner (1993b) used a TP-SE column to deoil soy lecithin proposing this technology as an alternative to batch SC-CO₂ processes, and conventional processes using organics solvents. The device can solve problems such as agglomeration when processing viscous solutions and avoid inefficiencies of batch operations. The technology is based on jet extraction (dispersion of a thin string of lecithin with a CO₂-jet) and the authors remarked the importance of the mixing device, responsible for the highly turbulent two-phase flow. The experiments were carried out in a semi-industrial scale apparatus, producing a powdery and well-deoiled product as the raffinate. Best deoiling results were obtained with a lecithin-to-CO₂ mass flow ratio of 1:40 kg·kg⁻¹, at 7.5 MPa and temperatures >373 K. Nevertheless, the authors pointed out that the problem of collecting continuously a raffinate stream still persisted.

Later, Wagner & Eggers (1996) optimized the geometry of the mixing device employing different designs. Fundamental formulations for particle formation in atomizers, the fluid dynamics, and the mass transfer in turbulent two-phase flows were successfully modified to match the problem of SFE. The process was patented by Eggers, Wagner, & Schneider (1999b).

Regarding the phenomenology of spraying of liquids in dense gases, Niels Czerwonatis & Eggers (2001) studied and characterized the disintegration of liquid jets and the size distribution of the drops in jets of water or vegetable oil pressurized with CO₂ or N₂. The authors observed the same shapes of disintegrating jets as those at atmospheric pressure (Rayleigh breakup, sinuous wave break up, and atomization). However, the empirical classification by dimensionless analysis (Ohnesorge number) applied only for atmospheric pressure. The authors modified the Ohnesorge number in order to take into account the density of the gas phase. Results showed that an additional correction for the viscosity of the dense gas was needed in order to describe the regimes of jet disintegration in one unified diagram (modified Ohnesorge *versus* Reynolds number) appropriately. With this approach, the authors were able to determine the range boundaries that describe the

disintegration of jets in pressurized gases. The main conclusions of Niels Czerwonatis & Eggers (2001) were that, compared to the disintegration of liquid jets at atmospheric pressure, the regime of atomization in pressurized gases is reached at lower nozzle outlet velocities, and lower liquid flows are necessary to reach atomization. As long as the generated drops maintain a spherical shape these were found to move faster than hard spheres because of the induced inner circulation flow.

A known application of CC-SE is the stripping of caffeine from CO₂ with water using a high-pressure washing tower (Kurt Zosel, 1974). To the best of the authors' knowledge, there are no other applications of CC-SE and TP-SE.

Particle size, size distribution, and morphology are characteristics that are highly dependent on process parameters that must be optimized based on an exhaustive knowledge of phase equilibria and thermodynamic behavior of the system (Knez et al., 2015). Additionally, relevant physicochemical properties such as density, viscosity, and interfacial tension play also a key role in fluid dynamics and mass transfer. Moreover, these properties are of the utmost importance to achieve optimum separation efficiencies for all the technologies described in Sections 2.1 to 2.5.

2.6 Phase equilibrium and relevant physicochemical properties

As mentioned above, the requirement of knowledge of phase equilibria is transversal to all technologies because they are essentially separation processes. Separation processes are based on phase equilibrium of adjacent fluid or fluid-solid phases. Consequently, the presence of an interphase is essential for mass transfer of the desired solute. However, the rate of mass transfer is dependent on both, equilibrium and hydrodynamic conditions. Physicochemical properties such as density, viscosity, and InterFacial Tension (IFT) are relevant parameters used to characterize the hydrodynamics of the phases inside any separation equipment.

2.6.1 Phase equilibrium

Table 2.5 lists selected experimental phase equilibrium data relevant to the fractionation technologies and areas of application described in this work. The information

listed in Table 2.5 includes the systems studied, experimental temperatures and pressures, and type of data. The information presented is limited to the three main areas of research described in this work: fractionation of edible oil components and derivatives, deterpenation of essential oils, and fractionation of alcoholic beverages. Thereby, only phase equilibrium measurements of ternary or more complex mixtures (real systems) are listed in Table 2.5. Comprehensive information of binary or other mixtures can be found in specific high-pressure phase equilibria reviews (Christov & Dohrn, 2002; Dohrn & Brunner, 1995; Dohrn, Peper, & Fonseca, 2010; J. M. S. Fonseca, Dohrn, & Peper, 2011; R. E. Fornari, Alessi, & Kikic, 1990).

Phase equilibrium of edible oil components and derivatives is an extensive field. However, the respective experimental data and available correlations for more than three components or real mixtures are scarce. Usually, the approach is to define pseudo-binary mixtures based on the predominant components of the real mixture. Experimental data of model mixtures containing valuable vegetable oil components such as methyl oleate, α -tocopherol, and triolein, among other components of edible oil plus CO₂ can be found in Gast et al. (2005a), Bharath, Inomata, Adschiri, & Arai (1992), T Fang, Goto, Sasaki, & Hirose (2005) and Tao Fang, Goto, Yun, Ding, & Hirose (2004), and Inomata et al. (1989). Partition coefficients and phase equilibrium of fish oil components can be found in W B Nilsson, Seaborn, & Hudson (1992), Catchpole, Grey, & Noermark (1998), and Riha & Brunner (1999). Comprehensive information on the separation of constituents of fish oil using supercritical fluids, including experimental solubility and extraction studies can be consulted in Staby & Mollerup (1993).

In the case of essential oils, information is available mainly for citrus fruits oil and some effort has been done to study the phase behavior of complex mixtures, at least ternary systems such as model mixtures of (CO₂ + limonene + linalool) and (CO₂ + limonene + citral) at 323 K and pressures <11 MPa (Benvenuti & Gironi, 2001; Cháfer, Berna, Montón, & Mulet, 2001; J. Fonseca et al., 2003; Vieira De Melo, Pallado, Guarise, & Bertucco, 1999). Binary systems composed of typical citrus terpenes with CO₂ have been reported by J. Fonseca et al. (2003).

The phase behavior, concerning the fractionation of alcoholic beverages, is relatively well studied. Nevertheless, mainly simple and model systems have been considered. The phase equilibrium of the binary system (CO_2 + ethanol) and other higher chain and substituted alcohols is readily accessible in literature (Christov & Dohrn, 2002; Dohrn & Brunner, 1995; Dohrn et al., 2010; J. M. S. Fonseca et al., 2011; R. E. Fornari et al., 1990). Information on more complex systems like the ternary (CO_2 + ethanol + water) are presented by T. Fornari, Hernández, Ruiz-Rodríguez, Señoráns, & Reglero (2009). Recent works focus on the thermodynamic modelling for the removal of ethanol from alcoholic beverages (brandy, wine, and cider) using predictive Equations of State (EoS) Ruiz-Rodríguez et al. (2012, 2010).

Table 2.5 Phase equilibria. Studied system, temperature and pressure ranges, and type of equilibrium data of selected references.

System	Temperature / K	Pressure / MPa	Type of data	Reference
Edible oil and derivatives				
(CO ₂ + oleic acid + triolein) (CO ₂ + kernel oil) (CO ₂ + sesame oil)	313; 323; 333; 253	20.0; 25.0; 30.0; 6.0–33.0	Pxy and partition coefficients of triglyceride groups.	(Bharath et al., 1992)
(CO ₂ + ethyl esters of menhaden oil) (CO ₂ + ethyl esters of menhaden oil + Ethanol)	333	12.5	Partition coefficients of ethyl esters in SC-CO ₂ and SC-CO ₂ with 5%wt ethanol.	(W B Nilsson et al., 1992)
(CO ₂ + cod liver oil) (CO ₂ + vitamin A palmitate + spiny dogfish liver oil) (CO ₂ + squalene + orange roughy oil + spiny dogfish liver oil + cod liver oil + ethanol)	313; 323; 333	10.0–30.0	Pxy: Solubility of Squalene, Orange Roughy oil, Spiny Dogfish liver oil, Cod liver oil and Vitamin A Palmitate in SC-CO ₂ and solubility of CO ₂ in liquid phase.	(Catchpole et al., 1998)
(CO ₂ + ethyl ester mixtures from sardine oil)	313; 333; 343; 353	9.0–25.0	Pxy: mass fraction ethyl esters (C14–C22) in both, gas and liquid phases. Peng-Robinson EoS correlation of ternary mixtures.	(Riha & Brunner, 1999)
(CO ₂ + methyl oleate + α -tocopherol)	313; 333; 353	10.0; 20.0; 29.0	xy: mol fraction of methyl oleate and α -tocopherol in both, gas and liquid phases.	(Fang et al., 2005)
(CO ₂ + Crude palm oil) (CO ₂ + SODD)	310; 340; 370 343; 353; 363	20.0–30.0	Pxy; mol fraction of crude palm oil and SODD in both, gas and liquid phases. Partition coefficients of minor components.	(Gast et al., 2005)
(CO ₂ + olive husk oil + methanol) (CO ₂ + olive husk oil + ethanol)	328; 338	30.0; 35.0	Solubility of olive husk oil in SC-CO ₂ with (1 and 5)%v/v of methanol and ethanol. Chrastil correlation.	(de Lucas, Gracia, Rincón, & García, 2007)

Table 2.5 cont'd Phase equilibria. Studied system, temperature and pressure ranges, and type of equilibrium data of selected references.

System	Temperature / K	Pressure / MPa	Type of data	Reference
(CO ₂ + β -carotene + ethanol) (CO ₂ + β -carotene + ethyl acetate)	303; 313; 323; 333; 343	3.0–12.0	Bubble and dew points: Synthetic method. β -carotene concentrations from (0.10 to 0.34) g·L ⁻¹ . Peng-Robinson EoS correlation.	(Borges et al., 2007)
(CO ₂ + caffeine + ethanol)	313	15.0	Solubility values of caffeine in CO ₂ + ethanol at various ethanol concentrations	(Iwai, Nagano, Lee, Uno, & Arai, 2006)
(CO ₂ + oleic acid + squalene)	313; 323; 333	14.0–22.0	Vapor and liquid phase compositions at various squalene global mass fractions (0.25, 0.50 and, 0.75).	(Ruivo, Couto, & Simões, 2007)
(CO ₂ + ethanol + sunflower oil)	313; 333	13.0; 20.0	LL and LSC phase compositions. GC-EoS modelling and prediction.	(Hernández et al., 2008)
(CO ₂ + propane + sunflower oil)	308	2.8–6.2	LL and LLV phase compositions. GC-EoS modelling and prediction.	(Hegel, Mabe, Pereda, Zabaloy, & Brignole, 2006)
(CO ₂ + carnosic acid + ethanol)	313; 323; 333	28.0–40.0	Solubility of solid carnosic acid in SC-CO ₂ with 0.7 to 10% of ethanol.	(Cháfer, Fornari, Berna, Ibañez, & Reglero, 2005)
Essential oils				
(Ethane + orange peel oil)	282–363	1.0–10.0	Bubble, dew and critical points: synthetic method. Peng-Robinson EoS correlation.	(Sampaio de Sousa, Raeissi, Aguiar-Ricardo, Duarte, & Peters, 2004)
(CO ₂ + orange peel oil)	303; 333; 343	4.0–13.0	Compositions of both phases at equilibrium	(Budich & Brunner, 1999; Budich et al., 1999; Budich, 1999)
(CO ₂ + lemon oil) (Ethane + lemon oil)	298–313	0.4–8.8	Solubility of lemon oil in SC-CO ₂ and ethane. Soave-Redlich-Kwong EoS correlation. Molar densities of saturated liquid phase.	(de la Fuente & Bottini, 2000)

Table 2.5 cont'd Phase equilibria. Studied system, temperature and pressure ranges, and type of equilibrium data of selected references.

System	Temperature / K	Pressure / MPa	Type of data	Reference
(CO ₂ + limonene + linalool)	333	7.5; 8.1; 8.8; 8.9	xy; compositions of both phases at equilibrium (tie lines). Selectivity between limonene and linalool in CO ₂ .	(Vieira De Melo et al., 1999)
(CO ₂ + limonene + linalool)	318; 328	7.0–11.0	xy; compositions of both phases of mixtures of global compositions (40:60%wt) limonene:linalool and (60:40%wt) linalool:limonene. Selectivity between limonene and linalool in CO ₂ .	(Cháfer et al., 2001)
(CO ₂ + limonene + linalool) (Ethane + limonene + linalool)	293–363	3.0–14.0	Bubble dew and critical points: synthetic method. Liquid-liquid-vapor equilibrium.	(Raeissi & Peters, 2005a, 2005b)
(CO ₂ + limonene + citral)	315	8.4; 9.0	xy; compositions of both phases at equilibrium (tie lines)	(Benvenuti & Gironi, 2001)
(CO ₂ + propane + camphor)	304–384	2.4–15.0	Bubble and dew points of the mixture: synthetic method. Peng-Robinson EoS correlation.	(Carvalho Jr, Corazza, Cardozo-Filho, & Meireles, 2006)
Aqueous systems				
(CO ₂ + ethanol + water)	271–280, 313; 323; 328; 333; 343.	1.3–30.0 21.0; 29.8.	Bubble points (synthetic method), xy data GC-EoS, PR-EoS modelling. Hydrate dissociation pressures and temperatures.	(de la Fuente, Núñez, & del Valle, 2007; Durling, Catchpole, Tallon, & Grey, 2007; T. Fornari, Hernández, et al., 2009; Mohammadi, Afzal, & Richon, 2008)
(CO ₂ + 1-butanol + water)	297	5.9–6.4	LL equilibrium. Cloud-point data	(Najdanovic-Visak, Rebelo, & Nunes da Ponte, 2005)
(CO ₂ + wine) (CO ₂ + whiskey)	308; 313; 318; 328	9.7–29.8	xy; compositions of both phases at equilibrium (tie lines), GC-EoS modelling pseudo ternary mixtures.	(T. Fornari, Hernández, et al., 2009)

Table 2.5 cont'd Phase equilibria. Studied system, temperature and pressure ranges, and type of equilibrium data of selected references.

System	Temperature / K	Pressure / MPa	Type of data	Reference
(CO ₂ + acetone + water)	314; 353; 395 270–279	0.1–10.0 0.8–3.5	Solubility of CO ₂ in acetone water solutions, Henry's constants and UNIQUAQ modelling. Hydrate dissociation pressures	(Jödecke, Pérez-Salado Kamps, & Maurer, 2007) (Seo, Kang, Lee, & Lee, 2008)
(CO ₂ + caffeine + water) (CO ₂ + caffeine + ethanol+ water)	313	15.0	Solubility of caffeine in (CO ₂ + water) and (CO ₂ + ethanol+ water) at various water and ethanol concentrations.	(Iwai et al., 2006)
(Propane + 2-propanol + water) (Propane + ethanol + water) (Ethane + 2-propanol + water) (Ethane + ethanol + water)	272–282	0.2–1.3	Hydrate dissociation pressures and temperatures.	(Mohammadi et al., 2008; Mohammadi & Richon, 2007)
(CO ₂ + ethanol + p-coumaric acid + water) (CO ₂ + ethanol + resveratrol + water) (CO ₂ + ethanol + quercetin-3-glucoside + water) (CO ₂ + ethanol + catechin + water)	313	15.0; 20.0	VL equilibrium. Separation factors of phenolic compounds between gaseous and liquid phases.	(Nunes, Matias, Nunes da Ponte, & Duarte, 2007)
(CO ₂ + ethanol + boldine + water) (CO ₂ + ethanol + catechin + water) (CO ₂ + ethanol + boldine + catechin + water) (CO ₂ + ethanol + boldo leaf tincture + water)	313; 323; 333; 343	5.1–17.0	Bubble-point pressures, xy data; Synthetic method.	(de la Fuente et al., 2007)

LL, (liquid + liquid); VL, (vapor + liquid); LSC, (liquid + SuperCritical); LLV, (liquid + liquid + vapor); SODD, Soybean oil deodorizer distillate.

In particular, the GC-EoS showed reasonable good results when applied to simulate the countercurrent SC-CO₂ dealcoholization of model systems representing wine, brandy, and cider (Ruiz-Rodríguez et al., 2010). Ruiz-Rodríguez et al. (2010) used experimental data of the (CO₂ + ethanol), and (CO₂ + water) binary mixtures, and the (CO₂ + ethanol + water) ternary mixture, and readjusted the interaction parameter of H₂O-CH₂OH in order to achieve good modeling results. With the model developed by Ruiz-Rodríguez et al. (2010) the authors were able to estimate process conditions to achieve an ethanol content reduction from 10 wt% to values lower than 1 wt%. Additionally, Ruiz-Rodríguez et al. (2012) used the model to develop a two-step process for the production of a low-alcohol beverage from wine, but maintaining the aroma and the antioxidant activity similar to that of the original wine.

There is limited information regarding experimental data on equilibrium of odorant compounds of non-alcoholic beverages plus CO₂ at elevated pressures. The main challenge in phase behavior is to study and model complex multicomponent mixtures in order to come closer to real mixtures, which is difficult from both the experimental and the mathematical standpoint. Phase equilibrium measurements are very time-consuming and complicated tasks, especially for heterogeneous and multicomponent mixtures at elevated pressures. Complex EoS models are needed to describe and predict these systems appropriately. Usually experimental data are obtained for a particular application in a relatively narrow range of pressures and temperatures.

In view of the difficulty in obtaining reliable phase equilibrium data and versatile models applicable to a wide range of mixtures and conditions, a common strategy in modelling CC-SFF and membrane contactors, is to use empirical correlations or a simple or a predictive EoS, such as the Peng-Robinson EoS or the GC-EoS.

Besides phase equilibrium, the hydrodynamics of the phases inside the separation equipment is decisive for obtaining high separation efficiencies by improving mass transfer rates. In order to characterize the hydrodynamics, it is important to study relevant physical properties such as density, viscosity, and IFT.

2.6.2 Density and viscosity

The density and viscosity of loaded supercritical fluids and expanded liquid phases in the three areas of research described in this work is scarce. Densities and viscosities of coexisting phases of lipid-type mixtures with CO₂ such as Anhydrous Milk Fat (AMF) fatty acids and derivatives (Kashulines, Rizvi, Harriott, & Zollweg, 1991; Siegfried Peter & Jakob, 1991; D. Q. Tuan, Zollweg, Harriott, & Rizvi, 1999; Yener, Kashulines, Rizvi, & Harriott, 1998), cocoa butter (Calvignac, Rodier, Letourneau, Almeida dos Santos, & Fages, 2010), fish oil fatty acid ethyl esters (Staby & Mollerup, 1993b), minor components of edible oils such as α -tocopherol and β -carotene (Pecar & Dolecek, 2007, 2008), and capsaicin (Elizalde-Solis & Galicia-Luna, 2006) are predominant. Experimental data on the volumetric behavior of essential oil constituents and aqueous systems with CO₂ or other gases were not found in the literature. Few studies reporting experimental data of binary mixtures of alcohols or acetone with CO₂ are reported in the literature (Kariznovi, Nourozieh, & Abedi, 2013a; Pöhler & Kiran, 1997; Zúñiga-Moreno & Galicia-Luna, 2002). Indeed, most studies reporting experimental values of the volumetric behavior of mixtures with CO₂ or other gases at high pressures relate to hydrocarbons (Bessièrès, Saint-Guirons, & Daridon, 2001; Kalaga & Trebble, 1999; Kariznovi, Nourozieh, & Abedi, 2013b; Kiran, Pöhler, & Xiong, 1996; Medina-Bermudez, Saavedra-Molina, Escamilla-Tiburcio, Galicia-Luna, & Elizalde-Solis, 2013; Pöhler et al., 1996; Sen & Kiran, 1990; Tilly, Foster, Macnaughton, & Tomasko, 1994). Fluid densities can also be obtained from phase equilibrium modelling by use of an appropriate EoS.

Siegfried Peter & Jakob (1991) reported that the viscosity and density of binary mixtures of pelargonic, oleic, linoleic, and valeric acid with CO₂ and ethane (C₂H₆) were similar. The authors found that the viscosity of the coexisting gas phase increases with increasing pressure whereas the viscosity of the liquid phase decreases. Additionally, the authors showed that the density of the liquid phase of systems containing C₂H₆ decreases with increasing pressure (increasing gas content) while that of systems containing CO₂ increases. Dilatant flow behavior was observed for the systems (CO₂ + pelargonic acid) and (C₂H₆ + pelargonic acid). The other binary systems showed Newtonian flow behavior.

A similar work carried out by Kashulines et al. (1991) and Yener et al. (1998) evaluated applicability of two viscosity models developed for liquid mixtures (Arrhenius and Grunberg equations) to SC-CO₂ / liquid mixtures. The authors measured the viscosity of several types of lipids saturated with SC-CO₂ such as oleic and linoleic acid, its methyl esters, and the complex mixture of AMF. The authors found that the viscosity of the fatty acid methyl esters saturated with SC-CO₂, decreased 5 to 10 times as pressure increased from 0.1 to 8.0 MPa. Similar behavior was observed for the fatty acids and the AMF. At constant pressure, the viscosity of the fatty acids and AMF decreased with increasing temperature, whereas the viscosity of the fatty acid methyl esters increased with increasing temperature.

Results of the modelling reported by Kashulines et al. (1991) and Yener et al. (1998) showed that if only pure component viscosities and mixture compositions are used, errors using the Arrhenius equation were 52% for the fatty acids, 10% for the fatty acid methyl esters, and 111% for the AMF. These large errors were partially attributed to the large difference in viscosity between the mixture components. By the introduction of an experimentally determined adjustable parameter (Grunberg equation) the model errors were reduced to 8% for the fatty acids, 10% for the fatty acid methyl esters, and 5% for AMF. The authors also showed that all the mixtures had Newtonian behavior. D. Tuan, Zollweg, & Harriott (1999) measured the viscosity of binary (CO₂ + methyl oleate) and (CO₂ + AMF) systems and evaluated the applicability of a modified Ely and Hanel's corresponding state model (addition of an adjustable parameter in energy shape term) in order to improve the prediction capability of the purely correlative Grunberg and Nissan models. With this approach the authors described well the viscosity of both the fluid and liquid phases with an average absolute deviation of 3 to 6%.

Staby & Mollerup, (1993b) reported the density of the liquid phase along with experimental solubility of fish oil fatty acid ethyl esters in SC-CO₂. They showed that the densities of the liquid phases were almost constant when the CO₂ content of the liquid phase (x_{CO_2}) was < 80% and that the highest densities occurred at the lowest temperature. The authors also observed that at $x_{\text{CO}_2} > 80\%$ the density suddenly decreased as the

supercritical region was approached, and that at x_{CO_2} in the range of 90 to 95% the density curves cross over.

For minor components of edible oil, Pecar & Dolecek (2007, 2008) reported experimental density data of β -carotene and α -tocopherol in SC-CO₂ at various concentrations within wide intervals of temperature (308 to 333 K) and pressure (10 to 40 MPa). The data obtained for α -tocopherol was successfully correlated with the Peng-Robinson EoS and the Panagiotopoulos-Reid mixing rule.

2.6.3 Interfacial tension and contact angle

Besides the important effect of density and viscosity of the coexisting phases in the operation of separation equipment, their sizing further needs to account for apparent interfacial effects. These are IFT and contact angles on the technical surfaces involved in the process. IFT is a key property, especially when drops are formed. In spray columns (and other processes which make use of the large exchange area of small liquid drops) knowledge of the IFT of the employed liquids is crucial. This property defines the area-to-volume ratio of a liquid embedded in another fluid and thus, the drop size distribution (Sutjiadi-Sia, Jaeger, & Eggers, 2008a).

The idea of employing structured and random packing columns is to enlarge the exchange area and in this way to increase the efficiency of the process. In packed columns, the property that controls the extent of the exchange area is called wettability, which is characterized by the so-called three-phase contact angle and influenced by the IFT. An appropriate wettability enhances mass transfer rates and, in consequence, improves the separation efficiency of the process. Other applications where the IFT is an important parameter are nucleation and bubble formation in polymer melts (Jaeger, Eggers, & Baumgartl, 2002; Liao, Li, Park, & Chen, 2010), reservoir systems and CO₂ storage (Georgiadis, Llovel, et al., 2010; Jaeger & Eggers, 2012; H. Y. Jennings & Newman, 1971), ionic liquids (Jaeger & Eggers, 2009), and the use of modern EoS based on the Statistical Association Fluid Theory (SAFT) for modelling and prediction of IFT and other interfacial properties (Hu, Chen, & Mi, 2012; Niño-Amézquita, Enders, Jaeger, & Eggers, 2010a, 2010b). However, the work of Niño-Amézquita, van Putten, & Enders (2012) and

Hu et al. (2012) contribute to the understanding of the interfacial phenomena of aqueous systems. The authors used the van der Waals density gradient theory in combination with the Perturbed Chain Polar (PCP-SAFT) and the First-order Mean Spherical Approximation (FMSA-SAFT) EoS to overcome the challenge correctly describe water, due to strong hydrogen bonding. Aqueous systems are involved in the fractionation of alcoholic beverages and removal of acetone from water.

Table 2.6 lists selected IFT datasets that provide relevant information regarding the main application areas in this work (edible oil components and derivatives, essential oils and alcoholic beverages).

Table 2.6 Interfacial tension (IFT) datasets from selected references, system under study, experimental temperatures and pressures, and IFT measurement method.

System	Temperature / K	Pressure / MPa	Method	Reference
Edible oil and derivatives				
Binary mixtures of pelargonic and linoleic acid + ethane and CO ₂	313; 333; 353	0.1–25.0	CR / DNR	(Hiller, Schiemann, Weidner, & Peter, 1993)
Binary mixtures of pelargonic acid + N ₂ , Ar, He, and H ₂ Binary mixtures of stearic acid + CO ₂ , ethane, He and H ₂	313–393	0.1–25.0	PD-DSA	(Schiemann, Weidner, & Peter, 1993)
Binary mixtures of methyl myristate, methyl palmitate and, pelargonic and oleic acid + CO ₂ Methyl myristate + Methyl palmitate + CO ₂	313; 323; 333	0.1–17.5	CR	(Lockemann, 1994)
Binary mixtures of coffee, walnut, wheat and olive oil + CO ₂	313–393	0.1–50.0	PD-DSA	(Jaeger et al., 1996)
α -Tocopherol + CO ₂	313– 402	0.1–37.0	PD-SP	(Moser, Pietzonka, & Trepp, 1996)
Olive oil + oleic acid + CO ₂	313; 353	0.1–40.0	PD-DSA	(Simões, Eggers, & Jaeger, 2000)
Binary mixtures of vegetable oil + N ₂ and CO ₂	343; 353	0.1–30.0	PD-DSA	(Czerwonatis & Eggers, 2001)
Binary mixtures of commercial corn germ oil, and wheat, palm and olive oil + CO ₂ and N ₂	313–393	0.1–50.0	PD-DSA	(Dittmar, Eggers, Kahl, & Enders, 2002)
Refined (Mazola®) and unrefined corn germ oil + CO ₂			PD-DSA	(Dittmar, De Arévalo, Beckmann, & Eggers, 2005)
Fish oil triglycerides + CO ₂ Fatty acids ethyl esters + CO ₂	313; 328; 343	0.1–25.0	PD-DSA	(Seifried & Temelli, 2010)
Corn germ oil + CO ₂	313	0.1–27.0	PD-DSA	(Sutjiadi-Sia et al., 2008a)
Essential oils				
Lemon oil + CO ₂	313–393	0.1–50.0	PD-DSA	(Jaeger et al., 1996)
Ethanol and Aqueous systems				
(Ethanol + water) + CO ₂	278–344	0.1–18.6	CR	(Chun & Wilkinson, 1995)

Table 2.6 cont'd Interfacial tension (IFT) datasets from selected references, system under study, experimental temperatures and pressures, and IFT measurement method.

System	Temperature / K	Pressure / MPa	Method	Reference
Binary mixtures of water + N ₂ and CO ₂	343; 353	0.1–30.0	PD-DSA	(Czerwonatis & Eggers, 2001)
Binary mixtures of ethanol and water + CO ₂	293–355	0.1–27.5	PD-DSA	(Dittmar, Oei, & Eggers, 2002; Oei, Dittmar, & Eggers, 2001)
Water + CO ₂	278–333	0.1–20.0	PD-DSA	(Hebach et al., 2002; Kvamme, Kuznetsova, Hebach, Oberhof, & Lunde, 2007)
Ethanol + N ₂	296; 314; 355	0.1–20.0	PD-DSA	(Dittmar, Fredenhagen, Oei, & Eggers, 2003)
Water + CO ₂ and brine + CO ₂	308–383	5.0–45.0	PD-DSA	(Chiquet, Daridon, Broseta, & Thibaud, 2007)
Ethanol and water + CO ₂ and (Ethanol + water) + CO ₂	313	0.1–27.0	PD-DSA	(Sutjiadi-Sia et al., 2008a)
IFT on solid materials of binary mixtures of water and ethanol + CO ₂ and binary mixtures of water, formamide, ethanediol, and toluene + N ₂	313	0.1–27.0	DSA	(Sutjiadi-Sia, Jaeger, & Eggers, 2008b)
Water + CO ₂ and brine + CO ₂	293–393	2.0–27.0	PD-DSA	(Bachu & Bennion, 2009)
Binary mixtures of (carbon dioxide + n-alkane) and (carbon dioxide + water)	298–443	0.1–60.0	PD-DSA	(Georgiadis, Llovel, et al., 2010)
Water + CO ₂	298–374	1.0–60.0	PD-DSA	(Georgiadis, Maitland, Trusler, & Bismarck, 2010)

PD=Pendant drop, CR= Capillary rise, DNR= Du Nouy Ring method, DSA=Drop shape analysis, SP= Selected plane.

It is well known that the IFT of a liquid in dense CO₂ declines with increasing pressure. In general, as pressure increases the surrounding CO₂ dissolves into the liquid decreasing the IFT of the liquid. The behavior of the IFT of several edible oils with temperature and pressure are relatively well known specially for CC-SFF of fish oil constituents (Seifried & Temelli, 2010), vegetable oil constituents (Hiller et al., 1993; Lockemann, 1994; Moser et al., 1996; Schiemann et al., 1993), vegetable oils such as walnut, wheat, olive, palm, and un- and refined corn oils (Dittmar et al., 2005; Dittmar, Eggers, et al., 2002; Jaeger et al., 1996; Simões et al., 2000), and lemon essential oil (Jaeger et al., 1996), and coffee oil (Jaeger et al., 1996).

In order to understand the transport phenomena that occurs at the interface of a fluid/liquid separation process, Jaeger et al. (1996) reported and compared the IFT data of different oils in contact with CO₂ (walnut, wheat, lemon, and coffee) and investigated the mass transport into pendant oil drops simultaneously. The authors observed the decreasing tendency of the IFT with increasing pressure due to increased adsorption of the compressed fluid at the interface. Additionally, the authors studied IFT at various conditions of pressure and temperature and as a function of time showing that in the case of considerable mutual solubility, IFT further decreases with time as mass transfer into the bulk phase proceeds. Similarly, Pedro C Simões et al. (2000) used Portuguese extra virgin olive oil, enriched with oleic acid to a known amount of free fatty acids (7.6% w/w), to compare the IFT data with those of other edible oils. They found that triglycerides (walnut and wheat) with low content of volatiles behaved similarly to the extra virgin olive oil. The behavior of coffee and lemon oil was different because of their strong IFT decrease at moderate pressures resulting in a vanishing interfacial tension at the point of complete miscibility (Jaeger et al., 1996).

A similar work was carried out by Dittmar, Eggers, et al. (2002) who modelled and compared for the first time the IFT and the mixture density of triglycerides in contact with CO₂ and N₂. The authors found that IFT of the triglyceride mixtures (corn, germ, palm, wheat, and olive oils) were similar. Additionally, the IFT in contact with CO₂ and N₂ decreased with increasing pressure. The modelling of the IFT of triglycerides in contact with CO₂ or N₂ using the density gradient theory and an EoS was successful. Nevertheless,

the authors suggested that it is essential to choose the appropriate EoS for modelling the IFT in systems of CO₂ at high pressure. Additionally, for complex systems, *e.g.*, for triglyceride mixtures, it is indispensable to check the EoS by means of experimental equilibrium data (*e.g.*, density, volume, or mole fraction). Dittmar et al. (2005) studied the IFT behavior of refined (Mazola®) and unrefined corn germ oil in contact with CO₂ at lower temperatures (263 to 295 K). The authors found that the unrefined corn germ oil showed lower IFT, possibly caused by the presence of minor components lost in the refining process, and the addition of vitamin E to the refined oil.

Regarding aqueous systems, available data on IFT and contact angles are limited to pure water in dense CO₂ (Bachu & Bennion, 2009; Chiquet et al., 2007; Georgiadis, Maitland, et al., 2010; Hebach et al., 2002; Kvamme et al., 2007) and (ethanol + water) solutions in dense CO₂ (Chun & Wilkinson, 1995; Sutjiadi-Sia et al., 2008a, 2008b).

Enders & Kahl (2008) measured and modelled IFT for (ethanol + water) and (1-butanol + water) solutions at atmospheric pressure. Other sources of IFT data of pure water in contact with different gases, other than CO₂, can be consulted in Dittmar et al. (2003). Information regarding IFT data for ethanol in CO₂ and N₂, are also available in Oei et al. (2001) and Dittmar et al. (2003). No data for other aqueous mixtures in contact with CO₂ at elevated pressures were found in the literature.

Sutjiadi-Sia et al. (2008a) studied the interfacial phenomena of aqueous systems in dense CO₂. The authors used the pendant drop method to measure IFT, and the sessile drop method to estimate contact angles of pure water and the system (water + ethanol) surrounded by CO₂ at 313 K and pressures ≤ 27 MPa. Wetting was studied on three different materials commonly found in industry: PTFE, steel, and glass. Sutjiadi-Sia et al. (2008a) observed the same decreasing tendency of the IFT as pressure increased as in the oily systems. The authors showed that the change in the IFT with increasing pressure is closely related to the mass transfer between the bulk phases, *i.e.*, in systems composed of water, ethanol, and CO₂ the IFT of a drop changes until ternary equilibrium is reached. Sutjiadi-Sia et al. (2008a) also reported drop phenomena such as kicking of the drop, upward motion of the continuous phase around the drop, rising bubbles in the drop phase,

and intense stirring in the drop during mass transfer. Additionally, the authors demonstrated that a precise estimation of the IFT requires the values of the instantaneous, mean densities of both phases, which sometimes are unavailable. Regarding the contact angles, Sutjiadi-Sia et al. (2008a) observed increasing values at higher pressures, and the water mixtures showed better wettability (lower contact angles) on glass than on the other materials.

Based on these observations, Sutjiadi-Sia et al. (2008a) concluded that when aqueous drops are desired in a spray column, it is advantageous to work with higher CO₂ pressures because the wetting becomes poorer (formation of small drops due to lower IFT). However, for such systems less liquid hold up is expected. The authors also concluded that when a wide covering film is expected for an optimal mass transfer between the phases, high CO₂ pressure might be disadvantageous in spite of the decreasing IFT, which should rather promote wetting. As a consequence, interfacial phenomena at high pressure need to be precisely characterized and accounted for in order to decide whether a packed or a spray column will achieve better separation results.

A comparison of available data on IFT of water in CO₂ at high pressures from different sources is shown in Fig 2.5. As it can be seen there are significant discrepancies between the data, especially at higher pressures. Moreover, as shown by Sutjiadi-Sia et al. (2008a), the effect of the density of the phases used in the calculation of IFT is significant. From the discussion above it becomes clear that, although IFT is an essential requirement for several processes, so far there is an important lack of relevant data for aqueous systems at elevated pressures.

As described at the beginning of the section, IFT and contact angles are key properties that define the separation efficiency of the separation process. Poor or imprecise knowledge of these properties may lead to errors in the design of high-pressure extraction columns, and to obtain separation efficiencies far from the optimum.

The IFT of the liquid phase plays an important role in the break-through pressure in membrane contactors. However, experimental studies of IFT and wetting behavior in membrane contactors are non-existent. The wetting of the membrane in membrane

contactors is a non-desirable event because CO_2 absorption can cause long-term operational concerns and mass transfer efficiency may decrease. A detailed discussion of the wetting phenomenon, as well as different methods to avoid membrane wetting, along with their advantages and disadvantages can be found in Mosadegh-Sedghi, Rodrigue, Brisson, & Iliuta (2014).

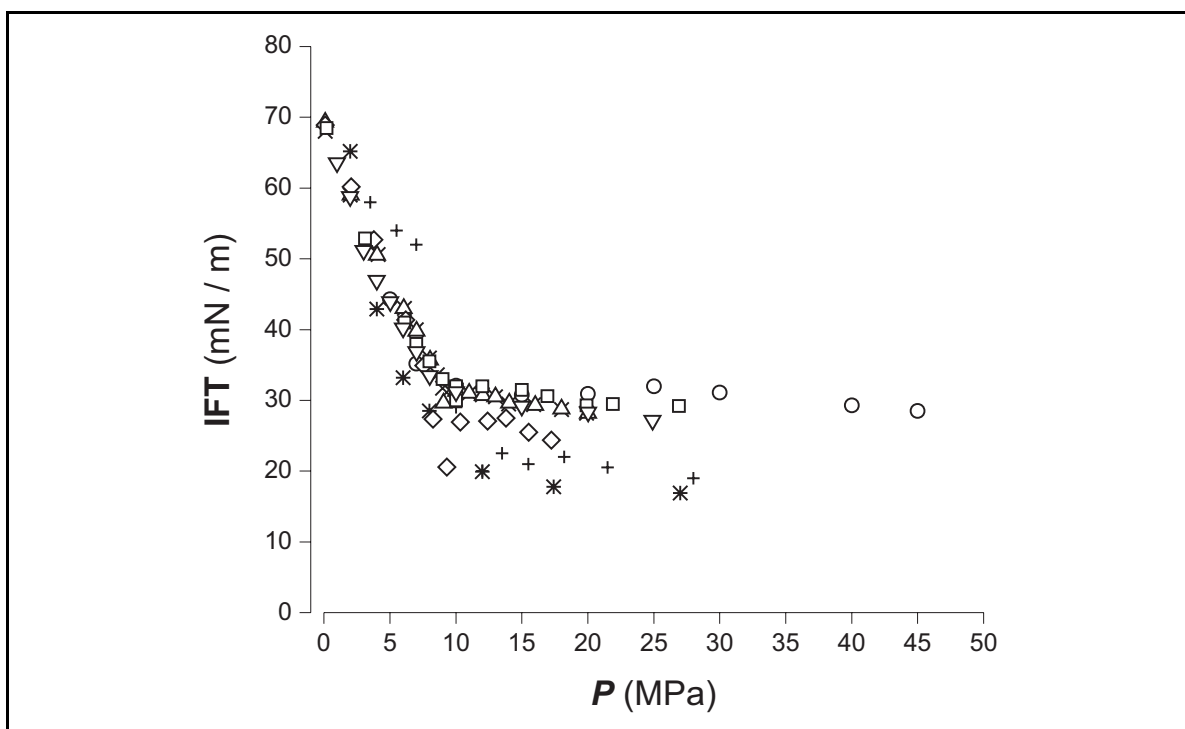


Figure 2.5 Interfacial tensions (IFT) at various pressures (P) for pure Water in contact with CO_2 . (*), Bachu & Bennion (2009) at 314 K; (\circ), Chiquet et al. (2007) at 308 K; (\diamond), Chun & Wilkinson (1995) at 311 K; (\square), Dittmar, Oei, et al. (2002) at 313 K; (∇), Georgiadis, Maitland, et al. (2010) at 313 K; (\triangle), Hebach et al. (2002) at 318 K; (\times), Kvamme et al. (2007) at 318 (+), Sutjiadi-Sia et al. (2008a) at 313 K.

3. HIGH-PRESSURE (VAPOR + LIQUID) EQUILIBRIA FOR TERNARY SYSTEMS COMPOSED BY (*E*)-2-HEXENAL OR HEXANAL + CARBON DIOXIDE + WATER: PARTITION COEFFICIENT MEASUREMENT

3.1 Introduction

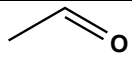
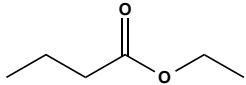
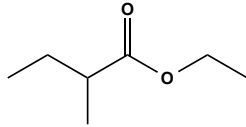
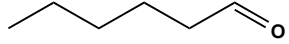
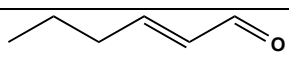
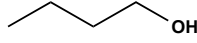
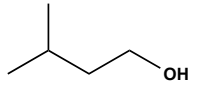
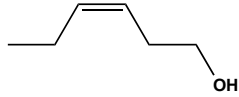
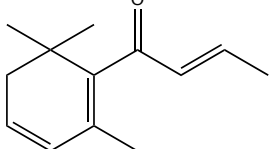
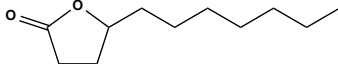
Fruit aroma is a complex combination of numerous volatile compounds that contribute to the overall sensory quality of the fruit and is specific to the species and cultivar (Sanz et al., 1997). Dimick et al. (1983) reviewed the apple aroma profile and reported an extensive list of over 300 volatile compounds that include alcohols, aldehydes, carboxylic esters, ketones, and ethers among others. Approximately 20 compounds including C-6 aldehydes and alcohols, usually present in very low concentrations, are considered essential constituents that contribute to strong characteristics typical of apple aroma (Dixon & Hewett, 2000). Table 3.1 includes some examples of key apple odorants along with their chemical structure, sensory descriptor, occurrence, and odor threshold.

Flath et al. (1967) identified and made an organoleptic evaluation of compounds in a 150-fold commercial “Delicious” apple essence. The authors found that (*E*)-2-hexenal, hexanal, hexanol, and ethyl-2-methylbutyrate were responsible for the apple odor. The apple-like odor was described as ‘good, green, ripe apple’ in over 85% of the responses. Although, (*E*)-2-hexenal and hexanal are not in significant amounts in the whole fruit, they are rapidly formed upon crushing (Drawert, Kuchendauer, Brickner, & Schreier, 1976), and they are mainly responsible for sensory impressions, such as ‘green, fresh, estery’ in commercial apple juices (Nikfardjam & Maier, 2011). Moreover, Koch (1976) demonstrated the importance of (*E*)-2-hexenal in the odor of apple essences. The concentration of these compounds in apple juice, and essence apple varies from (1 to 2400) $\text{mg}\cdot\text{dm}^{-3}$ (Carelli, Crapiste, & Lozano, 1991; Elss, Preston, Appel, Heckel, & Schreier, 2006; Jouquand, Ducruet, & Giampaoli, 2004; Nikfardjam & Maier, 2011; Versini, Franco, Moser, Barchetti, & Manca, 2009).

Traditionally, fruit aromas are recovered from the concentrated juice production process using techniques based on distillation/evaporation or partial condensation (Belitz et al., 2009; Birjessön et al., 1996). Alternative technologies for the recovery,

concentration and fractionation of fruit aromas are membrane processes, such as pervaporation, and less common techniques such as CounterCurrent Supercritical Fluid Fractionation (CC-SFF) in packed columns (Bejarano, Simões, & del Valle, 2016; Budich, 1999; Mukhopadhyay, 2000).

Table 3.1 Chemical structure, aroma, occurrence, and odor threshold of some apple key odorants.

Compound	Chemical structure	Aroma	Occurrence	Odour Threshold (Czerny et al., 2008)/ $\mu\text{g}\cdot\text{dm}^{-3}$
Acetaldehyde		Fresh green.	Apple and several fruits	15–120
Ethyl butyrate		Fruity.	Apple, strawberry, alcoholic beverages, cheese	0.0032–450
Ethyl 2-methylbutyrate		Fruity.	Apple, strawberry, wild berries, and citrus fruits	0.1–0.5
Hexanal		Green, grassy.	Apple, strawberry, orange, and lemon oil	4.5–479
(E)-2-Hexenal		Green apple-like, bitter almond like.	Apple, tomato	17–316
1-Butanol		Malty, solvent-like.	Apple and several fruits	500–1,240
3-Methyl-1-butanol		Fruity-winey, malty solvent-like.	Apple juice, Alcoholic beverages	71–1,900
(Z)-3-Hexenol		Green grassy odour, lettuce-like.	Apple and several Fruits	39–347
(E)- β -Damascenone		Baked apple-like, grape juice-like.	Apple and several fruits	0.00075–0.001
γ -Undecalactone		Sweet, oily-fruity, peach-like taste.	Apple and several fruits	4.2–150

The applications of CC-SFF in packed columns of aqueous solutions are mainly related to alcoholic beverages. The topics of most intense scientific research are

dealcoholization (Budich & Brunner, 2003; Gamse et al., 1999; Medina & Martínez, 1997; Ruiz-Rodríguez et al., 2010; Señoráns, Ruiz-Rodríguez, Ibáñez, et al., 2001; Señoráns, Ruiz-Rodríguez, Ibáñez, et al., 2001) and separation of the aroma of wine and other spirits (da Porto & Decorti, 2010; Gracia, Rodríguez, García, Alvarez, & García, 2007; Macedo et al., 2008; Ruiz-Rodríguez et al., 2012; Señoráns et al., 2003). However, information in literature concerning recovery and concentration of aromas from aqueous beverages (*e.g.*, natural fruit aromas) using CC-SFF is very scarce. Few works have been reported on CC-SFF of non-alcoholic beverages and they are mainly related to the separation of orange juice antioxidants (Señoráns, Ruiz-Rodríguez, et al., 2001; Simó et al., 2002). Nevertheless, the actual number of commercial scale CC-SFF processes is currently low (Brunner, 2010).

In general, for the design of packed columns, the separation is treated as a staged process, and uses the packed bed Height Equivalent to a Theoretical Plate (HETP) to convert the number of ideal stages required to a height of packing. According to the double-film theory the relationship between HETP and the Height of the mass-Transfer Unit for the gas phase (HTU_G) and for the liquid phase (HTU_L) is given by the following equations (Wang et al., 2005):

$$HETP = \frac{Z}{N}, \text{ and} \quad (3.1a)$$

$$HETP = \frac{\ln(\lambda)}{\lambda - 1} \cdot (HTU_G + HTU_L), \quad (3.1b)$$

where Z is the height of packing, N is the number of theoretical stages, and λ is the stripping factor defined as the ratio between the slope of the operating line (mass balance) and that of the equilibrium line, *i.e.*, vapor phase (y_i) *versus* liquid phase (x_i) mole fraction.

When assuming binary or pseudo-binary systems, low concentrations of the solute, straight equilibrium and operation lines (generally true in CC-SFF), and constant molar overflow throughout the column, the equations described above can be solved using conventional methods. The number of stages can be estimated by graphical methods such

as those of McCabe-Thiele or Ponchon-Savarit as described by Brunner (1994, 1998, 2009) or by numerical integration of traditional expressions for the Number of Transfer Units (NTU) (Sinnott, 1999).

It is clear that to successfully apply CC-SFF in packed columns of aqueous fruit aroma solutions both pilot plant experiments (mass transfer and hydrodynamics data) and (vapor + liquid) equilibrium (VLE) data of mixtures composed of (CO_2 + water + aroma compounds) are required. The main objective of this work was to contribute with the partition coefficients ($k_i = y_i/x_i$) of (*E*)-2-hexenal and hexanal between CO_2 and water in order to begin the construction the equilibrium line at several temperatures and pressures, and to suggest, from the equilibrium perspective, reasonable initial operation conditions of temperature and pressure for CC-SFF of aqueous apple aroma solutions. Conditions of temperature and pressure where high partition coefficients and separation factors are observed would be preferable for CC-SFF.

The k_i were determined by measuring the VLE, at fixed liquid phase composition, of the ternary systems (CO_2 + (*E*)-2-hexenal + water) and (CO_2 + hexanal + water). The experimental data was measured at a pressure range of (8 to 19) MPa and at temperatures of (313, 323 and 333) K. To the best of the authors' knowledge there is no experimental data regarding VLE of the ternary systems (CO_2 + (*E*)-2-hexenal + water) and (CO_2 + hexanal + water). Due to the lack of thermodynamic information of apple aromas, this work also contributed with a short article reporting the vapor pressure of some of the key apple aromas in the range of 25 to 190 kPa (for details see Appendix 1).

The experimental apparatus for high-pressure VLE was modified in order to measure multicomponent phase equilibrium; therefore, measurement of the isothermal VLE of the binary system (CO_2 + ethanol) and the ternary system (CO_2 + ethanol + water) were used to check the validity of the methodology.

3.2 Experimental

3.2.1 Materials

The reagents (*E*)-2-hexenal and hexanal were acquired from Sigma-Aldrich (St. Louis, MO). LiChrosolv® Ethanol was obtained from Merck (Darmstadt, Germany), HPLC water (specific conductance $<1.5 \mu\text{S cm}^{-1}$) from TEDIA (Fairfield, USA) and carbon dioxide and helium were purchased from Linde S.A. Specifications of all materials used in this work are summarized in Table 3.2. All substances were used without further purification.

Table 3.2 Chemical material specifications.

Chemical name	Source	Initial Purity / $\text{kg}\cdot\text{kg}^{-1}$	Purification method	Final purity $\text{kg}\cdot\text{kg}^{-1}$	Analysis method
Ethanol	Merck	>0.999	None	>0.999	GC ^(b)
(<i>E</i>)-2-Hexenal	Sigma-Aldrich	>0.995	None	0.995	GC ^(b)
Hexanal	Sigma-Aldrich	0.98	None	0.999	GC ^(b)
Water	Tedia	$<1.5^{(a)}$	None	$<1.5^{(a)}$	Specific conductance
Carbon dioxide	Linde S.A.	0.99999	None	0.99999	GC ^(b)
Helium	Linde S.A.	0.99995	None	0.99995	GC ^(b)

^(a) Specific conductance at 25°C / $\mu\text{S cm}^{-1}$ ^(b) Gas Chromatography

3.2.2 Experimental apparatus and procedure

The VLE measurements were carried out in a modified experimental apparatus assembled in this work. Originally, the experimental apparatus was used to measure high-pressure VLE of (CO_2 + alcohol) binary systems using the static-analytical method in which the phase compositions were determined gravimetrically as described in a previous work (Gutiérrez, Bejarano, & de la Fuente, 2010). The modifications of the experimental set up consisted in the implementation of a Rapid Online Sampler-Injector (ROLSI™, Armines/CEP/TEC, Paris, France) for the vapor phase (Guilbot, Valtz, Legendre, & Richon, 2000).

Fig. 3.1 shows a schematic diagram of the modified experimental set up. The main component of the system was a high-pressure equilibrium cell (1) (2.12 VID View Cell, Thar Technologies, Pittsburgh, PA) with 0.6 dm^3 of total volume, and three windows

used to verify the number of phases. The equilibrium pressure was measured using a pressure transducer (8) (Heise, Shelton, CT). The temperature inside the cell was measured and adjusted to the set value with a PID controller (9) (Digi-Sense, Vernon Hills, IL) connected to four electrical resistances on the cell (1000 W). The standard uncertainties (u) in the temperature and pressure were $u(T) = 0.1$ K and $u(p) = 0.05$ MPa. A syringe pump (13) (Teledyne ISCO, 206D, Lincoln, NE, USA) was used to feed CO₂ to the apparatus from the storage tank (10).

The sampling arrangement for the vapor phase included, the automatic electromagnetic capillary ROLSI™ sampler (2), the ROLSI™ control unit (19) which controls the sampler aperture time, the temperature of the sampler itself and that of the transfer line (6) to the gas chromatograph (7) (GC) (PerkinElmer, Clarus 500, Waltham, MA) used for detection and quantification. The liquid phase sampling setup included a needle valve (HiP model 15-11AF1, Erie, PA, USA), an expansion and flow control valve (3) (Butech, SFPMMV26V, Erie, PA, USA), a cold-trap (4) (home-made) for the phase separation, and a wet-test meter (5) (Ritter, TG 05/5, Bochum, Germany) to measure the CO₂ content. The volume (v) of CO₂ was measured in the wet-test meter with $u(v) = 2$ cm³. The experimental equipment can be operated up to a temperature of 373 K and a pressure of 68 MPa.

The experimental procedure was as follows; to start an experiment the equilibrium cell was cleaned and dried. The liquid mixture (250 cm³) with fixed composition (600 mg·kg⁻¹) was fed through the top window of the cell. The CO₂ was fed to the equilibrium cell (1) assisted by the syringe pump (13) operated at constant flow in the range of 0.02–0.04 dm³·min⁻¹. With all components loaded to the cell, the temperature of the cell was set to the desired value in the controller (9), after the system reached the desired temperature the pressure was registered with the pressure transducer (8) in periods of approximately 75 minutes. The equilibrium condition was reached when two consecutive measurements in pressure had a relative deviation <0.5% and when three to five injections of the vapor phase into the GC (7) gave peak areas with relative deviation <5%. The temperature value of the ROLSI™ sampler (2) and its transfer line (6) to the GC

was set at 10 K over the normal boiling point of less volatile component in the mixture (423 K).

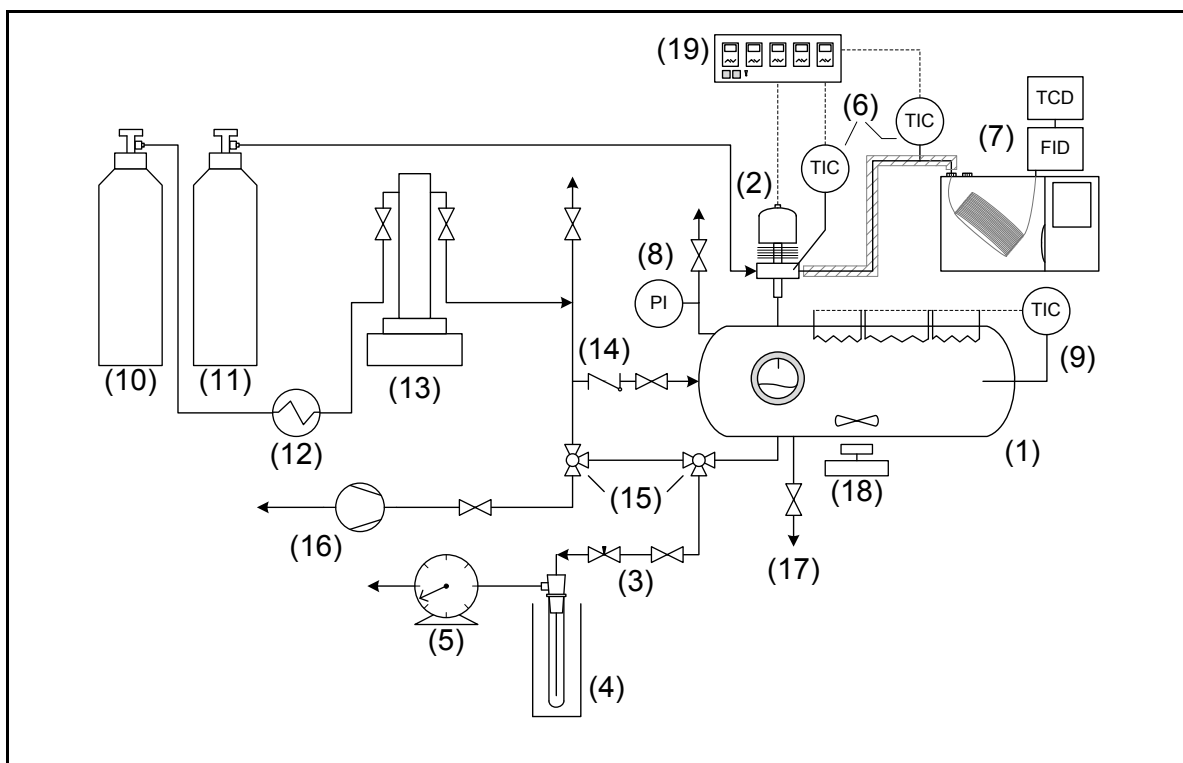


Figure 3.1 Schematic flow diagram of the experimental apparatus. (1) Equilibrium view cell, (2) Vapor phase auto-sampler (ROLSI™), (3) Liquid phase sampling valves, (4) Cold-trap, (5) Wet-test meter, (6) ROLSITM heated transfer line, (7) Gas chromatograph, (8) View cell pressure indicator, (9) View cell temperature control system, (10) CO₂ tank, (11) Carrier gas tank, (12) Cooler, (13) Syringe pump, (14) Feed line check valve, (15) Three-way valves, (16) Vacuum pump, (17) Liquid expulsion valve, (18) Magnetic stirrer, (19) ROLSITM control unit.

Immediately after the equilibrium criterion was met, three samples were withdrawn from the liquid phase using the needle valve and the flow control valve (3). The liquid sample was expanded into the cold-trap (4) placed in an ice bath at 273 K, where the condensable component (aqueous mixture) and CO₂ (non-condensable component) were separated. For the vapor phase, each reported point corresponds to the arithmetic average of the three to five experimental measurements after the equilibrium criterion was met. For the liquid phase, each reported point corresponds to the arithmetic average of the three

experimental measurements. After each point was measured, the liquid phase sampling line was cleaned with fresh CO₂, using two-way valves (15), and a vacuum pump (16). The vapor phase line was continuously cleaned by the carrier gas flow from its storage tank (11).

3.2.1 Analyses and quantification

In this work the molar composition of each component in both, liquid and vapor phases was calculated taking into account all components in the mixture. However, some approximations were found in literature, *e.g.*, Brudi et al. (1996) neglected the dissolved amount of water in the vapor phase and the quantity of dissolved CO₂ in the liquid phase.

Different analysis techniques were applied according to each system, solute in the liquid phase and phase sampled (vapor or liquid). All methods are described in detail below and are summarized in Table 3.3.

Table 3.3 Quantification methodology of each component according to system studied, phase sampled and sampling method.

System	Phase	Sampling method	Quantification	
			Component	Methodology
CO ₂ + ethanol	Vapor	ROLSI™	CO ₂ and ethanol	GC ^(a)
	Liquid	Cold-trap	CO ₂	Wet-test meter + density data ^(b)
			Ethanol	Analytic balance
CO ₂ + ethanol + water	Vapor	ROLSI™	CO ₂ , ethanol, and water	GC ^(a)
	Liquid	Cold-trap	CO ₂	Wet-test meter + density data ^(b)
			Ethanol + water	RI ^(c) + literature (Nowakowska, 1939) + analytic balance
CO ₂ + (<i>E</i>)-2-Hexenal + water	Vapor	ROLSI™	CO ₂ , (<i>E</i>)-2-Hexenal, and water	GC ^(a)
	Liquid	Cold-trap	CO ₂	Wet-test meter + density data ^(b)
			(<i>E</i>)-2-Hexenal + water	SP ^(d) + analytic balance
CO ₂ + Hexanal + water	Vapor	ROLSI™	CO ₂ , Hexanal, and water	GC ^(a)
	Liquid	Cold-trap	CO ₂	Wet-test meter + density data ^(b)
			Hexanal + water	SP ^(d) + analytic balance

^(a) Gas Chromatography, ^(b) Density data from (Lemmon, Huber, & McLinden, 2013), ^(c) Refractive Indices at 298 K, ^(d) SpectroPhotometry

For the vapor phase and all the systems studied, a gas chromatograph (GC) (PerkinElmer, Clarus 500, Waltham, MA) equipped with Flame Ionization Detector (FID) and Thermal Conductivity Detector (TCD), was used. Injection was made with the

automatic ROLSI™ sampler through a splitless injector. The separation was performed in a HayeSep C–ValcoPLOT® Capillary Column from VICI Metronics (Houston, TX) with 30 m long, internal diameter of 0.53 mm and film thickness of 20 µm. Samples of known mole content were previously injected to perform the calibration curves for each component in the system. Sample chromatograms of the vapor-phase for the ternary systems (CO₂ + (*E*)-2-hexenal + water) and (CO₂ + hexanal + water) can be seen in Appendix 2.

For the binary system (CO₂ + ethanol), the liquid phase composition was calculated from the mass (*m*) collected in the cold-trap, measured with an analytical balance (RADWAG, AS220/C/2, North Miami Beach, USA) with $u(m) = 1$ mg, the volume of CO₂ measured in the wet-test meter, and CO₂ density data (Lemmon et al., 2013).

For the ternary system (CO₂ + ethanol + water), the CO₂ composition of the liquid phase was calculated from the volume of CO₂ measured in the wet-test meter plus CO₂ density data. The ethanol and water content of the liquid mixture remaining in the cold-trap was calculated from the mass collected in the cold-trap, and the measurement of the refractive indices at 293 K in a refractometer (Bausch & Lomb, ABBE-32, Rochester, New York, USA) plus literature data (Nowakowska, 1939).

For the ternary systems (CO₂ + (*E*)-2-hexenal + water) and (CO₂ + hexanal + water), the quantification procedure was similar to the other cases. The determination of the (*E*)-2-hexenal, hexanal, and water content of the liquid mixture remaining in the cold-trap was calculated using a spectrophotometer (Thermo Scientific, G10S UV-Vis, PuDong, Shanghai, China). Samples of known mole content were used to perform the calibration curves for each component in the mixture (*i.e.*, (*E*)-2-hexenal and hexanal). The measurements were performed at the maximum absorption wavelength (λ) of each component, $\lambda = 225$ nm for (CO₂ + (*E*)-2-hexenal + water) and $\lambda = 281$ nm for (CO₂ + hexanal + water). The later were found by scanning the sample in the UV-Vis range (190 to 1,100 nm).

The experimental uncertainties for the molar composition in both phases, considering the variability in the measurements, the uncertainty of calibration curve, and

taking into account all sources of error were estimated according to Miller & Miller (2010) and Chirico et al. (2003). The results were similar for the four systems studied in this contribution. The standard combined uncertainties (u_{comb}) for the vapor phase were $u_{\text{comb}}(y) < 0.004$ and for the liquid phase, $u_{\text{comb}}(x) < 0.001$.

3.3. Results and discussion

3.3.1 Validation of the experimental apparatus and methodology: (CO₂ + ethanol) and (CO₂ + ethanol + water) systems

In order to verify the operation of the new static-analytic set-up described in Fig. 3.1, experimental VLE information from literature for the (CO₂ (1) + ethanol (2)) binary system at temperature of 313 K was compared with the data measured in this work. Each point was calculated as the arithmetic average of three to five experimental measurements as described in Table 3.3. The estimated combined uncertainties (u_{comb}) were $0.0002 \leq u_{\text{comb}}(x_1) \leq 0.0008 \text{ mol} \cdot \text{mol}^{-1}$ for the liquid phase and $0.001 \leq u_{\text{comb}}(y_1) \leq 0.002 \text{ mol} \cdot \text{mol}^{-1}$ for the vapor phase.

Fig. 3.2 shows the molar fraction of CO₂ in the vapor (y_1) and liquid (x_1) phases measured as a function of pressure (p) for the binary system (CO₂ (1) + ethanol (2)). Table 3.4 lists the experimental (vapor + liquid) equilibria data of the binary system (CO₂ (1) + ethanol (2)) at 313 K. Data selected from literature (Chang, Day, Ko, & Chiu, 1997; D. W. Jennings et al., 1991; Joung et al., 2001; Meneses, 2012; Secuianu, Feroiu, & Geană, 2008; K. Suzuki et al., 1990; Tsivintzelis, Missopolinou, Kalogiannis, & Panayiotou, 2004) were also included in Figure 3.2 for comparison. The discrepancies observed between the experimental data from this study and from the data reported in literature for the liquid phase was <6%, and for the vapor phase was <0.5%. As it can be seen from Fig. 3.2, the data reported by Gutiérrez et al. (2010) deviates significantly from the literature, especially for the vapor phase mole fraction at pressures below 5 MPa. Gutiérrez et al. (2010) used a manual gravimetric sampling method for the vapor phase. With this method, especially at low pressures, high uncertainties of ethanol content in the vapor phase were detected due to the amount of sample that can be withdrawn from the equilibrium cell without altering significantly the equilibrium pressure inside the cell.

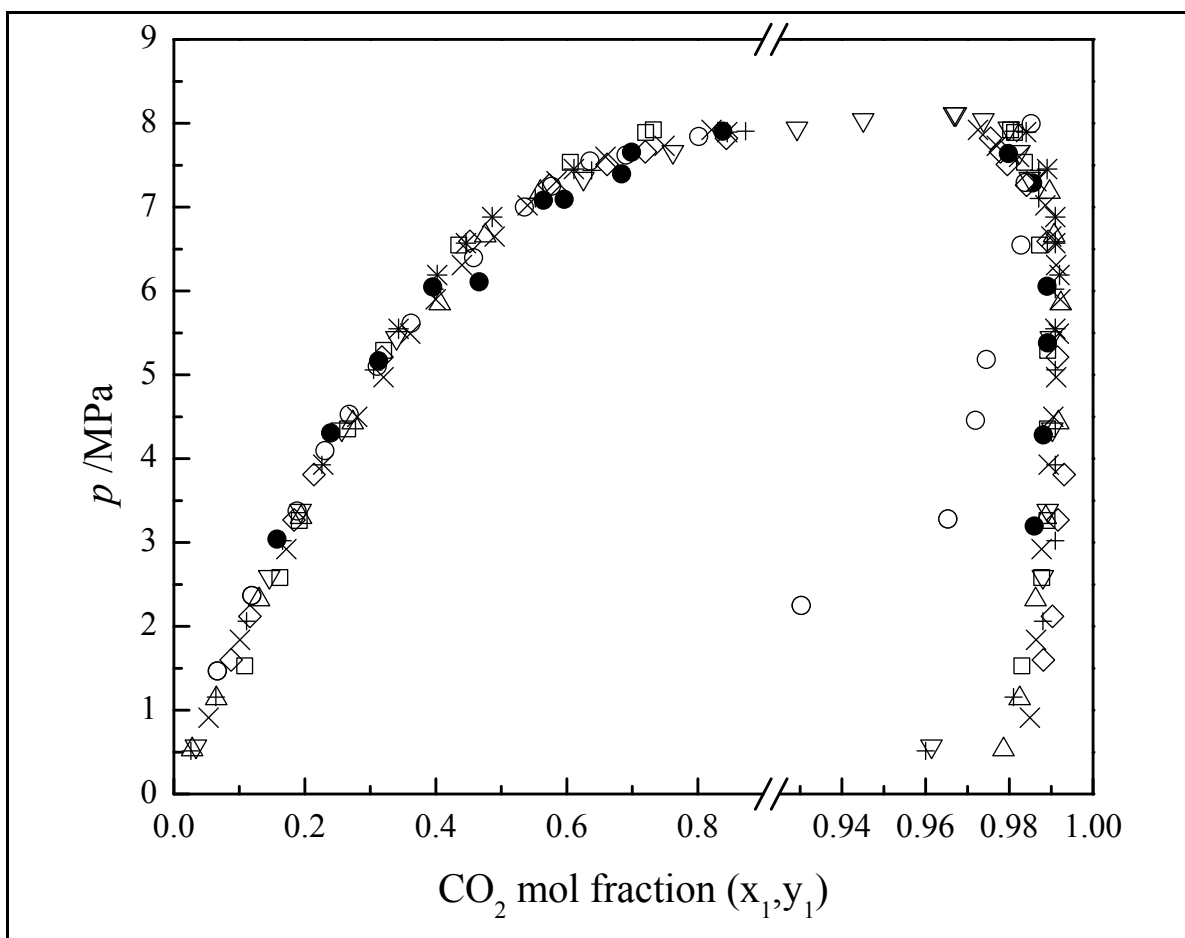


Figure 3.2 Isothermal (vapor + liquid) equilibria for the system (CO₂ (1) + ethanol (2)) at 313.2 K: (●) this work; (□) Meneses (2012); (○) Gutiérrez et al. (2010); (△) Secuianu et al. (2008); (◇) Tsvintzelis et al. (2004); (▽) Joung et al. (2001); (×) Chang et al. (1997); (*) Jennings et al. (1991); (+) Suzuki et al. (1990a).

In addition, to verify the validity of the methodology for ternary systems, literature VLE information from literature for the ternary system (CO₂ (1) + ethanol (2) + water (3)) 333 K and 10.1 MPa were compared with the data measured in this work. Table 3.5 lists the experimental y_i and x_i of each component i for the ternary system (CO₂ (1) + ethanol (2) + water (3)) at 333 K and 10.1 MPa. Each point was calculated as the arithmetic average of three to five experimental measurements as described in Table 3.3. For the liquid phase, the estimated uncertainties of each component were $0.0004 \leq u_{\text{comb}}(x_1) \leq 0.04 \text{ mol} \cdot \text{mol}^{-1}$, $0.003 \leq u_{\text{comb}}(x_2) \leq 0.06 \text{ mol} \cdot \text{mol}^{-1}$, and $0.0003 \leq u_{\text{comb}}(x_3) \leq$

$0.07 \text{ mol} \cdot \text{mol}^{-1}$. For the vapor phase, the estimated uncertainties of each component were $0.003 \leq u_{\text{comb}}(y_1), u_{\text{comb}}(y_3) \leq 0.004 \text{ mol} \cdot \text{mol}^{-1}$, and $0.0001 \leq u_{\text{comb}}(y_2) \leq 0.0003 \text{ mol} \cdot \text{mol}^{-1}$.

Table 3.4 Experimental (vapor + liquid) equilibria for the system (CO_2 (1) + ethanol (2)). Liquid (x_i) and vapor phase (y_i) mole fractions and combined standard uncertainties (u_{comb}) at pressures (p) and at $T=313 \text{ K}$.

p /MPa	x_1	$u_{\text{comb}}(x_1)$	p /MPa	y_1	$u_{\text{comb}}(y_1)$
	$\text{mol}\cdot\text{mol}^{-1}$			$\text{mol}\cdot\text{mol}^{-1}$	
3.04	0.1627	0.0007	3.20	0.986	0.002
4.31	0.2477	0.0008	4.28	0.988	0.001
5.17	0.3220	0.0008	5.38	0.989	0.001
6.05	0.4049	0.0008	6.05	0.989	0.001
6.11	0.4767	0.0007	7.29	0.986	0.001
7.09	0.6110	0.0005	7.64	0.980	0.001
7.08	0.5783	0.0005			
7.39	0.6916	0.0005			
7.65	0.7083	0.0004			
7.95	0.8441	0.0002			

$u(p)=0.05 \text{ MPa}$, $u(T)=0.1 \text{ K}$

Fig. 3.3 shows the results of the VLE measurements for the ternary system (CO_2 (1) + ethanol (2) + water (3)) in terms of the solvent free mass fraction of ethanol in the vapor (y_2) and liquid (x_2) phases. Additionally, Fig. 3.4 shows the triangular phase diagram for the same ternary system. Data reported in literature (Budich & Brunner, 2003; Furuta, Ikawa, Fukuzato, & Imanishi, 1989, 1990; J.-S. Lim, Lee, & Chun, 1994; T. Suzuki, Tsuge, & Nagahama, 1990) were also included in Figure 3.3 and Figure 3.4 for comparison. The discrepancies, observed between this work and the data reported in the literature, of the mole fractions of the liquid and vapor phases were $<4\%$ and $<2\%$, respectively.

In general, according to the comparison results above, the experimental results obtained in this work for the binary (CO_2 + ethanol) and ternary (CO_2 + ethanol + water) systems were found to be in very good agreement with those in the literature.

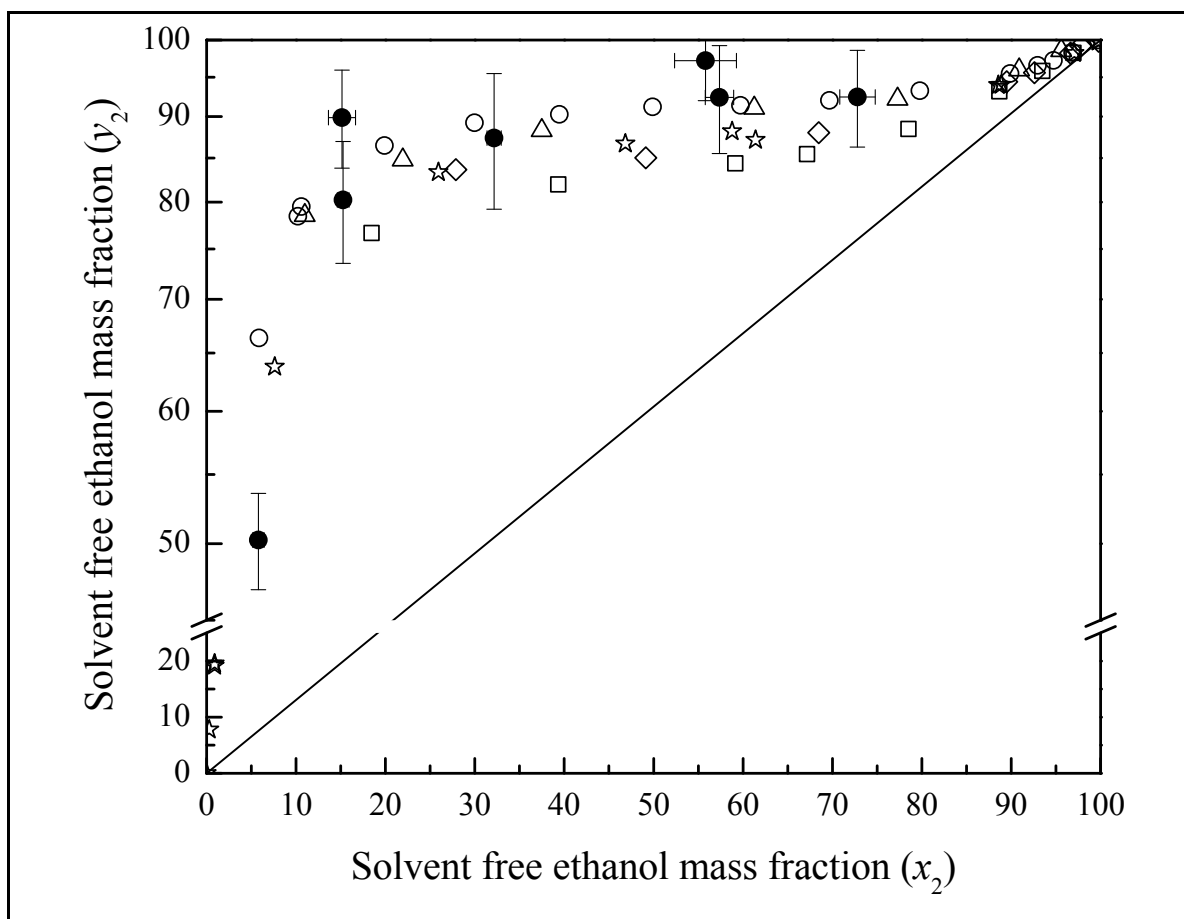


Figure 3.3 Solvent free mass fractions of the ternary (vapor + liquid) equilibria for the system (CO_2 (1) + ethanol (2) + water (3)) at 333.2 K and 10.1 MPa: (●) this work; (☆) Budich & Brunner (2003); (□) Lim et al. (1994); (○) Furuta et al. (1990); (△) Suzuki et al. (1990a); (◇) Furuta et al. (1989).

Table 3.5 Experimental (vapor + liquid) equilibria for the system (CO₂ (1) + ethanol (2) + water (3)). Liquid (x_i) and vapor phase (y_i) mass fractions and combined standard uncertainties (u_{comb}) at pressures (p) and at $T= 333$ K.

p / MPa	y_1	y_2	y_3	$u_{\text{comb}}(y_1)$	$u_{\text{comb}}(y_2)$	$u_{\text{comb}}(y_3)$	x_1	x_2	x_3	$u_{\text{comb}}(x_1)$	$u_{\text{comb}}(x_2)$	$u_{\text{comb}}(x_3)$
	$\text{kg} \cdot \text{kg}^{-1}$											
10.11	0.9821	0.0090	0.0089	0.0028	0.0001	0.0028	0.0345	0.0559	0.9096	0.0004	0.0028	0.0032
10.05	0.9906	0.0084	0.0009	0.0029	0.0001	0.0028	0.0374	0.1457	0.8168	0.0006	0.0049	0.0053
10.22	0.9859	0.0113	0.0028	0.0036	0.0002	0.0035	0.0399	0.1466	0.8135	0.0011	0.0061	0.0067
10.06	0.9844	0.0136	0.0020	0.0033	0.0002	0.0032	0.0635	0.3011	0.6354	0.0048	0.0169	0.0190
9.96	0.9821	0.0165	0.0014	0.0033	0.0003	0.0032	0.1529	0.4859	0.3612	0.0371	0.0595	0.0750
10.20	0.9789	0.0205	0.0006	0.0033	0.0002	0.0032	0.1628	0.4672	0.3700	0.0187	0.0425	0.0495
10.03	0.9764	0.0218	0.0018	0.0028	0.0001	0.0028	0.3364	0.4831	0.1805	0.0004	0.0028	0.0032

$u(p)= 0.05$ MPa, $u(T)= 0.1$ K

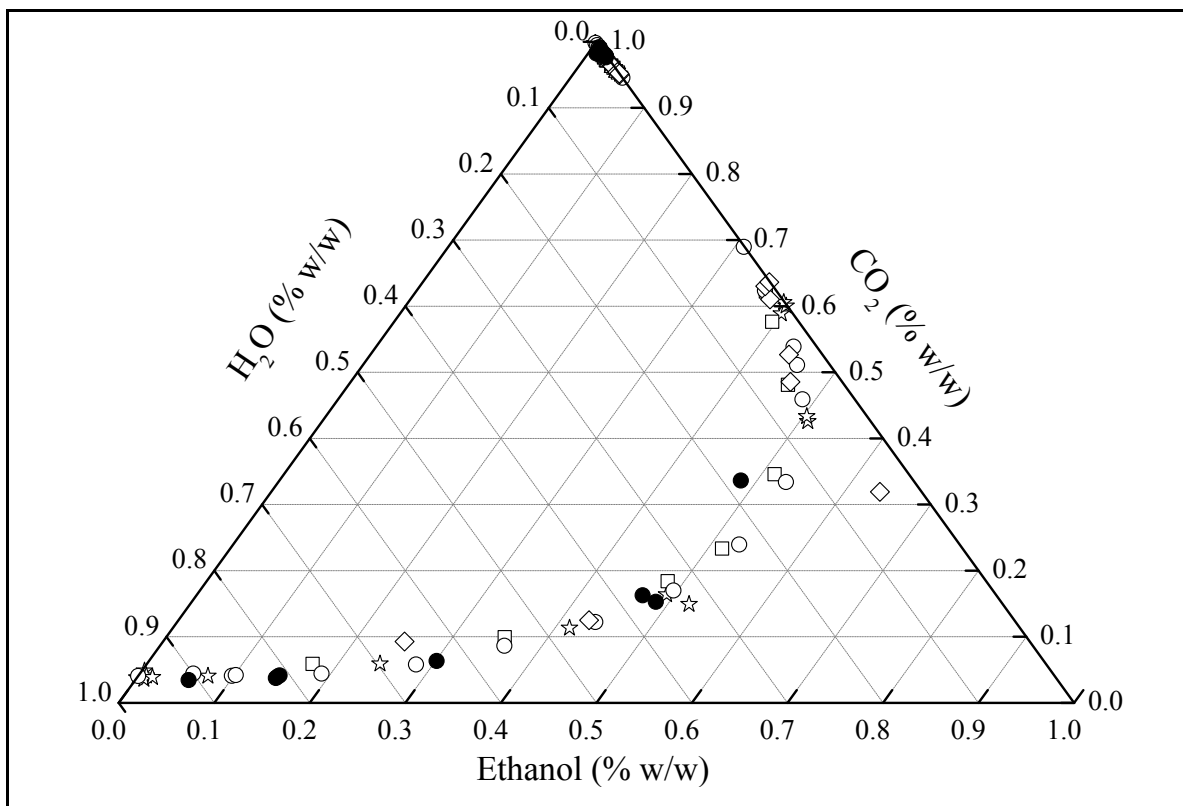


Figure 3.4 Ternary (vapor + liquid) equilibria for the system (CO_2 (1) + ethanol (2) + water (3)) at 333.2 K and 10.1 MPa: (●) this work; (☆) Budich & Brunner (2003); (□) Lim et al. (1994); (○) Furuta et al. (1990); (△) Suzuki et al. (1990a); (◇) Furuta et al. (1989).

3.3.2 Partition coefficients and separation factors of apple aroma constituents

In order to calculate the k_i of the apple aroma constituents i , (*E*)-2-hexenal and hexanal, VLE measurements of the ternary systems (CO_2 (1) + (*E*)-2-hexenal (2) + water (3)) and (CO_2 (1) + hexanal (2) + water (3)) were carried out at temperatures of (313, 323, and 333) K and at pressures from (8 to 19) MPa. The k_i of both (*E*)-2-hexenal and hexanal were calculated from the experimental VLE data ($k_2 = y_2/x_2$). The experimental x_i and y_i of the three components, along with the k_2 of (*E*)-2-hexenal and hexanal are listed in Table 3.6 and Table 3.7, respectively.

Table 3.6 Experimental (vapor + liquid) equilibria for the system (CO₂ (1) + (*E*)-2-Hexenal (2) + water (3)). Vapor (y_i) and liquid phase (x_i) mole fractions, partition coefficients of (*E*)-2-Hexenal (k_2), and combined standard uncertainties (u_{comb}) at pressures (p) and temperatures (313, 323 and 333) K.

p / MPa	y_1	$y_2 \cdot 10^3$	y_3	u_{comb} (y_1)	u_{comb} (y_2) $\cdot 10^3$	u_{comb} (y_3)	x_1	$x_2 \cdot 10^3$	x_3	u_{comb} (x_1)	u_{comb} (x_2) $\cdot 10^3$	u_{comb} (x_3)	$k_2 = y_2/x_2$	u_{comb} (k_2)
mol·mol ⁻¹														
$T = 313$ K														
8.6	0.9985	0.1061	0.0014	0.004	0.029	0.004	0.0143	0.00681	0.9857	0.0005	0.0003	0.0005	15.6	3.7
10.5	0.9975	0.1321	0.0024	0.003	0.022	0.003	0.0198	0.00261	0.9802	0.0004	0.0003	0.0004	50.6	8.3
12.6	0.9971	0.1455	0.0028	0.002	0.019	0.002	0.0202	0.00213	0.9798	0.0004	0.0003	0.0004	68.3	11.3
14.6	0.9963	0.1468	0.0036	0.002	0.016	0.002	0.0177	0.00179	0.9823	0.0004	0.0002	0.0004	82.0	14.3
15.9	0.9953	0.1525	0.0046	0.002	0.016	0.002	0.0176	0.00174	0.9824	0.0004	0.0002	0.0004	87.6	12.9
17.2	0.9939	0.1536	0.0059	0.002	0.013	0.002	0.0189	0.00168	0.9811	0.0004	0.0002	0.0004	91.7	12.7
$T = 323$ K														
8.2	0.9976	0.1622	0.0022	0.004	0.032	0.004	0.0133	0.0284	0.9866	0.0004	0.0014	0.0014	5.7	0.9
10.2	0.9975	0.1632	0.0024	0.003	0.024	0.003	0.0139	0.0082	0.9861	0.0004	0.0006	0.0006	19.9	8.3
12.1	0.9962	0.1251	0.0037	0.003	0.019	0.003	0.0156	0.0031	0.9844	0.0004	0.0005	0.0005	40.8	7.9
14.5	0.9956	0.1130	0.0043	0.002	0.016	0.002	0.0147	0.0020	0.9853	0.0003	0.0003	0.0003	57.8	10.9
15.9	0.9947	0.1085	0.0052	0.002	0.014	0.002	0.0188	0.0017	0.9812	0.0004	0.0004	0.0004	64.4	16.5
18.3	0.9948	0.1040	0.0051	0.002	0.011	0.002	0.0255	0.0014	0.9745	0.0004	0.0003	0.0003	73.2	16.4
$T = 333$ K														
7.9	0.9940	0.1599	0.0059	0.004	0.032	0.004	0.0112	0.0286	0.9888	0.0005	0.0015	0.0005	5.6	0.9
10.0	0.9950	0.1847	0.0050	0.004	0.030	0.004	0.0115	0.0168	0.9885	0.0005	0.0009	0.0005	11.0	1.4
12.2	0.9938	0.1786	0.0060	0.003	0.020	0.003	0.0131	0.0058	0.9869	0.0005	0.0006	0.0005	30.8	4.0
14.0	0.9950	0.1555	0.0052	0.002	0.017	0.002	0.0122	0.0029	0.9878	0.0005	0.0005	0.0005	53.6	10.3
15.7	0.9938	0.1365	0.0060	0.002	0.014	0.002	0.0149	0.0023	0.9851	0.0004	0.0004	0.0004	60.0	12.3
19.0	0.9931	0.1232	0.0068	0.001	0.011	0.001	0.0166	0.0017	0.9834	0.0004	0.0004	0.0004	74.3	17.3

$u(p) = 0.05$ MPa, $u(T) = 0.1$ K

Table 3.7 Experimental (vapor + liquid) equilibria for the system (CO₂ (1) + Hexanal (2) + water (3)). Vapor (y_i) and liquid phase (x_i) mole fractions, partition coefficients of Hexanal (k_2), and combined standard uncertainties (u_{comb}) at pressures (p) and temperatures (313, 323 and 333) K.

p / MPa	y_1	$y_2 \cdot 10^3$	y_3	u_{comb} (y_1)	u_{comb} (y_2) $\cdot 10^3$	u_{comb} (y_3)	x_1	$x_2 \cdot 10^3$	x_3	u_{comb} (x_1)	u_{comb} (x_2) $\cdot 10^3$	u_{comb} (x_3)	$k_2 = y_2/x_2$	u_{comb} (k_2)
mol · mol ⁻¹														
$T = 313$ K														
9.7	0.9967	0.2018	0.0031	0.003	0.010	0.003	0.0184	0.0213	0.9816	0.0004	0.007	0.0004	9.5	3.02
12.1	0.9957	0.1369	0.0042	0.002	0.008	0.002	0.0220	0.0111	0.9780	0.0003	0.002	0.0003	12.3	2.31
13.9	0.9951	0.1540	0.0047	0.002	0.006	0.002	0.0244	0.0108	0.9756	0.0003	0.002	0.0003	14.3	2.62
16.0	0.9953	0.1478	0.0045	0.002	0.005	0.002	0.0216	0.0098	0.9784	0.0003	0.002	0.0003	15.1	3.07
16.7	0.9952	0.1356	0.0047	0.001	0.005	0.001	0.0212	0.0085	0.9787	0.0002	0.002	0.0002	16.0	3.79
$T = 323$ K														
10.2	0.9968	0.1897	0.00300	0.003	0.010	0.003	0.0168	0.0203	0.9832	0.0003	0.002	0.0003	9.3	0.9
12.2	0.9951	0.1467	0.00477	0.002	0.008	0.002	0.0209	0.0139	0.9791	0.0003	0.002	0.0003	10.6	2.3
14.4	0.9943	0.1263	0.00554	0.002	0.006	0.002	0.0216	0.0118	0.9784	0.0003	0.002	0.0003	10.7	1.8
16.6	0.9937	0.1056	0.00618	0.001	0.005	0.001	0.0182	0.0073	0.9818	0.0003	0.002	0.0003	14.5	3.8
18.5	0.9940	0.0916	0.00591	0.001	0.004	0.001	0.0220	0.0058	0.9780	0.0002	0.002	0.0002	15.9	5.6
$T = 333$ K														
8.4	0.9932	0.2880	0.00648	0.003	0.013	0.003	0.0136	0.0265	0.9863	0.0003	0.002	0.0003	10.9	0.8
10.1	0.9947	0.2236	0.00508	0.002	0.009	0.002	0.0156	0.0153	0.9844	0.0003	0.002	0.0003	14.6	1.8
12.4	0.9942	0.1651	0.00563	0.002	0.007	0.002	0.0167	0.0102	0.9832	0.0003	0.002	0.0003	16.2	2.8
14.5	0.9935	0.1323	0.00635	0.002	0.006	0.002	0.0154	0.0085	0.9846	0.0002	0.002	0.0002	15.5	3.8
17.1	0.9926	0.1138	0.00731	0.001	0.005	0.001	0.0176	0.0068	0.9824	0.0003	0.002	0.0003	16.7	4.8
17.9	0.9928	0.1072	0.00712	0.001	0.005	0.001	0.0173	0.0063	0.9827	0.0002	0.002	0.0002	17.0	5.8

$u(p) = 0.05$ MPa, $u(T) = 0.1$ K

Fig. 3.5 shows the k_2 for the system (CO_2 (1) + (*E*)-2-hexenal (2) + water (3)) at temperatures (313, 323 and 333) K and as a function of pressure (p). The k_2 was in the range of 5 to 92, and the highest value was observed at a temperature 313 K and at pressures around 16 MPa. In general, the k_2 increased with increasing pressure at constant temperature. At constant pressure the k_2 decreased when temperature increased. Crossover was found between the curves at 323 K and 333 K near 8 MPa and again at 16 MPa. Additionally, the separation factor of (*E*)-2-hexenal from water ($a_{23} = k_2/k_3$) as a function of pressure is shown in Fig. 3.6. High a_{23} were observed, the highest value was found at a temperature of 313 K and at pressures around 12 MPa, at lower pressures the a_{23} decreased rapidly, and above 14 MPa it remained practically constant around 10^4 .

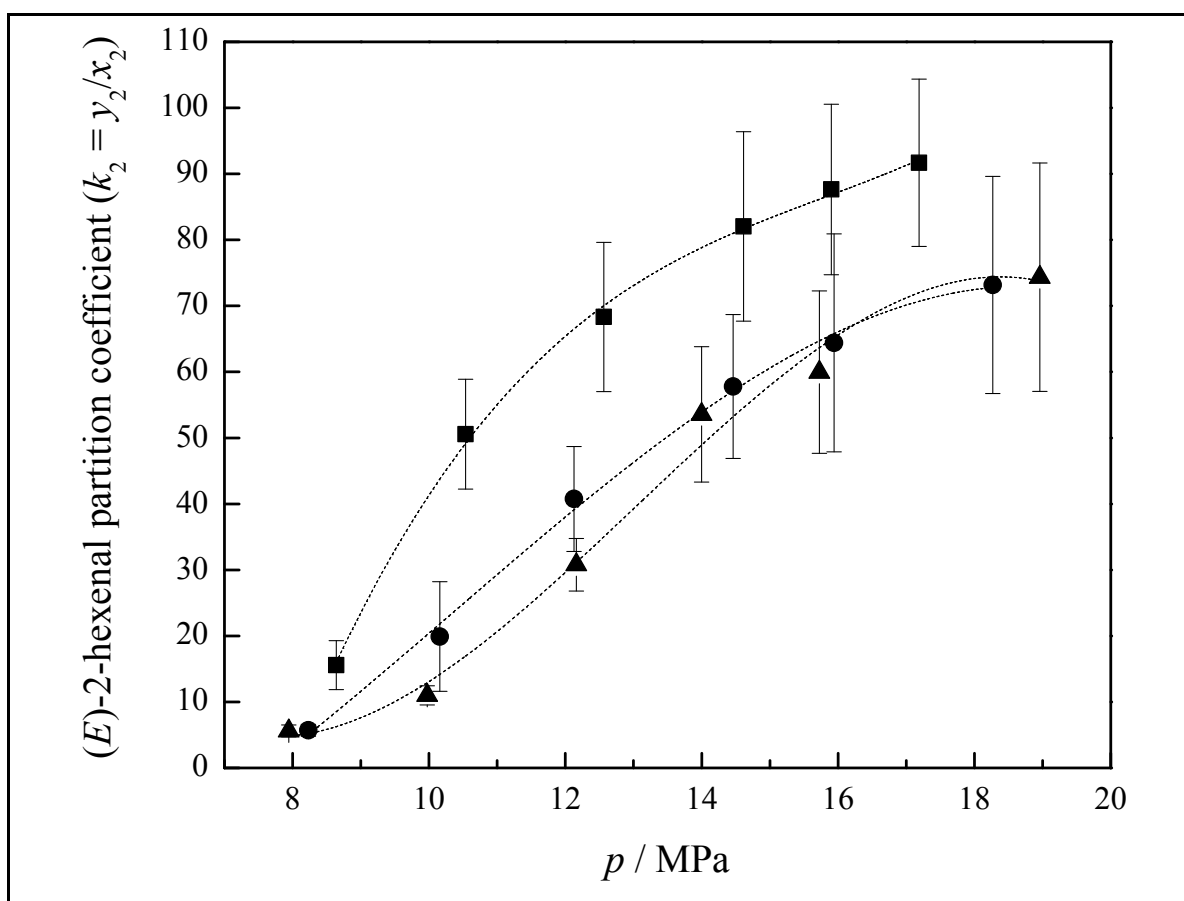


Figure 3.5 Isothermal partition coefficients of (*E*)-2-hexenal (k_2) at various pressures (p). This work: (■) 313 K; (●) 323 K; (▲) 333 K. (----) Trend line.

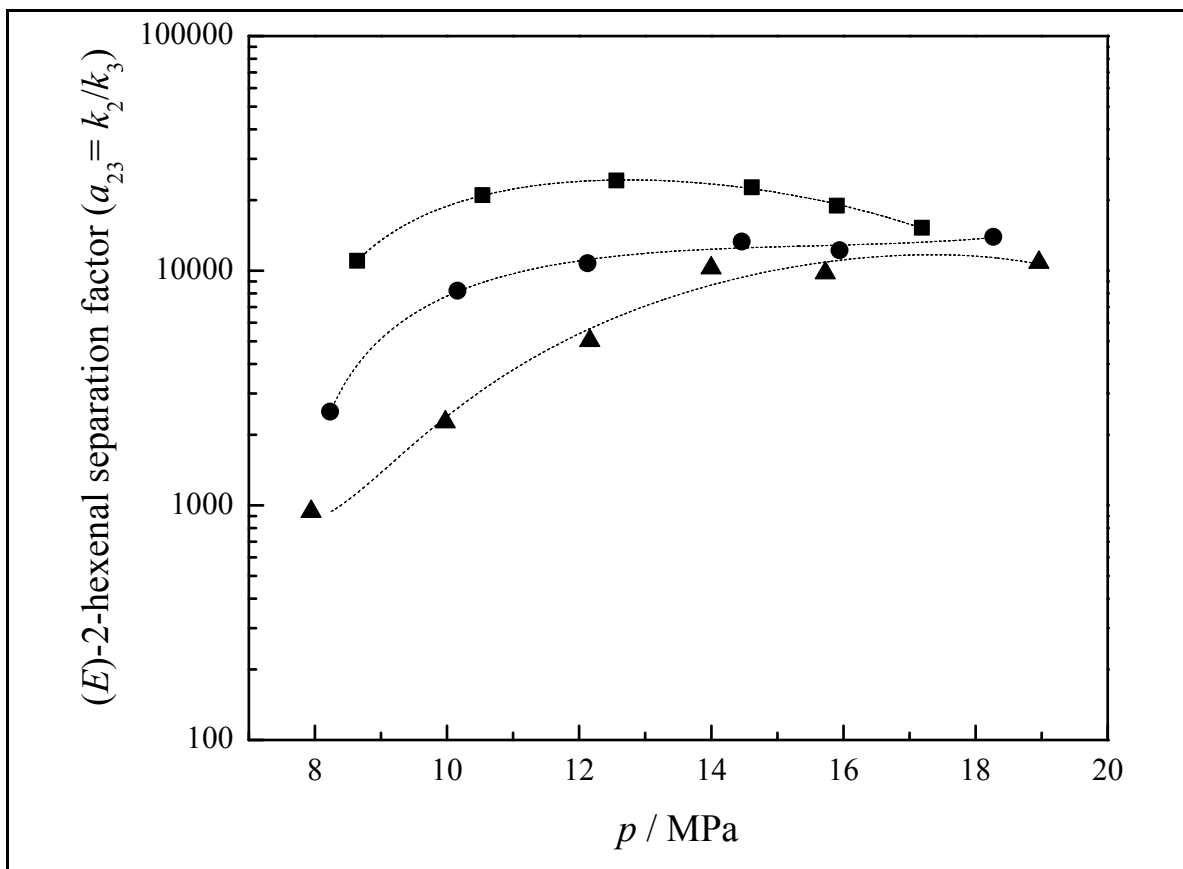


Figure 3.6 Isothermal separation factor (a_{23}) of (*E*)-2-hexenal (2) from water (3) at various pressures (p). This work: (■) 313 K; (●) 323 K; (▲) 333 K. (----) Trend line.

For the system (CO_2 (1) + hexanal (2) + water (3)) hexanal, the k_2 between CO_2 and water as a function of pressure at temperatures (313, 323, and 333) K is shown in Fig. 3.7. In this case, the values of the k_2 were in the range of (9 to 17), near six times lower than those of (*E*)-2-hexenal. For hexanal, the k_2 at 333 K was found to be higher than at 313 and 323 K nearly crossing over around 17 MPa. At all temperatures studied in this work, the hexanal k_2 increased as pressure increased. The a_{23} of hexanal from water, as a function of pressure, is shown in Fig. 3.8. High a_{23} were also found for hexanal. However, they were one order of magnitude lower than those of (*E*)-2-hexenal. For hexanal, the highest a_{23} was found at a temperature of 313 K and around 17 MPa. The tendency of hexanal a_{23} as a function of pressure showed different behavior than that of (*E*)-2-hexenal. At lower pressure (10 MPa) the a_{23} at all temperatures showed a similar value. As pressure increased lines crossed over; at 313 K the a_{23} decreased slightly until 12 MPa and then

increased to its maximum value around 17 MPa, at 323 K a_{23} decreased to a minimum near 14 MPa and increased again near 19 MPa to its maximum value, at 333 K a_{23} increased to its maximum around 11 MPa and then decreased until crossed over the 323 K isotherm near 16 MPa.

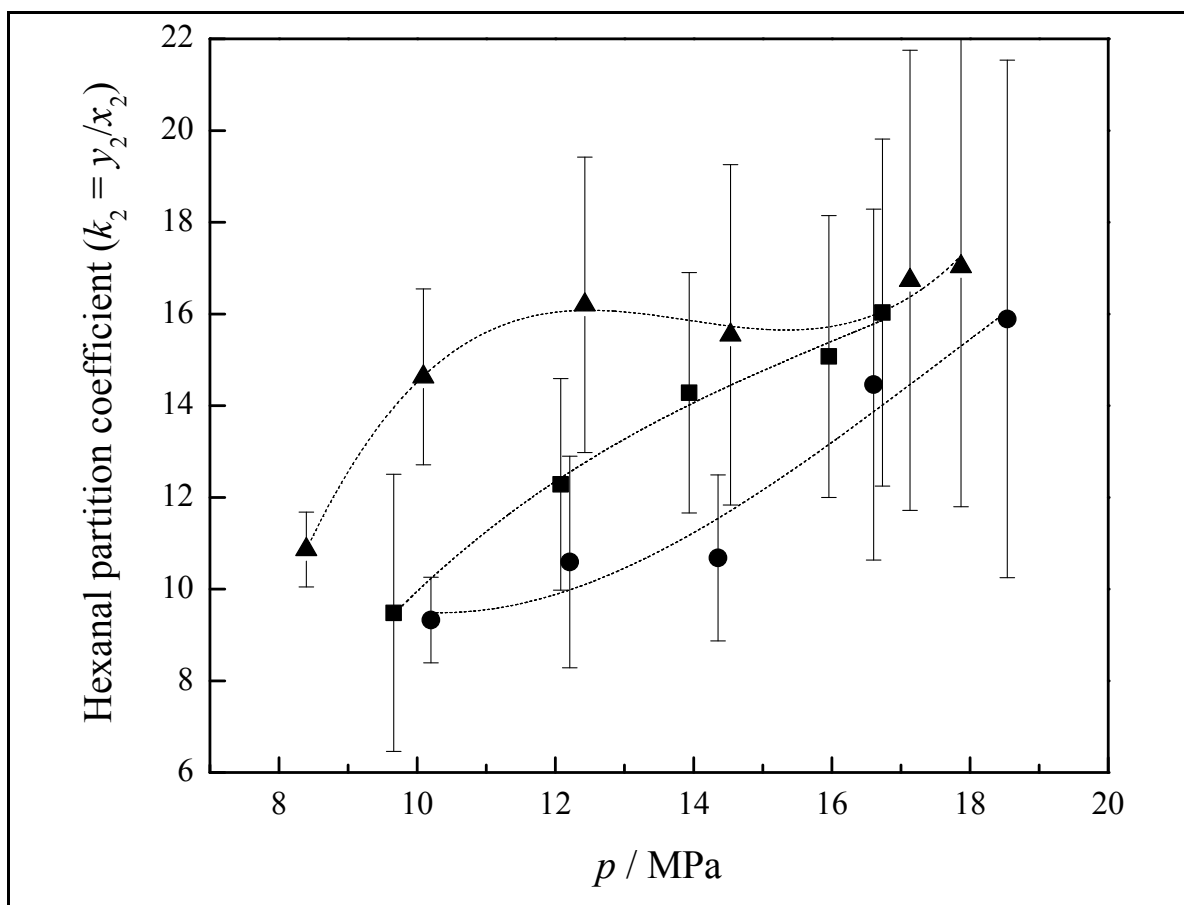


Figure 3.7 Isothermal partition coefficients of hexanal (k_2) at various pressures (p). This work: (■) 313 K; (●) 323 K; (▲) 333 K. (----) Trend line.

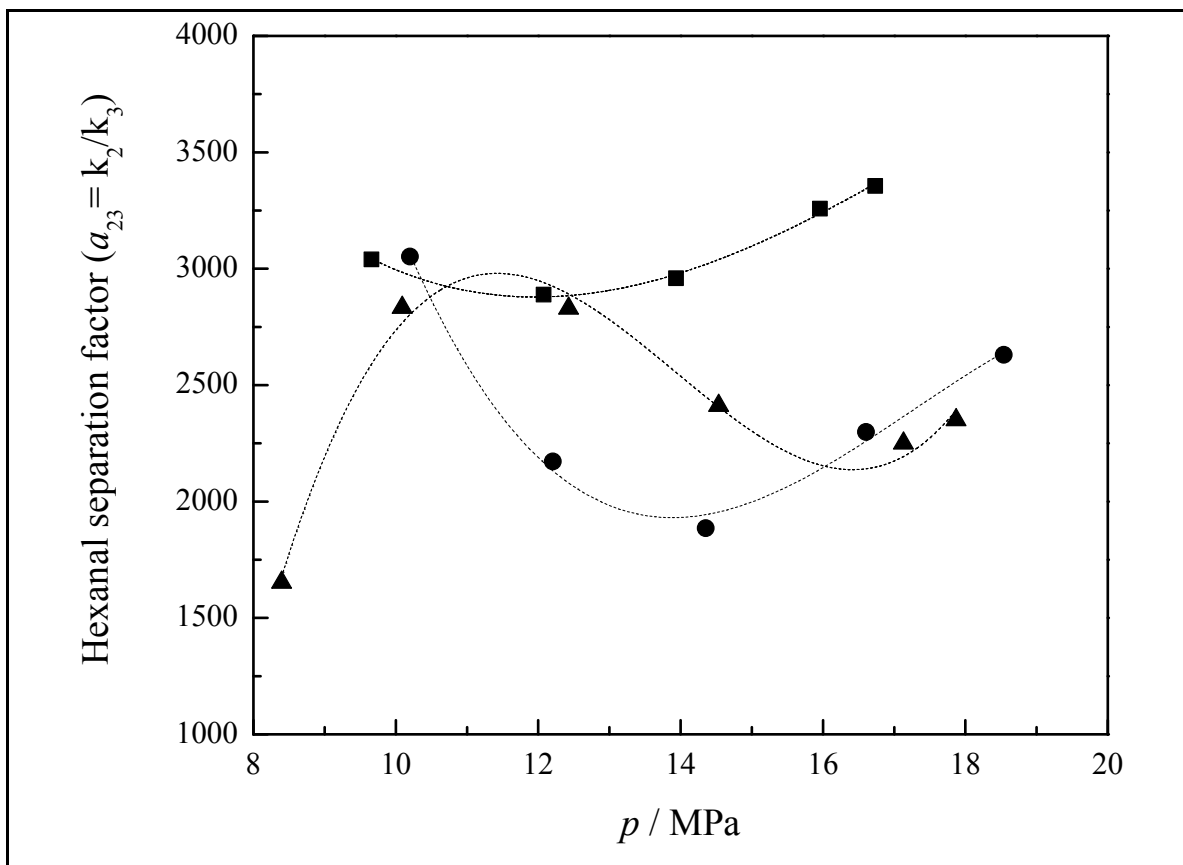


Figure 3.8 isothermal separation factors (a_{23}) of hexanal (2) from water (3) at various pressures (p). This work: (\blacksquare) 313 K; (\bullet) 323 K; (\blacktriangle) 333 K. (----) Trend line.

In general, k_i and a_{ij} are influenced by polarity, volatility and the affinity of CO_2 to certain functional groups. Although hexanal has a lower normal boiling point ($T_b = 402$ K (“NIST Chemistry WebBook”)) than that of (*E*)-2-hexenal ($T_b = 420$ K (“NIST Chemistry WebBook”)), as shown in Fig. 3.5 and Fig. 3.7, partition coefficients of (*E*)-2-hexenal were found to be near six times higher than those of hexanal. This behavior could be explained by the trans double bond in (*E*)-2-hexenal lower polarity compared with hexanal. This apparently increases CO_2 affinity for (*E*)-2-hexenal (despite its lower vapor pressure) over hexanal, which is slightly more soluble in water than (*E*)-2-hexenal probably due to higher dipole-dipole interactions. Brunner & Budich (2004) found the same behavior for ethyl acetate and ethyl butyrate under similar conditions. However, the

authors stated that this is not a general characteristic; the partition coefficients and separation factors can also decrease according to the components' vapor pressure.

To the best of the author's knowledge there is no experimental VLE data of the ternary system ($\text{CO}_2 + (E)\text{-2-hexenal} + \text{water}$) and ($\text{CO}_2 + \text{hexanal} + \text{water}$) in literature to compare and validate the results obtained in this work. However, Brudi et al. (1996) and Wagner et al. (1999) measured high-pressure k_i between CO_2 and water of several organic solvents as a function of pressure and found similar behavior such as crossover between isotherms at different conditions and a wide variety of tendencies. Apparently, there is no general tendency among the data found in literature.

4. COUNTERCURRENT FRACTIONATION OF AQUEOUS APPLE AROMA CONSTITUENTS USING SUPERCRITICAL CARBON DIOXIDE

4.1 Introduction

Supercritical Fluid Extraction (SFE) is a process that uses gases at high pressures as solvents to extract valuable materials. In contrast to SFE from solid matrices, in which the compounds of interest are directly extracted from its natural source, the SFE from liquid mixtures is typically used to fractionate materials extracted by conventional methods (Tabera et al., 2004), typically carried out continuously on packed columns operated in the countercurrent mode (Bejarano et al., 2016), and known as CounterCurrent Supercritical Fluid Fractionation (CC-SFF).

Early developments of the CC-SFF technology and its advantageous characteristics were first described in the late 1970's (Siegfried Peter & Brunner, 1978; K. Zosel, 1978). However, the number of industrial applications of CC-SFF nowadays is limited mainly because the process has to be designed for each application, and the required know-how is not universally shared by all members of the chemical engineering community (Brunner, 2010).

CC-SFF has been applied mainly to edible oil mixtures and derivatives (e.g., PUFAs from fish oil), essential oils (e.g., deterpenation of citrus oils), and alcoholic beverages (e.g., dealcoholization). Extensive reviews on CC-SFF applications are available in literature (Bejarano et al., 2016; Brunner, 1998, 2005, 2009, 2010). Concentration and fractionation of aroma constituents from aqueous solutions has been mainly applied to alcoholic beverages (Gamse et al., 1999; Macedo et al., 2008; Medina & Martínez, 1997; Ruiz-Rodríguez et al., 2010; Señoráns et al., 2003; Señoráns, Ruiz-Rodríguez, Ibáñez, et al., 2001; Señoráns, Ruiz-Rodríguez, Ibáñez, et al., 2001). The recovery of aromas from other liquid mixtures such as juices is even more limited. Señoráns, Ruiz-Rodríguez, et al. (2001) and Simó et al. (2002) isolated by CC-SFF and analyzed the antioxidant compounds in orange juice. The authors studied the effect of the solvent-to-feed ratio (S/F)

on the content of antioxidant compounds of the extracts. They found that when operating at low S/F (~ 3) the antioxidant compounds were more concentrated in the extract.

In the late and mid 70's Schultz et al. (T. H. Schultz et al., 1967) studied the extraction of volatiles from apple essences with different solvents including dense CO_2 . Later, Schultz (W. G. Schultz, 1969) patented the process, performed selective extraction of apple aroma (W. G. Schultz & Randall, 1970), and built a pilot plant for the extraction of volatiles from fruit essences using liquid CO_2 (W. G. Schultz et al., 1974). However, to the best of the authors knowledge further research on the subject is not available.

Chile is among the eleven top world producers of apples with 1.5% of the world production (Bravo Mina, 2011). Nearly 55% of the domestic production of apples is used to make concentrated juice with 95% being exported (Gálvez, 1996). This process is usually carried out by evaporation, and a significant amount of volatile aromas are lost. Actually, few companies in Chile recover the aroma fraction lost in the evaporation stage of the concentrated juice manufacturing process. Traditionally, fruit aromas are recovered from the concentrated juice using techniques based on distillation/evaporation or partial condensation (Belitz et al., 2009; Birjessön et al., 1996). CC-SFF can be used as an alternative technology to concentrate and fractionate natural fruit aroma essences with large amounts of water as described by Mukhopadhyay (2000). A super-concentrated aroma extract obtained by CC-SFF would be a product of higher added value than the fresh fruit, concentrated juice, and aqueous essences obtained by condensation. Therefore, the use of CC-SFF could be attractive to producers of concentrated fruit juices.

The objective of this work was to put into operation a new packed column designed for SFF by studying the effect of temperature, pressure, and S/F on the concentration and fractionation of a model aqueous apple aroma solution composed by two six-carbon aldehydes which contribute to the apple aroma, (*E*)-2-hexenal and hexanal; and a six-carbon alcohol which is not relevant for the apple aroma, 1-hexanol. Although (*E*)-2-hexenal and hexanal are not in significant amounts in the whole fruit, they are mainly responsible for sensory impressions, such as 'green, fresh, estery' in commercial apple juices (Bejarano, López, del Valle, & de la Fuente, 2015). Moreover, Koch (Koch, 1976)

demonstrated the importance of (*E*)-2-hexenal in the odor of apple essences. The concentration of these compounds in apple juice, apple, and essence varies from ca. 1 to 2400 mg·kg⁻¹ (Carelli et al., 1991; Nikfardjam & Maier, 2011; Versini et al., 2009). Response Surface Methodology (RSM) with a Box-Behnken Design (BBD) was used to investigate and optimize the process variables. This approach is an effective statistical method to define the effects of multiple independent variables and their interactions on the process response, and to optimize the process variables (Guthalugu, Balaraman, & Kadimi, 2006; Maran, Manikandan, Priya, & Gurumoorthi, 2013). The values of the variables used in the BBD were chosen based on previous ternary phase equilibrium measurements (Bejarano et al., 2015) to explore reasonable operating values. Experimental values of temperature ranged from 40 to 60 °C, pressure from 8 to 14 MPa, and *S/F* from 5 to 15 kg·kg⁻¹ CO₂/feed. At the selected temperature and pressure conditions CO₂ densities were in the range of 191.6 to 763.3 kg·m⁻³ (Lemmon et al., 2013).

4.2 Materials and Methods

4.2.1 Materials

Food grade CO₂ (≥99.9%) was supplied by Indura S.A. (Santiago, Chile). *E*-2-hexenal (≥99.5%), hexanal (98%), and 1-hexanol (≥99%) were purchased from Sigma-Aldrich (Saint Luis, MO). LiChrosolv® methanol (≥99.9%) was acquired from Merck (Darmstadt, Germany). Distilled water was used in all experiments. All materials were used without further purification.

4.2.2 Experimental apparatus and procedure

The new pilot-scale CC-SFF column was purchased from Eurotechnica GmbH (HPCC-500, Bargteheide, Germany) and was coupled to an existing SFE plant as depicted in Fig. 4.1. The main component of the experimental apparatus is the high-pressure column (1) of 4 m height and an internal diameter of 38 mm. Top operation condition of the column is 50 MPa at 100 °C. The column is equipped with structured packing Sulzer CY, and with a sapphire window to observe the wetting behavior of falling liquid in the middle section of the column (2). The column temperature inside the column is controlled by the

temperature of the CO₂ entering at the bottom of the column and by two heating mantles covering the upper (3) and bottom (4) part of the column. The temperature of the CO₂ entering at the bottom of column is adjusted in the heating thermostatic water bath (5) (8205, PolyScience, Niles, IL) and a 500 cm³ preheater filled with glass beads (6). The temperatures inside the column are measured by three type-k thermocouples, located at the top, middle, and bottom part of the column. The upper and bottom thermocouples are connected to the temperature controllers (7) (HT42-10P, Hillesheim GmbH, Waghäusel, Germany) of the heating mantles (3,4). All three temperatures are monitored and displayed in the column control panel. A backpressure regulator (8) (BPR-A-200B1, Thar Technologies, Pittsburgh, PA) controls the pressure inside the column and it is displayed in the column control panel by a pressure transmitter (A-10 Wika, Klingenberg, Germany). The liquid phase is pumped by a piston pump (9) (Novados H1, SPX Bran+Luebbe, Norderstedt, Germany) from the liquid feed storage tank (10). The liquid feed pump is equipped with a variable frequency drive to control the liquid mass flow rate, which is measured by a Coriolis mass flow meter (11) (MASS 2100, SITRANS FC MASSFLO®, Siemens, Nordborg, Denmark). Liquid CO₂ is pumped by a two-piston pump (12) (P-200A-220V, Thar Technologies, Pittsburgh, PA) from the buffer tank (13) of the solvent recovery cycle (14). A cooling thermostatic water bath (15) (9106A12E, PolyScience, Niles, IL) is installed at the suction side of the pump in order avoid gaseous CO₂ entering the pump head, and to achieve higher CO₂ mass flow rates. The CO₂ mass flow rate is measured and controlled by a Coriolis mass flow meter (16) (CNF010M324NU, Micro Motion Inc., Boulder, CO).

Sampling was done as follows. Dissolved substances in CO₂ coming out from the top of the column were collected in two 250 cm³ cyclonic separators (17,18). The pressure inside the CO₂ supply tank determined the pressure of both separators (5.0 MPa). The first separator was heated to 40 °C in order to avoid ice formation while sampling causing a controlled expansion while taking samples. The second separator (18) was cooled with water (at ~ -5 °C) from the cooling thermostatic water bath (15) to diminish aroma losses in the first separator (due to relative high temperature) and to the solvent cycle. Additional losses were quantified by a homemade cold-trap (19) set-up composed

by a needle valve (20) (HiP model 15-11AF1, Erie, PA, USA), an expansion and flow control valve (21) (Butech, SFPMMV26V, Erie, PA, USA), and a wet-test meter (22) (Ritter, TG 05/5, Bochum, Germany) to measure the CO₂ content using density data (Lemmon et al., 2013). Finally, CO₂ was recycled through the solvent cycle (14) before passing through a molecular sieve (23) to avoid clogging of pipes by gas hydrates. The raffinate was collected at the bottom of the column and withdrawn via a heated vessel (24) for gradual expansion to avoid ice formation. The temperature of the liquid in the feed tank (10) and the raffinate expansion vessel (24) is measured and controlled by a Pt-100 temperature sensor connected to a temperature controller (25) (AKO-D14726, Madrid, Spain).

The experimental procedure was as follows. Cooling of the solvent cycle (14) and cooling thermostatic water bath (15) were turned on, and by opening slowly the CO₂ storage tank (26) the column was pressurized. The operating temperature of the column was set on the column controllers (7) and on the heating bath (5). When the temperature values inside the column were near the set point and the buffer tank (13) was filled with liquid CO₂, the CO₂ flow rate was set on the flow controller (16) and CO₂ pump (12) was turned on. The desired operation pressure was set on the automatic backpressure regulator (8), which was initially closed up to when the pressure reached the set point when it began to open until a stable pressure within the column was achieved. When stable temperature and pressure conditions in the column were achieved, a previously prepared homogeneous aqueous liquid solution of 1750 mg·kg⁻¹ of organics (500 mg·kg⁻¹ of (*E*)-2-hexenal, 250 mg·kg⁻¹ of hexanal, and 1000 mg·kg⁻¹ of 1-hexanol) was fed to the liquid feed tank (10) and the magnetic stirrer (27) turned on. To establish the desired *S/F* the liquid flow rate was adjusted in the liquid pump mass flow controller (11) according to the CO₂ mass flow rate.

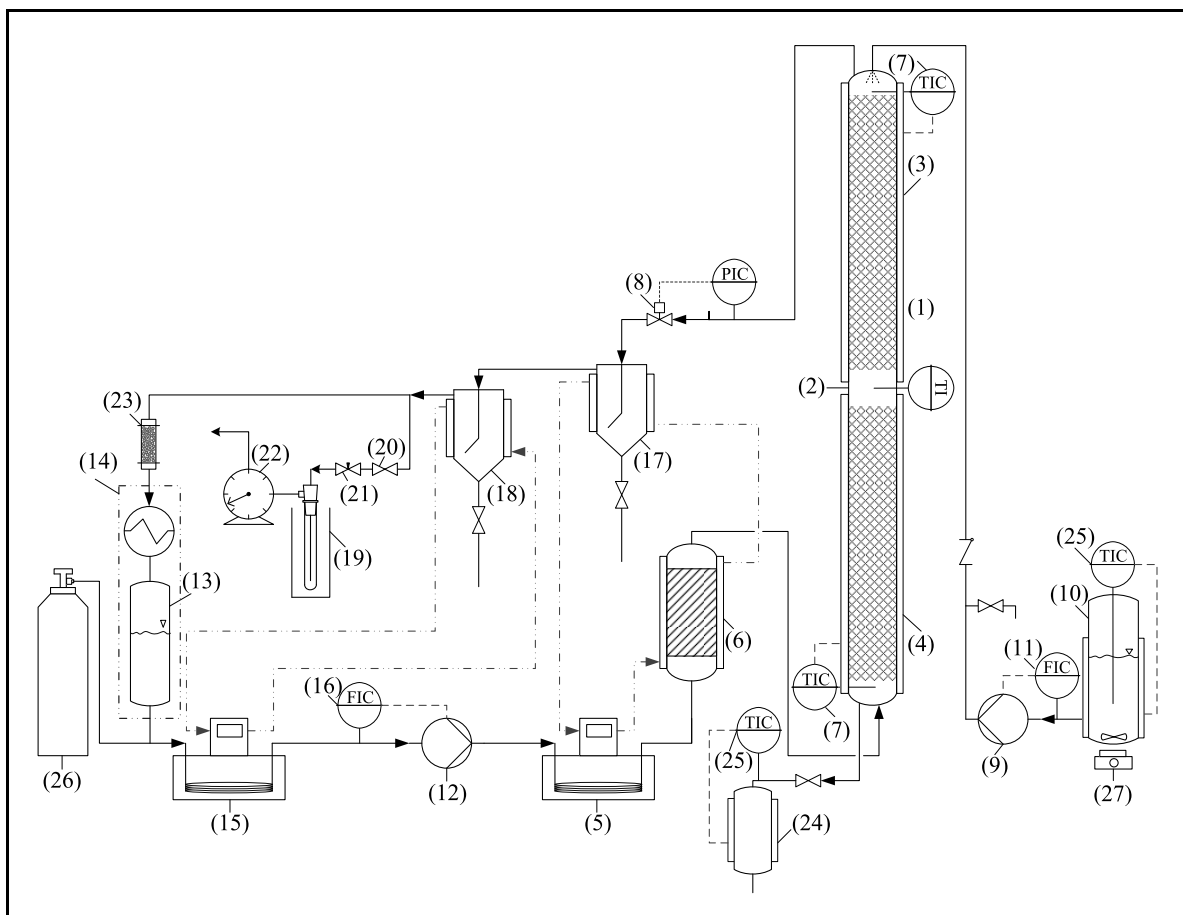


Figure. 4.1 Schematic flow diagram of experimental apparatus. (1), packed column; (2), sapphire window; (3) and (4), upper and bottom heating mantles; (5), heating bath; (6) preheater; (7), temperature controllers; (8), backpressure regulator; (9), liquid piston pump; (10), liquid storage tank; (11), liquid mass flow meter; (12), CO₂ piston pump; (13), CO₂ buffer tank; (14), CO₂ recovery cycle; (15), cooling bath; (16), CO₂ mass flow meter; (17) and (18), cyclonic separators; (19), cold-trap; (20), needle valve; (21), flow control valve; (22), wet test-meter; (23), molecular sieve; (24), raffinate expansion tank; (25), temperature controller; (26), CO₂ storage tank; (27), magnetic stirrer.

In order to establish steady state conditions the phase composition of the raffinate was monitored at the bottom of the column as a function of time (60, 80, 100, 110, and 120 min). Fig. 4.2 shows the composition of (*E*)-2-hexenal, hexanal, and 1-hexanol *versus* time. Based on this observation the extraction time was set to 2 h. This period of time was used in all experiments and was found to be in agreement with those in literature (da Porto & Decorti, 2010; Gracia et al., 2007; Lahiere & Fair, 1987; J. S. Lim et

al., 1995; Seibert & Moosberg, 1988; Señoráns et al., 2003; Señoráns, Ruiz-Rodríguez, Ibañez, et al., 2001) for a similar type of application and operation conditions.

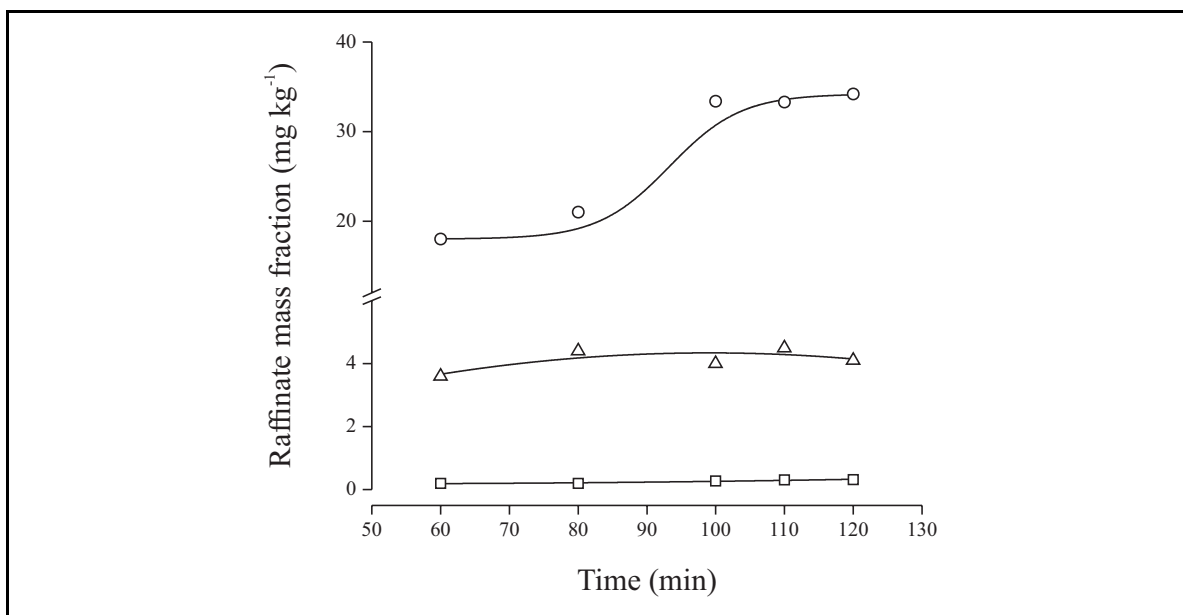


Figure 4.2 Raffinate mass fractions over time for steady state time estimation. (—○—), 1-Hexanol; (—□—), (E)-2-Hexenal; (—△—), Hexanal. Open symbols represent experimental values and lines signals trends.

The estimation of the aroma losses to the solvent cycle was as follows. After the first hour of constant operation, both separators (17,18) and the heated raffinate collector (24) were emptied, and the cold trap was slightly opened in order to quantify the aroma losses to the solvent cycle. Overall and component mass balances were checked for the next hour of operation. At the end of that period samples from both extract and raffinate were collected. The mass balance was checked with overall recovery value of >93%, >90% for (E)-2-hexenal, >80% hexanal, and >90% for 1-hexanol. The walls of the separators were cleaned with pure methanol in order to collect all the extract remaining, and samples were stored in the dark at -18 °C until analysis.

4.2.3 Analyses and quantification

The extract, raffinate, and feed samples were sent to a certified analytical laboratory at *Universidad Técnica Federico Santa María*. All samples were analyzed by

Gas Chromatography (GC) and Solid Phase Micro Extraction (SPME). Calibration curves were constructed for each compound in order to quantify the amount of organics ((*E*)-2-hexenal, hexanal, and 1-hexanol) in each sample. The amount of water in each sample was determined by difference. All samples were analyzed in triplicate and the estimated experimental uncertainty was $<12.0 \text{ mg}\cdot\text{kg}^{-1}$ for (*E*)-2-hexenal, $3.1 \text{ mg}\cdot\text{kg}^{-1}$ for hexanal, and $< 49.2 \text{ mg}\cdot\text{kg}^{-1}$ for 1-hexanol. Appendix 3 includes the analysis reports of each experiment.

4.2.4 Data analysis and statistics

Statistical calculation and analysis were performed in R (“R Core Team. R: A language and environment for statistical computing. R Foundation for Statistical Computing, Vienna, Austria. <http://www.R-project.org/>,” 2015) using the package RcmdrPlugin.DoE (Groemping, 2014). The significance of the models was determined through the ANalysis Of VAriance (ANOVA), the significance of each variable was determined by ANOVA followed by Fisher’s statistical test (F-test).

4.3 Results and discussion

The experimental conditions of each experiment used in the BBD are listed in Table 4.1. All compounds were identified by numbers as follows: (*E*)-2-hexenal ($i=1$), hexanal ($i=2$), 1-hexanol ($i=3$), and water ($i=4$). Additionally, Table 4.1 lists the results of the mass compositions of each compound in the extract (y_i) and raffinate (x_i). Other response variables such as the Organics Loading (OL), aroma extraction yield (Y_A), and selectivity of aroma from 1-hexanol ($\alpha_{A,3}$) were also considered and are listed in Table 4.1. The OL was expressed as the mg of extract dissolved per kilogram of CO_2 , and the Y_A and $\alpha_{A,3}$ were calculated using the following equations:

$$Y_A (\%) = 100 \cdot \frac{q_E(y_1 + y_2)}{q_F(z_1 + z_2)}, \text{ and} \quad (4.1)$$

$$\alpha_{A,3} = \frac{k_A}{k_3} = \frac{(y_1 + y_2)/y_3}{(x_1 + x_2)/x_3}, \quad (4.2)$$

where q_E and q_F are the solvent-free extract and feed mass flow rates, x_i , y_i , and z_i are the mass compositions of compound i in the raffinate, extract, and feed streams, and k_A and k_3 are the partition coefficients of apple aroma constituents (*E*)-2-hexenal and hexanal, and 1-hexanol ($k_i = y_i/x_i$).

4.3.1 Extraction yield of aromas and mass fractions of extract and raffinate streams

In all experiments, a good concentration of the apple aroma constituents was achieved (Table 4.1). The organic compounds were practically removed completely from the feed solution. The amount of organic compounds in the raffinate was $<200 \text{ mg}\cdot\text{kg}^{-1}$ in all experiments, and the minimum value was found to be $11 \text{ mg}\cdot\text{kg}^{-1}$. Fig. 4.3 shows the mass fraction of each sample, feed, raffinate, and extract, of the best run (first line in Table 4.1). This experimental run showed the highest organic compounds content in the extract, and the Y_A was around 92%. The mass fraction of organics in the best run was nearly 43 % w/w (14 %w/w of (*E*)-2-hexenal, 6 %w/w of hexanal, and 23 %w/w of 1-hexanol), raffinate composition was near $174 \text{ mg}\cdot\text{kg}^{-1}$ ($26 \text{ mg}\cdot\text{kg}^{-1}$ of (*E*)-2-hexenal, $3 \text{ mg}\cdot\text{kg}^{-1}$ of hexanal, and $145 \text{ mg}\cdot\text{kg}^{-1}$ of 1-hexanol).

Results of Table 4.1 and Fig. 4.3 show that the apple aroma constituents (*E*)-2-hexenal and hexanal were not successfully fractionated from the less relevant compound 1-hexanol. However, as it can be seen in Fig. 4.4, the extract collected in the separator was highly concentrated so that two separate phases were formed.

None of the RSM models gave satisfactory results for the Y_A , aroma selectivity (from 1-hexanol and water), and mass fractions of each compound in the extract (y_i) and raffinate (x_i) streams. The number of significant effects, the magnitude of the regressed parameters, and the determination coefficient (R^2) were low. This means that variability of the responses was not successfully explained by the variation of the chosen variables (T , P , and S/F) and such statistical models were not considered valid. However, qualitative consistent results were obtained for all the mass fractions; in general, temperatures around 45°C , low S/F levels, and pressures in the range of 8 to 11 MPa tend to increase the mass fraction of relevant apple aroma compounds in the extract, and maximize water and 1-hexanol content in the raffinate.

Table 4.1 Box-Behnken design and observed responses. Operational conditions of temperature (T), pressure (P), solvent-to-feed ratio (S/F), CO_2 density (ρCO_2), mass flow rates of feed (q_F), extract (q_E) and raffinate (q_R); mass fractions of component i in extract (y_i) and raffinate (x_i) streams; selectivity of aromas (A) from 1-hexanol ($\alpha_{A,3}$) and water ($\alpha_{A,4}$); extraction yield of aromas (Y_A) and total organics (Y_{tot}), and Organics Loading (OL).

Operational Conditions							Mass Fractions								Selectivity		Extraction Yield		Organics Loading
$T (X_1)$	$P (X_2)$	$S/F (X_3)$	ρCO_2	q_F	q_E	q_R	y_1	y_2	y_3	y_4	x_1	x_2	x_3	x_4	$\alpha_{A,3}$	$\alpha_{A,4}$	Y_A	Y_{tot}	OL
50 (0)	8 (-1)	5 (-1)	219	20.2	0.10	20.7	14.2	5.9	23.1	56.9	26.0	2.8	145.0	99.983	4.4	12232	91.5	87.4	0.26
50 (0)	11 (0)	5 (-1)	672	20.4	0.20	20.7	6.1	2.1	12.1	79.7	3.0	1.5	7.0	99.999	1.2	25622	93.8	96.0	0.27
50 (0)	8 (-1)	15 (1)	219	10.9	0.10	10.1	6.0	2.3	11.0	80.7	18.0	3.5	178.0	99.980	6.3	4804	90.6	88.8	0.11
40 (-1)	8 (-1)	10 (0)	278	15.5	0.10	15.8	5.6	2.0	10.5	81.9	17.0	1.6	112.0	99.987	4.3	4875	90.3	88.6	0.15
40 (-1)	11 (0)	5 (-1)	684	19.5	0.20	19.3	3.9	1.4	8.1	86.5	4.0	1.5	13.0	99.998	1.5	11095	66.9	95.5	0.27
60 (1)	11 (0)	5 (-1)	358	21.5	0.30	20.7	4.0	1.3	7.6	87.1	11.0	2.5	47.0	99.994	2.5	4635	93.6	93.1	0.28
40 (-1)	11 (0)	15 (1)	684	10.4	0.10	10.1	3.4	1.1	6.7	88.8	5.0	0.6	34.0	99.996	4.3	9538	91.2	93.4	0.11
40 (-1)	14 (1)	10 (0)	763	15.4	0.30	15.8	2.9	0.9	5.5	90.6	4.0	1.6	20.0	99.997	2.4	7276	94.0	95.9	0.17
60 (1)	8 (-1)	10 (0)	192	10.0	0.20	10.7	2.1	0.8	4.4	92.7	17.0	1.1	94.0	99.989	3.6	1803	85.1	85.8	0.14
60 (1)	14 (1)	10 (0)	561	15.5	0.40	15.9	1.9	0.7	4.0	93.5	6.0	1.6	18.0	99.997	1.6	3733	95.3	94.9	0.16
50 (0)	14 (1)	15 (1)	672	10.5	0.30	10.5	1.6	0.6	3.5	94.3	5.0	1.5	17.0	99.998	1.7	3809	86.7	92.5	0.11
60 (1)	11 (0)	15 (1)	358	10.3	0.30	10.2	1.5	0.6	2.9	95.1	6.0	0.3	25.0	99.997	2.8	3491	89.4	91.7	0.10
50 (0)	11 (0)	10 (0)	503	15.6	0.30	16.1	2.3	1.1	4.5	92.1	14.0	0.2	42.0	99.994	2.3	2677	92.0	89.4	0.16
50 (0)	11 (0)	10 (0)	503	15.6	0.30	14.3	2.2	1.1	4.5	92.3	11.0	0.2	33.0	99.996	2.2	3192	89.5	89.5	0.16
50 (0)	11 (0)	10 (0)	503	15.6	0.30	15.3	2.3	1.0	4.4	92.3	9.0	0.5	27.0	99.996	2.1	3723	95.9	91.8	0.16

(E)-2-hexenal ($i=1$); hexanal ($i=2$); 1-hexanol ($i=3$); water ($i=4$)

$[T] = ^\circ\text{C}$; $[P] = \text{MPa}$; $[S/F, \alpha_{A,3}, \alpha_{A,4}] = -$; $[\rho \text{CO}_2] = \text{kg}\cdot\text{m}^{-3}$; $[q] = \text{g}\cdot\text{min}^{-1}$; $[y_i] = \%\text{w/w}$; $[x_i] = \text{mg}\cdot\text{kg}^{-1}$; $[Y_A, Y_{\text{tot}}] = \%$; $[\text{OL}] = \text{gOrg}\cdot\text{kgCO}_2^{-1}$

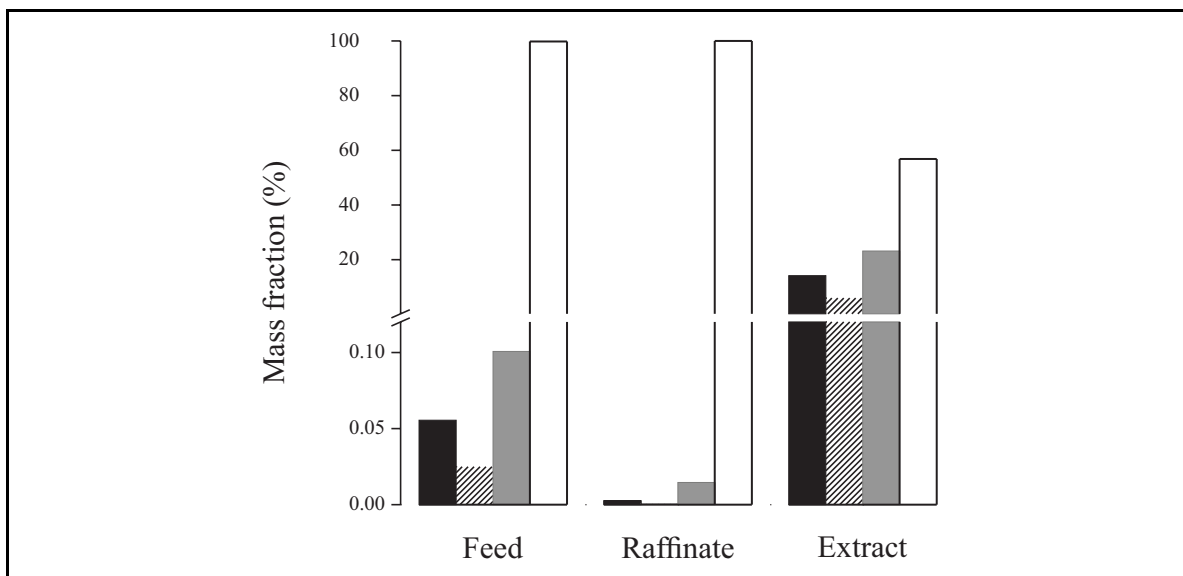


Figure 4.3 Aroma content in Feed, Raffinate, and Extract samples of best experimental run (first line of Table 4.1). (■), (*E*)-2-Hexenal; (▨) Hexanal; (■), 1-Hexanol; (□), Water.

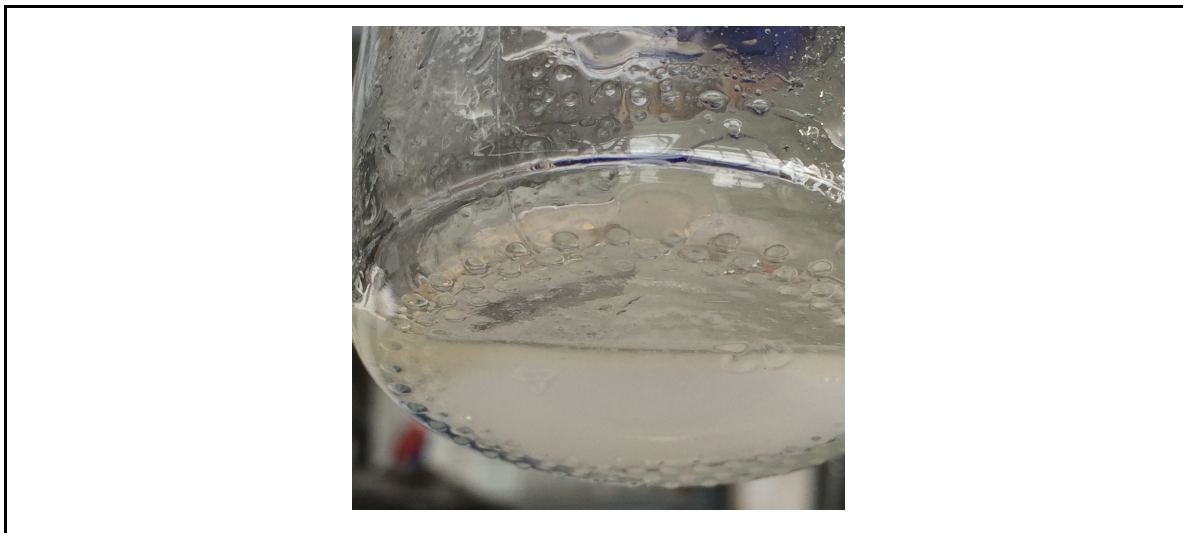


Figure 4.4 Super-concentrated extract, two-phase separation.

For all experiments, Y_A was $>86\%$. Fig. 4.5 shows Y_A versus CO_2 density at fixed temperatures: Y_A remained practically constant around 90% at all pressures and S/F . This result suggests that no relevant difference was observed in Y_A by varying temperature, pressure, or S/F . This may be due to the low solubility of the organic compounds in water

so that when in contact with a non-polar solvent such as CO₂ they are extracted easily. However, the highest Y_A was found to be at a temperature of 60 °C and showed a maximum of 99% near 350 kg·m⁻³ which occurred at $S/F = 5$ kg·kg⁻¹, and at a pressure of 11 MPa. These results agree with those of Señoráns et al. (Señoráns, Ruiz-Rodríguez, Ibáñez, et al., 2001) and da Porto and Decorti (da Porto & Decorti, 2010) who obtained the highest extraction yield of volatiles at the lowest S/F (~7 kg·kg⁻¹), for similar aqueous systems. Y_A showed a similar tendency at 50 °C and 60 °C. At 40 °C the Y_A showed a slightly increasing tendency with increasing CO₂ density. Y_A increased from 90 to 94% when density varied from 278 to 763 kg·m⁻³. These results are consistent with the observed tendency of the mass fractions in the extract and raffinate streams discussed above. In order to increase mass fraction of relevant apple aroma compounds in the extract, and maximize water and 1-hexanol content in the raffinate temperatures around 40 °C, low values of S/F , and pressures in the range of 8 to 11 MPa should be preferable.

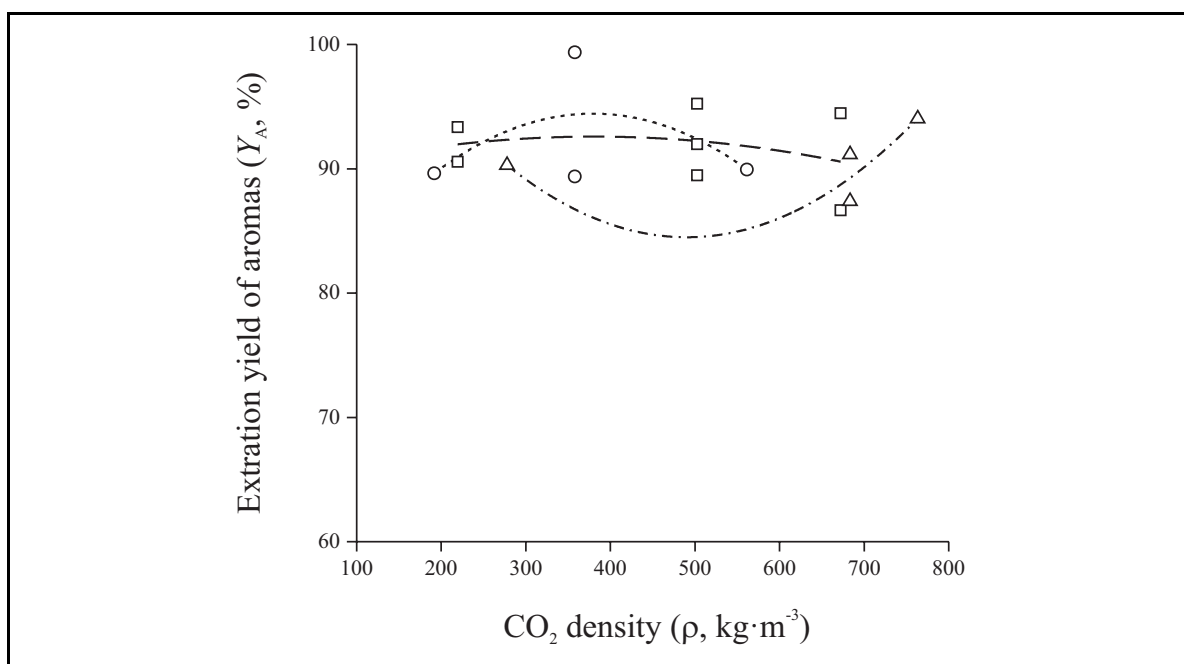


Figure 4.5 Aromas ((*E*)-2-Hexenal, Hexanal) extraction yield (Y_A). (---○---), 60 °C; (—□—), 50 °C; (----△----), 40 °C. Open symbols represent experimental values and lines signals trends.

4.3.2 Total extraction yield of organics and organics loading

The experimental data of the total extraction yield of organic compounds (Y_{tot}) and the organics loading (OL) was fitted to the quadratic response surface model depicted by Eq. (4.3) where Y is the estimated response, X_i and X_j are the independent coded variables (X_1 for temperature, X_2 for pressure, and X_3 for S/F) depicted by equations (3a) to (3c), and β_0 , β_j , β_{jj} , and β_{ij} are the regression coefficients for the intercept, First Order (FO), Pure Quadratic (PQ), and Two Factor Interaction (TFI), respectively.

$$Y = \beta_0 + \sum_{i=1}^3 \beta_i X_i + \sum_{i=1}^3 \beta_{ii} X_i^2 + \sum_{i=1}^2 \sum_{j=i+1}^3 \beta_{ij} X_i X_j \quad (4.3)$$

$$X_1 = \frac{T\{^{\circ}\text{C}\} - 50}{10} \quad (4.3a)$$

$$X_2 = \frac{P\{\text{MPa}\} - 11}{3} \quad (4.3b)$$

$$X_3 = \frac{S/F - 10}{5} \quad (4.3c)$$

The significance of the models was determined through the ANOVA, and the results are summarized in Table 4.2 for both estimated responses Y_{tot} , and OL. A large F-value indicates that most of the variation in the response can be explained by the regression model, Eq. (4.3). The results of the ANOVA indicated that both models showed a satisfactory representation of the relationship between the independent variables and responses. ANOVA results also showed that the R^2 and adjusted R^2 values were 0.96 and 0.92 for the Y_{tot} model and 0.99 for the OL model (Table 4.3). These results indicate the accuracy of the models.

Table 4.2 Analysis of variance (ANOVA) of total yield of organics (Y_{tot}) and Organics Loading (OL) models. First Order (FO), Two Factor Interaction (TFI), Pure Quadratic (PQ).

Source	Degrees of freedom	Sum of squares	Mean squares	F-value	Pr (>F)
Y_{tot}					
FO (X_1, X_2, X_3)	3	101	33.6	45.6	< 0.001 (***)
PQ (X_1, X_3)	2	19.0	9.52	12.9	0.003 (**)
TFI (X_2, X_3)	1	6.04	6.04	8.16	0.021 (*)
Residuals	8	5.92	0.740		
Lack of fit	6	2.35	0.391	0.219	0.938
Pure error	2	3.57	1.78		
OL					
FO (X_2, X_3)	2	$5.40 \cdot 10^4$	$2.70 \cdot 10^4$	855	< 0.001 (***)
PQ (X_2, X_3)	2	$4.05 \cdot 10^3$	$2.02 \cdot 10^3$	64.1	< 0.001 (***)
Residuals	10	316	31.6		
Lack of fit	4	158	39.5	1.50	0.313
Pure error	6	158	26.3		

Significance levels: (***), 0.1%; (**), 1%; (*), 5%.

In order to simplify the mathematical expressions of Y_{tot} and OL, the parameters of non-significant effects were excluded from the regression analysis. However, care was taken in order to maintain the significance of the expressions. The regression coefficient analysis of the models for the responses Y_{tot} and OL are summarized in Table 4.3. For Y_{tot} , all FO parameters were significant (P-values < 0.05), the PQ parameters of temperature and S/F were also significant (P-values < 0.05), and only the TFI parameter of pressure and S/F was significant (P-value = 0.05).

From the regression analysis for OL (Table 4.3), only pressure and S/F affected it significantly. FO parameters showed high significance (P-values < 0.01), none of the TFI parameters were significant, and the PQ parameter of S/F was highly significant (P-value < 0.01). The PQ parameter of pressure was not significant (P-value > 0.05), nevertheless the removal of this parameter causes that the lack of fit to become significant and the R^2 drops to unacceptable values.

Table 4.3 Regression coefficient analyses for total yield model (Y_{tot}) and Organics Loading (OL) models. Coded variables X_1 temperature, X_2 pressure, and X_3 , solvent-to-feed ratio; regressed coefficients ($\beta_0, \beta_{ii}, \beta_{ij}$); and model determination coefficient (R^2).

Coefficient	Estimated value	Standard error	t value	P-value ($\text{Pr} > t $)
Y_{tot}				
Intercept (β_0)	90.0	0.413	218	< 0.001 (***)
X_1 (β_1)	-0.791	0.304	-2.60	0.032 (*)
X_2 (β_2)	3.39	0.304	11.2	< 0.001 (***)
X_3 (β_3)	-0.704	0.304	-2.32	0.049 (*)
X_1^2 (β_{11})	1.89	0.446	4.23	0.003 (**)
X_3^2 (β_{33})	1.38	0.446	3.10	0.015 (*)
$X_2 \cdot X_3$ (β_{23})	-1.23	0.430	-2.86	0.021 (*)
R^2	0.955			
Adjusted R^2	0.922			
F-statistic	28.4			< 0.001 (***)
OL				
Intercept (β_0)	157	2.70	58.2	< 0.001 (***)
X_2 (β_2)	6.30	1.99	3.17	0.001 (**)
X_3 (β_3)	-81.9	1.99	-41.2	< 0.001 (***)
X_2^2 (β_{22})	-2.60	2.92	-0.893	0.393
X_3^2 (β_{33})	32.64	2.92	11.2	< 0.001 (***)
R^2	0.995			
Adjusted R^2	0.992			
F-statistic	460			< 0.001 (***)

Significance levels: (***), 0.1%; (**), 1%; (*), 5%.

The response surface generated from the regression model of Y_{tot} is shown in Fig. 4.6. As it can be seen from Fig. 4.6A, Y_{tot} decreases rapidly from approx. 96 to 86 % when pressure decreased from 14 to 8 MPa. The S/F affected Y_{tot} differently, with a slight convex tendency. Y_{tot} increased when S/F decreased from 10 to 5 to find a maximum of 96% at $S/F = 5 \text{ kg} \cdot \text{kg}^{-1}$. Fig. 4.6B shows effect of temperature and pressure on Y_{tot} . The maximum Y_{tot} was found to be at the lowest temperature (40 °C) and the highest pressure (14 MPa). As the temperature and S/F decreased, Y_{tot} increased (Fig. 4.6C).

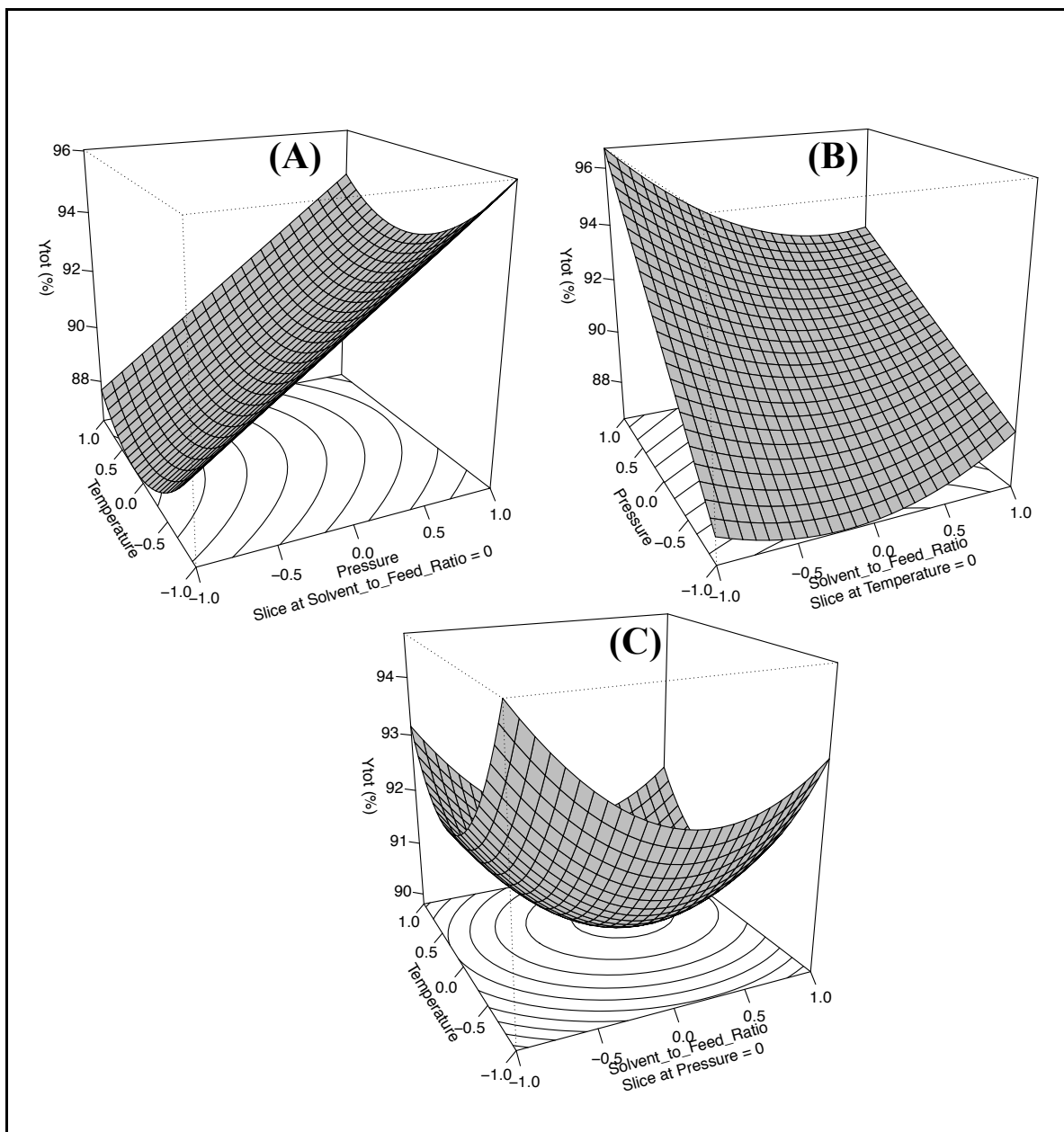


Figure 4.6 Response surface plot for total organics extraction yield (Y_{tot} , %) $Y_{tot} = 89.97 - 0.97X_1 + 3.39X_2 - 0.70X_3 + 1.89X_1^2 + 1.39X_3^2 - 1.23X_2X_3$. (A), effect of temperature and pressure; (B), effect of pressure and solvent-to-feed ratio; (C), effect of temperature and solvent-to-feed ratio.

On the other hand, only the pressure and the S/F showed significant effect on the OL. Fig. 4.7 shows the response surface plot for OL. As it can be observed, the OL decreased rapidly from ~ 300 to $125 \text{ mg} \cdot \text{kg}^{-1} \text{ Org/CO}_2$ when the S/F increased from 5 to 15

$\text{kg}\cdot\text{kg}^{-1}$. Pressure showed a slightly positive effect on OL; increasing from $100 \text{ mg}\cdot\text{kg}^{-1}$ at 8 MPa to $125 \text{ mg}\cdot\text{kg}^{-1}$ at 14 MPa.

As mentioned before, these results were found to be in good agreement with those found in literature (da Porto & Decorti, 2010; Señoráns, Ruiz-Rodríguez, Ibáñez, et al., 2001). The highest extraction yield of volatiles was observed at the lowest values of S/F ($\sim 7 \text{ kg}\cdot\text{kg}^{-1}$), and this variable was found to be the one with the most significant effect on the extraction of volatiles from similar aqueous systems.

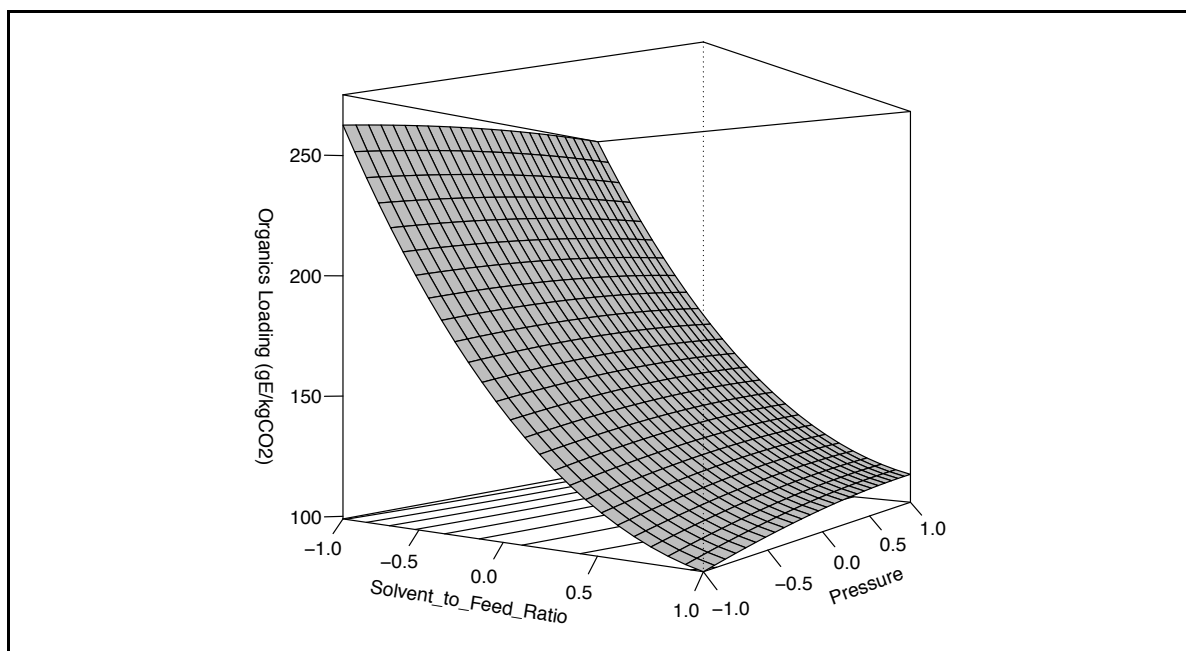


Figure 4.7 Response surface plot for Organics loading (OL, $\text{mg}\cdot\text{kg}^{-1} \text{ Org}/\text{CO}_2$)

$$\text{OL} = 157.06 - 6.30X_2 - 81.88X_3 - 2.60X_2^2 + 32.64X_3^2$$
 Effect of pressure and solvent-to-feed ratio.

4.3.3 Selectivity of CO_2 for aromas from 1-hexanol and water

The fractionation capability of CC-SFF for aqueous apple aromas (*E*)-2-hexenal and hexanal from 1-hexanol and water was analyzed by the comparison of selectivity factor (α_{ij}) Fig. 4.8 shows the selectivity factor of the apple aroma constituents aromas (*E*)-2-hexenal and hexanal from 1-hexanol ($\alpha_{A,3}$) versus CO_2 density at fixed temperature. In general the $\alpha_{A,3}$ showed a decreasing tendency with increasing CO_2 density. At a

temperature of 50 °C, $\alpha_{A,3}$ decreases from a maximum of 6.3 near 200 kg·m⁻³ to 1.2 near 750 kg·m⁻³. At temperatures of 60 °C and 40 °C the decreasing tendency was less steep than at 50 °C. At 60 °C, $\alpha_{A,3}$ decreased slowly approximately from 4 to 1.5. At 40 °C, $\alpha_{A,3}$ started approximately at 4 near 300 kg·m⁻³ and decreased to 2.5 near 750 kg·m⁻³. However, near 700 kg·m⁻³ and $S/F = 15$ the selectivity was approximately 4.5. Even though $\alpha_{A,3}$ showed reasonable values for feasible separation with CC-SFF (>1.3 (Brunner, 1998)), the presence of water made the fractionation of the relevant aroma constituents (*E*)-2-hexenal and hexanal from 1-hexanol unsuccessful.

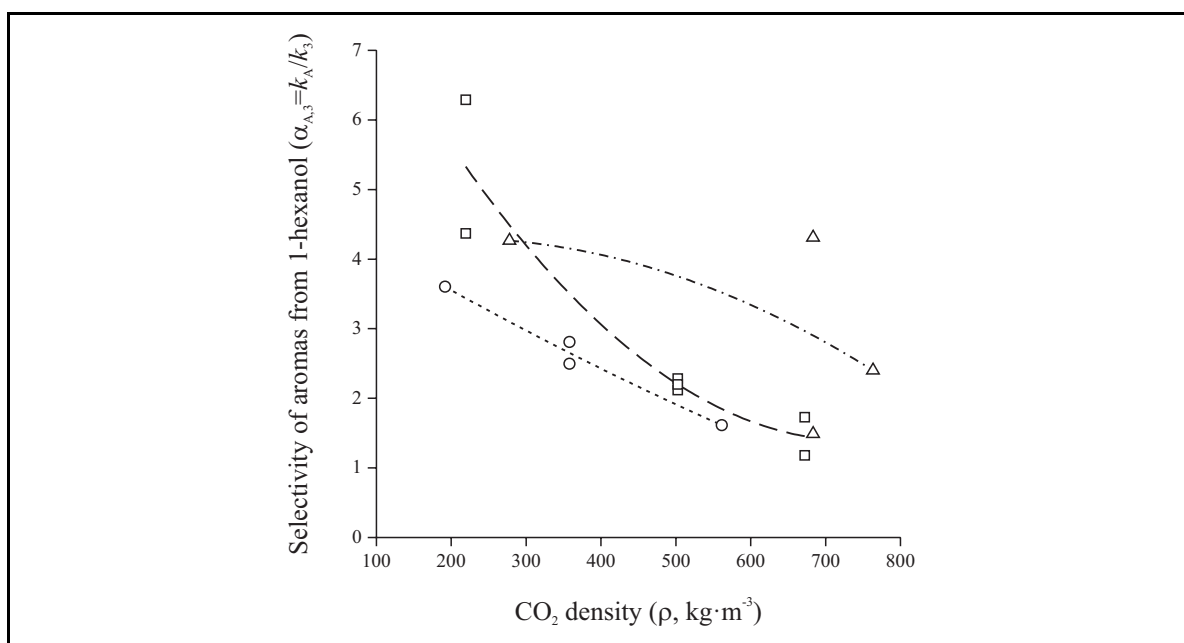


Figure 4.8 Selectivity of apple aroma constituents (*E*)-2-Hexenal, Hexanal from 1-Hexanol ($\alpha_{A,3}=k_A/k_3$). (---○---), 60 °C; (—□—), 50 °C; (----△----), 40 °C. Open symbols represent experimental values and lines signals trends.

As expected high separation factors between organic compounds and water were achieved. Fig 4.9 compares the selectivity of individual aromas from water ($\alpha_{i,4}=k_i/k_4$) calculated from column experiments and from (vapor + liquid) equilibria (VLE) data (Bejarano et al., 2015).

Selectivity values of (*E*)-2-hexenal from water ($\alpha_{1,4}=k_1/k_4$) calculated from column experiments were $\sim 10^4$ and were found to be in reasonable good agreement with those calculated from VLE data (Bejarano et al., 2015) (Fig. 4.9A). This result suggests that only one stage of equilibrium was achieved in the column, this could be explained by poor hydrodynamic characteristics inside the column due to high interfacial tension of aqueous systems and perhaps inappropriate packing type (IFT measurements for relevant apple aroma aqueous solutions are reported in Appendix 4). As it can be seen from Fig. 4.9B the separation factors for hexanal ($\alpha_{2,4}=k_2/k_4$) were higher than those calculated from VLE data nearly by an order of magnitude ($\sim 10^4$). The maximum separation factor was observed at 50 °C and CO₂ density of 500 kg·m⁻³. Nearly one order of magnitude lower ($\sim 10^3$) were the observed separation factors for 1-hexanol ($\alpha_{3,4}=k_3/k_4$) (Fig. 4.9C). This behavior is explained by the higher polarity of alcohols compared with that of aldehydes. However, a clear increasing tendency with increasing CO₂ density was observed for all temperatures suggesting that low pressure would be preferable for obtaining low separation factors between 1-hexanol and water. No experimental data was available to compare. However, from the behavior of (*E*)-2-hexenal and hexanal the $\alpha_{3,4}=k_3/k_4$ should not differ greatly from those calculated from VLE data.

As mentioned before, despite the higher polarity of alcohols compared to that of aldehydes, these were not sufficient for fractionation of 1-hexanol from the aroma compounds. This could explain why fractionation was not possible; the predominant effect was the concentration of organics in the extract.

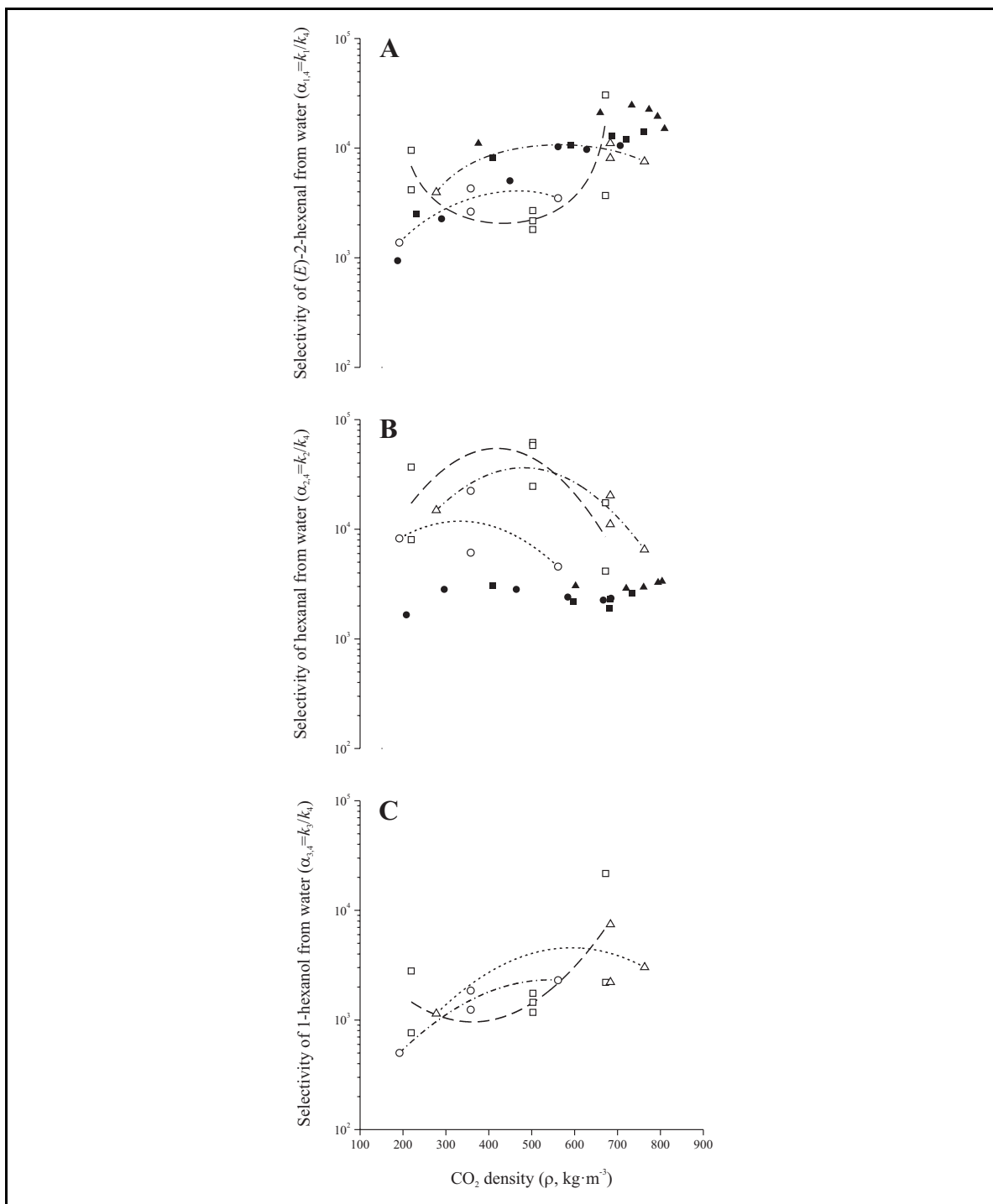


Figure 4.9 Selectivity of individual aromas from water ($\alpha_{i,4}=k_i/k_4$) calculated from column experiments and (vapor + liquid) equilibria (VLE) data (Bejarano et al., 2015). (A), (E)-2-hexenal; (B), Hexanal; (C), 1-hexanol; (---○---), 60 °C; (—□—), 50 °C; (----△----), 40 °C. Open symbols represent experimental values, closed symbols experimental values from VLE, and lines signal trends.

5. CONCLUSIONS AND PERSPECTIVES

This thesis describes in detail liquid fractionation technologies with SC-CO₂. Main applications are fractionation of lipids, deterpenation of essential oils, and fractionation of alcoholic beverages. Isolated applications also found in literature include fractionation of polymer mixtures and removal of organic solvents from water. The furthestmost explored technology is CC-SFF. Different types of operation were identified and described. Operating the column with an external reflux at the top (reflux mode) adds an extra equilibrium stage compared with the other modes of operation (stripping and semi-batch). This work also overviews comprehensively countercurrent packed columns in leading public research groups and some private institutions. Several random and structured packing materials have been tested. Internal column diameter ranges from 9 mm to 12.6 cm and the height ranges from 40 cm to 13.6 m, however, a standard height seems to be 3 m.

Less common technologies like membrane contactors are limited to aqueous solutions because they achieve a better immobile interphase. Care must be taken to not exceed ΔP_{crit} specially when operating a HFMC in the countercurrent mode. Fractionation of non-aqueous systems would probably lead to a mobile interphase in the pores causing the liquid phase to break into the CO₂ as drops or bubbles. In a single stage mixer-settler arrangement, as well as in a single HFMC module, only one equilibrium stage can be achieved. Therefore, these technologies are limited to mixtures that require a relatively small number of stages for a reasonable separation.

Columns without packing material are used in countercurrent and two-phase spray extractions. The absence of packing material (high specific surface for mass transfer) is overcome by generating very fine droplets by atomization. Therefore, the study and characterization of disintegration of liquid jets and atomization regimes at high pressures, where IFT plays a key role, are of great importance. Countercurrent and two-phase spray extractions are limited to mixtures with high separation factors (relatively small number of stages for a reasonable separation). Formation of particles using SC-CO₂ in spray

processes is a vast field of research and was not covered in this work. However, relevant references in this topic were provided to the interested reader.

Due to their design characteristics, static mixers are commonly used as mixing devices in mixer-settler arrangements as well as spray processes. Additionally, literature informs some successful attempts to use static mixers for equilibrium measurements and fractionation purposes. It is surprising that there are few comparisons between different technologies for a common application in literature.

This work also provides a general overview of fundamental equilibrium data and physicochemical properties of mixtures relevant to all the described applications and technologies. Densities and viscosities are commonly estimated from equilibrium data and are relevant to understand the hydrodynamics of the phases inside the separation equipment. IFT and contact angles of diverse aqueous mixtures surrounded by CO₂ at high pressures need to be studied in detail to improve the knowledge and application of CC-SFF for complex aqueous systems. Knowledge of IFT and contact angles of edible oil mixtures in contact with dense CO₂ is well studied. No wetting behavior studies were found for membrane contactors.

Regarding the fundamental equilibrium data for the CC-SFF of apple aromas, new high-pressure (vapor + liquid) equilibria data for the ternary systems {CO₂ + (*E*)-2-hexenal water} and (CO₂ + hexanal + water) was measured using a new apparatus and methodology assembled in this work with standard combined uncertainties for the vapor phase, $u_{\text{comb}}(y) < 0.004$ and for the liquid phase, $u_{\text{comb}}(x) < 0.001$.

The methodology includes the quantification of all components in each phase. The measurements were performed at fixed liquid phase composition (600 mg kg⁻¹) and at temperatures of (313, 323 and 333) K and pressures from (8 to 19) MPa. Partition coefficients and separation factors were derived from the measured values of the VLE in order to suggest reasonable temperature and pressure conditions for the separation of apple aromas from aqueous solutions by CC-SFF in packed columns. Partition coefficients of (*E*)-2-hexenal between CO₂ and water were in the range of (6 to 91) and were found to be near six times higher than those of hexanal (9 to 17). Higher separation factors for (*E*)-2-

hexenal were found to be at pressures from (10 to 14) MPa and at $T = 313$ K. For hexanal, higher separation factors were observed at pressures from (16 to 17) MPa and at $T = 313$ K. In addition, for both ternary systems temperature crossovers were detected. Even though this behavior could be a consequence of the physicochemical characteristics of the mixture, the estimated experimental uncertainties could, in part, explain the observed results. Preliminary studies on CC-SFF of these compounds should explore these conditions.

A newly acquired CounterCurrent Supercritical Fluid Fractionation (CC-SFF) packed column was started up by studying the separation of key apple aroma constituents ((*E*)-2-hexenal and hexanal) from aqueous solutions containing 1-hexanol using supercritical CO_2 .

CC-SFF of aqueous C-6 apple aromas is highly capable of producing a water-free super-concentrated product. Very high separation factors of individual aromas over water were observed ($\sim 10^4$). Therefore, all organic compounds were practically removed completely from the feed solution and a two-phase extract was collected in the separator.

However, polarity differences between (*E*)-2-hexenal, hexanal and 1-hexanol were not sufficient for fractionation of 1-hexanol from the aroma compounds and, consequently the predominant effect was the concentration of organics in the extract.

The extraction yield of aromas was > 86 % for all experiments and the highest organic compounds composition in the extract was 43 % w/w. The S/F had the most significant effect on the extraction of apple aroma compounds as observed by other authors, and according to the RSM models 40°C , 14 MPa, and $S/F = 4$ to would be optimum condition to concentrate C-6 apple aromas.

Phase equilibrium measurements are very time-consuming and complicated tasks, especially for heterogeneous and multicomponent mixtures at elevated pressures. Complex EoS models are needed to describe and predict these systems appropriately. Usually experimental data are obtained for a particular application in a relatively narrow range of pressures and temperatures.

In view of the difficulty in obtaining reliable phase equilibrium data and versatile models applicable to a wide range of mixtures and conditions, a common strategy in modelling CC-SFF, is to use empirical correlations or a simple or a predictive EoS, such as the Peng-Robinson EoS. However, even though the equilibrium data obtained in this thesis is valuable it is not sufficient for modelling and design of the CC-SFF process of apple C-6 aromas. Additionally, in order to come close to a real aroma mixture ethanol should be included in the mixture.

Future work should focus in expanding phase equilibrium measurements in order to model and design the process using graphical (such as those of McCabe-Thiele or Ponchon-Savarit) or computer-aided determination of NTU and HTU or HETP. Additionally, determination of hydrodynamic characteristics such as dry and wet pressure drops, flooding points, liquid holdups, and IFT on the column packing surface is necessary to completely understand the performance of SC-SFF of apple C-6 aromas.

NOMENCLATURE

Acronyms

AMF	Anhydrous Milk Fat
ANOVA	ANalysis Of VAriance
BBD	Box-Behnken Design
CC	CounterCurrent
CC-SE	CounterCurrent Spray Extraction
CC-SFF	CounterCurrent Supercritical Fluid Fractionation
CFD	Computer Fluid Dynamics
CIAL	<i>Instituto de Investigación en Ciencias de la Alimentación</i>
CR	Capillary Rise
CSIC	<i>Consejo Superior de Investigaciones Científicas</i>
DNR	Du Nouy Ring
DSA	Drop Shape Analysis
EoS	Equation of State
FMSA	First-order Mean Spherical Approximation
FO	First Order
GC	Gas Chromatography
GC	Group Contribution
HETP	Height Equivalent to a Theoretical Plate
HFMC	Hollow Fiber Membrane Contactor
HTU	Height of the mass-Transfer Unit
HTU _G	Height of the mass-Transfer Unit for the gas phase
HTU _L	Height of the mass-Transfer Unit for the liquid phase
IFT	InterFacial Tension
LL	Liquid + Liquid
LLV	Liquid + Liquid + Vapor
LSC	Liquid + SuperCritical
NTU	Number of transfer Units
OODD	Olive Oil Deodorizer Distillate
PCP	Perturbed Chain Polar
PD	Pendant Drop
PGSS	Particles from Gas Saturated Solutions
PQ	Pure Quadratic

REQUIMTE	<i>Laboratório Associado para a Química Verde – Tecnologias e Processos Limpos</i>
RESS	Rapid Expansion of Saturated Solutions
RSM	Response Surface Methodology
S/F	Solvent-to-Feed ratio
SAFT	Statistical Association Fluid Theory
SC-CO ₂	Supercritical CO ₂
SFE	Supercritical Fluid Extraction
SFF	Supercritical Fluid Fractionation
SLO	Shark Liver Oil
SODD	Soybean Oil Deodorizer Distillate
SP	Selected Plane
SPME	Solid Phase Micro Extraction
SS	Stainless Steel
TFI	Two Factor Interaction
TP-SE	Two-Phase Spray Extraction
TUHH	<i>Technische Universität Hamburg-Harburg</i>
UAM	<i>Universidad Autónoma de Madrid</i>
USDA	United States Department of Agriculture
VL	Vapor + Liquid

Variables and parameters

a	Packing specific surface [m^{-1}]
a_e	Effective specific interfacial area [m^{-1}]
ΔP_{Crit}	Critical pressure difference between fluids phases in membrane contactors [MPa]
G_m	Gas phase molar flow rate per unit cross sectional area [$\text{mol} \cdot \text{s}^{-1} \cdot \text{m}^{-2}$]
J_i	Mass flux of solute i [$\text{kg} \cdot \text{s}^{-1} \cdot \text{m}^{-2}$]
J_{CO_2}	Mass flux of CO ₂ [$\text{kg} \cdot \text{s}^{-1} \cdot \text{m}^{-2}$]
$K_{\text{CO}_2, \text{L}}$	SC-CO ₂ liquid phase overall mass-transfer coefficient [$\text{m} \cdot \text{s}^{-1}$]
k_G	Gas phase mass-transfer coefficient [$\text{mol} \cdot \text{s}^{-1} \cdot \text{m}^{-2}$]
k_i	Phase equilibrium partition coefficient [-]
$K_{i, \text{SC}}$	Solute i SuperCritical phase overall mass-transfer coefficient [$\text{m} \cdot \text{s}^{-1}$]
k_L	Liquid phase mass-transfer coefficient [$\text{mol} \cdot \text{s}^{-1} \cdot \text{m}^{-2}$]
L_m	Liquid phase molar flow rate per unit cross sectional area [$\text{mol} \cdot \text{s}^{-1} \cdot \text{m}^{-2}$]

N	Number of theoretical stages [-]
OL	Organics Loading [$\text{mgOrg} \cdot \text{kgCO}_2^{-1}$]
P	Pressure [MPa]
P_1	Pressure of fluid phase 1 in membrane contactors [MPa]
P_2	Pressure of fluid phase 2 in membrane contactors [MPa]
q_E	Extract mass flow rate [$\text{g} \cdot \text{min}^{-1}$]
q_F	Feed mass flow rate [$\text{g} \cdot \text{min}^{-1}$]
q_R	Raffinate mass flow rate [$\text{g} \cdot \text{min}^{-1}$]
S/F	Solvent-to-Feed ratio [$\text{kg} \cdot \text{kg}^{-1}$]
T	Temperature [$^{\circ}\text{C}$]
u_L	Liquid phase superficial velocity [$\text{m} \cdot \text{s}^{-1}$]
u_{SC}	SuperCritical phase superficial velocity [$\text{m} \cdot \text{s}^{-1}$]
x_i	Solute i mass fraction in the raffinate stream [%w/w]
x_{CO_2}	CO_2 liquid phase mole fraction [$\text{mol} \cdot \text{mol}^{-1}$]
$x_{\text{CO}_2}^*$	CO_2 liquid phase equilibrium mole fraction [$\text{mol} \cdot \text{mol}^{-1}$]
x_i^*	Solute i liquid phase equilibrium mole fraction [$\text{mol} \cdot \text{mol}^{-1}$]
y_i	Solute i gas phase mole fraction [$\text{mol} \cdot \text{mol}^{-1}$]
y_i	Solute i mass fraction in the extract stream [%w/w]
y_i^*	Solute i gas phase equilibrium mole fraction [$\text{mol} \cdot \text{mol}^{-1}$]
Y_A	Extraction yield of aromas [%]
Y_{tot}	Total yield Extraction yield of organics [%]
Z	Height of packing [m]
z_i	Solute i mass fraction in the feed stream [%w/w]
Greek symbols	
ε	Void fraction [-]
λ	Stripping factor [-]
ρ_L	Density of the Liquid phase [$\text{kg} \cdot \text{m}^{-3}$]
ρ_{SC}	Density of the SuperCritical phase [$\text{kg} \cdot \text{m}^{-3}$]
α_{ij}	Selectivity factor of compound i over compound j [-]

REFERENCES

- Al-darmaki, N., Lu, T., Al-duri, B., Harris, J. B., Favre, T. L. F., Bhaggan, K., & Santos, R. C. D. (2012). Isothermal and temperature gradient supercritical fluid extraction and fractionation of squalene from palm fatty acid distillate using compressed carbon dioxide. *The Journal of Supercritical Fluids*, 61, 108–114.
- Assaoui, M., Benadda, B., & Otterbein, M. (2007). Distillation under high pressure: a behavioral study of packings. *Chemical Engineering & Technology*, 30(6), 702–708.
- Bachu, S., & Bennion, D. B. (2009). Interfacial tension between CO₂, freshwater, and brine in the range of pressure from (2 to 27) MPa, temperature from (20 to 125) °C, and water salinity from (0 to 334 000) mg·l⁻¹. *Journal of Chemical & Engineering Data*, 54(3), 765–775.
- Becker, O., & Heydrich, G. (2004). Separation efficiency and axial mixing in packed high pressure extraction columns. In G. Brunner (Ed.), *Supercritical Fluids as Solvents and Reaction Media* (pp. 465–488). Hamburg: Elsevier Science and Technology Books.
- Bejarano, A., López, P. I., del Valle, J. M., & de la Fuente, J. C. (2015). High-pressure (vapour + liquid) equilibria for ternary systems composed by {(e)-2-hexenal or hexanal + carbon dioxide + water}: partition coefficient measurement. *The Journal of Chemical Thermodynamics*, 89, 79–88.
- Bejarano, A., Simões, P. C., & del Valle, J. M. (2016). Fractionation technologies for liquid mixtures using dense carbon dioxide. *The Journal of Supercritical Fluids*, 107, 321–348.
- Belitz, H.-D., Grosch, W., & Schieberle, P. (2009). *Food chemistry* (4th ed.). Berlin: Springer-Verlag.
- Benadda, B., Kafoufi, K., Monkam, P., & Otterbein, M. (2000). Hydrodynamics and mass transfer phenomena in counter-current packed column at elevated pressures. *Chemical Engineering Science*, 55(24), 6251–6257.
- Benadda, B., Otterbein, M., Kafoufi, K., & Prost, M. (1996). Influence of pressure on the gas/liquid interfacial area a and coefficient k_{la} in a counter-current packed column. *Chemical Engineering and Processing*, 35, 247–253.
- Benvenuti, F., & Gironi, F. (2001). High-pressure equilibrium data in systems containing supercritical carbon dioxide, limonene, and citral. *Journal of Chemical & Engineering Data*, 46, 795–799.
- Bessi eres, D., Saint-Guirons, H., & Daridon, J.-L. (2001). Volumetric behavior of decane + carbon dioxide at high pressures. measurement and calculation. *Journal of Chemical & Engineering Data*, 46(5), 1136–1139.
- Bharath, R., Inomata, H., Adschiri, T., & Arai, K. (1992). Phase-equilibrium study for the separation and fractionation of fatty oil components using supercritical carbon-dioxide. *Fluid Phase Equilibria*, 81(1-2), 307–320.
- Bhaskar, A. R., Rizvi, S. S. H., & Harriott, P. (1993). Performance of a packed column for continuous supercritical carbon dioxide processing of anhydrous milk fat.

Biotechnology Progress, 9, 70–74.

- Bhaskar, A. R., Rizvi, S. S. H., & Sherbon, J. W. (1993). Anhydrous milk-fat fractionation with continuous countercurrent supercritical carbon-dioxide. *Journal of Food Science*, 58(4), 748–752.
- Birjessön, J., Karlsson, H. O. E., Trägårdh, G., Börjesson, J., Karlsson, H. O. E., & Trägårdh, G. (1996). Pervaporation of a model apple juice aroma solution: comparison of membrane performance. *Journal of Membrane Science*, 119(2), 229–239.
- Bocquet, S., Romero, J., Sanchez, J., & Rios, G. M. (2007). Membrane contactors for the extraction process with subcritical carbon dioxide or propane: simulation of the influence of operating parameters. *The Journal of Supercritical Fluids*, 41(2), 246–256.
- Bocquet, S., Torres, A., Sanchez, J., Rios, G. M., & Romero, J. (2005). Modeling the mass transfer in solvent-extraction processes with hollow-fiber membranes. *AIChE Journal*, 51(4), 1067–1079.
- Bondioli, P., Mariani, C., Lanzani, A., Fedeli, E., Mossa, A., & Muller, A. (1992). Lampante olive oil refining with supercritical carbon-dioxide. *Journal of the American Oil Chemists' Society*, 69(5), 477–480.
- Bonthuys, G. J. K., Schwarz, C. E., Burger, A. J., & Knoetze, J. H. (2011). Separation of alkanes and alcohols with supercritical fluids. Part I: phase equilibria and viability study. *The Journal of Supercritical Fluids*, 57(2), 101–111.
- Borges, G. R., Junges, A., Franceschi, E., Corazza, F. C., Corazza, M. L., Oliveira, J. V., & Dariva, C. (2007). High-pressure vapor–liquid equilibrium data for systems involving carbon dioxide + organic solvent + β -carotene. *Journal of Chemical & Engineering Data*, 52(4), 1437–1441.
- Bothun, G. D., Knutson, B. L., Strobel, H. J., Nokes, S. E., Brignole, E. A., & Diaz, S. (2003). Compressed solvents for the extraction of fermentation products within a hollow fiber membrane contactor. *The Journal of Supercritical Fluids*, 25, 119–134.
- Bravo Mina, J., & Odepa. (2011). Mercado de la manzana, 16.
- Brudi, K., Dahmen, N., & Schmieder, H. (1996). Partition coefficients two-phase mixtures dioxide at pressures temperatures of 313 to 333 K. *The Journal of Supercritical Fluids*, 9(3), 146–151.
- Brunner, G. (1994). *Gas extraction: an introduction to fundamentals of supercritical fluids and the application to separation processes*. New York, NY: Springer.
- Brunner, G. (1998). Industrial process development countercurrent multistage gas extraction (SFE) processes. *The Journal of Supercritical Fluids*, 13(1-3), 283–301.
- Brunner, G. (2005). Supercritical fluids: technology and application to food processing. *Journal of Food Engineering*, 67(1-2), 21–33.
- Brunner, G. (2009). Counter-current separations. *The Journal of Supercritical Fluids*, 47(3), 574–582.
- Brunner, G. (2010). Applications of supercritical fluids. *Annual Review of Chemical and*

Biomolecular Engineering, 1(1), 321–342.

- Brunner, G., & Budich, M. (2004). Separation of organic compounds from aqueous solutions by means of supercritical carbon dioxide. In *Supercritical Fluids as Solvents and Reaction Media* (pp. 489–522). Elsevier.
- Brunner, G., & Machado, N. T. (2012). Process design methodology for fractionation of fatty acids from palm fatty acid distillates in countercurrent packed columns with supercritical CO₂. *The Journal of Supercritical Fluids*, 66, 96–110.
- Brunner, G., Malchow, T., Stürken, K., & Gottschau, T. (1991). Separation of tocopherols from deodorizer condensates by countercurrent extraction with carbon dioxide. *The Journal of Supercritical Fluids*, 4(1), 72–80.
- Budich, M. (1999). *Countercurrent extraction of citrus aroma from aqueous and nonaqueous solutions using supercritical carbon dioxide*. TU-Hamburg-Harburg, Germany.
- Budich, M., & Brunner, G. (1999). Vapor–liquid equilibrium data and flooding point measurements of the mixture carbon dioxide+orange peel oil. *Fluid Phase Equilibria*, 158–160, 759–773.
- Budich, M., & Brunner, G. (2003). Supercritical fluid extraction of ethanol from aqueous solutions. *The Journal of Supercritical Fluids*, 25(1), 45–55.
- Budich, M., Heilig, S., Wesse, T., Leibkuchler, V., & Brunner, G. (1999). Countercurrent deterpenation of citrus oils with supercritical CO₂. *The Journal of Supercritical Fluids*, 14(2), 105–114.
- Calvignac, B., Rodier, E., Letourneau, J.-J., Almeida dos Santos, P. M., & Fages, J. (2010). Cocoa butter saturated with supercritical carbon dioxide: measurements and modelling of solubility, volumetric expansion, density and viscosity. *International Journal of Chemical Reactor Engineering*, 8(A73), 1–29.
- Carelli, A. A., Crapiste, G. H., & Lozano, J. E. (1991). Activity coefficients of aroma compounds in model solutions simulating apple juice. *Journal of Agricultural and Food Chemistry*, 39(9), 1636–1640.
- Carlson, L. H. C., Bolzan, A., & Machado, R. A. F. (2005). Separation of d-limonene from supercritical CO₂ by means of membranes. *The Journal of Supercritical Fluids*, 34(2), 143–147.
- Carvalho Jr, R. N., Corazza, M. L., Cardozo-Filho, L., & Meireles, M. A. A. (2006). Phase equilibrium for (camphor + CO₂), (camphor + propane), and (camphor + CO₂ + propane). *Journal of Chemical and Engineering Data*, 51(3), 997–1000.
- Catchpole, O. J., Grey, J. B., & Noermark, K. A. (1998). Solubility of fish oil components in supercritical CO₂ and CO₂ plus ethanol mixtures. *Journal of Chemical & Engineering Data*, 43(6), 1091–1095.
- Catchpole, O. J., Grey, J. B., & Noermark, K. A. (2000). Fractionation of fish oils using supercritical CO₂ and CO₂ plus ethanol mixtures. *The Journal of Supercritical Fluids*, 19(1), 25–37.
- Catchpole, O. J., Simões, P. C., Grey, J. B., Nogueiro, E. M. M., Carmelo, P. J., & Nunes

- da Ponte, M. (2000). Fractionation of lipids in a static mixer and packed column using supercritical carbon dioxide. *Industrial & Engineering Chemistry Research*, 39(12), 4820–4827.
- Catchpole, O. J., & von Kamp, J.-C. (1997). Phase equilibrium for the extraction of squalene from shark liver oil using supercritical carbon dioxide. *Industrial & Engineering Chemistry Research*, 36(9), 3762–3768.
- Catchpole, O. J., von Kamp, J.-C., & Grey, J. B. (1997). Extraction of squalene from shark liver oil in a packed column using supercritical carbon dioxide. *Industrial & Engineering Chemistry Research*, 36(10), 4318–4324.
- Cháfer, A., Berna, A., Montón, J. B., & Mulet, A. (2001). High pressure solubility data of the system limonene + linalool + CO₂. *Journal of Chemical & Engineering Data*, 46(5), 1145–1148.
- Cháfer, A., Fornari, T., Berna, A., Ibañez, E., & Reglero, G. (2005). Solubility of solid carnosic acid in supercritical CO₂ with ethanol as a co-solvent. *The Journal of Supercritical Fluids*, 34(3), 323–329.
- Chang, C.-M. J., Chang, Y.-F., Lee, H., Lin, J., & Yang, P.-W. (2000). Supercritical carbon dioxide extraction of high-value substances from soybean oil deodorizer distillate. *Industrial & Engineering Chemistry Research*, 39(12), 4521–4525.
- Chang, C.-M. J., Day, C.-Y., Ko, C.-M., & Chiu, K.-L. (1997). Densities and p-x-y diagrams for carbon dioxide dissolution in methanol, ethanol, and acetone mixtures. *Fluid Phase Equilibria*, 131(1-2), 243–258.
- Charbit, G., Badens, E., & Boutin, O. (2004). Methods of particle production. In P. York, U. B. Kampella, & B. Y. Shekunov (Eds.), *Supercritical Fluid Technology for Drug Product Development* (pp. 159–212). New York, USA: Marcel Dekker.
- Chen, C.-R., Wang, C.-H., Wang, L.-Y., Hong, Z.-H., Chen, S.-H., Ho, W.-J., & Chang, C.-M. J. (2008). Supercritical carbon dioxide extraction and deacidification of rice bran oil. *The Journal of Supercritical Fluids*, 45(3), 322–331.
- Chiquet, P., Daridon, J.-L., Broseta, D., & Thibeau, S. (2007). CO₂/water interfacial tensions under pressure and temperature conditions of CO₂ geological storage. *Energy Conversion and Management*, 48(3), 736–744.
- Chirico, R. D., Frenkel, M., Diky, V. V., Marsh, K. N., & Wilhoit, R. C. (2003). Thermoml-an xml-based approach for storage and exchange of experimental and critically evaluated thermophysical and thermochemical property data. 2. uncertainties. *Journal of Chemical & Engineering Data*, 48(5), 1344–1359.
- Christov, M., & Dohrn, R. (2002). High-pressure fluid phase equilibria experimental methods and systems investigated (1994 – 1999). *Fluid Phase Equilibria*, 202, 153–218.
- Chuang, M.-H., & Brunner, G. (2006). Concentration of minor components in crude palm oil. *The Journal of Supercritical Fluids*, 37(2), 151–156.
- Chun, B.-S., & Wilkinson, G. T. (1995). Interfacial tension in high-pressure carbon dioxide mixtures. *Industrial & Engineering Chemistry Research*, 34, 4371–4377.

- Compton, D. L., Eller, F. J., Laszlo, J. A., & Evans, K. O. (2012). Purification of 2-monoacylglycerols using liquid CO₂ extraction. *Journal of the American Oil Chemists' Society*, 89(8), 1529–1536.
- Compton, D. L., Laszlo, J. A., Eller, F. J., & Taylor, S. L. (2008). Purification of 1,2-diacylglycerols from vegetable oils: comparison of molecular distillation and liquid CO₂ extraction. *Industrial Crops and Products*, 28(2), 113–121.
- Czerny, M., Christlbauer, M. M., Christlbauer, M. M., Fischer, A., Granvogl, M., Hammer, M., ... Schieberle, P. (2008). Re-investigation on odour thresholds of key food aroma compounds and development of an aroma language based on odour qualities of defined aqueous odorant solutions. *European Food Research and Technology*, 228(2), 265–273.
- Czerwonatis, N., & Eggers, R. (2001). Disintegration of liquid jets and drop drag coefficients in pressurized nitrogen and carbon dioxide. *Chemical Engineering & Technology*, 24(6), 619–624.
- da Porto, C., & Decorti, D. (2010). Countercurrent supercritical fluid extraction of grape-spirit. *The Journal of Supercritical Fluids*, 55(1), 128–131.
- Danielski, L., Brunner, G., Schwänke, C., Zetzl, C., Hense, H., & Donoso, J. P. M. (2008). Deterpenation of mandarin (citrus reticulata) peel oils by means of countercurrent multistage extraction and adsorption/desorption with supercritical CO₂. *The Journal of Supercritical Fluids*, 44(3), 315–324.
- Danielski, L., Zetzl, C., Hense, H., & Brunner, G. (2005). A process line for the production of raffinated rice oil from rice bran. *The Journal of Supercritical Fluids*, 34(2), 133–141.
- De Haan, A. B., & de Graauw, J. (1990). Extraction of flavors from milk fat with supercritical carbon dioxide. *The Journal of Supercritical Fluids*, 3(1), 15–19.
- De Haan, A. B., & De Graauw, J. (1991). Mass transfer in supercritical extraction columns with structured packings for hydrocarbon processing. *Industrial & Engineering Chemistry Research*, 30(11), 2463–2470.
- de la Fuente, J. C., & Bottini, S. B. (2000). High-pressure phase equilibria and thermodynamic modelling for the binary systems CO₂+lemon oil and C₂H₆+lemon oil. *Fluid Phase Equilibria*, 175(1-2), 45–52.
- de la Fuente, J. C., Núñez, G., & del Valle, J. M. (2007). Bubble-point measurements for the system CO₂+aqueous ethanol solutions of boldo leaf antioxidant components (boldine and catechin) at high pressures. *Fluid Phase Equilibria*, 259(1), 77–82.
- de Lucas, A., Gracia, I., Rincón, J., & García, M. T. (2007). Solubility determination and model prediction of olive husk oil in supercritical carbon dioxide and cosolvents. *Industrial & Engineering Chemistry Research*, 46(14), 5061–5066.
- Díaz, S., Espinosa, S., & Brignole, E. A. (2005). Citrus peel oil deterpenation with supercritical fluids - optimal process and solvent cycle design. *The Journal of Supercritical Fluids*, 35(1), 49–61.
- Diban, N., Athès-Dutour, V., Bes, M., & Souchon, I. (2008). Ethanol and aroma

- compounds transfer study for partial dealcoholization of wine using membrane contactor. *Journal of Membrane Science*, 311(1-2), 136–146.
- Dimick, P. S., Hoskin, J. C., & Acree, T. E. (1983). Review of apple flavor: state of the art. *Critical Reviews in Food Science and Nutrition*, 18(4), 387–409.
- Dittmar, D., De Arévalo, A. M., Beckmann, C., & Eggers, R. (2005). Interfacial tension and density measurement of the system corn germ oil - carbon dioxide at low temperatures. *European Journal of Lipid Science and Technology*, 107(1), 20–29.
- Dittmar, D., Eggers, R., Kahl, H., & Enders, S. (2002). Measurement and modelling of the interfacial tension of triglyceride mixtures in contact with dense gases. *Chemical Engineering Science*, 57(3), 355–363.
- Dittmar, D., Fredenhagen, A., Oei, S. B., & Eggers, R. (2003). Interfacial tensions of ethanol-carbon dioxide and ethanol-nitrogen. dependence of the interfacial tension on the fluid density - prerequisites and physical reasoning. *Chemical Engineering Science*, 58(7), 1223–1233.
- Dittmar, D., Oei, S. B., & Eggers, R. (2002). Interfacial tension and density of ethanol in contact with carbon dioxide. *Chemical Engineering & Technology*, 25(1), 23–27.
- Dixon, J., & Hewett, E. W. (2000). Factors affecting apple aroma / flavour volatile concentration : a review. *New Zealand Journal of Crop and Horticultural Science*, 28(February 2013), 155–173.
- Dohrn, R., & Brunner, G. (1995). High-pressure fluid-phase equilibria: experimental methods and systems investigated (1988–1993). *Fluid Phase Equilibria*, 106(1-2), 213–282.
- Dohrn, R., Peper, S., & Fonseca, J. M. S. (2010). High-pressure fluid-phase equilibria: experimental methods and systems investigated (2000–2004). *Fluid Phase Equilibria*, 288(1-2), 1–54.
- Drawert, F., Kuchendauer, F., Brickner, H., & Schreier, P. (1976). Über die quantitative gusammensetzung natürlicher und technologisch overanderter pflanzelicher aromen. *Chemie Mikrobiologie Technologie Der Lebensmittel*, 5(27).
- Dunford, N. T., & King, J. W. (2001). Thermal gradient deacidification of crude rice bran oil utilizing supercritical carbon dioxide. *Journal of the American Oil Chemists' Society*, 78(2), 121–125.
- Dunford, N. T., Teel, J. A., & King, J. W. (2003). A continuous countercurrent supercritical fluid deacidification process for phytosterol ester fortification in rice bran oil. *Food Research International*, 36(2), 175–181.
- Durling, N. E., Catchpole, O. J., Tallon, S. J., & Grey, J. B. (2007). Measurement and modelling of the ternary phase equilibria for high pressure carbon dioxide–ethanol–water mixtures. *Fluid Phase Equilibria*, 252(1-2), 103–113.
- Edwards, W. F., & Thies, M. C. (2006). Fractionation of pitches by molecular weight using continuous and semibatch dense-gas extraction. *Carbon*, 44(2), 243–252.
- Eggers, R., Wagner, H., & Schneider, M. (1999a). Process for high pressure spray extraction of liquids.

- Eggers, R., Wagner, H., & Schneider, M. (1999b). Process for high-pressure spray extraction of liquids.
- Eggers, R., Wagner, H., & Wag. (1993). Extraction device for high viscous media in a high-turbulent two-phase flow with supercritical CO₂. *The Journal of Supercritical Fluids*, 6(1), 31–37.
- Elizalde-Solis, O., & Galicia-Luna, L. A. (2006). Solubilities and densities of capsaicin in supercritical carbon dioxide at temperatures from 313 to 333 K. *Industrial & Engineering Chemistry Research*, 45(15), 5404–5410.
- Eller, F. J., Taylor, S. L., Compton, D. L., Laszlo, J. A., & Palmquist, D. E. (2008). Counter-current liquid carbon dioxide purification of a model reaction mixture. *The Journal of Supercritical Fluids*, 43(3), 510–514.
- Eller, F. J., Taylor, S. L., & Curren, M. S. S. (2004). Use of liquid carbon dioxide to remove hexane from soybean oil. *Journal of the American Oil Chemists' Society*, 81(10), 989–992.
- Eller, F. J., Taylor, S. L., Laszlo, J. A., Compton, D. L., & Teel, J. A. (2009). Counter-current carbon dioxide purification of partially deacylated sunflower oil. *Journal of the American Oil Chemists' Society*, 86(3), 277–282.
- Eller, F. J., Taylor, S. L., & Palmquist, D. E. (2007). Enhanced selective extraction of hexane from hexane/soybean oil mixture using binary gas mixtures of carbon dioxide. *Journal of Agricultural and Food Chemistry*, 55(8), 2779–83.
- Elss, S., Preston, C., Appel, M., Heckel, F., & Schreier, P. (2006). Influence of technological processing on apple aroma analysed by high resolution gas chromatography–mass spectrometry and on-line gas chromatography–combustion/pyrolysis-isotope ratio mass spectrometry. *Food Chemistry*, 98(2), 269–276.
- Enders, S., & Kahl, H. (2008). Interfacial properties of water+alcohol mixtures. *Fluid Phase Equilibria*, 263(2), 160–167.
- Estay, H., Bocquet, S., Romero, J., Sanchez, J., Rios, G. M., & Valenzuela, F. (2007). Modeling and simulation of mass transfer in near-critical extraction using a hollow fiber membrane contactor. *Chemical Engineering Science*, 62(21), 5794–5808.
- Fang, T., Goto, M., Sasaki, M., & Hirose, T. (2005). Phase equilibria for the ternary system methyl oleate plus tocopherol plus supercritical CO₂. *Journal of Chemical & Engineering Data*, 50(2), 390–397.
- Fang, T., Goto, M., Wang, X.-B., Ding, X., Geng, J.-G., Sasaki, M., & Hirose, T. (2007). Separation of natural tocopherols from soybean oil byproduct with supercritical carbon dioxide. *The Journal of Supercritical Fluids*, 40(1), 50–58.
- Fang, T., Goto, M., Yun, Z., Ding, X., & Hirose, T. (2004). Phase equilibria for binary systems of methyl oleate–supercritical CO₂ and α -tocopherol–supercritical CO₂. *The Journal of Supercritical Fluids*, 30(1), 1–16.
- Fernandes, J., Lisboa, P. F., Barbosa Mota, J. P., & Simões, P. C. (2011). Modelling and simulation of a complete supercritical fluid extraction plant with countercurrent

- fractionation column. *Separation Science and Technology*, 46(13), 2088–2098.
- Fernandes, J., Lisboa, P. F., Simões, P. C., Mota, J. P. B. B. P. B., & Saadjan, E. E. (2009). Application of cfd in the study of supercritical fluid extraction with structured packing: wet pressure drop calculations. *The Journal of Supercritical Fluids*, 50(1), 61–68.
- Fernandes, J., Ruivo, R. M., Mota, J. P. B., Simoes, P., & Simões, P. C. (2007). Non-isothermal dynamic model of a supercritical fluid extraction packed column. *The Journal of Supercritical Fluids*, 41(1), 20–30.
- Fernandes, J., Ruivo, R. M., & Simões, P. C. (2007). Dynamic model of a supercritical fluid extraction plant. *AIChE Journal*, 53(4), 825–837.
- Fernandes, J., Simões, P. C., Mota, J. P. B. B. P. B., Saadjan, E. E., Lisboa, P. F., Simões, P. C., ... Saadjan, E. E. (2008). Application of cfd in the study of supercritical fluid extraction with structured packing: dry pressure drop calculations. *The Journal of Supercritical Fluids*, 47(1), 17–24.
- Fernández-Ronco, M. P., Gracia, I., Zetzi, C., de Lucas, A., García, M. T., & Rodríguez, J. F. (2011). Equilibrium data for the separation of oleoresin capsicum using supercritical CO₂: a theoretical design of a countercurrent gas extraction column. *The Journal of Supercritical Fluids*, 57(1), 1–8.
- Flath, R. A., Black, D. R., Guadagni, D. G., McFadden, W. H., & Schultz, T. H. (1967). Identification and organoleptic evaluation of compounds in delicious apple essence. *Journal of Agricultural and Food Chemistry*, 15(1), 29–35.
- Fleck, U., Tieg, C., & Brunner, G. (1998). Fractionation of fatty acid ethyl esters by supercritical CO₂: high separation efficiency using an automated countercurrent column. *The Journal of Supercritical Fluids*, 14(1), 67–74.
- Fonseca, J. M. S., Dohrn, R., & Peper, S. (2011). High-pressure fluid-phase equilibria: experimental methods and systems investigated (2005–2008). *Fluid Phase Equilibria*, 300(1-2), 1–69.
- Fonseca, J., Simões, P. C., & Nunes da Ponte, M. (2003). An apparatus for high-pressure vle measurements using a static mixer. results for (CO₂+limonene+citral) and (CO₂+limonene+linalool). *The Journal of Supercritical Fluids*, 25(1), 7–17.
- Fornari, R. E., Alessi, P., & Kikic, I. (1990). High pressure fluid phase equilibria: experimental methods and systems investigated (1978–1987). *Fluid Phase Equilibria*, 57(1-2), 1–33.
- Fornari, T., Hernández, E. J., Ruiz-Rodríguez, A., Javier Señorans, F., Reglero, G., Ruiz-Rodríguez, A., ... Reglero, G. (2009). Phase equilibria for the removal of ethanol from alcoholic beverages using supercritical carbon dioxide. *The Journal of Supercritical Fluids*, 50(2), 91–96.
- Fornari, T., Torres, C. F., Señorans, F. J., & Reglero, G. (2009). Simulation and optimization of supercritical fluid purification of phytosterol esters. *AIChE Journal*, 55(4), 1023–1029.
- Fornari, T., Vázquez, L., Torres, C. F., Ibáñez, E., Señorans, F. J., & Reglero, G. (2008).

- Countercurrent supercritical fluid extraction of different lipid-type materials: experimental and thermodynamic modeling. *Journal of Supercritical Fluids*, 45(2), 206–212.
- Furuta, S., Ikawa, N., Fukuzato, R., & Imanishi, N. (1989). Extraction of ethanol from aqueous solutions using supercritical carbon dioxide. *Kagaku Kogaku Ronbunshu*, 15(3), 519–512.
- Furuta, S., Ikawa, N., Fukuzato, R., & Imanishi, N. (1990). Extraction of ethanol from aqueous solutions using supercritical carbon dioxide. In *Proceedings of the 2nd International Symposium on High-Pressure Chemical Engineering* (pp. 345–351). Erlangen, Germany.
- Gabelman, A., & Hwang, S.-T. (2005). Experimental results versus model predictions for dense gas extraction using a hollow fiber membrane contactor. *The Journal of Supercritical Fluids*, 35(1), 26–39.
- Gabelman, A., & Hwang, S.-T. (2006). A theoretical study of dense gas extraction using a hollow fiber membrane contactor. *The Journal of Supercritical Fluids*, 37(2), 157–172.
- Gabelman, A., Hwang, S.-T., & Krantz, W. B. (2005). Dense gas extraction using a hollow fiber membrane contactor: experimental results versus model predictions. *Journal of Membrane Science*, 257(1-2), 11–36.
- Gálvez, S. (1996). *El jugo de manzana. Tierra adentro*. Instituto de Investigaciones Agropecuarias (INIA), Gobierno de Chile, Ministerio de Agricultura.
- Gamse, T., Rogler, I., & Marr, R. (1999). Supercritical CO₂ extraction for utilisation of excess wine of poor quality. *The Journal of Supercritical Fluids*, 14(2), 123–128.
- Gañán, N., & Brignole, E. A. (2011). Fractionation of essential oils with biocidal activity using supercritical CO₂-experiments and modeling. *The Journal of Supercritical Fluids*, 58(1), 58–67.
- Gast, K., Jungfer, M., Saure, C., & Brunner, G. (2005). Purification of tocochromanols from edible oil. *Journal of Supercritical Fluids*, 34(1), 17–25.
- Georgiadis, A., Llovel, F., Bismarck, A., Blas, F. J., Galindo, A., Maitland, G. C., ... Jackson, G. (2010). Interfacial tension measurements and modelling of (carbon dioxide + n-alkane) and (carbon dioxide + water) binary mixtures at elevated pressures and temperatures. *The Journal of Supercritical Fluids*, 55, 743–754.
- Georgiadis, A., Maitland, G. C., Trusler, J. P. M., & Bismarck, A. (2010). Interfacial tension measurements of the (H₂O + CO₂) system at elevated pressures and temperatures. *Journal of Chemical & Engineering Data*, 55(10), 4168–4175.
- Gironi, F., & Maschietti, M. (2005). Supercritical carbon dioxide fractionation of lemon oil by means of a batch process with an external reflux. *The Journal of Supercritical Fluids*, 35(3), 227–234.
- Gironi, F., & Maschietti, M. (2008). Continuous countercurrent deterpenation of lemon essential oil by means of supercritical carbon dioxide: experimental data and process modelling. *Chemical Engineering Science*, 63(3), 651–661.

- Goto, M., Sato, M., Kodama, A., & Hirose, T. (1997). Application of supercritical fluid technology to citrus oil processing. *Physica B*, 239(1-2), 167–170.
- Gracia, I., Rodríguez, J. F., García, M. T., Alvarez, A., & García, A. (2007). Isolation of aroma compounds from sugar cane spirits by supercritical CO₂. *The Journal of Supercritical Fluids*, 43(1), 37–42.
- Groemping, U. (2014). Rcmdrplugin.doe: R commander plugin for (industrial) design of experiments. <https://cran.r-project.org/web/packages/rcmdrplugin.doe/index.html>.
- Güçlü-Üstündağ, Ö., & Temelli, F. (2007). Column fractionation of canola oil deodorizer distillate using supercritical carbon dioxide. *Journal of the American Oil Chemists' Society*, 84(10), 953–961.
- Guilbot, P., Valtz, A., Legendre, H., & Richon, D. (2000). Rapid on-line sampler-injector: a reliable tool for HT-HP sampling and on-line GC analysis. *Analisis*, 28, 426–431.
- Guthalugu, N. K., Balaraman, M., & Kadimi, U. S. (2006). Optimization of enzymatic hydrolysis of triglycerides in soy deodorized distillate with supercritical carbon dioxide. *Biochemical Engineering Journal*, 29(3), 220–226.
- Gutiérrez, J. E., Bejarano, A., & de la Fuente, J. C. (2010). Measurement and modeling of high-pressure (vapour + liquid) equilibria of (CO₂ + alcohol) binary systems. *The Journal of Chemical Thermodynamics*, 42(5), 591–596.
- Hanley, B., & Chen, C.-C. (2012). New mass-transfer correlations for packed towers. *AIChE Journal*, 58(1), 132–152.
- Hebach, A., Oberhof, A., Dahmen, N., Kögel, A., Ederer, H., & Dinjus, E. (2002). Interfacial tension at elevated pressures measurements and correlations in the water + carbon dioxide system. *Journal of Chemical & Engineering Data*, 47(6), 1540–1546.
- Hegel, P. E., Mabe, G. D. B., Pereda, S., Zabalo, M. S., & Brignole, E. A. (2006). Phase equilibria of near critical CO₂+propane mixtures with fixed oils in the LV, LL and LLV region. *The Journal of Supercritical Fluids*, 37(3), 316–322.
- Hernández, E. J., Mabe, G. D., Señoráns, F. J., Reglero, G., Fornari, T., Hernández, E. J., ... Fornari, T. (2008). High-pressure phase equilibria of the pseudoternary mixture sunflower oil + ethanol + carbon dioxide. *Journal of Chemical & Engineering Data*, 53(11), 2632–2636.
- Hiller, N., Schiemann, H., Weidner, E., & Peter, S. (1993). Interfacial tension in systems with a supercritical component at high pressures. *Chemical Engineering & Technology*, 16(3), 206–212.
- Hu, J., Chen, J., & Mi, J. (2012). Prediction of interfacial structure and tension of binary mixtures containing carbon dioxide. *Industrial & Engineering Chemistry Research*, 51, 1236–1243.
- Hurtado-Benavides, A. M., Señoráns, F. J., Ibáñez, E., & Reglero, G. (2004). Countercurrent packed column supercritical CO₂ extraction of olive oil. mass transfer evaluation. *The Journal of Supercritical Fluids*, 28(1), 29–35.
- Ibáñez, E., Hurtado-Benavides, A. M., Señoráns, F. J., & Reglero, G. (2002). Concentration of sterols and tocopherols from olive oil with supercritical carbon

- dioxide. *Journal of the American Oil Chemists' Society*, 79(12), 1255–1260.
- Ibáñez, E., Palacios, J., Señoráns, F. J., Santa-Maria, G., Tabera, J., & Reglero, G. (2000). Isolation and separation of tocopherols from olive by-products with supercritical fluids. *Journal of the American Oil Chemists' Society*, 77(2), 187–190.
- Inomata, H., Kondo, T., Hirohama, S., Arai, K., Suzuki, Y., & Konno, M. (1989). Vapour—liquid equilibria for binary mixtures of carbon dioxide and fatty acid methyl esters. *Fluid Phase Equilibria*, 46(1), 41–52.
- Iwai, Y., Nagano, H., Lee, G. S., Uno, M., & Arai, Y. (2006). Measurement of entrainer effects of water and ethanol on solubility of caffeine in supercritical carbon dioxide by FT-IR spectroscopy. *The Journal of Supercritical Fluids*, 38(3), 312–318.
- Jaeger, P. T., & Eggers, R. (2009). Interfacial tension of ionic liquids at elevated pressures. *Chemical Engineering and Processing: Process Intensification*, 48(6), 1173–1176.
- Jaeger, P. T., & Eggers, R. (2012). Interfacial properties at elevated pressures in reservoir systems containing compressed or supercritical carbon dioxide. *Journal of Supercritical Fluids*, 66, 80–85.
- Jaeger, P. T., Eggers, R., & Baumgartl, H. (2002). Interfacial properties of high viscous liquids in a supercritical carbon dioxide atmosphere. *The Journal of Supercritical Fluids*, 24(3), 203–217.
- Jaeger, P. T., Schnitzler, J. v., Eggers, R., v. Schnitzler, J., Eggers, R., von Schnitzler, J., & Eggers, R. (1996). Interfacial tension of fluid systems considering the nonstationary case with respect to mass transfer. *Chemical Engineering & Technology*, 19(3), 197–202.
- Jakobsson, M., Sivik, B., Bergqvist, P. A., Strandberg, B., & Rappe, C. (1994). Counter-current extraction of dioxins from cod liver oil by supercritical carbon dioxide. *The Journal of Supercritical Fluids*, 7(3), 197–200.
- Jaubert, J.-N. N., Gonçalves, M. M., & Barth, D. (2000). A theoretical model to simulate supercritical fluid extraction: application to the extraction of terpenes by supercritical carbon dioxide. *Industrial & Engineering Chemistry Research*, 39(12), 4991–5002.
- Jennings, D. W., Lee, R. J., Teja, A. S., Yoon, J.-H., Lee, H. H.-S., & Lee, H. H.-S. (1991). Vapor-liquid equilibria in the carbon dioxide + ethanol and carbon dioxide + 1-butanol systems. *Journal of Chemical and Engineering Data*, 36(3), 303–307.
- Jennings, H. Y., & Newman, G. H. (1971). Effect of temperature and pressure on the interfacial tension of water against methane - normal decane mixtures. *Society of Petrol Engineers Journal*, 11, 171–175.
- Jödecke, M., Pérez-Salado Kamps, Á., & Maurer, G. (2007). Experimental investigation of the solubility of CO₂ in (acetone + water). *Journal of Chemical & Engineering Data*, 52(3), 1003–1009.
- Joung, S. N., Yoo, C. W., Shin, H. Y., Kim, S. Y., Yoo, K.-P. P., Lee, C. S., & Huh, W. S. (2001). Measurements and correlation of high-pressure vle of binary CO₂-alcohol systems (methanol, ethanol, 2-methoxyethanol and 2-ethoxyethanol). *Fluid Phase Equilibria*, 185(1-2), 219–230.

- Jouquand, C., Ducruet, V., & Giampaoli, P. (2004). Partition coefficients of aroma compounds in polysaccharide solutions by the phase ratio variation method. *Food Chemistry*, 85(3), 467–474.
- Kalaga, A., & Trebble, M. (1999). Density changes in supercritical solvent + hydrocarbon solute binary mixtures. *Journal of Chemical & Engineering Data*, 44(5), 1063–1066.
- Kariznovi, M., Nourozieh, H., & Abedi, J. (2013a). Experimental measurements and predictions of density, viscosity, and carbon dioxide solubility in methanol, ethanol, and 1-propanol. *The Journal of Chemical Thermodynamics*, 57, 408–415.
- Kariznovi, M., Nourozieh, H., & Abedi, J. (2013b). Experimental results and thermodynamic investigation of carbon dioxide solubility in heavy liquid hydrocarbons and corresponding phase properties. *Fluid Phase Equilibria*, 339, 105–111.
- Kashulines, P., Rizvi, S. S. H., Harriott, P., & Zollweg, J. A. (1991). Viscosities of fatty acids and methylated fatty acids saturated with supercritical carbon dioxide. *Journal of the American Oil Chemists' Society*, 68(12), 912–921.
- Kawashima, A., Watanabe, S., Iwakiri, R., & Honda, K. (2009). Removal of dioxins and dioxin-like pcbs from fish oil by countercurrent supercritical CO₂ extraction and activated carbon treatment. *Chemosphere*, 75(6), 788–94.
- Kiran, E., Pöhler, H., & Xiong, Y. (1996). Volumetric properties of pentane + carbon dioxide at high pressures. *Journal of Chemical & Engineering Data*, 41(2), 158–165.
- Knez, Ž., Knez Hrnčič, M., & Škerget, M. (2015). Particle formation and product formulation using supercritical fluids. *Annual Review of Chemical and Biomolecular Engineering*, 6(1), 16.1–16.29.
- Koch, J. (1976). Zur beurteilung von natuerlichem fruchtsaftaroma. In *Kongress-Bericht XIV Internationaler Fruchtsaft-Kongress* (p. 18.–21.5. 219). Meran.
- Kondo, M., Akgun, N., Goto, M., Kodama, A., & Hirose, T. (2002). Semi-batch operation and countercurrent extraction by supercritical CO₂ for the fractionation of lemon oil. *The Journal of Supercritical Fluids*, 23(1), 21–27.
- Kondo, M., Goto, M., Kodama, A., & Hirose, T. (2000). Fractional extraction by supernatural carbon dioxide for the deterpenation of bergamot oil. *Industrial and Engineering Chemistry Research*, 39(12), 4745–4748.
- Kondo, M., Goto, M., Kodama, A., & Hirose, T. (2002). Separation performance of supercritical carbon dioxide extraction column for the citrus oil processing: observation using simulator. *Separation Science and Technology*, 37(15), 3391–3406.
- Köse, O., Akman, U., & Hortaçsu, Ö. (2000). Semi-batch deterpenation of origanum oil by dense carbon dioxide. *The Journal of Supercritical Fluids*, 18(1), 49–63.
- Kubat, H., Akman, U., & Hortaçsu, Ö. (2001). Semi-batch packed-column deterpenation of origanum oil by dense carbon dioxide. *Chemical Engineering and Processing*, 40(1), 19–32.
- Kvamme, B., Kuznetsova, T., Hebach, A., Oberhof, A., & Lunde, E. (2007). Measurements and modelling of interfacial tension for water+carbon dioxide systems

- at elevated pressures. *Computational Materials Science*, 38(3), 506–513.
- Lahiere, R. J., & Fair, J. R. (1987). Mass-transfer efficiencies of column contactors in supercritical extraction service. *Industrial & Engineering Chemistry Research*, 26(10), 2086–2092.
- Laitinen, A., & Kaunisto, J. (1998). Hydrodynamics and mass transfer in a rotating disk supercritical extraction column. *Industrial & Engineering Chemistry Research*, 37(6), 2529–2534.
- Laitinen, A., & Kaunisto, J. (1999). Supercritical fluid extraction of 1-butanol from aqueous solutions. *The Journal of Supercritical Fluids*, 15(3), 245–252.
- Laitinen, A., & Kaunisto, J. (2000). Acid gas extraction of pyridine from water. *Industrial & Engineering Chemistry Research*, 39(1), 168–174.
- Langmaack, T., Jaeger, P. T., & Eggers, R. (1996). The refinement of vegetable oils through countercurrent extraction with compressed carbon dioxide. *Fett-Lipid*, 98(7-8), 261–267.
- Lemmon, E. W., Huber, M. L., & McLinden, M. O. (2013). Standard reference database 23: reference fluid thermodynamic and transport properties-refprop. Gaithersburg: National Institute of Standards and Technology, Standard Reference Data Program.
- Liao, X., Li, Y. G., Park, C. B., & Chen, P. (2010). Interfacial tension of linear and branched pp in supercritical carbon dioxide. *The Journal of Supercritical Fluids*, 55(1), 386–394.
- Lim, J. S., Lee, Y.-W. Y., Kim, J.-D., Lee, Y.-W. Y., & Chun, H.-S. (1995). Mass-transfer and hydraulic characteristics in spray and packed extraction columns for supercritical carbon-dioxide ethanol-water system. *The Journal of Supercritical Fluids*, 8(2), 127–137.
- Lim, J.-S., Lee, Y.-Y., & Chun, H.-S. (1994). Phase equilibria for carbon dioxide-ethanol-water system at elevated pressures. *The Journal of Supercritical Fluids*, 7(4), 219–230.
- Lisboa, P. F., Fernandes, J., Simões, P. C., Mota, J. P. B., & Saadtdjian, E. (2010). Computational-fluid-dynamics study of a kenics static mixer as a heat exchanger for supercritical carbon dioxide. *The Journal of Supercritical Fluids*, 55(1), 107–115.
- Lockemann, C. A. (1994). Interfacial tensions of the binary systems carbon myristate, and carbon dioxide-methyl palmitate and of the ternary system carbon dioxide-methyl palmitate at high pressures. *Chemical Engineering and Processing*, 33, 193–198.
- Luis, V., Torres, C. F., Fornari, T., Se, F. J., Reglero, G., Vázquez, L., ... Reglero, G. (2007). Recovery of squalene from vegetable oil sources using countercurrent supercritical carbon dioxide extraction. *The Journal of Supercritical Fluids*, 40(1), 59–66.
- Macedo, S., Fernandes, S., Lopes, J. A., de Sousa, H. C., Pereira, P. J., Carmelo, P. J., ... Nunes da Ponte, M. (2008). Recovery of wine-must aroma compounds by supercritical CO₂. *Food and Bioprocess Technology*, 1(1), 74–81.
- Manninen, P., Pakarinen, J., & Kallio, H. (1997). Large-scale supercritical carbon dioxide

- extraction and supercritical carbon dioxide countercurrent extraction of cloudberry seed oil. *Journal of Agricultural and Food Chemistry*, 45(7), 2533–2538.
- Maran, J. P., Manikandan, S., Priya, B., & Gurumoorthi, P. (2013). Box-behnken design based multi-response analysis and optimization of supercritical carbon dioxide extraction of bioactive flavonoid compounds from tea (*camellia sinensis l.*) leaves. *Journal of Food Science and Technology*, 52(1), 92–104.
- Medina, I., & Martínez, J. L. (1997). Dealcoholisation of cider by supercritical extraction with carbon dioxide. *Journal of Chemical Technology & Biotechnology*, 68(1), 14–18.
- Medina-Bermudez, M., Saavedra-Molina, L. A., Escamilla-Tiburcio, W., Galicia-Luna, L. A., & Elizalde-Solis, O. (2013). (p , ρ , t) behavior for the binary mixtures carbon dioxide + heptane and carbon dioxide + tridecane. *Journal of Chemical & Engineering Data*, 58(5), 1255–1264.
- Meneses, D. A. (2012). *Personal communication*.
- Meterc, D., Petermann, M., & Weidner, E. (2008). Drying of aqueous green tea extracts using a supercritical fluid spray process. *The Journal of Supercritical Fluids*, 45(2), 253–259.
- Meure, L. A., Foster, N. R., & Dehghani, F. (2008). Conventional and dense gas techniques for the production of liposomes: a review. *AAPS PharmSciTech*, 9(3), 798–809.
- Miao, S. F., Yu, J. P., Du, Z., Guan, Y. X., Yao, S. J., & Zhu, Z. Q. (2010). Supercritical fluid extraction and micronization of ginkgo flavonoids from ginkgo biloba leaves. *Industrial & Engineering Chemistry Research*, 49(11), 5461–5466.
- Miller, J. N., & Miller, J. C. (2010). *Statistics and chemometrics for analytical chemistry* (6th ed.). Gosport, UK: Prentice Hall.
- Mohammadi, A. H., Afzal, W., & Richon, D. (2008). Experimental data and predictions of dissociation conditions for ethane and propane simple hydrates in the presence of distilled water and methane, ethane, propane, and carbon dioxide simple hydrates in the presence of ethanol aqueous solutions. *Journal of Chemical & Engineering Data*, 53, 73–76.
- Mohammadi, A. H., & Richon, D. (2007). Experimental gas hydrate dissociation data for methane, ethane, and propane + 2-propanol aqueous solutions and methane + 1-propanol aqueous solution systems. *Journal of Chemical & Engineering Data*, 52(6), 2509–2510.
- Mosadegh-Sedghi, S., Rodrigue, D., Brisson, J., & Iliuta, M. C. (2014). Wetting phenomenon in membrane contactors – causes and prevention. *Journal of Membrane Science*, 452, 332–353.
- Moser, M., Pietzonka, W., & Trepp, C. (1996). Interfacial tension measurements between α -tocopherol and carbon dioxide at high pressures. *Chemical Engineering & Technology*, 19(5), 462–466.
- Mukhopadhyay, M. (2000). *Natural extracts using supercritical carbon dioxide*. Florida,

Fl: CRC Press.

- Najdanovic-Visak, V., Rebelo, L. P. N., & Nunes da Ponte, M. (2005). Liquid–liquid behaviour of ionic liquid–1-butanol–water and high pressure CO₂-induced phase changes. *Green Chemistry*, 7(6), 443.
- Nieuwoudt, I., Crause, J. C., & du Rand, M. (2002). Oligomer fractionation with supercritical fluids. *The Journal of Supercritical Fluids*, 24(1), 47–55.
- Nikfardjam, M. P., & Maier, D. (2011). Development of a headspace trap HRGC/MS method for the assessment of the relevance of certain aroma compounds on the sensorial characteristics of commercial apple juice. *Food Chemistry*, 126(4), 1926–1933.
- Nilsson, W. B., Gauglitz, E. J., & Hudson, J. K. (1989). Supercritical fluid fractionation of fish oil esters using incremental pressure programming and a temperature gradient. *Journal of the American Oil Chemists Society*, 66(11), 1596–1600.
- Nilsson, W. B., Gauglitz, E. J., Hudson, J. K., Stout, V. F., & Spinelli, J. (1988). Fractionation of menhaden oil ethyl-esters using supercritical fluid CO₂. *Journal of the American Oil Chemists' Society*, 65(1), 109–117.
- Nilsson, W. B., Seaborn, G. T., & Hudson, J. K. (1992). Partition-coefficients for fatty-acid esters in supercritical fluid CO₂ with and without ethanol. *Journal of the American Oil Chemists' Society*, 69(4), 305–308.
- Niño-Amézquita, O. G., Enders, S., Jaeger, P. T., & Eggers, R. (2010a). Interfacial properties of mixtures containing supercritical gases. *The Journal of Supercritical Fluids*, 55(2), 724–734.
- Niño-Amézquita, O. G., Enders, S., Jaeger, P. T., & Eggers, R. (2010b). Measurement and prediction of interfacial tension of binary mixtures. *Industrial & Engineering Chemistry Research*, 49(2), 592–601.
- Niño-Amézquita, O. G., van Putten, D., & Enders, S. (2012). Phase equilibrium and interfacial properties of water + CO₂ mixtures. *Fluid Phase Equilibria*, 332, 40–47.
- Nist chemistry webbook. <webbook.nist.gov/chemistry>.
- Nowakowska, J. (1939). *The refractive indices of ethyl alcohol and water mixtures*. Loyola University.
- Nunes, A. V. M., Matias, A. A., Nunes da Ponte, M., & Duarte, C. M. M. (2007). Quaternary phase equilibria for SCCO₂ + biophenolic compound + water + ethanol. *Journal of Chemical & Engineering Data*, 52(1), 244–247.
- Oei, S. B., Dittmar, D., & Eggers, R. (2001). Grenzflächenspannung und dichte von ethanol in kontakt mit kohlendioxid. *Chemie Ingenieur Technik*, 73(7), 830–834.
- Oliveira, E. L. G. G., Silvestre, A. J. D. D., & Silva, C. M. (2011). Review of kinetic models for supercritical fluid extraction. *Chemical Engineering Research and Design*, 89(7), 1104–1117.
- Ooi, C. K., Bhaskar, A. R., Yener, M. S., Tuan, D. Q., Hsu, J., Rizvi, S. S. H., & Lumpur, K. (1996). Continuous supercritical carbon dioxide processing of palm oil. *Journal of the American Oil Chemists' Society*, 73(2), 233–237.

- Osséo, L. S., Caputo, G., Gracia, I., & Reverchon, E. (2004). Continuous fractionation of used frying oil by supercritical CO₂. *Journal of the American Oil Chemists' Society*, 81(9), 879–885.
- Pecar, D., & Dolecek, V. (2007). Densities of b-carotene - supercritical carbon dioxide mixtures. *Journal of Chemical & Engineering Data*, 52(6), 2442–2445.
- Pecar, D., & Dolecek, V. (2008). Densities of a-tocopherol + supercritical carbon dioxide mixtures. *Journal of Chemical & Engineering Data*, 53(4), 929–932.
- Perre, C., Delestre, G., Shrive, L., & M, C. (1994). Deterpenation process for citrus oils by supercritical CO₂ extraction in a packed column. In *3th International Symposium on Supercritical Fluids* (p. 456). Strasbourg.
- Perretti, G., Motori, A., Bravi, E., Favati, F., Montanari, L., & Fantozzi, P. (2007). Supercritical carbon dioxide fractionation of fish oil fatty acid ethyl esters. *The Journal of Supercritical Fluids*, 40(3), 349–353.
- Persson, P., Barisic, Z., Cohen, A., Thörneby, L., & Gorton, L. (2002). Countercurrent supercritical fluid extraction of phenolic compounds from aqueous matrices. *Analytica Chimica Acta*, 460(1), 1–12.
- Peter, S., & Brunner, G. (1978). The separation of nonvolatile substances by means of compressed gases in countercurrent processes. *Angewandte Chemie International Edition in English*, 17(10), 746–750.
- Peter, S., & Jakob, H. (1991). The rheological behavior of coexisting phases in systems containing fatty acids and dense gases. *The Journal of Supercritical Fluids*, 4, 166–172.
- Peter, S., Schneider, M., Weidner, E., Ziegelitz, R., Schneider, M., & Ziegelitz, R. (1987). The separation of lecithin and soya oil in a countercurrent column by near critical fluid extraction. *Chemical Engineering & Technology*, 10(1), 37–42.
- Peter, S., Zhang, Z., Grüning, B., & Weidner, E. (2001). Purification of alkylpolyglucosides by extraction with near-critical gases. In *2nd International Meeting on High Pressure Chemical Engineering* (pp. 1–13). TUHH, Hamburg-Harbug.
- Pieck, C. A., Crampon, C., Chanton, F., & Badens, E. (2013). Determination of operative parameters of a countercurrent column for the supercritical fractionation process. In *6th International Symposium on High Pressure Processes Technology* (p. O41). Belgrade.
- Pietsch, A., & Eggers, R. (1999). The mixer-settler principle as a separation unit in supercritical fluid processes. *The Journal of Supercritical Fluids*, 14(2), 163–171.
- Pietsch, A., & Swidersky, P. (2012). Erfahrungen mit dem einsatz einer hochdruckextraktionsanlage in der ingenieursausbildung. In *ProcessNet Meeting High Pressure*. Hamburg.
- Pöhler, H., & Kiran, E. (1997). Volumetric properties of carbon dioxide + ethanol at high pressures. *Journal of Chemical Engineering Data*, 42(2), 384–388.
- Pöhler, H., Kiran, E., Pohler, H., Kiran, E., Pöhler, H., & Kiran, E. (1996). Volumetric properties of carbon dioxide + toluene at high. *Journal of Chemical & Engineering*

Data, 41(3), 482–486.

- Poiana, M., Mincione, A., Gionfriddo, F., & Castaldo, D. (2003). Supercritical carbon dioxide separation of bergamot essential oil by a countercurrent process. *Flavour and Fragrance Journal*, 18(5), 429–435.
- R core team. R: a language and environment for statistical computing. R Foundation for Statistical Computing. <<http://www.r-project.org/>>. (2015). Vienna, Austria.
- Raeissi, S., & Peters, C. J. (2005a). Experimental determination of high-pressure phase equilibria of the ternary system carbon dioxide+limonene+linalool. *The Journal of Supercritical Fluids*, 35(1), 10–17.
- Raeissi, S., & Peters, C. J. (2005b). Liquid–vapor and liquid–liquid–vapor equilibria in the ternary system ethane+limonene+linalool. *The Journal of Supercritical Fluids*, 33(3), 201–208.
- Reverchon, E. (1997). Supercritical fluid extraction and fractionation of essential oils and related products. *The Journal of Supercritical Fluids*, 10(1), 1–37.
- Reverchon, E., Marciano, A., & Poletto, M. (1997). Fractionation of a peel oil key mixture by supercritical CO₂ in a continuous tower. *Industrial & Engineering Chemistry Research*, 36(11), 4940–4948.
- Rezayat, M., & Ghaziaskar, H. S. (2011). Continuous extraction of glycerol acetates from their mixture using supercritical carbon dioxide. *The Journal of Supercritical Fluids*, 55(3), 937–943.
- Riha, V., & Brunner, G. (1999). Phase equilibrium of fish oil ethyl esters with supercritical carbon dioxide. *The Journal of Supercritical Fluids*, 15(1), 33–50.
- Riha, V., & Brunner, G. (2000). Separation of fish oil ethyl esters with supercritical carbon dioxide. *The Journal of Supercritical Fluids*, 17(1), 55–64.
- Rincón, J., Cañizares, P., & García, M. T. (2007). Improvement of the waste-oil vacuum-distillation recycling by continuous extraction with dense propane. *Industrial & Engineering Chemistry Research*, 46(1), 266–272.
- Rincón, J., Martínez, F., Rodríguez, L., Ancillo, V., Martínez, F., Rodríguez, L., & Ancillo, V. (2011). Recovery of triglycerides from used frying oil by extraction with liquid and supercritical ethane. *The Journal of Supercritical Fluids*, 56(1), 72–79.
- Rizvi, S. S. H., & Bhaskar, A. R. (1995). Supercritical-fluid processing of milk-fat - fractionation, scale-up, and economics. *Food Technology*, 49(2), 55–90.
- Romero, P., Rizvi, S. S. H., Kelly, M. L., & Bauman, D. E. (2000). Short communication: concentration of conjugated linoleic acid from milk fat with a continuous supercritical fluid processing system. *Journal of Dairy Science*, 83(1), 20–22.
- Rubio-Rodríguez, N., Beltrán, S., Jaime, I., de Diego, S. M., Sanz, M. T., & Carballido, J. R. (2010). Production of omega-3 polyunsaturated fatty acid concentrates: a review. *Innovative Food Science & Emerging Technologies*, 11(1), 1–12.
- Ruivo, R. M., Cebola, M. J., Simões, P. C., & Nunes da Ponte, M. (2001). Fractionation of edible oil model mixtures by supercritical carbon dioxide in a packed column. Part I: experimental results. *Industrial & Engineering Chemistry Research*, 40(7), 1706–

1711.

- Ruivo, R. M., Cebola, M. J., Simões, P. C., & Nunes da Ponte, M. (2002). Fractionation of edible oil model mixtures by supercritical carbon dioxide in a packed column. Part II: a mass-transfer study. *Industrial & Engineering Chemistry Research*, 41(9), 2305–2315.
- Ruivo, R. M., Couto, R. M., & Simões, P. C. (2007). High-pressure phase equilibria of the ternary system oleic acid + squalene + carbon dioxide. *Journal of Chemical & Engineering Data*, 52(2), 566–570.
- Ruivo, R. M., Couto, R. M., & Simões, P. C. (2008). Supercritical carbon dioxide fractionation of the model mixture squalene/oleic acid in a membrane contactor. *Separation and Purification Technology*, 59(3), 231–237.
- Ruivo, R. M., Paiva, A., Mota, J. P. B., & Simões, P. C. (2004). Dynamic model of a countercurrent packed column operating at high pressure conditions. *The Journal of Supercritical Fluids*, 32(1-3), 183–192.
- Ruivo, R. M., Paiva, A., & Simões, P. C. (2006). Hydrodynamics and mass transfer of a static mixer at high pressure conditions. *Chemical Engineering and Processing*, 45(3), 224–231.
- Ruiz-Rodríguez, A., Fornari, T., Hernández, E. J., Señoráns, F. J., Reglero, G., Ruiz-Rodríguez, A., ... Reglero, G. (2010). Thermodynamic modeling of dealcoholization of beverages using supercritical CO₂: application to wine samples. *The Journal of Supercritical Fluids*, 52(2), 183–188.
- Ruiz-Rodríguez, A., Fornari, T., Jaime, L., Vázquez, E., Amador, B., Nieto, J. A., ... Reglero, G. (2012). Supercritical CO₂ extraction applied toward the production of a functional beverage from wine. *The Journal of Supercritical Fluids*, 61, 92–100.
- Sahena, F., Zaidul, I. S. M., Jinap, S., Saari, N., Jahurul, H. a., Abbas, K. A., & Norulaini, N. A. (2009). Pufas in fish: extraction, fractionation, importance in health. *Comprehensive Reviews in Food Science and Food Safety*, 8(2), 60–74.
- Sahle-Demessie, E. (1997a). Fractionation of glycerides using supercritical carbon dioxide. *Industrial & Engineering Chemistry Research*, 36(11), 4906–4913.
- Sahle-Demessie, E. (1997b). Thermal gradient fractionation of glyceride mixtures under super-critical fluid conditions. *The Journal of Supercritical Fluids*, 10(2), 127–137.
- Salas-Salazar, N., & Olivas-Orozco, G. (2011). El aroma de la manzana. *Interciencia*, 36(4), 265–272.
- Sampaio de Sousa, A. R., Raeissi, S., Aguiar-Ricardo, A., Duarte, C. M. M., & Peters, C. J. (2004). High pressure phase behavior of the system ethane+orange peel oil. *The Journal of Supercritical Fluids*, 29(1-2), 59–67.
- Sanz, C., Olias, J. M., & Perez, A. G. (1997). Aroma biochemistry of fruits and vegetables. In F. A. Tomas-Barberan & R. J. Robins (Eds.), *Phytochemistry of fruit and vegetables* (pp. 125–155). New York, USA: Oxford University Press Inc.
- Sarrade, S., Guizard, C., & Rios, G. M. (2003). New applications of supercritical fluids and supercritical fluids processes in separation. *Separation and Purification*

Technology, 32(1-3), 57–63.

- Sato, M., Goto, M., & Hirose, T. (1995). Fractional extraction with supercritical carbon-dioxide for the removal of terpenes from citrus oil. *Industrial & Engineering Chemistry Research*, 34(11), 3941–3946.
- Sato, M., Goto, M., & Hirose, T. (1996). Supercritical fluid extraction on semibatch mode for the removal of terpene in citrus oil. *Industrial & Engineering Chemistry Research*, 35(6), 1906–1911.
- Sato, M., Kondo, M., Goto, M., Kodama, A., & Hirose, T. (1998). Fractionation of citrus oil by supercritical countercurrent extractor with side-stream withdrawal. *The Journal of Supercritical Fluids*, 13(1-3), 311–317.
- Schaffner, D., & Trepp, C. (1995). Improved mass transfer for supercritical-fluid extraction - a new mixer-settler system. *The Journal of Supercritical Fluids*, 8(4), 287–294.
- Schiemann, H., Weidner, E., & Peter, S. (1993). Interfacial tension in binary systems containing a dense gas. *The Journal of Supercritical Fluids*, 6(3), 181–189.
- Schultz, T. H., Flath, R. A., Black, D. R., Guadagni, D. G., Schultz, W. G., & Teranishi, R. (1967). Volatiles from delicious apple essence-extraction methods. *Journal of Food Science*, 32(3), 279–283.
- Schultz, W. G. (1969). Process for extraction of flavors US Patent N° 3477856.
- Schultz, W. G., & Randall, J. M. (1970). Liquid carbon dioxide for selective aroma extraction. *Food Technology*, 24(11), 94–98.
- Schultz, W. G., Schultz, T. H., Carston, R. A., & Hudson, J. S. (1974). Pilot plant extraction with liquid CO₂. *Food Technology*, 28, 32–88.
- Schwarz, C. E., Bonthuys, G. J. K., van Schalkwyk, R. F., Laubscher, D. L., Burger, A. J., & Knoetze, J. H. (2011). Separation of alkanes and alcohols with supercritical fluids. part ii. influence of process parameters and size of operating range. *The Journal of Supercritical Fluids*, 58(3), 352–359.
- Schwarz, C. E., Nieuwoudt, I., & Knoetze, J. H. (2010). Additional pilot plant measurements with incorporation of reflux for the fractionation of wax derivatives with supercritical propane. *Industrial & Engineering Chemistry Research*, 49(9), 4462–4467.
- Secuianu, C., Feroiu, V., & Geană, D. (2008). Phase behavior for carbon dioxide+ethanol system: experimental measurements and modeling with a cubic equation of state. *The Journal of Supercritical Fluids*, 47(2), 109–116.
- Seibert, A. F., & Moosberg, D. G. (1988). Performance of spray, sieve tray, and packed contactors for high pressure extraction. *Separation Science and Technology*, 23(12-13), 2049–2063.
- Seifried, B., & Temelli, F. (2010). Interfacial tension of marine lipids in contact with high pressure carbon dioxide. *The Journal of Supercritical Fluids*, 52(2), 203–214.
- Sen, Y. L., & Kiran, E. (1990). A new experimental system to study the temperature and pressure dependence of viscosity, density, and phase behavior of pure fluids and

- solutions. *The Journal of Supercritical Fluids*, 3(2), 91–99.
- Señoráns, F. J., Ruiz-Rodríguez, A., Cavero, S., Cifuentes, A., Ibáñez, E., Reglero, G., ... Reglero, G. (2001). Isolation of antioxidant compounds from orange juice by using countercurrent supercritical fluid extraction (cc-sfe). *Journal of Agricultural and Food Chemistry*, 49(12), 6039–6044.
- Señoráns, F. J., Ruiz-Rodríguez, A., Ibáñez, E., Tabera, J., Reglero, G., Ruiz-Rodríguez, A., ... Reglero, G. (2001). Optimization of countercurrent supercritical fluid extraction conditions for spirits fractionation. *The Journal of Supercritical Fluids*, 21(1), 41–49.
- Señoráns, F. J., Ruiz-Rodríguez, A., Ibáñez, E., Tabera, J., Reglero, G., Senorans, F. J., ... Reglero, G. (2003). Isolation of brandy aroma by countercurrent supercritical fluid extraction. *The Journal of Supercritical Fluids*, 26(2), 129–135.
- Señoráns, F. J., Ruiz-Rodríguez, A., Ibáñez, E., Tabera, J., Reglero, G., Señoráns, F. J., ... Reglero, G. (2001). Countercurrent supercritical fluid extraction and fractionation of alcoholic beverages. *Journal of Agricultural and Food Chemistry*, 49(4), 1895–1899.
- Seo, Y., Kang, S.-P., Lee, S., & Lee, H. (2008). Experimental measurements of hydrate phase equilibria for carbon dioxide in the presence of THF, propylene oxide, and 1,4-dioxane. *Journal of Chemical & Engineering Data*, 53(12), 2833–2837.
- Shaw, P. E. (1986). The flavour of non-alcoholic fruit beverages. In I. D. Morton & A. J. Macleod (Eds.), *Food Flavors*. Elsevier.
- Shi, B., Jin, J., Yu, E., & Zhang, Z. (2011). Concentration of natural vitamin e using a continuous countercurrent supercritical CO₂ extraction-distillation dual column. *Chemical Engineering & Technology*, 34(6), 914–920.
- Shirazian, S., & Ashrafizadeh, S. N. (2010). Mass transfer simulation of caffeine extraction by subcritical CO₂ in a hollow-fiber membrane contactor. *Solvent Extraction and Ion Exchange*, 28(2), 267–286.
- Simó, C., Ibáñez, E., Señoráns, F. J., Barbas, C., Reglero, G., & Cifuentes, A. (2002). Analysis of antioxidants from orange juice obtained by countercurrent supercritical fluid extraction, using micellar electrokinetic chromatography and reverse-phase liquid chromatography. *Journal of Agricultural and Food Chemistry*, 50(23), 6648–6652.
- Simões, P. C., Afonso, B., Fernandes, J., & Barbosa Mota, J. P. (2008). Static mixers as heat exchangers in supercritical fluid extraction processes. *The Journal of Supercritical Fluids*, 43(3), 477–483.
- Simões, P. C., Carmelo, P. J., Pereira, P. J., Lopes, J. A., Nunes da Ponte, M., & Brunner, G. (1998). Quality assessment of refined olive oils by gas extraction. *The Journal of Supercritical Fluids*, 13(1-3), 337–341.
- Simões, P. C., & Catchpole, O. J. (2002). Fractionation of lipid mixtures by subcritical R134a in a packed column. *Industrial & Engineering Chemistry Research*, 41(2), 267–276.
- Simões, P. C., Eggers, R., & Jaeger, P. T. (2000). Interfacial tension of edible oils in

- supercritical carbon dioxide. *European Journal of Lipid Science and Technology*, 102(4), 263–265.
- Simões, P. C., Matos, H. A., Carmelo, P. J., Gomes de Azevedo, E., & Nunes da Ponte, M. (1995). Mass transfer in countercurrent packed columns: application to supercritical CO₂ extraction of terpenes. *Industrial & Engineering Chemistry Research*, 34(2), 613–618.
- Sinnott, R. K. (1999). Separation columns (distillation, absorption and extraction). In *Coulson & Richardson's CHEMICAL ENGINEERING* (3th ed., Vol. 6, pp. 592–603). Oxford, UK: Butterworth-Heinemann.
- Sirkar, K. K. (2008). Membranes, phase interfaces, and separations: novel techniques and membranes - an overview. *Industrial & Engineering Chemistry Research*, 47(15), 5250–5266.
- Staby, A., & Mollerup, J. (1993a). Separation of constituents of fish oil using supercritical fluids: a review of experimental solubility, extraction, and chromatographic data. *Fluid Phase Equilibria*, 91(2), 349–386.
- Staby, A., & Mollerup, J. (1993b). Solubility of fish oil fatty acid ethyl esters in sub-and supercritical carbon dioxide. *Journal of the American Oil Chemists' Society*, 70(6), 583–588.
- Stockfleth, R., & Brunner, G. (1999). Hydrodynamics of a packed countercurrent column for the gas extraction. *Industrial & Engineering Chemistry Research*, 38(10), 4000–4006.
- Stockfleth, R., & Brunner, G. (2001a). Film thickness, flow regimes, and flooding in countercurrent annular flow of a falling film at high pressures. *Industrial & Engineering Chemistry Research*, 40(25), 6014–6020.
- Stockfleth, R., & Brunner, G. (2001b). Holdup, pressure drop, and flooding in packed countercurrent columns for the gas extraction. *Industrial & Engineering Chemistry Research*, 40(1), 347–356.
- Sutjiadi-Sia, Y., Jaeger, P. T., & Eggers, R. (2008a). Interfacial phenomena of aqueous systems in dense carbon dioxide. *Journal of Supercritical Fluids*, 46(3), 272–279.
- Sutjiadi-Sia, Y., Jaeger, P. T., & Eggers, R. (2008b). Interfacial tension of solid materials against dense carbon dioxide. *Journal of Colloid and Interface Science*, 320(1), 268–274.
- Suzuki, K., Sue, H., Itou, M., Smith, R. L., Inomata, H., Arai, K., & Saito, S. (1990). Isothermal vapor-liquid equilibrium data for binary systems at high pressures: carbon dioxide-methanol, carbon dioxide-ethanol, carbon dioxide-1-propanol, methane-ethanol, methane-1-propanol, ethane-ethanol, and ethane-1-propanol systems. *Journal of Chemical Engineering Data*, 35(1), 63–66.
- Suzuki, T., Tsuge, N., & Nagahama, K. (1990). Supercritical extraction of alcohol from aqueous solutions using only carbon dioxide. In T. Sekine (Ed.), *Solvent Extraction* (pp. 1701–1706).
- Tabera, J., Guinda, Á., Ruiz-Rodríguez, A., Señoráns, F. J., Ibáñez, E., Albi, T., &

- Reglero, G. (2004). Countercurrent supercritical fluid extraction and fractionation of high-added-value compounds from a hexane extract of olive leaves. *Journal of Agricultural and Food Chemistry*, 52(15), 4774–4779.
- Terada, A., Kitajima, N., Machmudah, S., Tanaka, M., Sasaki, M., & Goto, M. (2010). Cold-pressed yuzu oil fractionation using countercurrent supercritical CO₂ extraction column. *Separation and Purification Technology*, 71(1), 107–113.
- Thakur, R. R. K., Vial, C., Nigam, K. D. P. K., Nauman, E. B., & Djelveh, G. (2003). Static mixers in the process industries—a review. *Chemical Engineering Research and Design*, 81(7), 787–826.
- Tilly, K. D., Foster, N. R., Macnaughton, S. J., & Tomasko, D. L. (1994). Viscosity correlations for binary supercritical fluids. *Industrial & Engineering Chemistry Research*, 33, 681–688.
- Torres, C. F., Fornari, T., Torrelo, G., Señoráns, F. J., & Reglero, G. (2009). Production of phytosterol esters from soybean oil deodorizer distillates. *European Journal of Lipid Science and Technology*, 111(5), 459–463.
- Torres, C. F., Torrelo, G., Señoráns, F. J., & Reglero, G. (2009). Supercritical fluid fractionation of fatty acid ethyl esters from butteroil. *Journal of Dairy Science*, 92(5), 1840–5.
- Tsivintzelis, I., Missopolinou, D., Kalogiannis, K., & Panayiotou, C. (2004). Phase compositions and saturated densities for the binary systems of carbon dioxide with ethanol and dichloromethane. *Fluid Phase Equilibria*, 224(1), 89–96.
- Tuan, D. Q., Zollweg, J. A., Harriott, P., & Rizvi, S. S. H. (1999). Measurement and modeling of viscosity of supercritical carbon dioxide/biomaterial(s) mixtures. *Industrial and Engineering Chemistry Research*, 38(5), 2129–2136.
- Unlusu, B., & Sunol, A. K. (2004a). Modeling of equilibration times at high pressure for multicomponent vapor-liquid diffusional processes. *Fluid Phase Equilibria*, 226, 15–25.
- Unlusu, B., & Sunol, A. K. (2004b). Multicomponent interphase diffusion of carbon dioxide-methanol-water under near-critical conditions. *Chemical Engineering Science*, 59(10), 1923–1929.
- Valsecchi, R., Mutta, F., De Patto, U., & Tonelli, C. (2014). Countercurrent fractionation of methylol-terminated perfluoropolyoxyalkylene oligomers by supercritical carbon dioxide. *The Journal of Supercritical Fluids*, 88, 85–91.
- Varona, S., Martín, Á., Cocero, M. J., & Gamse, T. (2008). Supercritical carbon dioxide fractionation of lavandin essential oil: experiments and modeling. *The Journal of Supercritical Fluids*, 45(2), 181–188.
- Vázquez, L., Fornari, T., Señoráns, F. J., Reglero, G., & Torres, C. F. (2008). Supercritical carbon dioxide fractionation of nonesterified alkoxyglycerols obtained from shark liver oil. *J. Agric. Food Chem.*, 56, 1078–1083.
- Vazquez, L., Fornari, T., Senorans, F. J., Reglero, G., Torres, C. F., Vázquez, L., ... Torres, C. F. (2008). Supercritical carbon dioxide fractionation of nonesterified

- alkoxyglycerols obtained from shark liver oil. *Journal of Agricultural and Food Chemistry*, 56(3), 1078–1083.
- Vázquez, L., Hurtado-Benavides, A. M., Reglero, G., Fornari, T., Ibáñez, E., & Señoráns, F. J. (2009). Deacidification of olive oil by countercurrent supercritical carbon dioxide extraction: experimental and thermodynamic modeling. *Journal of Food Engineering*, 90(4), 463–470.
- Vázquez, L., Torres, C. F., Fornari, T., Grigelmo, N., Señoráns, F. J., & Reglero, G. (2006). Supercritical fluid extraction of minor lipids from pretreated sunflower oil deodorizer distillates. *European Journal of Lipid Science and Technology*, 108(8), 659–665.
- Versini, G., Franco, M. A., Moser, S., Barchetti, P., & Manca, G. (2009). Characterisation of apple distillates from native varieties of sardinia island and comparison with other italian products. *Food Chemistry*, 113(4), 1176–1183.
- Vieira De Melo, S. A. B., Pallado, P., Guarise, G. B., & Bertucco, A. (1999). High-pressure vapor-liquid equilibrium data for binary and ternary systems formed by supercritical CO₂, limonene and linalool. *Brazilian Journal of Chemical Engineering*, 16(1), 1–10.
- Visentín, A., Cismondi, M., & Maestri, D. (2011). Supercritical CO₂ fractionation of rosemary ethanolic oleoresins as a method to improve carnosic acid recovery. *Innovative Food Science and Emerging Technologies*, 12(2), 142–145.
- Visentín, A., Rodríguez-Rojo, S., Navarrete, A., Maestri, D., & Cocero, M. J. (2012). Precipitation and encapsulation of rosemary antioxidants by supercritical antisolvent process. *Journal of Food Engineering*, 109(1), 9–15.
- Vyhmeister, E., Estay, H., Romero, J., & Cubillos, F. (2012). Simulation and process optimization of a membrane-based dense gas extraction using hollow fiber contactors. *Chemical Engineering Communications*, 199(5), 644–657.
- Wagner, H., & Eggers, R. (1996). Extraction of spray particles with supercritical fluids in a two-phase flow. *AIChE Journal*, 42(7), 1901–1910.
- Wagner, K., Brudi, K., Dahmen, N., & Schmieder, H. (1999). Partition coefficients of aromatic organic substances in two-phase mixtures of water and carbon dioxide at pressures from 8 to 30 MPa and at temperatures of 313 to 333 K . Part II. *Journal of Supercritical Fluids*, 15(2), 109–116.
- Wang, G. Q., Yuan, X. G., & Yu, K. T. (2005). Review of mass-transfer correlations for packed columns. *Industrial & Engineering Chemistry Research*, 44(23), 8715–8729.
- Weidner, E. (2009). High pressure micronization for food applications. *Journal of Supercritical Fluids*, 47(3), 556–565.
- Wilke, G. (1978). Extraction with supercritical gases—a foreword. *Angewandte Chemie International Edition in English*, 17(10), 701–702.
- Yener, M. E., Kashulines, P., Rizvi, S. S. H., & Harriott, P. (1998). Viscosity measurement and modeling of lipid-supercritical carbon dioxide mixtures. *The Journal of Supercritical Fluids*, 11(3), 151–162.

- Yu, Z.-R., Bhaskar, A. R., & Rizvi, S. S. H. (1995). Modeling of triglyceride distribution and yield of anhydrous milk-fat in a continuous supercritical carbon-dioxide extraction system. *Journal of Food Process Engineering*, 18(1), 71–84.
- Zosel, K. (1974). Process for recovering caffeine US Patent 3806619.
- Zosel, K. (1978). Separation with supercritical gases: practical applications. *Angewandte Chemie International Edition in English*, 17(10), 702–709.
- Zúñiga-Moreno, A., & Galicia-Luna, L. A. (2002). Compressed liquid densities of carbon dioxide + ethanol mixtures at four compositions via a vibrating tube densimeter up to 363 K and 25 MPa. *Journal of Chemical & Engineering Data*, 47(2), 149–154.

APPENDIXES

Appendix 1 Vapor pressures data for ethyl-2-methylbutyrate, hexanal, and *E*-2-hexenal at a pressure range of (25 to 190) kPa.

In the process of defining a model mixture of aqueous apple aroma, little information was found in literature regarding vapor pressures of several apple aroma constituents. Vapor pressure is a relevant parameter involved in VLE calculations and modeling. For that reason I supervised the measurement of this property for three constituents of apple aroma, and the redaction of a peer-reviewed scientific article (Fig. A1). This article fulfilled the part of the requirements of David A. Menses M.Sc. thesis, which I codirected.



Contents lists available at ScienceDirect

J. Chem. Thermodynamics

journal homepage: www.elsevier.com/locate/jct

Vapor pressure data for ethyl-2-methylbutyrate, hexanal and (*E*)-2-hexenal at a pressure range of (25 to 190) kPa

David A. Meneses^a, Arturo Bejarano^a, Juan C. de la Fuente^{a,b,*}^a Departamento de Ingeniería Química y Ambiental, Universidad Técnica Federico Santa María, Avda. España 1680, Valparaíso, Chile^b Centro Regional de Estudios en Alimentos Saludables, Blanco 1623, Valparaíso, Chile

ARTICLE INFO

Article history:

Received 7 October 2013

Received in revised form 28 February 2014

Accepted 5 March 2014

Available online 22 March 2014

Keywords:

Dynamic recirculation method

Ethyl-2-methylbutyrate

Hexanal

(*E*)-2-hexenal

Vapor pressure

Apple aroma

ABSTRACT

The saturated vapor pressures of pure ethyl-2-methylbutyrate, hexanal and (*E*)-2-hexenal, which are volatile compounds characteristic of apple aroma, were measured with a dynamic recirculation apparatus at a pressure range of (24.5 to 190.0) kPa. Measurements were made over the temperature range of (362.1 to 429.9) K for ethyl-2-methylbutyrate, (358.1 to 425.8) K for hexanal, and (373.5 to 446.2) K for (*E*)-2-hexenal. The maximum likelihood method was used to estimate the parameters of the Antoine equation, whereas the parameters of an extended Antoine equation and the Wagner equation were determined by non linear least square method. The three models showed root mean square deviations (*rmsd*) of 0.29%, 0.28%, and 0.27% for ethyl-2-methylbutyrate, 0.58%, 0.48%, and 0.38% for hexanal, and 0.89%, 0.62% and 0.36% for (*E*)-2-hexenal, respectively. Additionally, the experimental data and correlation were compared with those available in the literature.

© 2014 Elsevier Ltd. All rights reserved.

1. Introduction

Fruit aroma is a complex mixture of a large number of volatile compounds that contribute to the overall sensory quality of fruit specific to species and cultivar [1]. Over 300 volatile compounds have been measured in the aroma profile of apples. These compounds include alcohols, aldehydes, carboxylic esters, ketones, and ethers [2]. Flath *et al.* [3] studied odor thresholds of the volatile compounds of “Delicious” apples and pointed out ethyl-2-methylbutyrate, hexanal, and (*E*)-2-hexenal as essential constituents of apple aroma.

The use of (counter-current) supercritical CO₂ fractionation (CC-SCF) is an alternative technology for the recovery and concentration of fruit aromas [4]. The applications of CC-SCF of aqueous solutions are mainly related to alcoholic beverages. The topics of most intense scientific research are the dealcoholization [5–9] and recovery and separation of the aroma [10–14] of wine and other spirits. However, the information on recovery and concentration of aromas from non-alcoholic beverages (e.g., natural fruit aromas) using CC-SCF is very limited in the literature, and the existence of commercial scale CC-SCF processes is currently low [15].

To successfully apply CC-SCF to the fruit aroma recovery, (vapor + liquid) equilibrium data are required for the mixture of CO₂ + volatile compounds. Data of vapor pressure of pure volatile

compounds is a relevant property on which the (vapor + liquid) calculations have a strong dependence and therefore it is of great importance in the design of separation processes. Moreover, other (physical + chemical) properties can be derived based on the vapor pressure data [16]. Additionally, limited information regarding vapor pressure data were reported in the literature, mainly for ethyl-2-methylbutyrate and (*E*)-2-hexenal.

The aim of this research was to measure the isobaric (vapor + liquid) equilibrium in terms of temperature and vapor pressure for these three representative flavor compounds, namely, ethyl-2-methylbutyrate, hexanal and (*E*)-2-hexenal, for a pressure range of (24.5 to 190) kPa. The ester group was represented by ethyl-2-methylbutyrate, while hexanal and (*E*)-2-hexenal belonged to the aldehyde group. The experimental values were fit to the Antoine, extended Antoine, and Wagner vapor pressure equations.

2. Experimental

2.1. Materials

The reagents, ethyl-2-methylbutyrate (99%), hexanal (98%), and (*E*)-2-hexenal (≥95%) were purchased from Sigma–Aldrich (St. Louis, MO). These materials were used without further purification.

2.2. Apparatus and procedures

The vapor pressure was measured using a commercial all-glass dynamic recirculation isobaric (vapor + liquid) equilibrium (VLE)

* Corresponding author. Tel.: +56 32 2654110; fax: +56 32 2654478.

E-mail address: juan.delafuente@usm.cl (J.C. de la Fuente).<http://dx.doi.org/10.1016/j.jct.2014.03.006>

0021-9614/© 2014 Elsevier Ltd. All rights reserved.

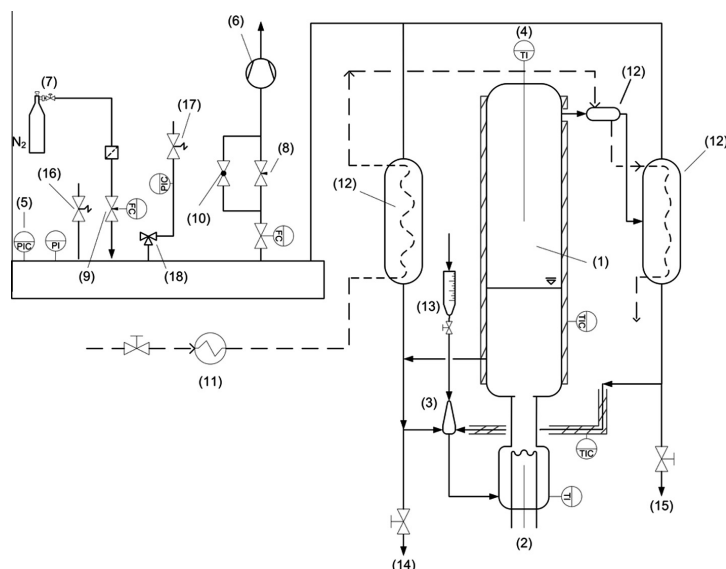


FIGURE 1. Experimental apparatus: (1), Cottrell pump; (2), immersion heater; (3), mixing chamber; (4), vapor Pt-100 temperature probe; (5) pressure controller; (6), vacuum pump; (7), N₂ supply; (8), vacuum throttle valve; (9), pressure throttle valve; (10), vacuum by-pass; (11), thermo regulated bath; (12), vapor condensers; (13), filling tunnel; (14) and (15), liquid and vapor samplers; (16), overpressure relief valve; (17), vacuum relief valve; (18), 3/2 way valve.

apparatus shown in figure 1 (Labodest model 602D, i-Fischer Engineering GmbH, Waldbüttelbrunn, Germany) [17]. Its operation procedure relies on the principle of the recirculation of both liquid and vapor phases at controlled pressure. The advantage of the recirculation method is the rapid appearance of the equilibrium simultaneously with the exact measurement of the boiling temperature. The experimental procedure used was as follows: the pure compound was charged in the apparatus by the filling tunnel (13), the N₂ supply (7) to the system was opened, once the liquid is at the desired level the magnetic stirrer bar was activated (3), the pressure throttle valve (9) is opened, and the vacuum pump (10) was started to work. The desired value of pressure was set on the controller panel, the immersion heater (2) was activated and finally, fine adjustments of pressure were made by manual operation of valve (8). In order to verify that system reached the equilibrium, the temperature stability had to remain constant (within ± 0.1 K) for a period of time of (15 to 30) min [17]. The experimental uncertainty was the uncertainty associated to the equipment, which was estimated $<0.2\%$ [18]. This estimation was calculated by comparison between the measurements for *n*-heptane made in our equipment and those reported in literature. The comparison, the apparatus and methodology are described in more detail in a previous work [18].

3. Results and discussion

Experimental temperature and vapor pressures are listed in table 1, along with the percent deviations ($10^2 \cdot (p - p_{\text{cal}})/p$) between the observed and calculated (p_{cal}) pressures from the Wagner equation (4), for ethyl-2-methylbutyrate, hexanal, and (E)-2-hexenal.

The maximum likelihood method was used to estimate the parameters of the Antoine equation (1) in order to take into account its non-linear mathematical form and the fact that both temperature and pressure are subject to experimental variability [19].

$$\ln\{p_{\text{cal}}/\text{kPa}\} = A - \frac{B}{T/K + C}, \quad (1)$$

where A , B and C are adjustable parameters. The maximum likelihood objective function to be minimized has the form:

$$S = \sum_i \left[\left(\frac{T - T_{\text{cal}}}{\sigma_{T,i}} \right)^2 + \left(\frac{p - p_{\text{cal}}}{\sigma_{p,i}} \right)^2 \right], \quad (2)$$

where $\sigma_{T,i}$ and $\sigma_{p,i}$ are estimated standard deviations in the measured temperature and pressure for the i th observation. These values were assigned from the experimental set up as $\sigma_{T,i} = 0.1$ K and $\sigma_{p,i} = 0.1$ kPa.

The extended Antoine equation (3) [20] has the form:

$$\ln\{p_{\text{cal}}/\text{kPa}\} = A + \frac{B}{T/K} + C \cdot \{T/K\} + D \cdot \ln\{T/K\} + E \cdot \{T/K\}^6, \quad (3)$$

where A , B , C , D and E are adjustable parameters.

The Wagner equation (4) [21] with four different functional forms, with exponent $i \leq 6$, was evaluated to represent the measured vapor pressures. The results for the regression analysis have shown that there were not significant differences, in terms of root mean square deviation (*rmsd*), among the four functional forms selected for the ester and both aldehydes. However, the functional form depicted by equation (4), with parameters ($c_3 = c_6 = 0$), showed the best representation for the vapor pressures measured for ethyl-2-methylbutyrate and (E)-2-hexenal, while the same functional form, with parameters ($c_{2.5} = c_5 = 0$), showed the best representation for hexanal.

$$\ln(p_{\text{cal}}/p_c) = \{T_c/(T/K)\} \{c_1 \cdot \tau + c_{1.5} \cdot \tau^{1.5} + c_{2.5} \cdot \tau^{2.5} + c_3 \cdot \tau^3 + c_5 \cdot \tau^5 + c_6 \cdot \tau^6\}, \quad (4)$$

where p_{cal} is the calculated vapor pressure, T_c and p_c are the critical temperature and pressure, c_i are the fitting model parameters, and $\tau = 1 - T/T_c$ is a reversed reduced temperature variable. The critical

TABLE 1

Experimental temperature and vapor pressures (T, p), and percent deviations ($10^2 \cdot (p - p_{\text{cal}})/p$) from the Wagner equation (4) for ethyl-2-methylbutyrate, hexanal, and (*E*)-2-hexenal.

p/kPa	Ethyl-2-methylbutyrate		Hexanal		(E)-2-hexenal	
	T/K	$10^2 \cdot (p - p_{\text{cal}})/p$	T/K	$10^2 \cdot (p - p_{\text{cal}})/p$	T/K	$10^2 \cdot (p - p_{\text{cal}})/p$
24.5	362.1	0.06	358.1	0.45	373.5	0.09
34.0	371.2	−0.11	367.3	−0.97	383.0	−0.49
43.5	378.3	−0.06	374.2	−0.11	390.4	0.28
53.0	384.2	0.08	380.0	0.35	396.9	0.20
62.5	389.5	−0.31	385.3	0.13	402.6	0.04
72.0	394.0	−0.07	389.9	0.28	407.7	−0.14
81.5	397.9	0.57	394.0	0.42	412.0	0.53
91.0	401.8	0.26	397.8	0.47	416.1	0.64
101.3	405.6	0.18	401.9	−0.31	420.7	−0.61
110.0	408.7	−0.17	404.9	−0.41	423.8	−0.21
119.5	411.7	−0.05	407.9	−0.25	427.1	−0.19
129.0	414.5	0.14	410.6	0.17	430.3	−0.41
138.5	417.3	−0.05	413.4	−0.05	433.1	−0.13
148.0	420.1	−0.55	416.0	−0.16	435.9	−0.21
157.5	422.5	−0.37	418.6	−0.56	438.4	0.10
167.0	424.8	−0.18	420.8	−0.25	441.0	−0.19
176.5	427.0	0.00	422.8	0.29	443.4	−0.27
186.0	429.1	0.22	424.9	0.35	445.4	0.36
190.0	429.9	0.46	425.8	0.28	446.2	0.64

temperature and pressure in equation (4) plus normal boiling point obtained from the literature are listed in table 2 for ethyl-2-methylbutyrate, hexanal and (*E*)-2-hexenal.

Non linear least squares method was used to estimate the parameters of the equations (3) and (4) by minimizing the objective function:

$$S = \left(\frac{1}{N} \sum_i \left(\frac{p - p_{\text{cal}}}{p} \right)^2 \right)^{1/2}. \quad (5)$$

The regressed parameters of the three vapor pressure equations, along with their *rmsd* are reported in table 3.

The Wagner equation (4) was selected to compare the model results with information found in the literature, due to its better representation of the experimental data. The data sets selected from the literature for the vapor pressures of the three compounds studied in this work are listed in table 4. The relation between natural logarithm of the vapor pressure and the inverse of temperature for the experimental data and the calculated pressure from Wagner equation (4) is shown in figure 2 for ethyl-2-methylbutyrate, hexanal and (*E*)-2-hexenal.

The percent deviations from equation (4), with parameters ($c_3 = c_6 = 0$), for the vapor pressure values of ethyl-2-methylbutyrate with the data sets included in table 4 are compared in figure 3. Values of vapor pressure obtained by using the correlation from Yaws *et al.* [22], in the temperature range of (365 to 425) K, are compared with a standard deviation of 1.11 kPa. The percent deviations were in the range of (−1.13% to 4.17%). These deviations show a decreasing tendency as temperature increases, and the minimum deviation from this work was shown at temperatures around 395 K.

TABLE 2

Critical properties and normal boiling point of: ethyl-2-methylbutyrate, hexanal and (*E*)-2-hexenal.

Component	T_b/K	T_c/K	p_c/kPa
Ethyl-2-methylbutyrate	406.2 ^a	578.11 ^b	2838 ^b
Hexanal ^c	404.2	592.8	3460
(E)-2-hexenal	419.65 ^c	615.15 ^b	3594 ^b

^a Data from NIST Chemistry WebBook [32].

^b Data calculated using the Joback method [16].

^c Data from CRC [31].

Figure 4 shows for hexanal, in the temperature range of (350 to 430) K, the comparison of the vapor pressure among the selected data from the literature (included in table 4) and equation (4) with parameters ($c_2.5 = c_5 = 0$). Experimental vapor pressure data from Markovnik *et al.* [23] was represented using equation (4) with a standard deviation of 0.16 kPa, and percent deviations in the range of (−0.19% to 1.13%). These results were in very good agreement with this work. Palczewska-Tulinska and Oracz [24] reported vapor pressure measurements in a narrower temperature range. Equation (4) represented this data set with comparatively large negative percent deviations from this work, from (−4.09% to 2.86%), and significantly higher compared with the rest of the references listed in table 4. A slight convex tendency of the percent deviations along with standard deviation of 0.73 kPa was observed for the data set reported by [24]. Vapor pressures obtained by using the correlation from The Design Institute for Physical Properties (DIP-PR) [25] presented systematically positive deviations from equation (4), with the lowest value at temperature 375 K of 0.77%, increasing from (1.34% to 1.46%) at temperatures (360 and 420) K, respectively. For this data set, the standard deviation from equation (4) was 0.85 kPa. A similar tendency was displayed by the percent deviations from the vapor pressures calculated by using the correlation from Liessmann *et al.* [26] with deviations in the band of (0.82% to 3.51%) at temperatures (375 and 425) K, respectively. Deviations from equation (4) for the correlation obtained from [26] were in the range of (−1.64% to 2.95%) with standard deviation of 2.05 kPa. It can be seen from figure 4 that the correlation from [26] indicates a minor increasing trend of the percent deviations as temperature increases. The minimum percent deviation from this work took place at temperatures near to 395 K and was 0.13%. As it can be seen from figure 4, the data sets [22,24] showed significant differences among them and with the results obtained in this work, mainly at low temperatures. Another region can be described in figure 4, between temperatures of (395 to 425) K, where the calculated vapor pressures from the correlations from [22,25,26] showed positive deviations. Covarrubias-Cervantes *et al.* [27], Verevkin *et al.* [28], Hahn and Moerke [29], and Linek and Wichterle [30] reported vapor pressure measurements for hexanal in a lower temperature range than that of this work. Palczewska-Tulinska and Oracz [24], and Linek and Wichterle [30] published Antoine coefficients by fitting pressure boiling point data from their experimental measurements.

TABLE 3

Estimated parameters (A , B , C , D , E , and c_i) and root mean square deviation ($rmsd$) from the Antoine, extended Antoine, and Wagner equations for ethyl-2-methylbutyrate, hexanal and (*E*)-2-hexenal.

Component	Parameter					Deviation ($10^2 \cdot rmsd$)
	Antoine (1)					
	A	B	C			
Ethyl-2-methylbutyrate	13.032	2534.144	−104.451			0.29
Hexanal	14.070	3191.429	−64.140			0.58
(E)-2-hexenal	14.636	3872.094	−33.992			0.89
	Ext. Antoine (3)					
	A	B	C	D	E	
Ethyl-2-methylbutyrate	−164.775	−5.216	−0.050	2.903	4.778	0.28
Hexanal	−154.258	−4.881	−0.046	5.570	3.997	0.48
(E)-2-hexenal	−152.052	−4.861	−0.043	5.903	3.836	0.62
	Wagner (4)					
	c ₁	c _{1.5}	c _{2.5}	c ₃	c ₅	c ₆
Ethyl-2-methylbutyrate	−16.611	26.050	−35.597		43.695	
Hexanal	−6.130	−3.475		8.513		−58.985
(E)-2-hexenal	−2.045	−19.416	33.919		−77.454	

TABLE 4

Vapor pressure datasets for ethyl-2-methylbutyrate, hexanal and (*E*)-2-hexenal selected from the literature.

Type of information	Temperature range/K	Reference
<i>Ethyl-2-methylbutyrate</i>		
Experimental: T , p	362 to 430	This work
Correlation: Antoine equation	263 to 464	Yaws et al. [22]
<i>Hexanal</i>		
Experimental: T , p	233 to 298	Covarrubias-Cervantes et al. [27]
	287 to 309	Verevkin et al. [28]
	303 to 354	Hahn and Moerke [29]
	315 to 402	Markovnik et al. [23]
	322 to 402	Palczewska-Tulinska and Oracz [24]
	329 to 352	Linek and Wichterle [30]
	358 to 426	This Work
Correlation: DIPPR equation	215 to 594	DIPPR [25]
Correlation: Antoine equation	217 to 591	Yaws et al. [22]
Correlation: Antoine equation	281 to 585	Liessmann et al. [26]
<i>(E)-2-hexenal</i>		
Experimental: T , p	374 to 446	This work
Correlation: Antoine equation	278 to 475	Yaws et al. [22]

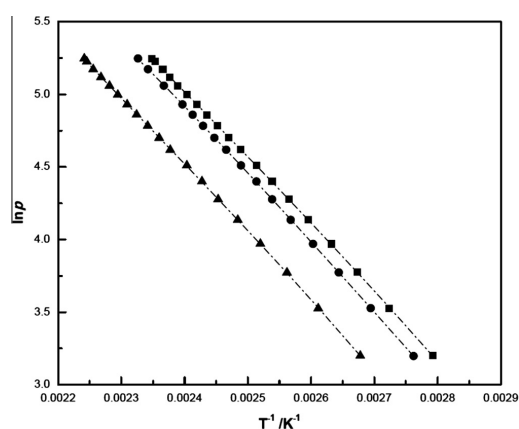


FIGURE 2. Natural logarithm of vapor pressure ($\ln p$) vs. the inverse of temperature (T^{-1}) for the calculated pressure (—, —) from Wagner equation (4), and the experimental data for ethyl-2-methylbutyrate (●), hexanal (■), and (*E*)-2-hexenal (□).

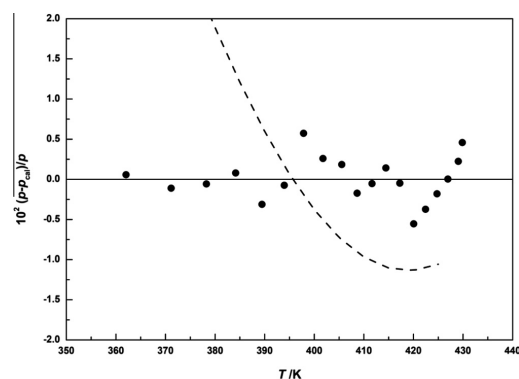


FIGURE 3. Percent deviations ($10^2 \cdot (p - p_{cal}) / p$) from the Wagner equation (4) for ethyl-2-methylbutyrate at temperatures T : (●), this work; (—, —), Yaws et al. [22].

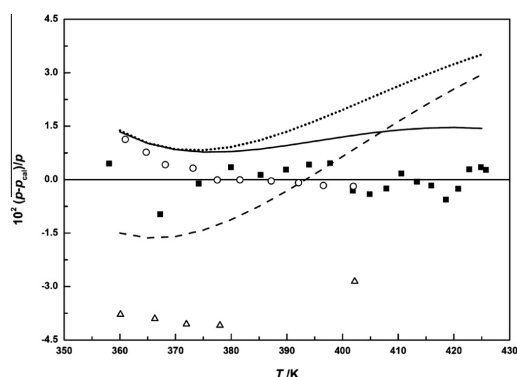


FIGURE 4. Percent deviations ($10^2 \cdot (p - p_{\text{sat}})/p$) from the Wagner equation (4) for hexanal at temperatures T : (■), this work; (○), Markovnik *et al.* [23]; (Δ), Palczewska-Tulinska and Oracz [24]; (— · —), Yaws *et al.* [22]; (·····), DIPPR [25]; (— · — · —), Liessmann *et al.* [26].

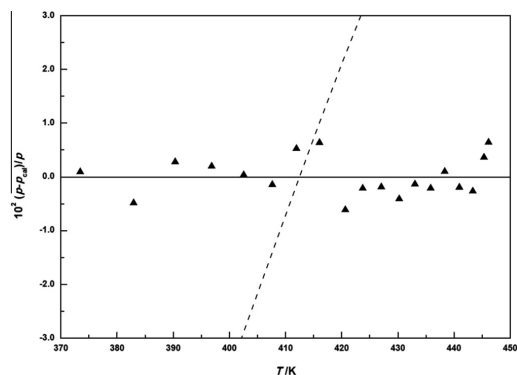


FIGURE 5. Percent deviations ($10^2 \cdot (p - p_{\text{sat}})/p$) from the Wagner equation (4) for (E)-2-hexenal at temperatures T : (·····), this work; (— · —), Yaws *et al.* [22].

Figure 5 compares for (E)-2-hexenal the percent deviations from equation (4), with parameters ($c_3 = c_6 = 0$), with the data included in table 4, in the temperature range of (370 to 450) K. Deviations from equation (4) for the correlation obtained from [22] were in the range of (−9.38% to 7.72%) with standard deviation of 5.87 kPa. As can be seen from figure 5, the correlation from [22] indicates an increasing trend of the percent deviations as temperature increases. Additionally, at the normal boiling point, reported by CRC Handbook of Data on Organic Compounds [31], the vapor pressure predicted by the correlation from [22] showed a difference of 2.0% from this work. However, the normal boiling point reported in this work ($T = 420.7$ K) was in very good agreement with the values reported in the literature [22,31] showing differences <0.25%.

4. Conclusions

New and complementary information for the vapor pressure of pure ethyl-2-methylbutyrate, hexanal, and (E)-2-hexenal was presented in this work for the temperature ranges of (362.1 to 429.9) K, (358.1 to 425.8) K, and (373.5 to 446.2) K, respectively.

The measurements were carried out using a VLE apparatus with an uncertainty <0.2%. The parameters of three common vapor pressure equations were estimated. The Antoine, extended Antoine and Wagner equations represented the experimental data of this work with $r_{\text{msd}} < 0.9\%$. A Wagner-type equation was selected to compare with selected database information from the literature, due to its better representation. Experimental data of saturated vapor pressures in literature are scarce, mainly for ethyl-2-methylbutyrate and (E)-2-hexenal. Two tendencies of the percent deviations among the data selected from the literature and the Wagner equation from this work were seen for both compounds as temperature increases; a slight decreasing tendency for ethyl-2-methylbutyrate, and a minor increasing trend for (E)-2-hexenal. Maximum discrepancies between this work and the literature were 4.2% and −9.4% for ethyl-2-methylbutyrate and (E)-2-hexenal, respectively. Values for the vapor pressure of hexanal from the selected database showed discrepancies among them and with the results obtained in this work, especially at low temperatures. For hexanal, the highest discrepancy between this work and the literature was −4.1%.

Acknowledgements

The present work was funded by the Chilean Agency Fondecyt (Regular Project 111-1008). The assistance of Ana I. González and Carolina A. Ugaldé is highly appreciated.

References

- [1] C. Sanz, J.M. Olias, A.G. Perez, Aroma biochemistry of fruits and vegetables, in: F.A. Tomas-Barberan, R.J. Robins (Eds.), *Phytochemistry of Fruit and Vegetables*, Oxford University Press Inc., New York, USA, 1997, pp. 125–155.
- [2] P.S. Dimick, J.C. Hoskin, *Crit. Rev. Food Sci. Nutr.* 18 (1983) 387–409.
- [3] R. Flath, D. Black, D. Guadagni, W. McFadden, T. Schultz, *J. Agric. Food Chem.* 15 (1967) 29–35.
- [4] M. Mukhopadhyay, *Natural Extracts Using Supercritical Carbon Dioxide*, first ed., CRC Press, Boca Raton, Florida, 2000.
- [5] I. Medina, J.L. Martínez, *J. Chem. Technol. Biotechnol.* 68 (1997) 14–18.
- [6] T. Gamse, I. Rogler, R. Marr, *J. Supercrit. Fluids* 14 (1999) 123–128.
- [7] F.J. Señoráns, A. Ruiz-Rodríguez, E. Ibañez, J. Tabera, G. Reglero, *J. Supercrit. Fluids* 21 (2001) 41–49.
- [8] F.J. Señoráns, A. Ruiz-Rodríguez, E. Ibañez, J. Tabera, G. Reglero, *J. Agric. Food Chem.* 49 (2001) 1895–1899.
- [9] M. Budich, G. Brunner, *J. Supercrit. Fluids* 25 (2003) 45–55.
- [10] F.J. Señoráns, A. Ruiz-Rodríguez, E. Ibañez, J. Tabera, G. Reglero, *J. Supercrit. Fluids* 26 (2003) 129–135.
- [11] I. Gracia, J.F. Rodríguez, M.T. García, A. Alvarez, A. García, *J. Supercrit. Fluids* 43 (2007) 37–42.
- [12] S. Macedo, S. Fernandes, J.A. Lopes, H.C. de Sousa, P.J. Pereira, P.J. Carmelo, C. Menduiña, P.C. Simões, M. Nunes da Ponte, *Food Bioprocess Technol.* 1 (2008) 74–81.
- [13] C. Da Porto, D. Decorti, *J. Supercrit. Fluids* 55 (2010) 128–131.
- [14] A. Ruiz-Rodríguez, T. Fornari, L. Jaime, E. Vázquez, B. Amador, J.A. Nieto, M. Yuste, M. Mercader, G. Reglero, *J. Supercrit. Fluids* 61 (2012) 92–100.
- [15] G. Brunner, *Annu. Rev. Chem. Biomol. Eng.* 1 (2010) 321–342.
- [16] B.E. Poling, J.M. Prausnitz, J.P. O'Connell, *The Properties of Gases and Liquids*, fifth ed., McGraw-Hill Co., New York, 2001.
- [17] FISCHER Technology <<http://www.fischer-technology.de>>.
- [18] A. Bejarano, N. Quezada, J.C. de la Fuente, *J. Chem. Thermodyn.* 41 (2009) 1020–1024.
- [19] M. Čenský, P. Vrbka, K. Růžicka, M. Fulem, *Fluid Phase Equilib.* 298 (2010) 199–205.
- [20] Aspen Technology Inc., Aspen Plus® Version 10.2: User Guide, Cambridge, MA, 2001.
- [21] W. Wagner, A. Pruss, *J. Phys. Chem. Ref. Data* 22 (1993) 783–787.
- [22] C.L. Yaws, P.K. Narasimhan, C. Gabbula, Yaws' Handbook of Antoine Coefficients for Vapor Pressure, second electronic Ed., Knovel, 2009 (accessed 22.04.13).
- [23] V.S. Markovnik, A.I. Sachek, A.D. Peshchenko, O.V. Sharro, D.N. Andreevskii, N.M. Olizarevich, *Termodin. Org. Soedin.* (1979) 107–110.
- [24] M. Palczewska-Tulinska, P. Oracz, *J. Chem. Eng. Data* 51 (2006) 639–641.
- [25] DIPPR Project 801, Physical and Thermodynamic Properties of Pure Chemicals, 1993.

<i>D.A. Meneses et al./J. Chem. Thermodynamics 74 (2014) 16–21</i>		21
[26] G. Liessmann, W. Schmidt, S. Reiffarth, Data Compilation of the Saechsische Olefinwerke Boehlen, vol. 33, Germany, 1995.	[30] J. Linek, I. Wichterle, ELDATA: Int. Electron. J. Phys. Chem. Data 2 (1996) 19–22.	
[27] M. Covarrubias-Cervantes, I. Mokbel, D. Champion, J. Jose, A. Voilley, Food Chem. 85 (2004) 221–229.	[31] R.C. Weast, M.J. Astle, CRC Handbook of Data on Organic Compounds, vol. 1 and 2, CRC Press Inc., Florida, 1992.	
[28] S.P. Verevkin, E.L. Krasnykh, T.V. Vasiltsova, B. Koutek, J. Doubsky, A. Heintz, Fluid Phase Equilib. 206 (2003) 331–339.	[32] NIST Chemistry WebBook < http://webbook.nist.gov/chemistry >.	
[29] J. Hahn, K. Moerke, Leuna Protocol (1984) 10161.	JCT 13-590	

Figure A1 Vapor pressure article *J. Chem. Thermodyn.* 74 (2014) 16-21

Appendix 2 High-pressure VLE measurements vapor phase chromatograms.

Figure A2 show typical chromatograms obtained of the vapor-phase sample injected for quantification by GC-TCD.

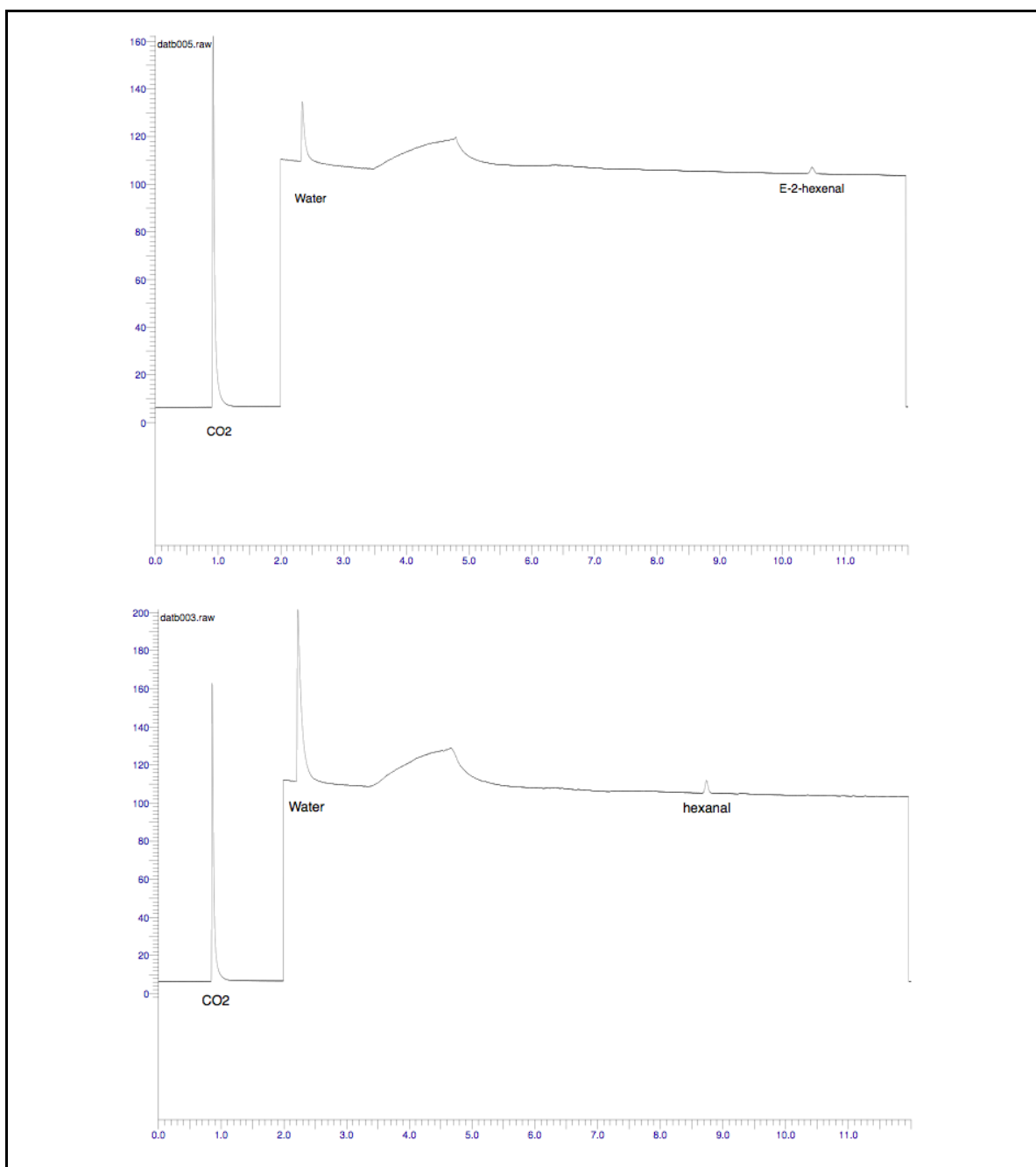


Figure A2 Chromatograms of the vapor-phase. (A), (CO₂ + Water +E-2-Hexenal) at 313 K; (B), (CO₂ + Water + Hexanal).

Appendix 3 Analytical reports of countercurrent supercritical fluid fractionation experiments: feed, raffinate, and extract samples.



UNIVERSIDAD TÉCNICA
FEDERICO SANTA MARÍA

Departamento de Química

CENTRO DE ANÁLISIS QUÍMICO E INSTRUMENTAL
Avenida España 1680, Valparaíso Fono: (32) 2654219. FAX: (32) 2654782
Correo electrónico: servicios.analiticos@usm.cl

INFORME DE ANALISIS N° QUI-246-A/14

REFERENCIA : Pontificia Universidad Católica de Chile.
Atn: Sr. Arturo Bejarano.

IDENTIFICACIÓN MUESTRA : 3 muestras líquidas rotuladas Experimento 1 :
1 Refinado, 2 Extracto, 3 Alimentación .
Recibidas en nuestro laboratorio el 15/10/2014.

ANÁLISIS SOLICITADOS : E-2- Hexenal, 1-Hexanal, 1- Hexanol.

MÉTODO BASE DE ANÁLISIS : Cromatografía de Gases con detector de Ionización de Llama (CG-FID) y SPME

Muestras	Resultados análisis Experimento 1		
	1 Refinado [µg/g]	2 Extracto [mg]	3 Alimentación [mg/g]
E-2- Hexenal	20,5 – 12,5	60,8 – 68,2	0,55 – 0,61
1-Hexanal	1,2 – 0,95	18,3 – 23,9	0,16 – 0,19
1-Hexanol	112 - 77	212 - 237	1,06 – 1,07

María Elena Ortiz
Jefe Laboratorio
Análisis Químicos

Valparaíso, 28 de Julio de 2015.

Nota: Los resultados entregados en este Informe sólo se refieren a los ítems ensayados.
Este Informe no debe ser reproducido parcialmente sin la aprobación escrita de este Laboratorio.



UNIVERSIDAD TÉCNICA
FEDERICO SANTA MARÍA

Departamento de Química

CENTRO DE ANÁLISIS QUÍMICO E INSTRUMENTAL
Avenida España 1680, Valparaíso Fono: (32) 2654219. FAX: (32) 2654782
Correo electrónico: servicios.analiticos@usm.cl

INFORME DE ANALISIS N° QUI-247-A/14

REFERENCIA : Pontificia Universidad Católica de Chile.
Atn: Sr. Arturo Bejarano.

IDENTIFICACIÓN MUESTRA : 3 muestras líquidas rotuladas Experimento 2 :
1 Refinado, 2 Extracto, 3 Alimentación .
Recibidas en nuestro laboratorio el 15/10/2014.

ANÁLISIS SOLICITADOS : E-2- Hexenal, 1-Hexanal, 1- Hexanol.

MÉTODO BASE DE ANÁLISIS : Cromatografía de Gases con detector de Ionización de Llama (CG-FID) y SPME

Muestras	Resultados análisis Experimento 2		
	1 Refinado [µg/g]	2 Extracto [mg]	3 Alimentación [mg/g]
E-2- Hexenal	6,2 – 5,5	107 – 80,7	0,60 – 0,61
1-Hexanal	0,12 – 0,39	31,2 – 23,5	0,19 – 0,17
1-Hexanol	23,9 – 25,8	250 - 232	1,1 – 1,0

María Elena Ortiz
Jefe Laboratorio
Análisis Químicos

Valparaíso, 28 de Julio de 2015.

Nota: Los resultados entregados en este Informe sólo se refieren a los ítems ensayados.
Este Informe no debe ser reproducido parcialmente sin la aprobación escrita de este Laboratorio.



UNIVERSIDAD TÉCNICA
FEDERICO SANTA MARÍA

Departamento de Química

CENTRO DE ANÁLISIS QUÍMICO E INSTRUMENTAL
Avenida España 1680, Valparaíso Fono: (32) 2654219. FAX: (32) 2654782
Correo electrónico: servicios.analiticos@usm.cl

INFORME DE ANALISIS N° QUI –248-A/14

REFERENCIA : Pontificia Universidad Católica de Chile.
Atn: Sr. Arturo Bejarano.

IDENTIFICACIÓN MUESTRA : 3 muestras líquidas rotuladas Experimento 3 :
1 Refinado, 2 Extracto, 3 Alimentación .
Recibidas en nuestro laboratorio el 15/10/2014.

ANÁLISIS SOLICITADOS : E-2- Hexenal, 1-Hexanal, 1- Hexanol.

MÉTODO BASE DE ANÁLISIS : Cromatografía de Gases con detector de Ionización de Llama (CG-FID) y SPME

Muestras	Resultados análisis Experimento 3		
	1 Refinado [µg/g]	2 Extracto [mg]	3 Alimentación [mg/g]
E-2- Hexenal	4,9 – 4,5	38,1 – 37,8	0,55 – 0,54
1-Hexanal	0,54 – 0,7	10 – 11,4	0,12 – 0,13
1-Hexanol	37,1 – 30,9	165 - 173	1,11 – 1,07

María Elena Ortiz
Jefe Laboratorio
Análisis Químicos

Valparaíso, 28 de Julio de 2015.

Nota: Los resultados entregados en este Informe sólo se refieren a los ítems ensayados.
Este Informe no debe ser reproducido parcialmente sin la aprobación escrita de este Laboratorio.



UNIVERSIDAD TÉCNICA
FEDERICO SANTA MARÍA

Departamento de Química

CENTRO DE ANÁLISIS QUÍMICO E INSTRUMENTAL
Avenida España 1680, Valparaíso Fono: (32) 2654219. FAX: (32) 2654782
Correo electrónico: servicios.analiticos@usm.cl

INFORME DE ANALISIS N° QUI -249-A/14

REFERENCIA : Pontificia Universidad Católica de Chile.
Atn: Sr. Arturo Bejarano.

IDENTIFICACIÓN MUESTRA : 3 muestras líquidas rotuladas Experimento 4 :
1 Refinado, 2 Extracto, 3 Alimentación .
Recibidas en nuestro laboratorio el 15/10/2014.

ANÁLISIS SOLICITADOS : E-2- Hexenal , 1-Hexanal, 1- Hexanol.

MÉTODO BASE DE ANÁLISIS : Cromatografía de Gases con detector de Ionización de Llama (CG-FID) y SPME

Muestras	Resultados análisis Experimento 4		
	1 Refinado [µg/g]	2 Extracto [mg]	3 Alimentación [mg/g]
E-2- Hexenal	20,7 – 14,8	29,8 – 24,9	0,47 – 0,57
1-Hexanal	4,5 – 2,6	9,5 – 7,8	0,11 – 0,16
1-Hexanol	203 - 154	62,1 – 59,7	0,97 – 1,1

María Elena Ortiz
Jefe Laboratorio
Análisis Químicos

Valparaíso, 28 de Julio de 2015.

Nota: Los resultados entregados en este Informe sólo se refieren a los ítems ensayados.
Este Informe no debe ser reproducido parcialmente sin la aprobación escrita de este Laboratorio.



UNIVERSIDAD TÉCNICA
FEDERICO SANTA MARÍA

Departamento de Química

CENTRO DE ANÁLISIS QUÍMICO E INSTRUMENTAL
Avenida España 1680, Valparaíso Fono: (32) 2654219. FAX: (32) 2654782
Correo electrónico: servicios.analiticos@usm.cl

INFORME DE ANALISIS N° QUI –266-A14

REFERENCIA : Pontificia Universidad Católica de Chile.
Atn: Sr. Arturo Bejarano.

IDENTIFICACIÓN MUESTRA : 3 muestras líquidas rotuladas Experimento 5 :
1 Refinado, 2 Extracto, 3 Alimentación .
Recibidas en nuestro laboratorio el 29/10/2014.

ANÁLISIS SOLICITADOS : E-2- Hexenal , 1-Hexanal, 1- Hexanol.

MÉTODO BASE DE ANÁLISIS : Cromatografía de Gases con detector de Ionización de Llama (CG-FID) y SPME

Muestras	Resultados análisis Experimento 5		
	1 Refinado [µg/g]	2 Extracto [mg]	3 Alimentación [µg/g]
E-2- Hexenal	6,3 – 2,8	54,7 – 53,3	229 - 110
1-Hexanal	1,7 – 1,2	12,4 – 16,7	95 - 26
1-Hexanol	23,7 – 9,6	382 - 356	552 - 319

María Elena Ortiz
Jefe Laboratorio
Análisis Químicos

Valparaíso, 28 de Julio de 2015.

Nota: Los resultados entregados en este Informe sólo se refieren a los ítems ensayados.
Este Informe no debe ser reproducido parcialmente sin la aprobación escrita de este Laboratorio.



UNIVERSIDAD TÉCNICA
FEDERICO SANTA MARÍA

Departamento de Química

CENTRO DE ANÁLISIS QUÍMICO E INSTRUMENTAL
Avenida España 1680, Valparaíso Fono: (32) 2654219. FAX: (32) 2654782
Correo electrónico: servicios.analiticos@usm.cl

INFORME DE ANALISIS N° QUI –267-A/14

REFERENCIA : Pontificia Universidad Católica de Chile.
Atn: Sr. Arturo Bejarano.

IDENTIFICACIÓN MUESTRA : 3 muestras líquidas rotuladas Experimento 6 :
1 Refinado, 2 Extracto, 3 Alimentación .
Recibidas en nuestro laboratorio el 29/10/2014.

ANÁLISIS SOLICITADOS : E-2- Hexenal , 1-Hexanal, 1- Hexanol.

MÉTODO BASE DE ANÁLISIS : Cromatografía de Gases con detector de Ionización de Llama (CG-FID) y SPME

Muestras	Resultados análisis Experimento 6		
	1 Refinado [µg/g]	2 Extracto [mg]	3 Alimentación [µg/g]
E-2- Hexenal	19,6 – 32,3	166 - 141	139 - 138
1-Hexanal	2,5 – 3,2	24,3 – 21,4	64,8 – 66,6
1-Hexanol	126 - 164	405 - 369	377 - 360

María Elena Ortiz
Jefe Laboratorio
Análisis Químicos

Valparaíso, 28 de Julio de 2015.

Nota: Los resultados entregados en este Informe sólo se refieren a los ítems ensayados.
Este Informe no debe ser reproducido parcialmente sin la aprobación escrita de este Laboratorio.



UNIVERSIDAD TÉCNICA
FEDERICO SANTA MARÍA

Departamento de Química

CENTRO DE ANÁLISIS QUÍMICO E INSTRUMENTAL
Avenida España 1680, Valparaíso Fono: (32) 2654219. FAX: (32) 2654782
Correo electrónico: servicios.analiticos@usm.cl

INFORME DE ANALISIS N° QUI-268-A/14

REFERENCIA : Pontificia Universidad Católica de Chile.
Atn: Sr. Arturo Bejarano.

IDENTIFICACIÓN MUESTRA : 3 muestras líquidas rotuladas Experimento 7 :
1 Refinado, 2 Extracto, 3 Alimentación .
Recibidas en nuestro laboratorio el 29/10/2014.

ANÁLISIS SOLICITADOS : E-2- Hexenal , 1-Hexanal, 1- Hexanol.

MÉTODO BASE DE ANÁLISIS : Cromatografía de Gases con detector de Ionización de Llama (CG-FID) y SPME

Muestras	Resultados análisis Experimento 7		
	1 Refinado [µg/g]	2 Extracto [mg]	3 Alimentación [mg/g]
E-2- Hexenal	2,7 – 2,3	163 - 149	131 - 143
1-Hexanal	1,6 – 1,5	21 - 18	77,8 - 70
1-Hexanol	7,2 – 6,8	639 - 607	270 - 310

María Elena Ortiz
Jefe Laboratorio
Análisis Químicos

Valparaíso, 28 de Julio de 2015.

Nota: Los resultados entregados en este Informe sólo se refieren a los ítems ensayados.
Este Informe no debe ser reproducido parcialmente sin la aprobación escrita de este Laboratorio.



UNIVERSIDAD TÉCNICA
FEDERICO SANTA MARÍA

Departamento de Química

CENTRO DE ANÁLISIS QUÍMICO E INSTRUMENTAL
Avenida España 1680, Valparaíso Fono: (32) 2654219. FAX: (32) 2654782
Correo electrónico: servicios.analiticos@usm.cl

INFORME DE ANALISIS N° QUI-269-A/14

REFERENCIA : Pontificia Universidad Católica de Chile.
Atn: Sr. Arturo Bejarano.

IDENTIFICACIÓN MUESTRA : 3 muestras líquidas rotuladas Experimento 8 :
1 Refinado, 2 Extracto, 3 Alimentación .
Recibidas en nuestro laboratorio el 29/10/2014.

ANÁLISIS SOLICITADOS : E-2- Hexenal , 1-Hexanal, 1- Hexanol.

MÉTODO BASE DE ANÁLISIS : Cromatografía de Gases con detector de Ionización de Llama (CG-FID) y SPME.

Muestras	Resultados análisis Experimento 8		
	1 Refinado [µg/g]	2 Extracto [mg]	3 Alimentación [µg/g]
E-2- Hexenal	10,1 – 11,1	486 - 507	152 - 154
1-Hexanal	2,1 – 2,9	120 - 124	80,9 – 75,9
1-Hexanol	49 – 44,9	948 - 926	269 - 351

María Elena Ortiz
Jefe Laboratorio
Análisis Químicos

Valparaíso, 28 de Julio de 2015.

Nota: Los resultados entregados en este Informe sólo se refieren a los ítems ensayados.
Este Informe no debe ser reproducido parcialmente sin la aprobación escrita de este Laboratorio.



UNIVERSIDAD TÉCNICA
FEDERICO SANTA MARÍA

Departamento de Química

CENTRO DE ANÁLISIS QUÍMICO E INSTRUMENTAL
Avenida España 1680, Valparaíso Fono: (32) 2654219. FAX: (32) 2654782
Correo electrónico: servicios.analiticos@usm.cl

INFORME DE ANALISIS N° QUI-281-A/14

REFERENCIA : Pontificia Universidad Católica de Chile.
Atn: Sr. Arturo Bejarano.

IDENTIFICACIÓN MUESTRA : 3 muestras líquidas rotuladas Experimento 9 :
1 Refinado, 2 Extracto, 3 Alimentación .
Recibidas en nuestro laboratorio el 05/11/2014.

ANÁLISIS SOLICITADOS : E-2- Hexenal , 1-Hexanal, 1- Hexanol.

MÉTODO BASE DE ANÁLISIS: Cromatografía de Gases con detector de Ionización de Llama (CG-FID) y SPME

Muestras	Resultados análisis Experimento 9		
	1 Refinado [µg/g]	2 Extracto [mg]	3 Alimentación [µg/g]
E-2- Hexenal	5,9 – 5,6	305 - 352	150 - 122
1-Hexanal	1,8 – 1,3	96,1 - 114	58,5 – 42,5
1-Hexanol	16,9 – 19,6	836 - 801	335 - 332

María Elena Ortiz
Jefe Laboratorio
Análisis Químicos

Valparaíso, 28 de Julio de 2015.

Nota: Los resultados entregados en este Informe sólo se refieren a los ítems ensayados.
Este Informe no debe ser reproducido parcialmente sin la aprobación escrita de este Laboratorio.



UNIVERSIDAD TÉCNICA
FEDERICO SANTA MARÍA

Departamento de Química

CENTRO DE ANÁLISIS QUÍMICO E INSTRUMENTAL
Avenida España 1680, Valparaíso Fono: (32) 2654219. FAX: (32) 2654782
Correo electrónico: servicios.analiticos@usm.cl

INFORME DE ANALISIS N° QUI-282-A/14

REFERENCIA : Pontificia Universidad Católica de Chile.
Atn: Sr. Arturo Bejarano.

IDENTIFICACIÓN MUESTRA : 3 muestras líquidas rotuladas Experimento 10 :
1 Refinado, 2 Extracto, 3 Alimentación .
Recibidas en nuestro laboratorio el 05/11/2014.

ANÁLISIS SOLICITADOS : E-2- Hexenal , 1-Hexanal, 1- Hexanol.

MÉTODO BASE DE ANÁLISIS: Cromatografía de Gases con detector de Ionización de Llama (CG-FID) y SPME

Muestras	Resultados análisis Experimento 10		
	1 Refinado [µg/g]	2 Extracto [mg]	3 Alimentación [µg/g]
E-2- Hexenal	20,1 – 14,6	175 - 165	211 - 136
1-Hexanal	1,4 – 1,7	25,4 – 24,8	68 – 66,3
1-Hexanol	125 - 100	546 - 461	397 - 288

María Elena Ortiz
Jefe Laboratorio
Análisis Químicos

Valparaíso, 28 de Julio de 2015.

Nota: Los resultados entregados en este Informe sólo se refieren a los ítems ensayados.
Este Informe no debe ser reproducido parcialmente sin la aprobación escrita de este Laboratorio.



UNIVERSIDAD TÉCNICA
FEDERICO SANTA MARÍA

Departamento de Química

CENTRO DE ANÁLISIS QUÍMICO E INSTRUMENTAL
Avenida España 1680, Valparaíso Fono: (32) 2654219. FAX: (32) 2654782
Correo electrónico: servicios.analiticos@usm.cl

INFORME DE ANALISIS N° QUI –283-A/14

REFERENCIA : Pontificia Universidad Católica de Chile.
Atn: Sr. Arturo Bejarano.

IDENTIFICACIÓN MUESTRA : 3 muestras líquidas rotuladas Experimento 11 :
1 Refinado, 2 Extracto, 3 Alimentación .
Recibidas en nuestro laboratorio el 05/11/2014.

ANÁLISIS SOLICITADOS : E-2- Hexenal , 1-Hexanal, 1- Hexanol.

MÉTODO BASE DE ANÁLISIS: Cromatografía de Gases con detector de Ionización de Llama (CG-FID) y SPME

Muestras	Resultados análisis Experimento 11		
	1 Refinado [µg/g]	2 Extracto [mg]	3 Alimentación [µg/g]
E-2- Hexenal	4,7 – 3,6	54,8 – 35,8	181 - 111
1-Hexanal	1,7 – 1,4	11,5 – 5,9	63,3 – 46,4
1-Hexanol	23 – 17,4	316 - 206	413 - 330

María Elena Ortiz
Jefe Laboratorio
Análisis Químicos

Valparaíso, 28 de Julio de 2015.

Nota: Los resultados entregados en este Informe sólo se refieren a los ítems ensayados.
Este Informe no debe ser reproducido parcialmente sin la aprobación escrita de este Laboratorio.



UNIVERSIDAD TÉCNICA
FEDERICO SANTA MARÍA

Departamento de Química

CENTRO DE ANÁLISIS QUÍMICO E INSTRUMENTAL
Avenida España 1680, Valparaíso Fono: (32) 2654219. FAX: (32) 2654782
Correo electrónico: servicios.analiticos@usm.cl

INFORME DE ANALISIS N° QUI-284-A14

REFERENCIA : Pontificia Universidad Católica de Chile.
Atn: Sr. Arturo Bejarano.

IDENTIFICACIÓN MUESTRA : 3 muestras líquidas rotuladas Experimento 12 :
1 Refinado, 2 Extracto, 3 Alimentación .
Recibidas en nuestro laboratorio el 05/11/2014.

ANÁLISIS SOLICITADOS : E-2- Hexenal , 1-Hexanal, 1- Hexanol.

MÉTODO BASE DE ANÁLISIS: Cromatografía de Gases con detector de Ionización de Llama (CG-FID) y SPME

Muestras	Resultados análisis Experimento 12		
	1 Refinado [µg/g]	2 Extracto [mg]	3 Alimentación [µg/g]
E-2- Hexenal	6,2 – 2,1	390 - 529	131 - 121
1-Hexanal	1,9 – 1	77,5 - 107	40,8 – 40,1
1-Hexanol	17,7 – 7,2	1.347 – 1.362	419 - 369

María Elena Ortiz
Jefe Laboratorio
Análisis Químicos

Valparaíso, 28 de Julio de 2015.

Nota: Los resultados entregados en este Informe sólo se refieren a los ítems ensayados.
Este Informe no debe ser reproducido parcialmente sin la aprobación escrita de este Laboratorio.



UNIVERSIDAD TECNICA
FEDERICO SANTA MARIA

Departamento de Química

CENTRO DE ANÁLISIS QUÍMICO E INSTRUMENTAL
Avenida España 1680, Valparaíso Fono: (32) 2654219. FAX: (32) 2654782
Correo electrónico: servicios.analiticos@usm.cl

INFORME DE ANALISIS N° QUI –290-A/14

REFERENCIA : Pontificia Universidad Católica de Chile.
Atn: Sr. Arturo Bejarano.

IDENTIFICACIÓN MUESTRA : 3 muestras líquidas rotuladas Experimento 13 :
1 Refinado, 2 Extracto, 3 Alimentación .
Recibidas en nuestro laboratorio el 14/11/2014.

ANÁLISIS SOLICITADOS : E-2- Hexenal , 1-Hexanal, 1- Hexanol.

MÉTODO BASE DE ANÁLISIS: Cromatografía de Gases con detector de Ionización de Llama (CG-FID) y SPME

Muestras	Resultados análisis Experimento 13		
	1 Refinado [µg/g]	2 Extracto [mg]	3 Alimentación [µg/g]
E-2- Hexenal	15,9 – 11,4	242 - 252	176 - 165
1-Hexanal	0,26 – 0,22	214 - 199	74,5 – 67,7
1-Hexanol	46,7 – 37,1	645 - 773	316 - 256

María Elena Ortiz
Jefe Laboratorio
Análisis Químicos

Valparaíso, 29 de Julio de 2015.

Nota: Los resultados entregados en este Informe sólo se refieren a los ítems ensayados.
Este Informe no debe ser reproducido parcialmente sin la aprobación escrita de este Laboratorio.



UNIVERSIDAD TECNICA
FEDERICO SANTA MARIA

Departamento de Química

CENTRO DE ANÁLISIS QUÍMICO E INSTRUMENTAL
Avenida España 1680, Valparaíso Fono: (32) 2654219. FAX: (32) 2654782
Correo electrónico: servicios.analiticos@usm.cl

INFORME DE ANALISIS N° QUI-291-A/14

REFERENCIA : Pontificia Universidad Católica de Chile.
Atn: Sr. Arturo Bejarano.

IDENTIFICACIÓN MUESTRA : 3 muestras líquidas rotuladas Experimento 14 :
1 Refinado, 2 Extracto, 3 Alimentación .
Recibidas en nuestro laboratorio el 14/11/2014.

ANÁLISIS SOLICITADOS : E-2- Hexenal , 1-Hexanal, 1- Hexanol.

MÉTODO BASE DE ANÁLISIS: Cromatografía de Gases con detector de Ionización de Llama (CG-FID) y SPME

Muestras	Resultados análisis Experimento 14		
	1 Refinado [µg/g]	2 Extracto [mg]	3 Alimentación [µg/g]
E-2- Hexenal	12,2 – 6,2	164 - 177	166 - 158
1-Hexanal	0,45 - < 0,2	157 - 171	50,5 – 53,3
1-Hexanol	34,2 – 19,6	449 - 457	311 - 327

María Elena Ortiz
Jefe Laboratorio
Análisis Químicos

Valparaíso, 29 de Julio de 2015.

Nota: Los resultados entregados en este Informe sólo se refieren a los ítems ensayados.
Este Informe no debe ser reproducido parcialmente sin la aprobación escrita de este Laboratorio.



UNIVERSIDAD TÉCNICA
FEDERICO SANTA MARÍA

Departamento de Química

CENTRO DE ANÁLISIS QUÍMICO E INSTRUMENTAL
Avenida España 1680, Valparaíso Fono: (32) 2654219. FAX: (32) 2654782
Correo electrónico: servicios.analiticos@usm.cl

INFORME DE ANALISIS N° QUI –292-A/14

REFERENCIA : Pontificia Universidad Católica de Chile.
Atn: Sr. Arturo Bejarano.

IDENTIFICACIÓN MUESTRA : 3 muestras líquidas rotuladas Experimento 15 :
1 Refinado, 2 Extracto, 3 Alimentación .
Recibidas en nuestro laboratorio el 14/11/2014.

ANÁLISIS SOLICITADOS : E-2- Hexenal , 1-Hexanal, 1- Hexanol.

MÉTODO BASE DE ANÁLISIS: Cromatografía de Gases con detector de Ionización de Llama (CG-FID) y SPME

Muestras	Resultados análisis Experimento 15		
	1 Refinado [µg/g]	2 Extracto [mg]	3 Alimentación [µg/g]
E-2- Hexenal	6,1 – 15,5	187	150 - 153
1-Hexanal	< 0,2 – 0,24	167	39,2 – 44,1
1-Hexanol	21,5 – 45,2	522	302 - 300

María Elena Ortiz
Jefe Laboratorio
Análisis Químicos

Valparaíso, 29 de Julio de 2015.

Nota: Los resultados entregados en este Informe sólo se refieren a los ítems ensayados.
Este Informe no debe ser reproducido parcialmente sin la aprobación escrita de este Laboratorio.



UNIVERSIDAD TÉCNICA
FEDERICO SANTA MARÍA

Departamento de Química

CENTRO DE ANÁLISIS QUÍMICO E INSTRUMENTAL
Avenida España 1680, Valparaíso Fono: (32) 2654219. FAX: (32) 2654782
Correo electrónico: servicios.analiticos@usm.cl

INFORME DE ANALISIS N° QUI –293-A/14

REFERENCIA : Pontificia Universidad Católica de Chile.
Atn: Sr. Arturo Bejarano.

IDENTIFICACIÓN MUESTRA : 3 muestras líquidas rotuladas Experimento 15 :
1 Refinado 1 h, 2 Refinado 1:20 h, 3 Refinado 1:40 h .
Recibidas en nuestro laboratorio el 14/11/2014.

ANÁLISIS SOLICITADOS : E-2- Hexenal , 1-Hexenal, 1- Hexanol.

MÉTODO BASE DE ANÁLISIS: Cromatografía de Gases con detector de Ionización de Llama (CG-FID) y SPME

Muestras	Resultados análisis Experimento 15		
	[µg/g]		
	1 Refinado 1 h	2 Refinado 1:20 h	3 Refinado 1:40 h
E-2- Hexenal	6,1 – 1,2	4,4 – 4,4	10,4 – 9,5
1-Hexenal	< 0,2 - < 0,2	< 0,2 - < 0,2	0,28 - < 0,2
1-Hexanol	26,5 – 9,7	22,3 – 19,6	34,9 – 31,9

María Elena Ortiz
Jefe Laboratorio
Análisis Químicos

Valparaíso, 29 de Julio de 2015.

Nota: Los resultados entregados en este Informe sólo se refieren a los ítems ensayados.
Este Informe no debe ser reproducido parcialmente sin la aprobación escrita de este Laboratorio.

Appendix 4 Interfacial Tension of aqueous apple aroma solutions surrounded by CO₂ at elevated pressures.

As described in Section 2.6.3, information regarding interfacial effects of aqueous solutions surrounded by CO₂ at elevated pressures is scarce. To the best of the authors knowledge there is no information for aqueous aroma solutions surrounded by CO₂.

A short research stay at Eurotechnica GmbH, Bargteheide, Germany, allowed the measurements of IFT of some aqueous aroma solutions (Table A4.1) surrounded by CO₂ at elevated pressures. The main results are shown in Figure A4.1

Table A4.1 Composition of aqueous solutions used in IFT measurements.

	Ethanol	Ethyl-buturate	Hexanal	Ethyl-2-Methylbuturate	trans 2 Hexanal	Hexanol	Others
Water+ EtOH	2,35%wt	-	-	-	-	-	No
Model system	2,34%wt	7,5 mg/kg	8,9 mg/kg	6,3 mg/kg.	100 mg/kg	277 mg/kg	No
Natural Apple juice concentrate	2,44% wt	7,5 mg/kg	8,9 mg/kg	6,3 mg/kg	100 mg/kg	277 mg/kg	Yes

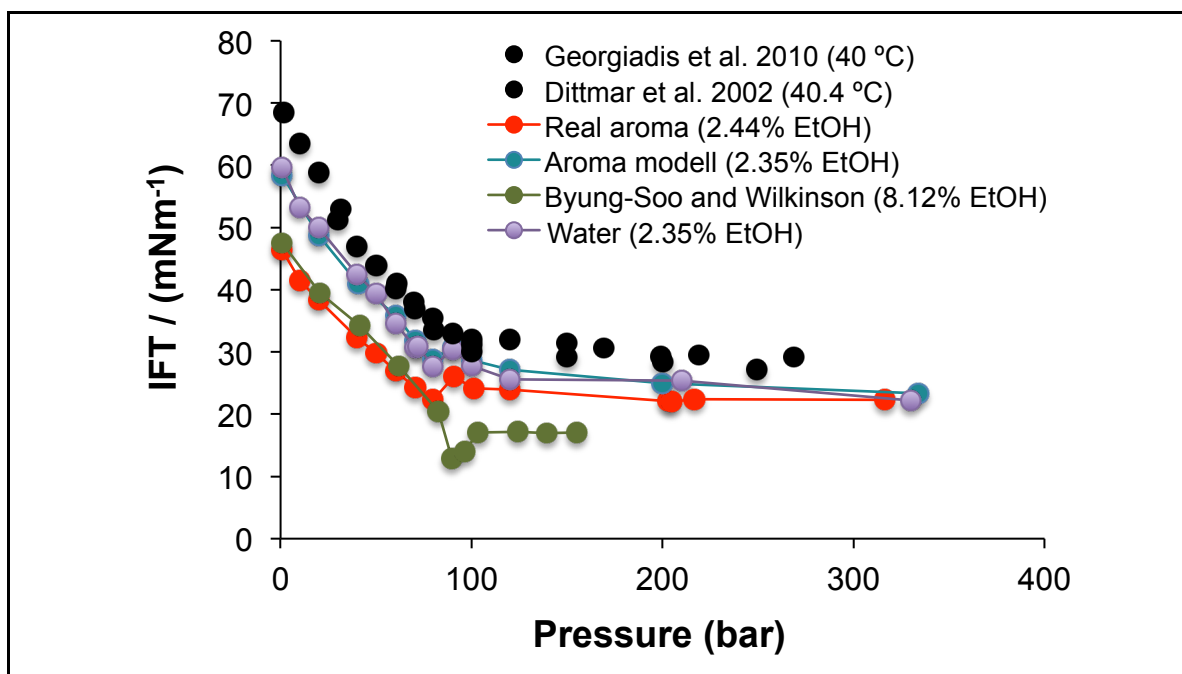


Figure A4.1 Interfacial tension of aqueous aroma solutions surrounded by CO₂ at elevated pressures

This work was presented in collaboration with Prof. Dr.-Ing. Arne Pietsch of the *Fachhochschule Lübeck* in the Annual ProcessNet meeting "High pressure technology" held in Merseburg, Germany 2014 (Fig. A4.2)

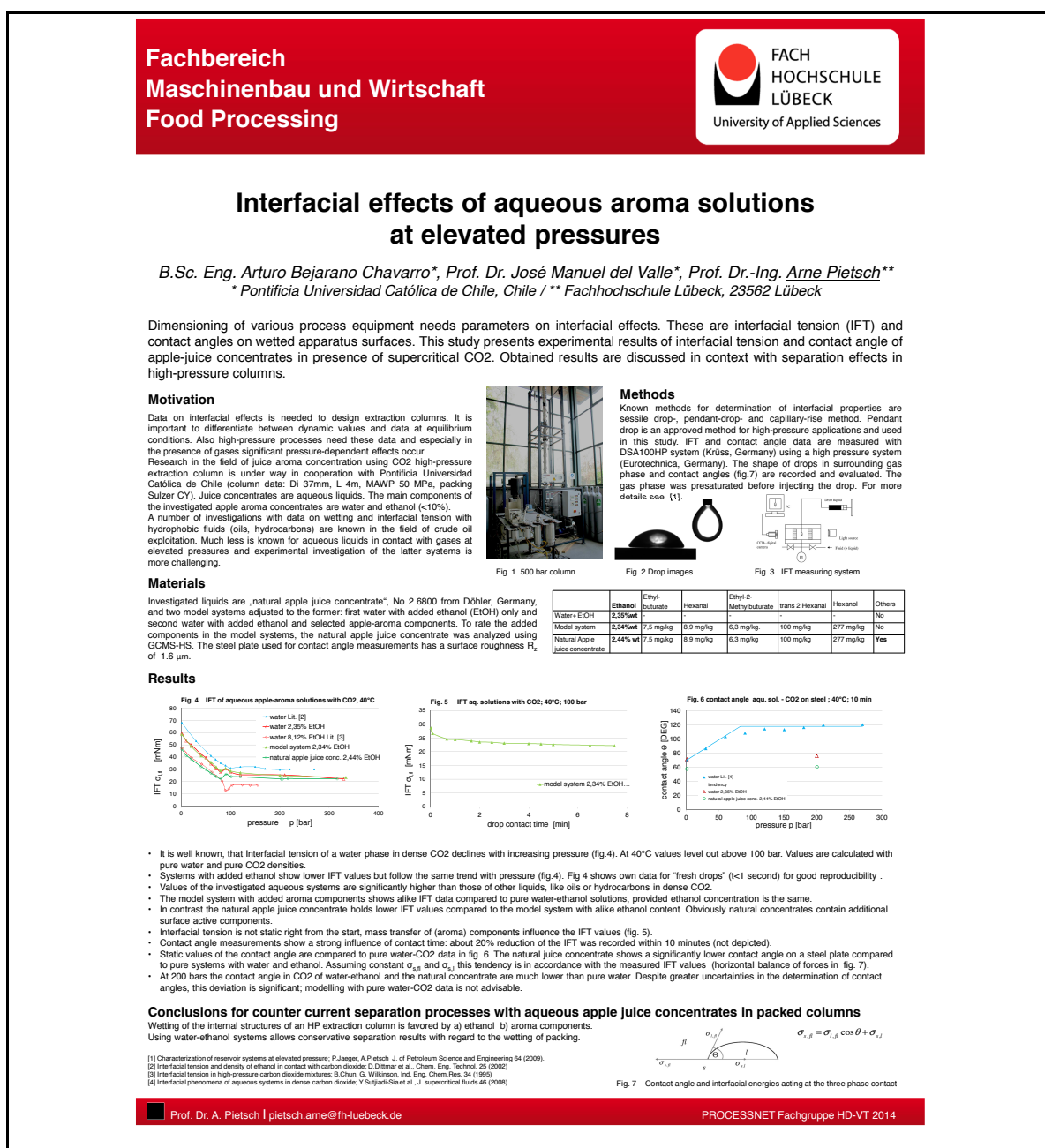


Figure A4.2

Poster presented in the Annual ProcessNet meeting "High pressure technology" held in Merseburg, Germany 2014.